



KINETIC AND EQUILIBRIUM STUDIES OF
CYCLODEXTRIN-AZO DYE INCLUSION COMPLEXES

Ronald James Clarke, B.Sc.(Hons.) (Adelaide)
Department of Physical and Inorganic Chemistry,
The University of Adelaide,
South Australia.

A thesis submitted for the degree of
Doctor of Philosophy.

February, 1985

Completed 12-7-85

"Wohin irgend die Neigung, Zufall oder Gelegenheit den Menschen führt, welche Phänomene besonders ihm auffallen, ihm einen Anteil abgewinnen, ihn festhalten, ihn beschäftigen, immer wird es zum Vorteil der Wissenschaft sein. Denn jedes neue Verhältnis, das an den Tag kommt, jede neue Behandlungsart, selbst das Unzulängliche, selbst der Irrtum ist brauchbar oder aufregend und für die Folge nicht verloren."

J.W. v. Goethe (1808)

"Zur Farbenlehre"

CONTENTS

	<u>Page</u>
<u>INTRODUCTION</u>	1
Bibliography	10
<u>CHAPTER I</u> <u>HISTORICAL REVIEW</u>	
1.1 The Discovery of the Cyclodextrins	13
1.2 The Determination of the Cyclodextrin Structure	16
1.3 The Formation of the Cyclodextrins from Starch	20
1.4 Cyclodextrin Inclusion Compounds	24
Bibliography	26
<u>CHAPTER II</u> <u>INCLUSION COMPLEX FORMATION</u>	
2.1 Detection of Complex Formation	28
2.2 Thermodynamics of Complex Formation	30
Bibliography	44
<u>CHAPTER III</u> <u>EXPERIMENTAL TECHNIQUES</u>	
3.1 Temperature-Jump Relaxation Spectrophotometry	47
3.1.1 Principles of Chemical Relaxation	48
3.1.2 The Temperature-Jump Method	53
3.1.3 Experimental Procedure	58
3.1.4 Data Acquisition and Analysis	59
3.1.5 Calibration of the Temperature Rise	61
3.2 UV/Visible Absorption Spectroscopy	63
3.2.1 Apparatus	63
3.2.2 Experimental Procedure	65

cont'd...

	<u>Page</u>
<u>CHAPTER III cont'd.</u>	
3.3 Circular Dichroism	66
3.4 Linear Dichroism	67
3.4.1 Preparation of Films	67
3.4.2 Measurement of Spectra	68
3.5 Fluorescence Spectroscopy	69
Bibliography	70

<u>CHAPTER IV</u>	<u>THE INTERACTION OF METHYL ORANGE WITH THE CYCLODEXTRINS</u>	
4.1 Introduction		71
4.2 Properties of the Methyl Orange Anion		79
4.3 The Interaction of Methyl Orange with α -Cyclodextrin		88
4.3.1 Results at pH 9.0.		88
4.3.2 Results at pH 13.4		93
4.4 The Interaction of Methyl Orange with β -Cyclodextrin		99
4.4.1 Results at pH 9.0.		99
4.4.2 Results at pH 13.4		106
4.5 The Interaction of Methyl Orange with γ -Cyclodextrin		109
4.5.1 Results at pH 9.0.		109
4.5.2 Results at pH 13.4		118
Bibliography		128

<u>CHAPTER V</u>	<u>THE INTERACTION OF TROPAEOLIN WITH THE CYCLODEXTRINS</u>	
5.1 Introduction		131
5.2 Properties of the Tropaeolin Anion		132
5.3 The Interaction of Tropaeolin with α -Cyclodextrin		140

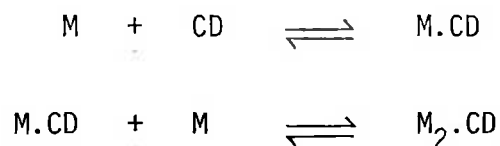
cont'd...

	<u>Page</u>
<u>CHAPTER V</u> cont'd.	
5.4 The Interaction of Tropaeolin with β -Cyclodextrin	140
5.5 The Interaction of Tropaeolin with γ -Cyclodextrin	145
5.6 The Interaction of the Tropaeolin Di-anion with the Cyclodextrins	151
Bibliography	155
<u>CHAPTER VI</u>	<u>THE INTERACTION OF ROCELLIN WITH THE CYCLODEXTRINS</u>
6.1 Introduction	156
6.2 Properties of the Roccellin Anion	156
6.3 The Interaction of Roccellin with α -Cyclodextrin	163
6.4 The Interaction of Roccellin with β -Cyclodextrin	166
6.5 The Interaction of Roccellin with γ -Cyclodextrin	168
6.6 The Interaction of the Roccellin Di-anion with the Cyclodextrins	173
Bibliography	177
<u>CHAPTER VII</u>	<u>GENERAL DISCUSSION AND CONCLUSIONS</u> . . .
Bibliography	178 185
<u>APPENDICES</u>	
A. Materials	186
B. Computational Methods	188
C. Isosbestic Points	192
D. Molecular Exciton Theory	195
E. Derivation of Reciprocal Relaxation Time Expressions	210
Bibliography	216

ABSTRACT

The cyclodextrins are cyclic oligosaccharides, which are able to form inclusion complexes with various organic molecules. The guest molecule is held within the hydrophobic cavity of the cyclodextrin by secondary forces alone. Whereas α -cyclodextrin is usually only capable of including a single guest molecule, it has been shown recently that the larger cyclodextrins, β and γ , are able to include two guest molecules simultaneously. This behaviour has been found for the series of azo dyes: methyl orange, tropaeolin and roccellin.

The presence of a guest dimer within the cyclodextrin cavity was detected by spectroscopic techniques: UV/visible absorption, induced circular dichroism and luminescence. The mechanism of one host-two guest complexation, given below, was determined by temperature-jump relaxation spectrophotometry.



where M = dye monomer

CD = cyclodextrin

In the case of the dyes investigated, dimer formation within β - and γ -cyclodextrin occurs at dye concentrations at which the amount of dimer in free solution is negligible in the absence of cyclodextrin. Hence, β - and γ -cyclodextrin effectively increase the dimerisation constant of the dyes.

The ability of the cyclodextrins to include two guest molecules simultaneously has significance in the field of directed synthesis. It may be possible to use the cyclodextrins to facilitate the association of molecules, which could lead to an increase in the rate of certain reactions which the two molecules might undergo.

To the best of my knowledge and belief, this thesis contains no material previously published or written by another person, nor any material previously submitted for a degree or diploma in any University, except where due reference is made in the text. I give my permission for this thesis to be photocopied.

R.J. Clarke

ACKNOWLEDGEMENTS

I wish to thank my supervisors, Dr. J.H. Coates and Dr. S.F. Lincoln, for their encouragement and guidance throughout the course of this work. I would also like to thank Dr. T. Kurucsev for many helpful discussions on the spectroscopic and computing aspects of this project.

My thanks are also due to the technical and ancillary staff of this Department, particularly Mr. J. Netting, Mr. R. Morris and Mr. K.R. Shepherdson, who have helped me in numerous ways. For their fellowship and advice I would like to express my gratitude to my colleagues, especially Robert Schiller, Bruce Doddridge, Ian Brereton, Daniel Fornasiero and Karen Connell.

To the many friends and relatives who have helped me in various different ways I am very grateful. I would particularly like to thank Robert Jones, Margrit Keck and Peter Cassidy.

Danke schön to Miss Christina Schoene for assistance with German translations, and for her invaluable moral support. I would also like to thank Mrs. Lyn Williams for the typing of this thesis.

Finally, to my parents for their support and encouragement throughout the course of this work I would like to express my thanks.

INTRODUCTION

INTRODUCTION

Inclusion complexes are chemical species consisting of two or more associated molecules, in which one of the molecules, the "host", forms or possesses a cavity, into which it can admit "guest" molecules, resulting in a stable association without any covalent bonds being formed. Weak secondary forces alone are responsible for the maintenance of the integrity of all inclusion complexes.

Over the past twenty-five years interest in the physical and chemical properties of inclusion complexes has grown considerably. One of the most important reasons for this is the relevance which inclusion complexes have to enzyme-substrate and drug-receptor interactions.¹⁻⁸ Inclusion complexes have also been found to have wide application in the food and pharmaceutical industries,^{5,6,9} e.g. microencapsulation of a volatile or reactive substance within a suitable host molecule can often lead to a decrease in the substance's susceptibility to hydrolysis, oxidation, photolysis, etc. Because they are non-toxic and are able to form complexes with numerous small organic molecules, perhaps the most important of the compounds capable of acting as host components are the cyclodextrins.

The cyclodextrins (CD) are cyclic (1 → 4)-linked oligomers of D-glucopyranose, each glucopyranose unit being in the C₁ chair conformation. The three most important cyclodextrins are the α-, β- and γ-cyclodextrins, which consist of six, seven, and eight glucopyranose units respectively. Higher homologues do exist, however they are difficult to purify and their complexing ability appears to be poor.¹⁰ Cyclodextrins having less than six

glucopyranose units are unknown, probably because of steric reasons.¹¹ As a consequence of the C1 chair conformation of the glucopyranose units and the lack of free rotation about the glycosidic bonds, the cyclodextrins are not perfectly cylindrical molecules, but are somewhat cone-shaped, with all of the secondary hydroxyl groups situated on one of the edges of the ring and all of the primary hydroxyls on the other edge. The cavity is lined by a ring of hydrogen atoms (bonded to C-5), a ring of glucosidic oxygens, and another ring of hydrogen atoms (bonded to C-3), thus making it relatively apolar. The shape of the molecule is stabilised by hydrogen bonds between the secondary hydroxyl groups of adjacent glucopyranose units. The numbering system and structure of β -cyclodextrin is shown in Fig.I. The molecular dimensions of the cyclodextrins are given in Table I.

The cyclodextrins are produced through the degradation of starch by the enzyme cyclodextrin transglycosylase (EC 2.4.1.19¹²), which is obtained from the bacterium *Bacillus macerans*. The crude starch digests contain α -, β -, and γ -cyclodextrin, as well as smaller amounts of the higher cyclodextrins and linear dextrans. The cyclodextrins can be separated by selective precipitation with complexing solvents, and then purified by the decomposition of the complex, removal of the guest compound and crystallisation of the cyclodextrin from water. The reason that the cyclodextrin transglycosylase enzyme only occurs in *Bacillus macerans* and a few other thermophilic bacteria has not, as yet, been determined. Nevertheless, it is interesting to speculate about the possible evolutionary advantage which a bacterium might have by possessing

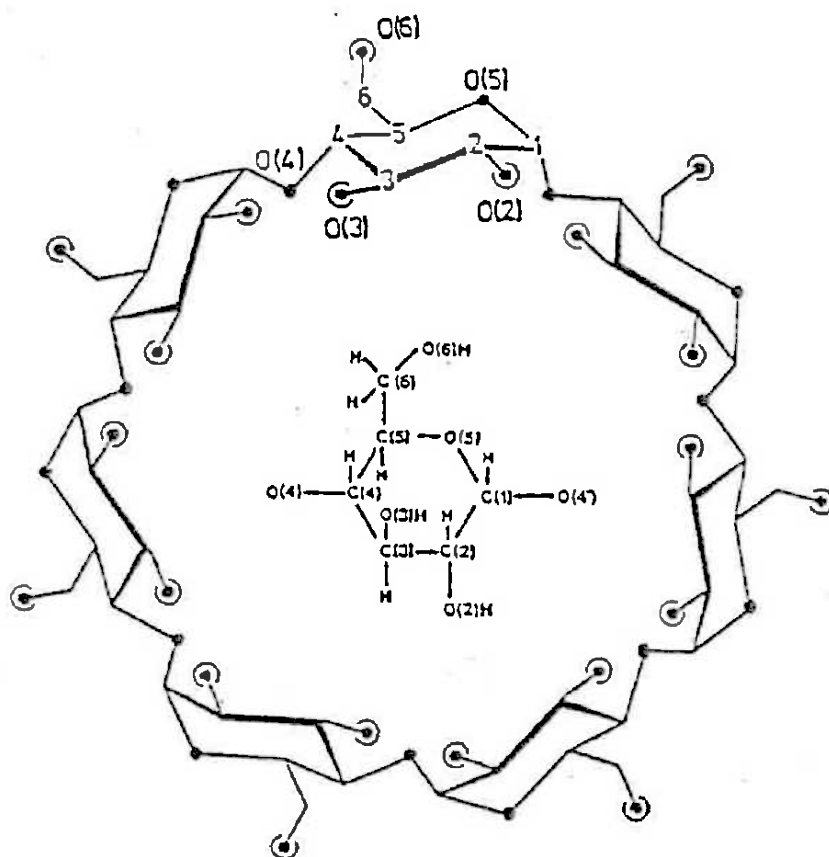


Figure I: Chemical structure and numbering of the atoms for β -cyclodextrin;⁵

- oxygen atoms
- ⊕ hydroxyl groups

No. of Glucose Units	Name	Molecular Weight	Water Solubility (g/100 ml)	Cavity Dimensions (Å)	
				Internal Diameter	Depth
6	α -Cyclodextrin	972	14.5	5.0	8.0
7	β -Cyclodextrin	1135	1.85	6.2	8.0
8	γ -Cyclodextrin	1297	23.2	8.0	8.0

Table I: Physical Properties of the Cyclodextrins

the cyclodextrin transglycosylase enzyme. Since the cyclodextrins have no end groups susceptible to attack, they are completely resistant towards degradation by β -amylases and are only slowly degraded by the α -amylases.⁶ Thus bacteria, which are capable of producing cyclodextrins, effectively convert starch into a form which is very difficult for all other bacteria to digest. It is possible, then, that bacteria possessing the cyclodextrin transglycosylase enzyme use the cyclodextrins as a form of extracellular energy storage.

An important advantage of the inclusion complexes of the cyclodextrins over those of other host compounds, particularly in regards to their use as models of enzyme-substrate complexes, is their ability of formation in aqueous solution. In the case of clathrates, gas hydrates, and the inclusion complexes of hosts such as urea and deoxycholic acid, the cavity in which the guest molecule is situated is formed by the crystal lattice of the host.¹ Thus, these inclusion complexes disintegrate once the crystal is dissolved. The cavity of the cyclodextrins, however, is a property of the size and shape of the molecule and hence persists in solution. In fact, there is evidence that suggests the ability of the cyclodextrins to form inclusion compounds is dependent on the presence of water.^{13,14} Once an inclusion complex has formed in solution it can be crystallised, however in the solid state additional cavities appear in the lattice, as in the case of the hosts mentioned above, which enable the inclusion of further guest molecules.¹⁵

As shown in Table I, the space within the cyclodextrin cavity increases with the number of D-glucopyranose

units. Thus, as would be expected, the stability of an inclusion compound depends to a large degree on the relative sizes of the cyclodextrin cavity and the portion of the guest molecule to be included. For example, a molecule may be too large to fit within the cavity of α -cyclodextrin, but might form a stable complex with the larger β -cyclodextrin. In solution the most common cyclodextrin-guest stoichiometric ratio is 1:1. In the case of guest molecules which cannot be totally included by a single cyclodextrin molecule, however, a further cyclodextrin molecule may occasionally bind, e.g. the complex of methyl orange with α -cyclodextrin.^{16,17}

Recently it has been found by various workers that certain guest molecules exhibit an enhancement of their excimer^{*} fluorescence band on the addition of γ -cyclodextrin.¹⁹⁻²⁷ The presence of β -cyclodextrin has also been found to produce a similar effect, although in a smaller number of cases.^{21,27,28} It has been suggested that this effect indicates one host-two guest complexation.¹⁹ Thus, it seems that the cavities of β - and γ -cyclodextrin are sufficiently large to be able to accommodate two molecules of certain guest compounds simultaneously. Further evidence for one host-two guest complexation has come from the measurement of induced circular dichroism,^{24,26,29-36} the measurement of the UV-visible absorption spectrum,^{24,28-30,33,35-37}

* Excimers are excited dimers (D^*) produced by collisional interaction between excited (M^*) and unexcited monomers (M), i.e. $M^* + M \rightarrow D^*$ ¹⁸

Job's method of continuous variation,^{29,34} as well as additional fluorescence measurements^{32,38}. It should be noted that 2:2 complex formation has also been recently reported for β -^{28,39,40} and γ -cyclodextrin.^{26,35,36}

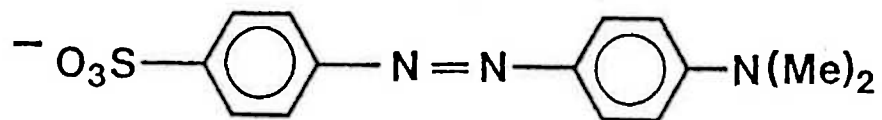
The ability of the cyclodextrins to form one host-two guest complexes has particular significance in the field of catalysis. The facilitation of the association of molecules through the presence of cyclodextrin could lead to an increase in the rate of certain reactions which the two molecules might undergo. One example of this has already appeared in the literature. Tamaki⁴¹ found that 2-anthracenesulphonate formed a one host-two guest inclusion complex with γ -cyclodextrin, and that this complex formation greatly enhanced the efficiency of photodimerisation of the 2-anthracenesulphonate.

The majority of reported studies of cyclodextrin inclusion complex formation in solution have been concerned predominantly with the determination of stability constants using equilibrium spectroscopic techniques, and the measurement of the enthalpy and entropy changes characterising the complexation reaction. The aim of much of this work has been to determine the driving force of complex formation. Despite the amount of research in this area, however, no general agreement has been reached, and several alternative hypotheses have been proposed. A critical review of these hypotheses is presented in Chapter II.

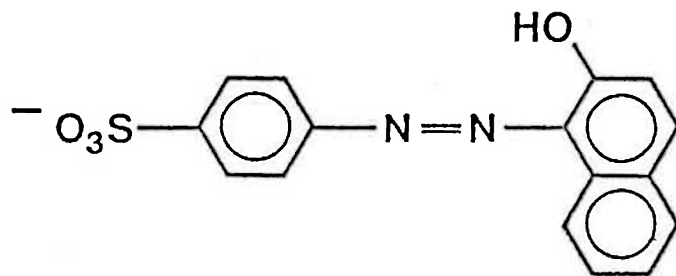
In order to determine the mechanism of complex formation, however, one must use kinetic methods. Consider one host-two

guest complexation. The two possible mechanisms are dimerisation outside the cyclodextrin cavity followed by inclusion, and dimerisation within the cyclodextrin cavity. Equilibrium measurements alone cannot distinguish between these two possibilities. The same is the case for 2:2 complex formation, where a larger number of possible mechanisms exist.

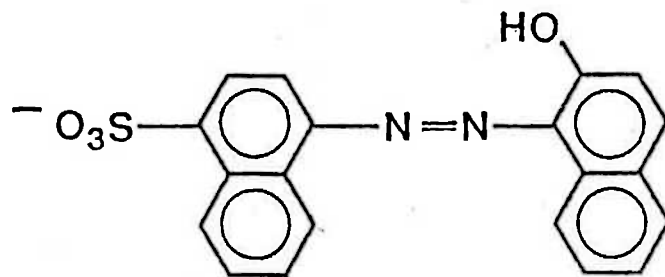
The aim of this study is to determine the effect of a variation of guest size on the stoichiometry and complex stability of a series of azo dyes with α -, β - and γ - cyclodextrin. The dyes investigated are shown in Fig. II. As can be seen, the main variation in the structures of the dyes is in the size of the aromatic rings. The study begins with methyl orange (two benzene rings), proceeds with tropaeolin 000 no. 2 (one benzene and one naphthalene ring) and concludes with roccellin (two naphthalene rings). By the use of the temperature-jump technique it was hoped that some insight might be gained into the mechanism of cyclodextrin inclusion complex formation, particularly one host-two guest complexation. It was also hoped that the application of various spectroscopic techniques might give information regarding the structures of the complexes formed.



METHYL ORANGE (MO)



TROPAEOLIN 000 NO.2 (TRP)



ROCCELLIN (ROC)

Figure II: Chemical structures of the azo dyes investigated

Bibliography

1. Cramer, F., *Revs.Pure Appl.Chem.*, 5, 143 (1955).
2. Griffiths, D.W. and M.L. Bender, *Adv.Cat.*, 23, 209 (1973).
3. Bergeron, R.J., *J.Chem.Ed.*, 54, 204 (1977).
4. Bender, M.L. and M. Komiyama, "Cyclodextrin Chemistry", Springer-Verlag, Berlin, 1978.
5. Saenger, W., *Angew.Chem.Int.Ed.Engl.*, 19, 344 (1980).
6. Szejtli, J., "Cyclodextrins and Their Inclusion Complexes", Akademiai Kiado, Budapest, 1982.
7. Tabushi, I., *Acc.Chem.Res.*, 15, 66, (1982).
8. Breslow, R., *Chemistry in Britain, 1983*, 126.
9. Proceedings of the First International Symposium on Cyclodextrins (J. Szejtli, ed.), Akademiai Kiado, Budapest, 1982.
10. French, D., A.O. Pulley, J.A. Effenberger, M.A. Rougvie and M. Abdullah, *Arch.Biochem.Biophys.*, 111, 153 (1965).
11. Sundararajan, P.R. and V.S.R. Rao, *Carbohydr.Res.*, 13, 351 (1970).
12. Florkin, M. and E.H. Stotz (eds.), "Comprehensive Biochemistry", Vol. 13, Elsevier, Amsterdam (1973).
13. Lach, J.L. and T.-F. Chin, *J.Pharm.Sci.*, 53, 69 (1964).
14. Siegel, B. and R. Breslow, *J.Am.Chem.Soc.*, 97, 6869 (1975).
15. Lammers, J.N.J.J., J.L. Koole and J. Hurkmans, *Die Stärke*, 23, 167 (1971).
16. Cramer, F., W. Saenger, and H.-Ch. Spatz, *J.Am.Chem.Soc.*, 89, 14 (1967).

17. Harata, K., *Bull.Chem.Soc.Jpn.*, 49, 1493 (1976).
18. Birks, J.B., "Photophysics of Aromatic Molecules", Wiley-Interscience, London, 1970.
19. Ueno, A., K. Takahashi and T. Osa., *J.Chem.Soc.Chem. Commun.*, 1980, 921.
20. Emert, J., D. Kodali and R. Catena, *J.Chem.Soc.Chem. Commun.*, 1981, 758.
21. Turro, N.J., T. Okubo and G.C. Weed, *Photochem.Photobiol.*, 35, 325 (1982).
22. Kano, K., I. Takenoshita and T.Ogawa, *Chem.Lett.*, 1982, 321.
23. Yorozu, T., M. Hoshino and M. Imamura, *J.Phys.Chem.*, 86, 4426 (1982).
24. Kobayashi, N., Y. Hino, A. Ueno and T. Osa, *Bull.Chem.Soc. Jpn.*, 56, 1849 (1983).
25. Ueno, A., Y. Tomita and T. Osa, *Chem.Lett.*, 1983, 1635.
26. Kobayashi, N., R. Saito, H. Hino, Y. Hino, A. Ueno and T. Osa, *J.Chem.Soc.Perkin Trans II*, 1983, 1031.
27. Arad-Yellin, R. and D.F. Eaton, *J.Phys.Chem.*, 87, 5051 (1983).
28. Hamai, S., *Bull.Chem.Soc.Jpn*, 55, 2721 (1982).
29. Hirai, H., N. Toshima and S. Uenoyama, *Polymer J.*, 13, 607 (1981).
30. Kobayashi, N., A. Ueno and T. Osa, *J.Chem.Soc.Chem. Commun.*, 1981, 340.
31. Kobayashi, N., R. Saito, Y. Hino, A. Ueno and T. Osa, *J.Chem.Soc.Chem. Commun.*, 1982, 706.
32. Ueno, A., Y. Tomita and T. Osa, *J.Chem.Soc.Chem. Commun.*, 1983, 976.

33. Kobayashi, N., R. Saito, A. Ueno and T. Osa, *Makromol.Chem.*, 184, 837 (1983).
34. Suzuki, M. and Y. Sasaki, *Chem.Pharm.Bull.*, 32, 832 (1984).
35. Clarke, R.J., J.H. Coates and S.F. Lincoln, *Carbohydr.Res.*, 127, 181 (1984).
36. Clarke, R.J., J.H. Coates and S.F. Lincoln, *J.Chem.Soc. Faraday Trans.I*, 80, 3119 (1984).
37. Schiller, R.L., J.H. Coates and S.F. Lincoln, *J.Chem.Soc. Faraday Trans.I*, 80, 1257 (1984).
38. Ueno, A., K. Takahashi, Y. Hino and T. Osa, *J.Chem.Soc. Chem.Comm.*, 1981, 194.
39. Uekama, K., F. Hirayama, T. Imai, M. Otagiri and K. Harata, *Chem.Pharm.Bull.*, 31, 3363 (1983).
40. Uekama, K., T. Imai, F. Hirayama, M. Otagiri and K. Harata, *Chem.Pharm.Bull.*, 32, 1662 (1984).
41. Tamaki, T., *Chem.Lett.*, 1984, 53.

CHAPTER I



CHAPTER I: HISTORICAL REVIEW

1.1 The Discovery of the Cyclodextrins

The first report in the literature of the isolation of a substance attributable as a cyclodextrin was that of Villiers¹ which appeared in 1891. From digests of *Bacillus amylobacter* on potato starch Villiers obtained a small amount (3 g. per 1000 g. of starch) of a crystalline material, which he named "cellulosine" because of its resemblance in some respects to cellulose. The foundations of cyclodextrin chemistry were laid down, however, in the period 1903-11 by Franz Schardinger, and in fact some of the older literature frequently refers to the cyclodextrins as Schardinger's dextrans.

During the course of his work on food spoilage Schardinger's attention had been drawn to various strains of bacteria, which survived the cooking process and which were thought to be responsible for some cases of food poisoning.² Schardinger found³ that one of these heat-resistant or "thermophilic" bacteria, which he called strain II, was able to dissolve starch and form crystalline polysaccharides (dextrans). He distinguished two of these crystalline polysaccharides, which he named crystalline dextrin A and crystalline dextrin B. The latter he observed was probably identical to the cellulosine of Villiers. The yield of B, however, was increased approximately ten-fold, which Schardinger explained by referring to Koch's assertion⁴ that Villiers had used impure cultures.

Schardinger intended to continue his work on these crystalline dextrans in the hope that they might shed some light on the

processes of starch synthesis and degradation or on its composition. However, when after a long suspension he again took up work in this direction, the strain used had almost completely lost its ability of starch decomposition.⁵ Fortunately in the meantime Schardinger had isolated a new organism,⁶ which he had discovered as an accidental contaminant in a nutrient medium. Initially he named the organism "Rottebazillus I", because of its rotting action on potato starch, but later, in order to conform to Latin nomenclature, he gave it the currently accepted name of "*Bacillus macerans*". Using this new organism Schardinger found that he was able to prepare crystalline dextrans identical to those he had previously described.

Bearing in mind the reactions of his A and B dextrans with iodine, Schardinger proposed the names "crystalline amylose" and "crystalline amyloextrin". Later, however, Schardinger considered that these names were inappropriate⁷ and he thus decided upon the less specific names of "crystalline dextrin α " and "crystalline dextrin β ".

At the conclusion of Schardinger's final paper on the crystalline dextrans⁷ he summarised his findings on their properties and their formation from starch. The following is a translation of that summary:

- 1) Starch paste is changed by specific microbes in such a way that water-soluble substances can be obtained, whose behaviour is in close chemico-physical relation to the well-known dextrans.
- 2) The amylolytic process caused by one of these microbes (*Bac. macerans*) is different under similar external conditions depending on the type of starch. In the case

of potato starch there is complete solution, for arrowroot it is almost complete, but for rice and wheat starch it is relatively slight. (The first two types of starch are obtained from root sections or rhizomes, the latter two from above-ground fruit. Perhaps the types of starch have different interior constitutions).

- 3) One part of the dextrans produced is crystalline, another part amorphous, gumlike. The amount of crystalline raw-product amounts to 25-30 per cent of the starch used (determined in the case of maranta^{*} and potato starch).
- 4) Crystalline dextrans have been obtained hitherto from potato, maranta, rice and wheat starch. Moreover from all the types of starch mentioned two different types of dextrin were obtained, which are denoted as crystalline dextrin α and β . The major product is the dextrin α .
- 5) The crystalline dextrans are precipitable from aqueous solution by alcohol as well as by ether, chloroform and iodine solution. Copper salts (Fehling's solution) are not reduced; yeast (top yeast, bottom yeast^{**}) produces no fermentation.
- 6) The iodine reaction offers the simplest means of discrimination of the two crystalline dextrans α and β . In a thin film crystalline iodo-dextrin α is blue when

*

**

Maranta is the scientific name for arrowroot.

Top yeast \equiv baker's yeast, bottom yeast \equiv brewer's yeast.

damp, grey-green when dry; crystalline iodo-dextrin
 β is brownish (red-brownish) whether damp or dry.

Although Schardinger did not propose a structure for his crystalline dextrans, he made several observations⁷ which can now be attributed to their cyclic structure. For example, he discovered their ability of complex formation: "With various substances the crystalline dextrans form loose complexes which, as those produced with alcohol, ether and chloroform, are indeed partly decomposed by water, while the iodine complexes are more stable toward water." He also found, as quoted above, that the crystalline dextrans were non-reducing toward copper salts and non-fermentable by yeast. This last observation he considered was ". . . the most essential thing, that I was able to mention concerning the formation of crystalline dextrans by microbes". Both of these observations can be explained by the lack of a chain termination.

Schardinger brought his work on the crystalline dextrans to a close in 1911. He ended his work with the statement: "I realise that still very many questions remain unsolved. The answer to these I must leave to another, who, owing to more favourable external conditions, can deal with the subject more intensively". It was to be another twenty-five years before the cyclic nature of Schardinger's dextrans was recognised.

1.2 The Determination of the Cyclodextrin Structure

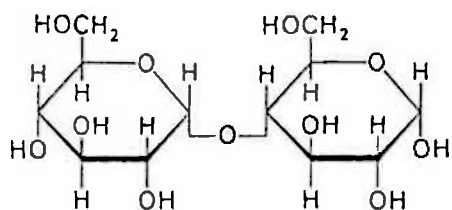
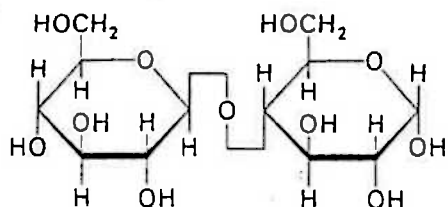
The next major contributor to cyclodextrin chemistry was Karl Freudenberg, who developed a method of obtaining pure α - and β -dextrans,⁸ and in the process also isolated another crystalline dextrin, which he named γ -dextrin. The period between

the publication of Schardinger's last paper and Freudenberg's work had been relatively fruitless, mainly due to the difficulty in separating the crystalline dextrans and obtaining pure samples. Once this hurdle had been overcome, research into Schardinger's dextrans accelerated.

Credit for the determination of the structure of Schardinger's dextrans must also go to Freudenberg, who first tentatively proposed a ring structure in 1936.⁹ In the next few years Freudenberg tested his hypothesis, and came to the conclusion¹⁰ that Schardinger's dextrans were cyclic oligosaccharides composed solely of glucose residues bonded by α -1,4-glycosidic linkages.* In support of this assignment Freudenberg cited the following pieces of experimental evidence:

- 1) the rate of hydrolysis of Schardinger's dextrans in 51% sulphuric acid is too slow for there to be any labile β -linkages present.
- 2) enzymic hydrolysis gave no trace of a sugar unit other than D-glucose.

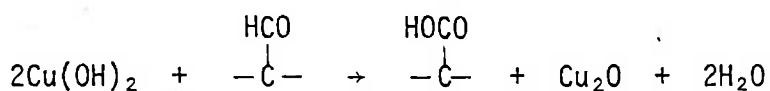
*

 α -1,4-glycosidic linkage β -1,4-glycosidic linkage

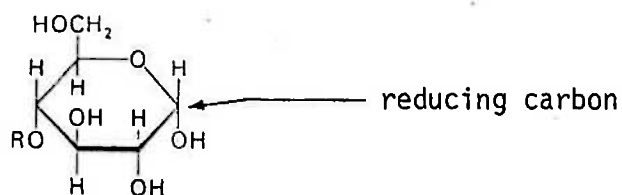
- 3) the Schardinger dextrans are non-reducing,^{*} i.e. they do not have a reducing chain termination.
- 4) methylation studies^{**} on the Schardinger dextrans gave no products other than 2,3,6-tri-O-methyl-D-glucose.

Although Freudenberg had determined the correct chemical structure for Schardinger's dextrans, the number of glucose units which he quoted⁸ for the α - and β -dextrin rings (five and six respectively) were incorrect. These values he determined from molecular weights obtained by the cryoscopic method, which is known to be sensitive to low molecular weight impurities. The correct values of six and seven glucose residues per molecule were determined by Dexter French,¹¹ who obtained the molecular weight by X-ray diffraction combined with crystal density measurement.

- * Reducing sugars are normally identified by their ability to reduce metallic salts, e.g. Fehling's solution.



In order to do this the sugar must have a carbonyl function in the form of a hemiacetal.



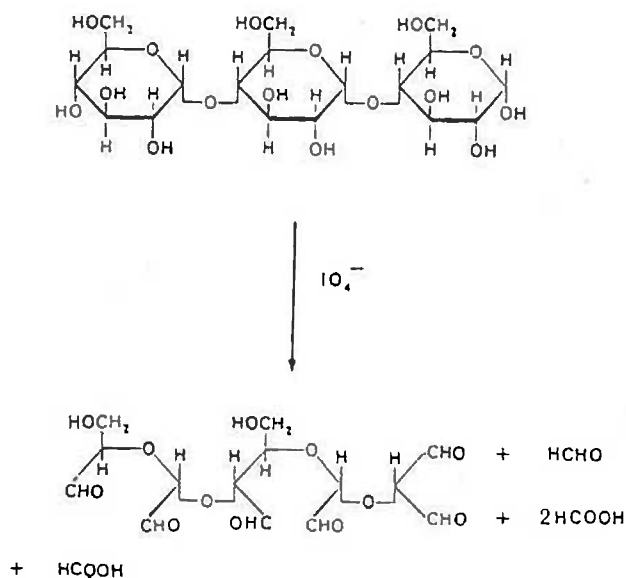
- ** The methylation technique consists of total methylation of the oligosaccharide, followed by hydrolysis to the partially methylated monosaccharide units, and determination of the unmethylated positions in each unit, these being the positions of linkage between units.

On the basis of these values French proposed the names "cyclohexaamylose" and "cycloheptaamylose" for Schardinger's α - and β -dextrins respectively.

Freudenberg later concurred with French's results, after studying the X-ray measurements of Borchert¹² and also his own optical rotational data.¹³ He also proposed that the γ -dextrin consisted of eight D-glucose units joined by α -linkages in a cyclic structure, as in the case of the α - and β -dextrins.

Finally French¹⁴ studied the periodate oxidation* of α -, β - and γ -dextrin, and found that no formic acid nor formaldehyde was produced, and concluded that all three have a cyclic structure as earlier proposed by Freudenberg. He also supported¹⁵ the γ -dextrin structure proposed by Freudenberg, on the basis of acid hydrolysis experiments and crystallographic data.

* Open chain 1 \rightarrow 4 linked polysaccharides yield one molecule of formic acid from the non-reducing end and two molecules of formic acid as well as one molecule of formaldehyde from the reducing end on periodate oxidation.



In keeping with his previously proposed names he suggested the name "cyclooctaamylose" for the γ -dextrin. The name "cyclodextrin", which is now most commonly used for the homologous series, seems to have been originated by Friedrich Cramer,¹⁶ who used this name in the title of his Ph.D. dissertation.

1.3 The Formation of the Cyclodextrins from Starch

Since the time of Schardinger one of the most important reasons for studying the cyclodextrins was for the information which they might yield on the structure of starch and of the well-known blue iodine-starch complex. In fact, the similarity between the iodine-starch reaction and the iodine- α -cyclodextrin reaction was first noted by Schardinger⁷ in his final paper on the cyclodextrins.

Prior to 1939, however, it was not known whether the cyclodextrins were products of the synthetic metabolism of the *Bacillus macerans* and therefore perhaps quite different from the components of starch, or whether they were formed by a single enzyme and therefore closely related to the starch structure. Then Tilden and Hudson¹⁷ announced the discovery of a cell-free enzyme preparation from cultures of *Bacillus macerans*, which had the ability to convert starch to the Schardinger dextrans without the production of maltose, glucose or any other reducing sugars. They thus concluded that the Schardinger dextrans were either the true components of starch or closely related to such true components.

The first to propose a mechanism for the formation of the cyclodextrins was again Freudenberg, who suggested that the

cyclodextrins were pre-formed in starch,¹⁰ and that they were formed by the cleavage of side branches by the *Bacillus macerans*¹⁸ (see Fig. 1.1). Freudenberg, however, soon abandoned his proposed starch structure,¹⁹ because it did not agree with the usual conceptions regarding the linkage of the glucose units, e.g. it required certain glucose units to be linked to three others. In its place Freudenberg adopted the screw model of starch first proposed by Hanes,²⁰ which represents starch as α -linked glucose units in a helical arrangement. On the basis of this model Freudenberg interpreted the formation of the cyclodextrins by the *Bacillus macerans* amylase as a transglucosidation, i.e. he suggested that a winding of the helix is cleaved by the enzyme and, because of the helical arrangement, the first and fifth or sixth glucose residues are situated close to one another and are able to unite and form rings of five or six glucose units (see Fig. 1.2).

Thus Freudenberg concluded that the cyclodextrins are not pre-formed in starch, but that their formation is made possible by the helicity of the starch chain. Freudenberg's hypotheses concerning the starch structure (i.e. the amylose fraction) and the *Bacillus macerans* amylase mechanism have subsequently been confirmed by X-ray crystallography²¹ and chromatographic techniques.²²

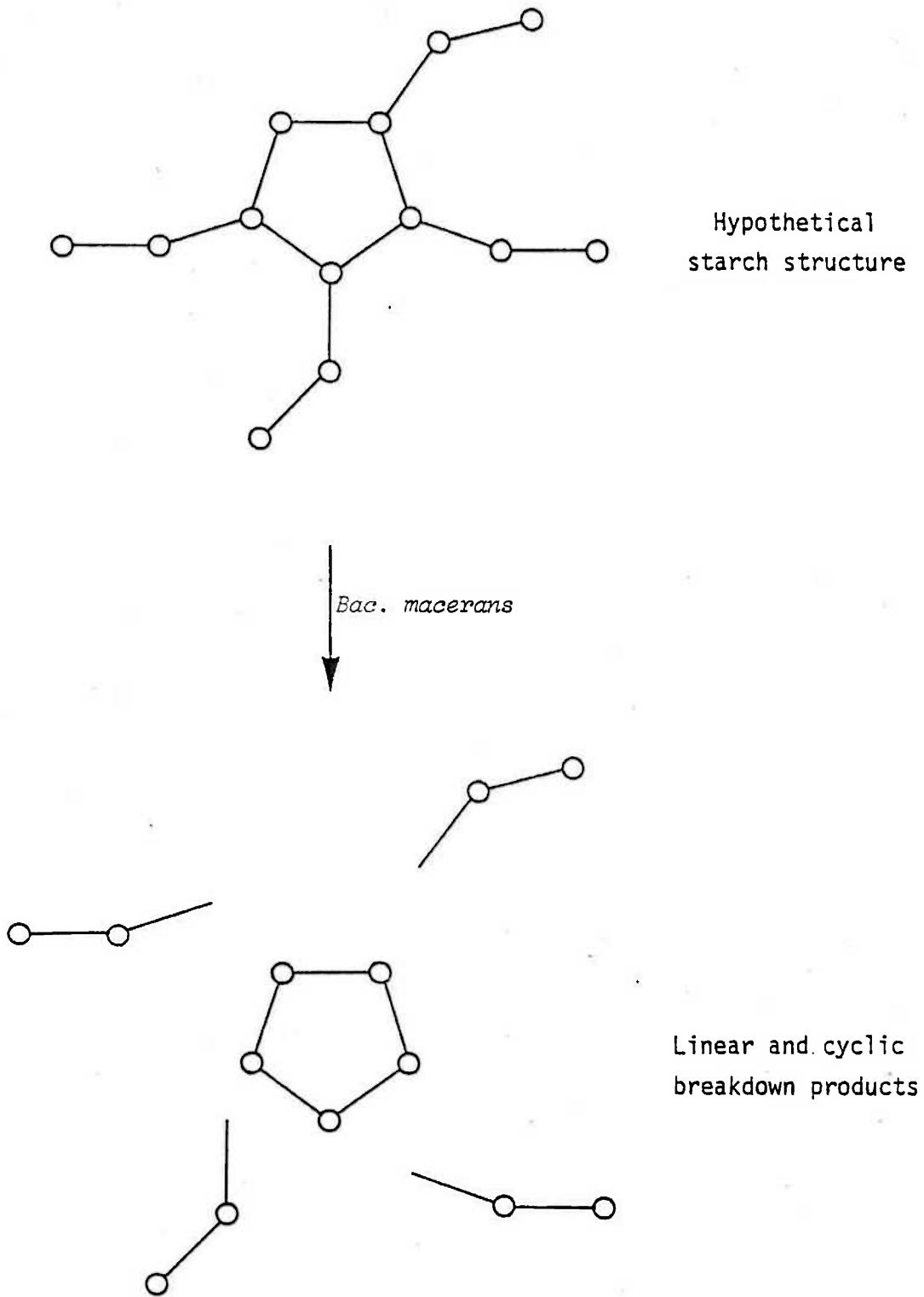
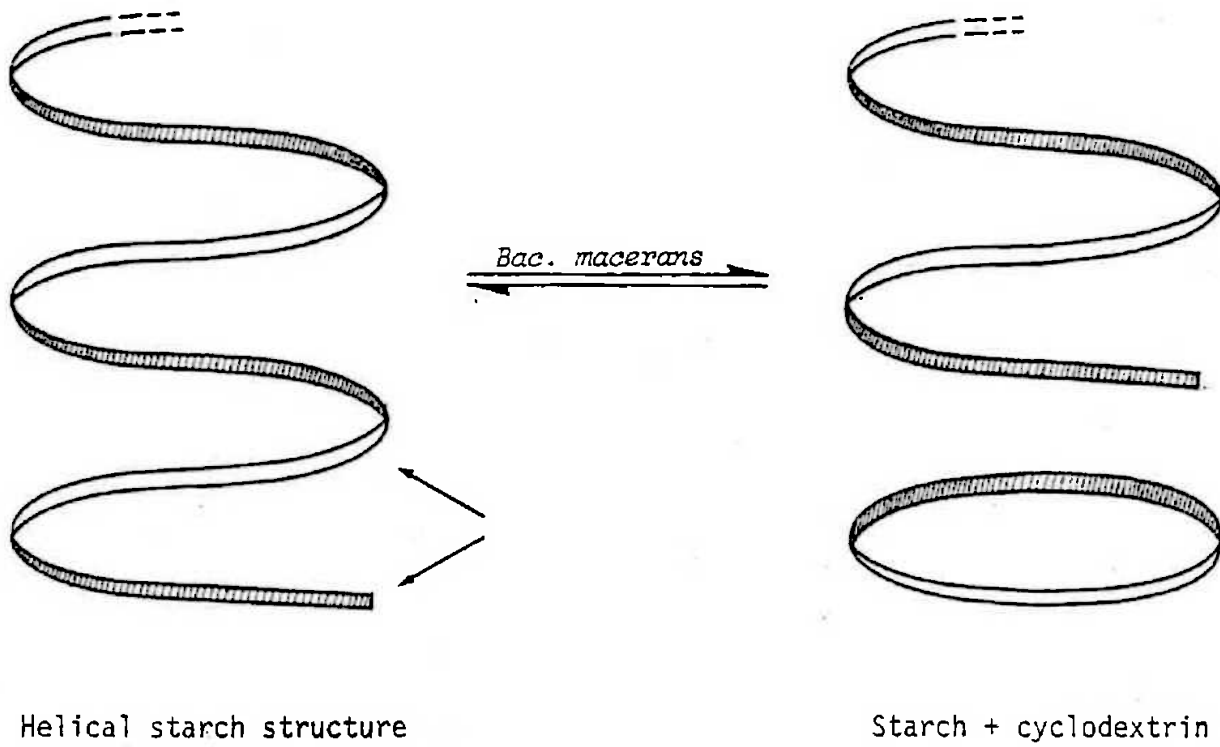
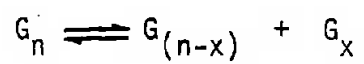


Fig. 1.1: Freudenberg's initial model of cyclodextrin formation.



i.e. If G = glucose, then the reaction can be written



where x is the no. of residues in the cyclodextrin ring.

Fig. 1.2: Freudenberg's final model of cyclodextrin formation.

1.4 Cyclodextrin Inclusion Compounds

Probably the most important property of the cyclodextrins is their ability to form complexes with a variety of organic and inorganic compounds. This property was first discovered by Schardinger,⁷ who used the complexes with alcohol, chloroform and ether as a means of precipitation of his crystalline dextrans and the complexes with iodine for the discrimination of his α and β dextrans. Freudenberg¹⁹ first interpreted these complexes as being formed by molecular inclusion into the cyclodextrin cavity. He also suggested that hydrophobic forces might be responsible for the binding of molecules within the cavity.

The cyclodextrins are not the only molecules capable of forming inclusion compounds ("Einschlussverbindungen"*). In contrast to the inclusion compounds of most other "host" molecules, however, those of the cyclodextrins are able to form in solution as well as in the solid state, a fact which was first recognised by Cramer,²⁴ after he had observed that a number of dyes showed characteristic changes in their absorption spectra in aqueous solutions of the cyclodextrins.

Although Freudenberg's hypothesis that complex formation occurred by inclusion within the cavity was generally accepted, there was no direct evidence for this either in solution or in the solid state. Broser and Lautsch^{25,26} had found by spectrophotometric titration that the complexes of a series of dyes

* The term "Einschlussverbindung" was coined by W. Schlenk Jr. in 1951.²³

with the cyclodextrins in solution obeyed the mass action law with a stoichiometry of 1:1. They suggested that association on the outside of the ring might not have a defined stoichiometric composition, and they thus interpreted their results as being consistent with inclusion by cyclodextrin. Their results were not conclusive, however.

The first direct evidence for molecular inclusion came from X-ray crystallography. Hybl et al.²⁷ determined the structure of the α -cyclodextrin/potassium acetate complex using three dimensional X-ray diffraction data. They found that in the solid state the acetate anions are included by the cyclodextrin. In the process they also found that every glucose residue of the cyclodextrin is in the C1 chair conformation.

Nuclear magnetic resonance provided the first direct evidence of inclusion within the cyclodextrin cavity in solution. Using aromatic "guest" molecules Demarco and Thakkar²⁸ found that on the addition of the guest the resonances of the hydrogen atoms of the cyclodextrin situated on the inside of the cavity were shifted significantly upfield due to shielding by the aromatic guest. They noted little effect on the resonances of the hydrogens on the exterior of the cyclodextrin torus.

Bibliography

1. Villiers, A., *Comptes Rendus*, 112, 536 (1891).
2. Schardinger, F., *Wiener klinischen Wochenschrift*, 16, 468 (1903).
3. Schardinger, F., *Zeitschrift für Untersuchung der Nahrungs- und Genussmittel*, 6, 865 (1903).
4. Koch, R., *Jahresbericht über Gärungsorganismen*, 2, 242 (1891).
5. Schardinger, F., *Zentralblatt für Bakteriologie II*, 22, 98 (1909).
6. Schardinger, F., *Wiener klinischen Wochenschrift*, 17, 207 (1904).
7. Schardinger, F., *Zentralblatt für Bakteriologie II*, 29, 188 (1911).
8. Freudenberg, K. and R. Jacobi, *Ann.*, 518, 102 (1935).
9. Freudenberg, K., G. Blomquist, L. Ewald and K. Soff, *Ber.*, 69, 1258 (1936).
10. Freudenberg, K. and M. Meyer-Delius, *Ber.*, 71, 1596 (1938).
11. French, D. and R.E. Rundle, *J. Am. Chem. Soc.*, 64, 1651 (1942).
12. Borchert, W., *Z. Naturforsch.*, 3b, 464 (1948).
13. Freudenberg, K. and F. Cramer, *Z. Naturforsch.*, 3b, 464 (1948).
14. French, D. and R.L. McIntire, *J. Am. Chem. Soc.*, 72, 5148 (1950).
15. French, D., D.W. Knapp and J.H. Pazur, *J. Am. Chem. Soc.*, 72, 5150 (1950).
16. Cramer, F., "Die Cyclodextrine aus Stärke", Dissertation, Heidelberg (1949).
17. Tilden, E.B. and C.S. Hudson, *J. Am. Chem. Soc.*, 61, 2900 (1939).

18. Freudenberg, K., *Ann.Rev.Biochem.*, 8, 81 (1939).
19. Freudenberg, K., E. Schaaf, G. Dumpert and T. Ploetz, *Naturwissenschaften*, 27, 850 (1939).
20. Hanes, C.S., *New Phytologist*, 36, 189 (1937).
21. Takeo, K. and T. Kuge, *Agric.Biol.Chem.(Tokyo)*, 33, 1174 (1969).
22. French, D., M.L. Levine, E. Norberg, P. Nordin, J.H. Pazur and G.M. Wild, *J.Am.Chem.Soc.*, 76, 2387 (1954).
23. Schlenk Jr., W., *Fortschr.Chem.Forsch.*, 2, 92 (1951).
24. Cramer, F., *Angew.Chemie*, 64, 437 (1952).
25. Broser, W. and W. Lautsch, *Z.Naturforsch.*, 8b, 711 (1953).
26. Broser, W., *Z.Naturforsch.*, 8b, 722 (1953).
27. Hybl, A., R.E. Rundle and D.E. Williams, *J.Am.Chem.Soc.*, 87, 2779 (1965).
28. Demarco, P.V. and A.L. Thakkar, *Chem.Commun.*, 1970, 2.

CHAPTER II

CHAPTER II: INCLUSION COMPLEX FORMATION

2.1 Detection of Complex Formation

Upon inclusion within the cyclodextrin cavity a guest molecule experiences changes in its physicochemical properties (due to the change in its environment), as well as changes in its reactivity (due to its removal from the bulk solution). These changes in behaviour have great practical significance (e.g. for the stabilisation of reactive substances, reduction in volatility, and improvement of solubility). In research, however, the changes in the guest's physicochemical properties provide an easy method of detecting inclusion complex formation.

A variety of techniques can be used for studying complex formation, a number of which are listed below:

1) UV/visible Absorption

Many aromatic organic molecules show changes in their UV/visible absorption spectrum on inclusion by cyclodextrin.^{1,2} Generally the spectral changes observed are similar to the effects caused by changes in solvent. These changes must be due to a perturbation of the guest's electronic system, caused either by its interaction with the cyclodextrin or by the exclusion of solvating water molecules or by a combination of these two effects.

2) Fluorescence

When fluorescent molecules are included by cyclodextrin a fluorescence enhancement usually occurs. This enhancement has been attributed as being due to the reduction in collisional quenching (by water and oxygen) of the guest's fluorescence upon its fixation within the cyclodextrin cavity.³

3) Circular Dichroism

The cyclodextrins are chiral molecules, since they are composed entirely of D-glucose units in a symmetrical arrangement. Thus a guest molecule exhibits changes in its circular dichroic spectrum on inclusion due to the interaction of the guest's transition dipoles with those of the glucose units of the cyclodextrins.⁴ Even achiral molecules show an induced circular dichroic spectrum upon inclusion due to this interaction.

4) Nuclear Magnetic Resonance

Upon inclusion of a guest molecule, changes in the chemical shifts of the atoms of both the cyclodextrin⁵ and the guest molecule⁶ are frequently observed. These changes are due to a change in the environment of the atom concerned, e.g. because of anisotropic shielding, interactions between the guest and the cyclodextrin, conformational changes in the cyclodextrin or expulsion of water from the cavity.

5) Acid-Base Titration

Acidic and basic guest molecules often show apparent changes in their acidity or basicity on inclusion, i.e. changes in pK_a are observed.⁷ Depending on the guest used, these changes can be followed spectrophotometrically or potentiometrically.

6) Solubility

Substances which are only sparingly soluble in water often show an increase in solubility on complexation with cyclodextrin.⁸ In contrast, the inclusion complex is generally less soluble than the free cyclodextrin.⁹

Although the techniques considered above have been widely used in research for the development of practical uses of the cyclodextrins, the underlying forces responsible for the stability of the inclusion complexes as well as the mechanism of their formation remain somewhat of a mystery.

2.2 Thermodynamics of Complex Formation

The stability of cyclodextrin inclusion complexes is generally due to a favourable enthalpy change (ΔH°) during the inclusion process. Depending on the guest molecule, the entropy change (ΔS°) can be either favourable or unfavourable, although the majority of guest molecules studied appear to give an unfavourable ΔS° .

Values of ΔH° and ΔS° for complex formation between α - and β -cyclodextrin and a variety of guest molecules have been collected from the literature (see Tables 2.1 and 2.2). If ΔH° is plotted against ΔS° a linear relationship is observed, in which ΔH° and ΔS° are compensating (see Figures 2.1 and 2.2). The slope of the graph is called the "compensation temperature" or "isoequilibrium temperature" and is denoted by T_c . The values of T_c thus determined for the α -cyclodextrin and β -cyclodextrin complexes are 272 (± 14) and 308 (± 15) K respectively.

This correlation implies a common interaction mechanism between the cyclodextrins and the various substrates. Since the substrates have widely varying structures, this mechanism cannot be associated with the substrate structure, but rather with a common attribute of these systems, i.e. the solvent, water, and/or the host, cyclodextrin. Compensation effects of this type have frequently been observed

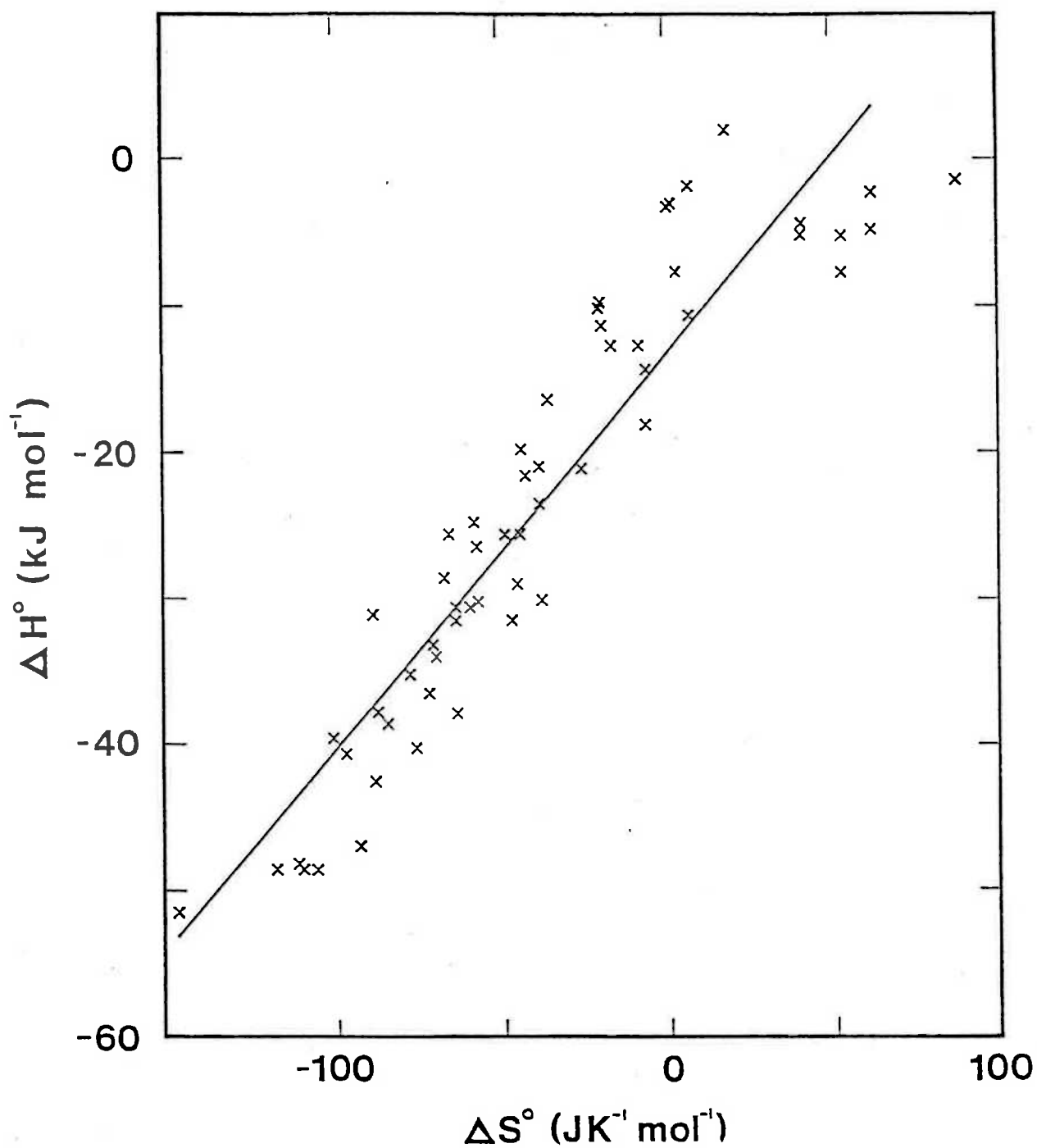


Fig. 2.1: Enthalpy-entropy compensation for α -cyclodextrin inclusion compounds.

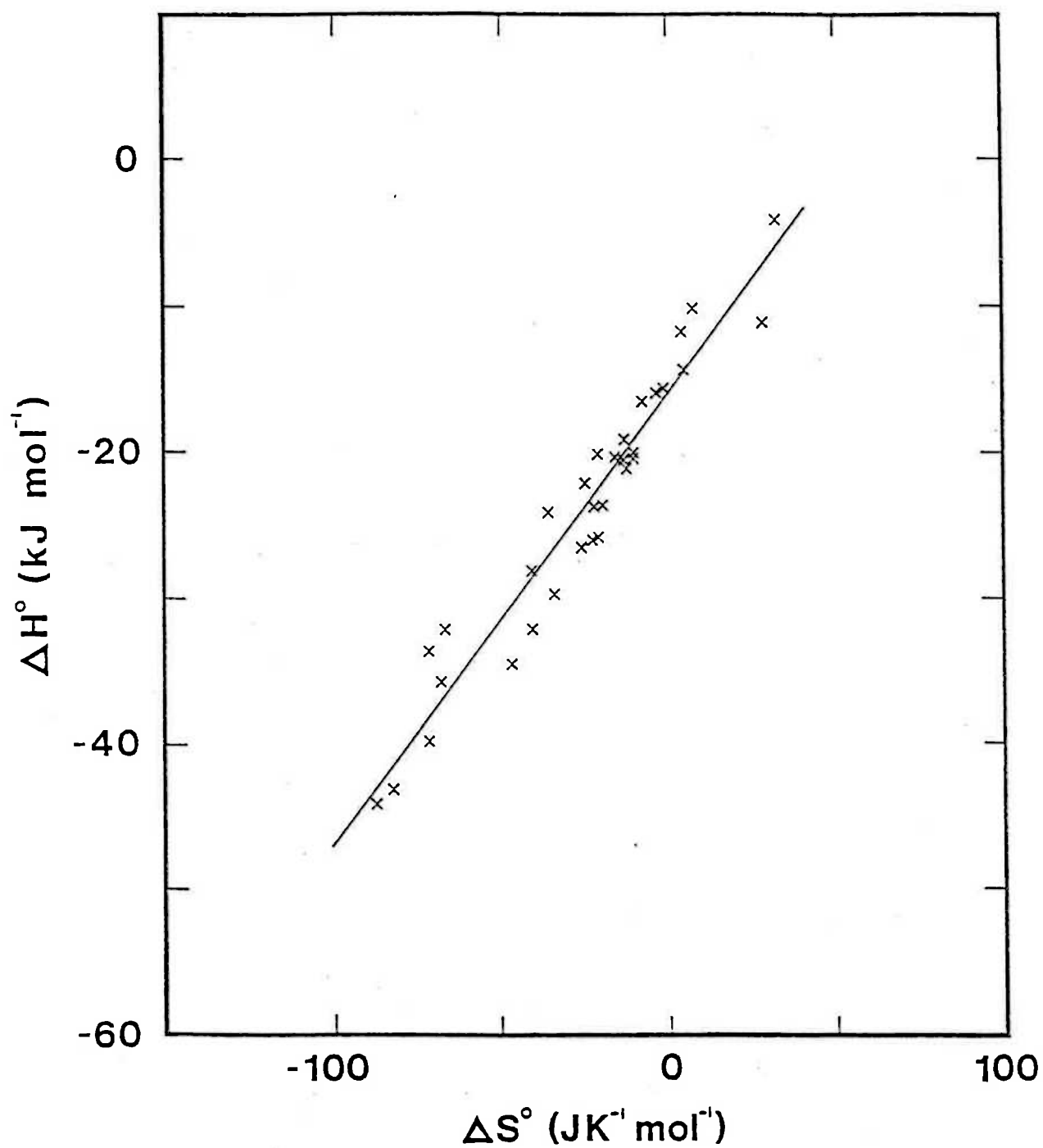


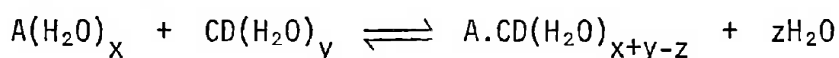
Fig. 2.2: Enthalpy-entropy compensation for β -cyclodextrin inclusion compounds.

in water,²⁴ and have been attributed to changes in the solvation of the participating molecules during the reaction. The values of T_c determined are well within the 250-315 K range characteristic of processes dominated by solvation phenomena. Thus, it seems most likely that changes in the solvation of the guest molecule and the cyclodextrin play an important role in determining the stability of the resultant inclusion complex.

An alternative explanation for the observed enthalpy-entropy compensation has been proposed by Gelb and co-workers,¹² who suggested that the cyclodextrin structure is responsible for the compensation. According to Gelb, polar interactions between α -cyclodextrin and the substrate provide the driving force for the complexation reaction. These interactions then result in torsional constraint of the α -cyclodextrin structure, reflected in the usually substantially negative entropy change. Having found a T_c value of 410 (± 15) K,¹⁸ i.e. outside the normal range for solvation phenomena, Gelb proposed that the complexation process involves no changes in the solvation of the guest molecule or the cyclodextrin.

Although Gelb's suggestions of polar interactions between the guest and the cyclodextrin and torsional constraint of the cyclodextrin structure appear feasible, his hypothesis that neither the host nor the guest undergo solvation changes on complexation seems untenable. It can be seen from published crystal structures of inclusion complexes²⁵ and also from molecular model building that in the case of the most stable complexes the fit between substrate and cyclodextrin is very tight, thus providing very little space for any

solvating water molecules. Thus, although it may not be the case that all solvating water molecules are removed from the guest and excluded from the cyclodextrin cavity prior to complex formation, it seems that significant changes in solvation must occur in most cases. This is further supported by the results of Mochida et al.,²⁶ who investigated the effect of inorganic salts on the dissociation of an azo dye/ β -cyclodextrin inclusion complex. Mochida found that increases in the concentration of salts such as phosphate, sulphate, iodate and fluoride caused a decrease in the apparent dissociation constant of the complex, i.e. an increase in the apparent association constant. Mochida attributed this effect to a change in the activity of the water, thus implying its participation in the inclusion reaction. Consider the reaction of a hydrated guest molecule, $A(H_2O)_x$, with a hydrated cyclodextrin, $CD(H_2O)_y$. The association can be expressed as follows:



The association constant, K , for this equilibrium is given by:

$$K = K_{app} \times a_{H_2O}^z$$

where K_{app} is the apparent association constant

a_{H_2O} is the activity of water.

Thus, the addition of inorganic salts, providing they are not included by cyclodextrin themselves, results in a decrease in the activity of water due to hydration of the salts, causing an increase in K_{app} . Mochida found that the cation used also affected the association, the K_{app} value increasing with the extent of hydration of the cation, i.e.

$$K_{app}(K^+) < K_{app}(Na^+) < K_{app}(Li^+)$$

Now if it is assumed that water molecules are excluded from the cyclodextrin cavity upon inclusion of a guest, then in order for a complex to form, solvation of the cyclodextrin-guest complex must be energetically more favourable than solvation of the individual molecules. There are two basic reasons which could account for this:

- 1) an interaction between the guest and the cyclodextrin drives the inclusion process.
- 2) the large internal cohesion of water (due to hydrogen bonding) forces the cyclodextrin and the guest together, i.e. a hydrophobic interaction.

The fact that inclusion complexes are formed most readily in aqueous solution^{27,28} suggests the importance of hydrophobic interactions. It has also been found that guest molecules with apolar groups favour the inclusion process,²⁹ thus giving further weight to the assignment of complex stability to hydrophobic interactions. Classical hydrophobic interactions, however, are characterised by a favourable entropy of association,³⁰ in contrast to the cyclodextrin inclusion complexes, for which the driving force of inclusion is derived primarily from a favourable enthalpy change. Thus, it has been suggested by Griffiths and Bender³¹ that the driving force of inclusion is an example of an "atypical" hydrophobic interaction.

The explanation that Griffiths and Bender offered to explain the favourable enthalpy change is that the "empty" cyclodextrin contains water molecules which are unable to form their full complement of hydrogen bonds to adjacent water molecules, and thus

may be considered as "enthalpy rich". The inclusion of a guest molecule would then displace this "high energy" water from the cyclodextrin cavity, leading to a net increase in solvent-solvent hydrogen bonds and a favourable enthalpy of association.

An additional contribution to the enthalpy of association has been proposed by Saenger et al.³². From an X-ray diffraction study of the solid α -cyclodextrin hexahydrate, Saenger found that one of the glucose units is rotated into a nearly orthogonal position relative to the other five, in order to form hydrogen bonds to the included water, and also that the ring of interglucosidic hydrogen bonds around the rim of the cyclodextrin torus is disrupted.³³ This unusual arrangement of the glucose units seems only to occur in the α -cyclodextrin hexahydrate structure. When α -cyclodextrin is complexed with other guest molecules the crystal structures determined show a complete ring of hydrogen bonds and no rotation of any glucose units. Thus, it has been suggested by Saenger that in water the α -cyclodextrin molecule is in a "strained" high energy conformation, and that when another guest molecule displaces the water, thus forming an inclusion complex, a conformational change of the α -cyclodextrin molecule occurs, transforming the α -cyclodextrin structure into an unstrained "relaxed" state. According to Saenger then, inclusion complex formation is accompanied in the case of α -cyclodextrin by relief of strain in the cyclodextrin ring, thus contributing to the enthalpy of association and to the stability of the inclusion complex. In the cases of β - and γ -cyclodextrin this strain energy relief mechanism does not seem to be operative, since the β - and γ -cyclodextrin/water adducts are not strained.^{34,35}

So far only hydrophobic interactions have been considered as the source of inclusion complex stability. Some experimental observations, however, cannot be explained by hydrophobic interactions alone. For example, from a study of a series of substituted phenyl acetates van Etten et al.²³ observed an approximately linear relationship between the dissociation constant of the cyclodextrin-guest complex and the molar refraction of the guest. Since the molar refraction is related to the polarisability, this suggests the participation in the inclusion process of van der Waals forces, i.e. permanent dipole-induced dipole interactions and London dispersion forces. Further support for this comes from the work of Bergeron and co-workers.³⁶ Bergeron found that the p-nitrophenolate anion binds over one hundred times more effectively in the α -cyclodextrin cavity than p-nitrophenol, although both guest molecules penetrate the cavity nitro group first. This difference in stability had previously been noted by Connors and Lipari,⁷ who attributed it to the extensive charge delocalisation in the p-nitrophenolate anion.

This dependence of the stability of cyclodextrin inclusion on the polarisability of the guest molecule was correctly predicted years earlier by Broser,³⁷ who used the concept to explain the perturbation of the visible absorption spectra of several dye molecules. According to Broser the fact that the cyclodextrin ring has a top and a bottom means that the dipole moments of the individual glucose units do not cancel, thus giving the cyclodextrin a resultant dipole moment directed along the cyclodextrin axis, passing through the cavity. This dipole moment produces an electrical

field within the cavity, which is thus responsible for the preference of the cyclodextrins for molecules of high polarisability. The dependence of complex stability on polarisability is a useful concept for explaining differences in the affinity of structurally similar guest molecules for cyclodextrin. In considering guest molecules of significantly different structures, however, steric effects and differences in solvation may be more important.

The participation of van der Waals forces in inclusion complex formation is also found to be consistent with crystal structure analyses. Interatomic distances between the guest and the cyclodextrin thus determined are characteristic of van der Waals type interactions.²⁵ Hydrogen bonding between the guest and hydroxyl groups of the cyclodextrin has also been demonstrated crystallographically in certain cases.²⁵

Thus, it seems that both hydrophobic interactions and van der Waals interactions undoubtedly play a part in inclusion complex formation, although the relative contribution of each type of interaction may vary with the chemical properties of the guest; which accounts for the ability of the cyclodextrins to form complexes with a wide variety of guest molecules. The existence of a good spatial fit between the guest and the cyclodextrin cavity is, however, a necessary requirement for the formation of a stable inclusion complex.

Table 2.1: Standard formation enthalpies and entropies of α -cyclodextrin inclusion complexes (1:1).

<u>Substrate</u>	<u>ΔH° (kJmol⁻¹)</u>	<u>ΔS° (JK⁻¹mol⁻¹)</u>	<u>Ref.</u>
formic acid	-3.10	1.3	10
acetic acid	-11.21	-18.8	10
acetic acid	-5.02	54	11
propionic acid	-21.51	-41.84	12
cyclohexanecarboxylic acid	-39.50	-100.00	12
trimethylacetic acid	-19.7	-43.1	12
adamantenecarboxylic acid	-23.4	-37.7	13
adamantenecarboxylate	-14.2	-5.4	13
adamantenecarboxylate	-5.0	41.8	14
benzoic acid	-42.47	-87.4	10
benzoic acid	-40.17	-75	11
benzoate	-16.3	-35.1	10
p-hydroxybenzoic acid	-48.53	-105.02	13
p-hydroxybenzoate	-25.52	-64.9	13
p-nitrophenol	-30.5	-58.6	15
p-nitrophenol	-30.5	-63	11
p-nitrophenol	-30.12	-56.1	16
p-nitrophenol	-18	-5.4	2
p-nitrophenolate	-46.9	-92.0	15
p-nitrophenolate	-30	-37	2
p-nitrophenolate	-37.8	-62.63	17
p-cyanophenol	-25.5	-43.5	12
p-cyanophenolate	-28.9	-44.4	12
p-nitrobenzoic acid	-33.89	-69.0	12

Table 2.1 cont'd.

<u>Substrate</u>	<u>ΔH° (kJmol⁻¹)</u>	<u>ΔS° (JK⁻¹mol⁻¹)</u>	<u>Ref.</u>
m-hydroxybenzoic acid	-48.12	-110.5	12
m-nitrophenol	-37.7	-86.6	12
m-nitrophenol	-33.05	-69.9	16
m-nitrophenolate	-38.5	-83.7	12
m-cyanophenol	-25.5	-48.1	12
m-cyanophenolate	-36.4	-71.1	12
m-nitrobenzoic acid	-35.1	-77	12
perchlorate	-26.36	-56.5	18
iodide	-24.69	-57.3	18
thiocyanate	-28.5	-66.5	18
hydroxide	-20.9	-37.7	12
acetonitrile	-10.0	-19.7	19
ethanol	-2.9	2.5	19
2-propanol	-1.7	7.9	19
2-methyl-2-propanol	2.09	19.2	19
cyclohexanol	-12.6	-7.5	19
dioxane	-9.62	-19.2	19
phenol	-12.6	-15.9	19
phenol	-7.53	54	11
anilinium perchlorate	-51.5	-146	11
4-aminobenzoic acid	-48.5	-109	11
3-methylbenzoic acid	-48.5	-117	11
sodium perchlorate	-40.6	-96	11
diisopropyl phosphofluoridate	-31	-88	20
perchloric acid	-31.4	-63	11

Table 2.1 cont'd.

<u>Substrate</u>	<u>ΔH° (kJmol⁻¹)</u>	<u>ΔS° (JK⁻¹mol⁻¹)</u>	<u>Ref.</u>
hydrocinnamic acid	-31.38	-46	11
L-mandelic acid	-21	-25	11
pyridine	-10.5	8	11
L-tryptophan	-7.53	4	11
L-phenylalanine	-4.6	63	11
L-tyrosine	-4.2	42	11
2-nitrophenol	-2.09	63	11
2-aminobenzoic acid	-1.26	88	11

Table 2.2: Standard formation enthalpies and entropies of β -cyclodextrin inclusion complexes (1:1).

<u>Substrate</u>	<u>ΔH° (kJmol⁻¹)</u>	<u>ΔS° (JK⁻¹mol⁻¹)</u>	<u>Ref.</u>
4-nitrophenol	-44	-88	11
phenobarbital	-43	-83	21
mephobarbital	-39.7	-72	21
2-aminobenzoic acid	-35.6	-68.3	4
thiophenobarbital	-34.4	-47	21
2-hydroxybenzoic acid	-33.5	-72	4
benzoic acid	-32	-67	11
C ₇ H ₁₅ barbituric acid	-32.0	-40.8	21
C ₆ H ₁₃ thiobarbituric acid	-29.6	-34.2	21
p-methylbenzoyl acetic acid	-28	-41	22
amobarbital	-26.4	-26.1	21
C ₆ H ₁₃ barbituric acid	-25.9	-22.8	21
thiopental	-25.7	-21.0	21
benzoyl acetic acid	-24	-36	22
C ₅ H ₁₁ thiobarbituric acid	-23.6	-22.3	21
hexobarbital	-23.5	-19.7	21
m-chlorobenzoyl acetic acid	-22	-25	22
C ₅ H ₁₁ barbituric acid	-21.0	-12.3	21
C ₄ H ₉ thiobarbituric acid	-20.4	-13.2	21
pentobarbital	-20.3	-10.2	21
cyclobarbital	-20.2	-15.9	21
4-hydroxybenzoic acid	-20.0	-21.1	4
4-aminobenzoic acid	-19.9	-10.1	4
m-ethylphenyl acetate	-19	-13	23

Table 2.2 cont'd.

<u>Substrate</u>	<u>ΔH° (kJmol⁻¹)</u>	<u>ΔS° (JK⁻¹mol⁻¹)</u>	<u>Ref.</u>
C ₃ H ₇ thiobarbituric acid	-16.4	-7.4	21
C ₄ H ₉ barbituric acid	-15.8	-3.2	21
C ₂ H ₅ thiobarbituric acid	-15.5	-0.92	21
p-nitrophenolate	-14.2	5.06	17
CH ₃ barbituric acid	-11.6	4.5	21
phenol	-11	29	11
3,4,5 trimethylphenyl acetate	-10	8	23
m-chlorophenyl acetate	-4	33	23

Bibliography

1. Broser, W. and W. Lautsch, *Z.Naturforsch.*, 8b, 711 (1953).
2. Cramer, F., W. Saenger and H. -Ch. Spatz, *J.Am.Chem.Soc.*, 89, 14 (1967).
3. Nakajima, A., *Spectrochimica Acta*, 39A, 913 (1983).
4. Kajtar, M., Cs. Horvath-Toro, E. Kuthi and J. Szejtli, *Acta Chimica Acad.Sci.Hung.*, 110, 327 (1982).
5. Demarco, P.V. and A.L. Thakkar, *Chem.Comm.*, 1970, 2.
6. MacNicol, D.D., *Tetrahedron Lett.*, 1975, 3325.
7. Connors, K.A. and J.M. Lipari, *J.Pharm.Sci.*, 65, 379 (1976).
8. Schlenk, H. and D.M. Sand, *J.Am.Chem.Soc.*, 83, 2312 (1961).
9. French, D., M.L. Levine, J.H. Pazur and E. Norberg, *J.Am.Chem.Soc.*, 71, 353 (1949).
10. Gelb, R.I., L.M. Schwartz, R.F. Johnson and D.A. Laufer, *J.Am.Chem.Soc.*, 101, 1869 (1979).
11. Lewis, E.A. and L.D. Hansen, *J.Chem.Soc.*, 2, 2081 (1973).
12. Gelb, R.I., L.M. Schwartz, B. Cardelino, H.S. Fuhrmann, R.F. Johnson and D.A. Laufer, *J.Am.Chem.Soc.*, 103, 1750 (1981).
13. Gelb, R.I., L.M. Schwartz and D.A. Laufer, *Bioorg.Chem.*, 9, 450 (1980).
14. Komiyama, M. and M.L. Bender, *J.Am.Chem.Soc.*, 100, 2259 (1978).
15. Gelb, R.I., L.M. Schwartz, B. Cardelino and D.A. Laufer, *Anal.Biochem.*, 103, 362 (1980).
16. Harata, K., *Bull.Chem.Soc.Jpn.*, 51, 2737 (1978).
17. Takeo, K. and T. Kuge, *Die Stdrke*, 24, 331 (1972).
18. Gelb, R.I., L.M. Schwartz, M. Radeos and D.A. Laufer, *J.Phys.Chem.*, 87, 3349 (1983).

19. Gelb, R.I., L.M. Schwartz, M. Radeos, R.B. Edmonds and D.A. Laufer, *J. Am. Chem. Soc.*, 104, 6283 (1982).
20. van Hoodonk, C. and J.C.A.E. Breebaart-Hansen, *Rec. Trav. Chim. Pay-Bas.*, 90, 680 (1971).
21. Otagiri, M., T. Miyaji, K. Uekama and K. Ikeda, *Chem. Pharm. Bull.*, 24, 1146 (1976).
22. Straub, T.S. and M.L. Bender, *J. Am. Chem. Soc.*, 94, 8881 (1972).
23. van Etten, R.L., J.F. Sebastian, G.A. Clowes and M.L. Bender, *J. Am. Chem. Soc.*, 89, 3242 (1967).
24. Lumry, R. and S. Rajender, *Biopolymers*, 9, 1125 (1970).
25. Saenger, W., Proc. 1st Int. Symp. on Cyclodextrins, Budapest, 1981, 141.
26. Mochida, K., A. Kagita, Y. Matsui and Y. Date, *Bull. Chem. Soc. Jpn.*, 46, 3703 (1973).
27. Lach, J.L. and T.-F. Chin, *J. Pharm. Sci.*, 53, 69 (1964).
28. Siegel, B. and R. Breslow, *J. Am. Chem. Soc.*, 97, 6869 (1975).
29. van Hoodonk, C. and J.C.A.E. Breebaart-Hansen, *Rec. Trav. Chim. Pay-Bas.*, 91, 958 (1972).
30. Kauzmann, W., *Adv. Protein Chem.*, 14, 1 (1959).
31. Griffiths, D.W. and M.L. Bender, *Adv. Cat.*, 23, 209 (1973).
32. Saenger, W., M. Noltemeyer, P.C. Manor, B. Hingerty and B. Klar, *Bioorg. Chem.*, 5, 187 (1976).
33. Manor, P.C. and W. Saenger, *J. Am. Chem. Soc.*, 96, 3630 (1974).
34. Lindner, K. and W. Saenger, *Angew. Chem. Int. Ed. Engl.*, 17, 694 (1978).

35. MacLennan, J.M. and J.J. Stezowski, *Biochem. Biophys. Res. Commun.*, *92*, 933 (1980).
36. Bergeron, R.J., M.A. Channing, G.J. Gibeily and D.M. Pillor, *J. Am. Chem. Soc.*, *99*, 5146 (1977).
37. Broser, W., *Z. Naturforsch.*, *8b*, 722 (1953).

CHAPTER III

CHAPTER III: EXPERIMENTAL TECHNIQUES

3.1 Temperature-Jump Relaxation Spectrophotometry

Chemical relaxation methods involve the rapid perturbation of the equilibrium of a reaction mixture, followed by observation of the mixture as it adjusts or "relaxes" to a new equilibrium position. In the case of the temperature-jump technique the perturbation is achieved by a rapid rise in temperature, which is usually brought about by the discharging of a high-voltage capacitor through the reaction mixture. The time which the system takes to reach its new equilibrium position is dependent on the rates of the chemical reactions involved. It will be shown that the concentration dependence of the "relaxation time"* can yield a great deal of kinetic information, and may ultimately aid in the assignment of a particular mechanism to the reaction under study.

The temperature-jump technique was first proposed in 1954 by Manfred Eigen,¹ who suggested conductimetric detection for following the relaxation process. In the first operational instrument, however, optical detection was used.² Since then the temperature-jump method has rapidly increased in popularity, and is now perhaps the most widely used of the relaxation methods. The basis of the temperature-jump method is the temperature dependence of the equilibrium constant, i.e.

$$\left(\frac{\partial \ln K}{\partial T} \right)_P = \frac{\Delta H^\circ}{RT^2} \quad (3.1)$$

* The time characterising the approach to the new equilibrium position.

Thus, a reaction mechanism, in which any one of the steps has a finite standard enthalpy change, will exhibit a change in the concentrations of the reactants on perturbation of the temperature. The fact that this requirement is met by most chemical equilibria explains the wide application of the temperature-jump method in the study of the kinetics of fast reactions.

3.1.1 Principles of Chemical Relaxation

Consider the single step equilibrium,



with the forward and backward rate constants k_1 and k_{-1} respectively.

The general rate equation is then given by

$$-\frac{dC_A}{dt} = -\frac{dC_B}{dt} = \frac{dC_C}{dt} = k_1 C_A C_B - k_{-1} C_C \quad (3.3)$$

If the system, initially at equilibrium, is perturbed by a sudden change in an external parameter (e.g. temperature, pressure, pH, electric field intensity, etc.), the system will adjust to the new external conditions and approach a new equilibrium position. The concentrations of the species immediately after the perturbation can then be expressed as

$$C_A = \bar{C}_A^f + \Delta C_A \quad (3.4a)$$

$$C_B = \bar{C}_B^f + \Delta C_B \quad (3.4b)$$

$$C_C = \bar{C}_C^f + \Delta C_C \quad (3.4c),$$

where \bar{C}^f corresponds to the concentration of a species once the new equilibrium position has been reached, and ΔC is the deviation

of the actual concentration from the new equilibrium value.

Applying the principle of mass conservation it can be shown that

$$\Delta C_A + \Delta C_C = 0 \quad (3.5a)$$

$$\Delta C_B + \Delta C_C = 0 \quad (3.5b)$$

Combining these two expressions yields,

$$\Delta C_A = \Delta C_B = -\Delta C_C \quad (3.6)$$

Thus, the rate equation can be written as,*

$$-\frac{d(\bar{C}_A + \Delta C_A)}{dt} = k_1(\bar{C}_A + \Delta C_A)(\bar{C}_B + \Delta C_A) - k_{-1}(\bar{C}_C - \Delta C_A) \quad (3.7)$$

Since, by definition, $-\frac{d\bar{C}_A}{dt} = 0$, this expression simplifies to

$$-\frac{d\Delta C_A}{dt} = [k_1(\bar{C}_A + \bar{C}_B) + k_{-1}] \Delta C_A + k_1(\Delta C_A)^2 \quad (3.8)$$

If only small perturbations are considered, i.e. $\Delta C_A \ll \bar{C}_A$, then this equation further simplifies to

$$\frac{d\Delta C_A}{dt} = -[k_1(\bar{C}_A + \bar{C}_B) + k_{-1}] \Delta C_A \quad (3.9)$$

The reciprocal of the proportionality factor, $[k_1(\bar{C}_A + \bar{C}_B) + k_{-1}]$, has the dimensions of time, and is thus defined as the "relaxation time", τ . Equation (3.9) can then be written as

$$\frac{d\Delta C_A}{dt} = -\left(\frac{1}{\tau}\right)\Delta C_A \quad (3.10)$$

or more generally,

* Henceforward all rate constants and equilibrium concentrations refer to the new equilibrium conditions.

$$\frac{d\Delta C_i}{dt} = -\left(\frac{1}{\tau}\right)\Delta C_i \quad (3.11)$$

The physical significance of the relaxation time can easily be determined by integration of equation (3.11), i.e.

$$\int_{\Delta C^\circ}^{\Delta C} \frac{d\Delta C_i}{\Delta C_i} = -\left(\frac{1}{\tau}\right) \int_0^t dt \quad (3.12)$$

which leads to

$$\ln \left(\frac{\Delta C_i}{\Delta C_i^\circ} \right) = -t/\tau \quad (3.13)$$

or

$$\Delta C_i = \Delta C_i^\circ \exp \left(-t/\tau \right) \quad (3.14)$$

where ΔC_i° is the difference between the initial and final equilibrium concentrations. Substituting $t = \tau$ into equation (3.14) leads to

$$\Delta C_i = \Delta C_i^\circ / e$$

Thus, it can be seen that the relaxation time corresponds to the time taken for the initial deviation from the final equilibrium concentration to decrease by a factor of e .

Once the expression relating the relaxation time to the rate constants and the equilibrium concentrations of the species involved has been derived for a particular mechanism, the basic experimental approach is to determine $1/\tau$ over a range of concentrations. The agreement between the experimental dependence of $1/\tau$ on concentration and that predicted using a proposed mechanism can then be used as a criterion for accepting or discarding the mechanism. If it is accepted, estimates of the

rate constants can then be determined from the same data. For example, consider again the scheme (3.2). It has been shown that for this mechanism the reciprocal of the relaxation time is given by the expression,

$$\frac{1}{\tau} = k_1(\bar{C}_A + \bar{C}_B) + k_{-1} \quad (3.15)$$

Thus, if a system is to be consistent with this mechanism, then a plot of $1/\tau$ versus $(\bar{C}_A + \bar{C}_B)$ must be a straight line. Estimates of the forward and backward rate constants can, in principle, be obtained from the slope and intercept of the plot respectively.

Reactions which involve more than one step usually cannot be characterised by a single relaxation time. For a mechanism involving a number of coupled reaction steps the number of relaxation times is equal to the number of independent concentration variables. Because the individual equilibria are coupled, the relaxation times are generally a function of all the equilibrium concentrations of the species present and the associated rate constants, and cannot be attributed to any single step of the mechanism. Thus, for a mechanism involving n independent concentration variables, the rate of decay of the deviation of the concentration of a component from its final equilibrium value is given by the general equation,

$$\frac{d\Delta C_i}{dt} = - \sum_{i=1}^n \left(\frac{1}{\tau_i} \right) \Delta C_i \quad (3.16)$$

Alternatively the rate equation can be expressed as follows,

3.1.2 The Temperature-Jump Method

The temperature-jump method involves the perturbation of the equilibrium of a solution by means of a sudden temperature rise. This can be brought about by discharging a high-voltage capacitor to ground through a sample cell containing the reaction mixture. The energy previously stored in the capacitor is then dissipated in the solution, causing an increase in temperature of a few degrees. At the same time as the discharge, a recording device is triggered for the observation of the relaxation effect.

In order to determine the relaxation times for a reaction, the time taken for the temperature rise must be much shorter than the relaxation time to be measured. This is achieved by using solutions of sufficiently low resistance such that the passage of the charge through the solution is much more rapid than the chemical relaxation to be observed. The extent of the temperature rise as well as the time taken for the rise are determined by the characteristics of the circuit and the applied voltage.^{2,9,10} Assuming negligible circuit inductance, the current delivered during the discharge of the capacitor is given by

$$i = \left(\frac{U_0}{R} \right) e^{-t/RC} \quad (3.20)$$

where U_0 = voltage to which the capacitor is charged (volts)

R = total resistance of the circuit (ohms)

t = time after the discharge (seconds)

C = capacitance of the condenser (farads).

The rate of dissipation of the energy stored in the capacitor is

$$\frac{dE}{dt} = i^2 R \quad (3.21)$$

If it is assumed that all the energy is transferred to the solution, then the rate of change of temperature is given by

$$\frac{dT}{dt} = \frac{i^2 R}{C_p \rho V} \quad (3.22)$$

where C_p = heat capacity of the solution ($\text{JK}^{-1}\text{g}^{-1}$)

ρ = density of the solution (gcm^{-3})

V = volume occupied by the solution (cm^3)

Substituting for i from equation (3.20) and integration from $t = 0$ to $t = t$ gives,

$$\Delta T(t) = \frac{CU_o^2}{2C_p \rho V} (1 - e^{-2t/RC}) \quad (3.23)$$

Thus, as with chemical relaxation, the heating of the solution proceeds exponentially with a characteristic time constant, τ_o , termed the "heating time". The total temperature rise can be found by substituting $t = \infty$ into equation (3.23), which gives

$$\Delta T_\infty = \frac{CU_o^2}{2C_p \rho V} \quad (3.24)$$

Now if we define τ_o in an analogous fashion to the chemical relaxation case, such that at τ_o , $(\Delta T_\infty - \Delta T_{\tau_o}) = \frac{1}{e} \Delta T_\infty$, it is found by setting $t = \tau_o$ in equation (3.23) that

$$\tau_o = \frac{1}{2} RC \quad (3.25)$$

Strictly R represents the total resistance of the circuit. However, in practice, it is found that by far the greatest contribution comes from the resistance of the sample cell. Thus, all the other contributing resistances may be neglected without appreciable error.

A schematic diagram of the temperature-jump apparatus, which has been developed in this laboratory, is shown in Figure 3.1. A Brandenburg E.H.T. generator is used to charge a 0.2 microfarad capacitor to a voltage of 20 kilovolts, using a 25 megohm charging resistor incorporated in series with the capacitor. Both the capacitor and the charging resistor are shielded from the remaining circuitry by means of aluminium and iron boxes to reduce electrical and magnetic disturbances. The discharge of the stored energy of the capacitor is brought about by manually closing a spark gap, causing a surge of current across the stainless steel electrodes of the sample cell (see Fig. 3.2), and an increase in temperature of the solution.

The course of the relaxation is followed spectrophotometrically. The light from a high intensity tungsten lamp passes through a Bausch and Lomb grating monochromator, set to a wavelength corresponding to a principal absorption band of one of the reaction components. The light beam then traverses the sample cell and the resulting light intensity is detected using a photomultiplier/emitter-follower circuit. The photomultiplier consists of six dynodes, and is powered by a Nuclear Enterprises Ltd. E.H.T. supply.

Two methods have been used for the recording of the photomultiplier voltages. The simpler method utilises a Tektronix storage oscilloscope, which is triggered by the discharge of the capacitor via an unshielded wire antenna inside the capacitor discharge box, connected to the external trigger of the oscilloscope. The data are then displayed as a trace on the oscilloscope's screen.

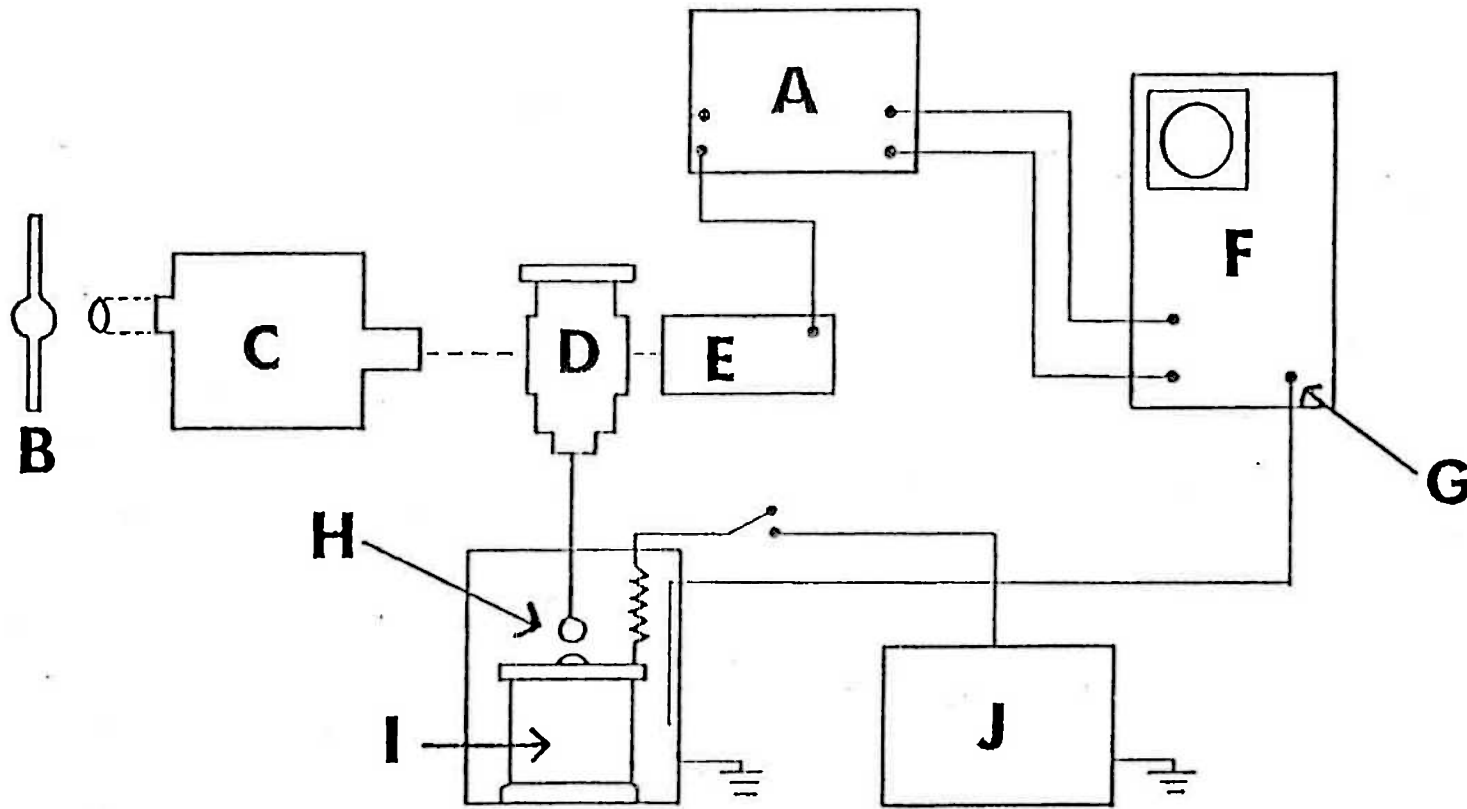
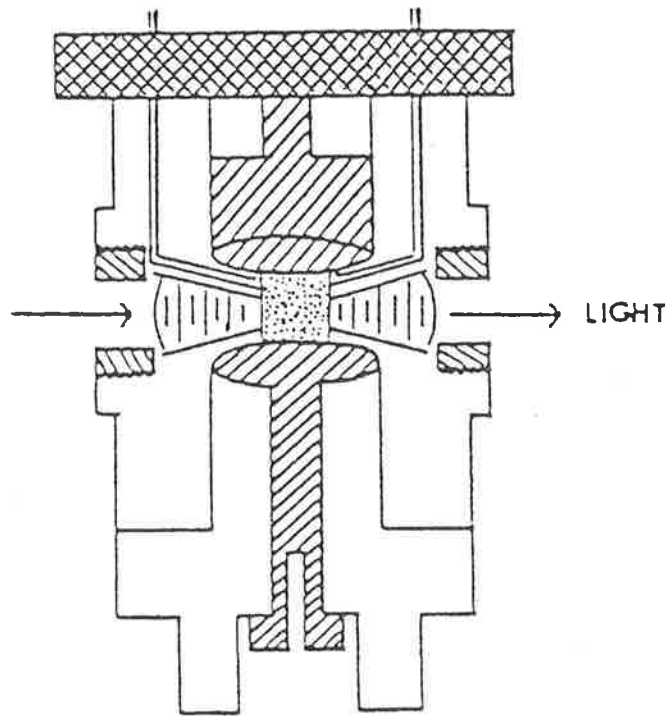


Fig. 3.1: Schematic diagram of the temperature-jump apparatus¹¹

- | | |
|----------------------|--------------------------|
| A = emitter-follower | F = storage oscilloscope |
| B = lamp | G = external trigger |
| C = monochromator | H = moveable spark gap |
| D = cell assembly | I = capacitor |
| E = photomultiplier | J = power supply |









Perspex			Quartz
Steel			Teflon
Brass			Solution

Fig. 3.2: Schematic diagram of the temperature-jump cell¹¹

A more sophisticated method of data acquisition, utilising a transient recorder, and its advantages over the simpler method will be discussed in a subsequent section.

3.1.3 Experimental Procedure

The sample solution is passed through a millipore filter to remove any foreign matter, and then degassed several times using the "freeze pump thaw" method. The purpose of degassing is to minimise bubble formation within the sample cell, which could cause distortions of the light beam and irregular oscilloscope traces. The temperature-jump cell is then filled with the sample solution through one of the capillary inlets. During filling the cell is tilted, so that any bubbles are forced out through the opposite inlet.

Once filled, the cell is placed in a thermostatted brass cell jacket, situated in the light path. After waiting fifteen minutes for thermal equilibrium to be reached, the intensity of the light incident on the solution is maximised by rotating the cell in the jacket until the photomultiplier voltage, read off a digital voltmeter, is at its maximum value. By a suitable choice of the photomultiplier load resistor and cathode voltage, a two volt signal is obtained. This is then backed-off to zero by using a potentiometer, thus allowing amplification of the voltage change caused by the perturbation of the reaction mixture.

Once the capacitor has been charged, it is discharged through the reaction mixture, the data recording system is triggered by the current flow, and a voltage trace is displayed on the oscilloscope. A time interval of at least 250 seconds is

left between the recording of successive traces to allow for the complete recharging of the capacitor and for the solution to return to the thermostat temperature. Depending on the method of data acquisition being used, the traces obtained are either photographed using an oscilloscope camera, or transferred in digital form onto cassette tape.

3.1.4 Data Acquisition and Analysis

a) Storage Oscilloscope Method

The simplest method of recording the data is to use a storage oscilloscope, which is triggered by the capacitor discharge, as described earlier. A permanent record of the resultant trace is then obtained by photographing the trace with an oscilloscope camera loaded with polaroid film. The photograph is then mounted on a digital measuring device with a sliding vernier scale, which gives a digital readout of the distance that the vernier moves. For the calculation of the relaxation time, τ , a time infinity base-line is drawn on the trace, and the difference in voltage between the trace and the infinity line at various times is measured. The voltage difference is proportional to the change in light intensity, and for small perturbations this, in turn, is proportional to the change in absorbance. Thus, equation (3.13), for a single exponential relaxation, can be rewritten as

$$\ln \frac{\Delta V}{\Delta V_0} = -t/\tau \quad (3.26)$$

which can also be expressed as

$$\ln \Delta V = \ln \Delta V_0 - t/\tau \quad (3.27)$$

Therefore, a plot of $\ln \Delta V$ versus time should give a straight line with a slope equal to $-1/\tau$. In practice, however, the true value of $1/\tau$ is obtained by dividing the slope by the factor -1.136, which takes into account the photographic reduction of the oscilloscope scale. Errors in the $1/\tau$ values can be estimated from the standard deviation of a number of repetitive measurements on the same solution.

b) Computer Averaged Transients (CAT) Scanning Method

A more sophisticated method of data acquisition and analysis has recently been developed in this laboratory.¹² Rather than using a storage oscilloscope for the recording of the data, this method utilises a Data Lab DL905 or DL910 transient recorder, which collects the photomultiplier voltages for each transient as 1,024 8-bit data points or as 4,096 8-bit data points respectively. The transient recorder is externally triggered in an identical fashion to the storage oscilloscope. An oscilloscope is connected to the recorder to enable the display of each digitally stored transient. Acceptable traces can be transferred from the memory of the transient recorder, and stored on cassette tape via an Intel SDK-8085 microprocessor and CDB-150 cassette interface system.

Once a series of temperature-jump experiments has been completed, the data, stored on cassette tape, can be transferred to a Computer Products LSI-11 minicomputer. This transfer process is also mediated by the microprocessor and cassette interface system mentioned above. Repetitive transients for each solution are then averaged using software developed for the minicomputer, thus increasing the signal-to-noise ratio. The pretrigger facility of

the transient recorder enables the synchronisation of successive transients recorded on the same time scale. Further programs enable the determination of the reciprocal relaxation time for the averaged scan using a non-linear least squares fitting procedure. Greater detail concerning this method of data acquisition may be found in reference 12.

This method has a number of advantages over the storage oscilloscope method, e.g. increased speed of data analysis, a permanent computer record of the data, and greatly improved signal-to-noise ratio. This last point is particularly important, since it allows the determination of relaxation times for processes with small amplitudes, and makes detection of double exponential relaxations much easier.

3.1.5 Calibration of the Temperature Rise

The rate constants determined by the temperature-jump method refer to the temperature after the jump, not the temperature at which the solution is initially thermostatted. Thus, it is necessary to know the temperature rise expected for each capacitor voltage setting. This can be calculated theoretically using equation (3.24); however, the assumption made here is that all the energy stored in the capacitor is dissipated in the reaction mixture. Since this assumption may not necessarily be valid, the temperature rise must be determined experimentally.

The method generally used for the calibration is to use a buffer-indicator system, in which the pH of the buffer shows a marked temperature dependence. The changing temperature of the

solution can then be followed by the change in photomultiplier voltage as the indicator changes colour with pH. If the photomultiplier voltage is equated to the light intensity, then the change in absorbance is given by the expression,

$$\Delta A = \log \frac{V_f}{V_o} \quad (3.28)$$

where V_f = photomultiplier voltage at the final temperature

V_o = photomultiplier voltage at the initial temperature.

Now if V_f is replaced by $(V_o + \Delta V)$, this expression can be written as

$$\Delta A = \log \left(1 + \frac{\Delta V}{V_o} \right) \quad (3.29)$$

The experimental procedure is to charge the capacitor to a range of voltages, and then to discharge it through the buffer-indicator solution. The change in photomultiplier voltage can be determined from the vertical amplitude of the oscilloscope traces obtained, and the corresponding absorbance change calculated using equation (3.29). If the absorbance of the solution is determined spectrophotometrically at a range of temperatures, the resulting plot of absorbance versus temperature enables the absorbance change for each capacitor voltage to be related to a temperature rise.

The buffer-indicator system used for the calibration was a tris-phenol red solution at pH 7.4. All measurements were made at 555 nm. The plot of absorbance versus temperature was obtained using a Zeiss DMR-10 spectrophotometer with a thermostatted cell

holder. The temperature was constantly monitored by using a previously calibrated type F53 thermistor situated in the sample cell, and connected to a digital multimeter. The final calibration curve obtained is shown in Figure 3.3.

The usual capacitor voltage employed is 20 kilovolts, i.e. $U_0^2 = 400 \text{ kV}^2$. Thus, from the graph it can be seen that the corresponding temperature rise is $8.9 (\pm 0.1)^\circ\text{C}$. The temperature rise expected theoretically can be calculated using the equation

$$\Delta T_\infty = \frac{CU_0^2}{2C_p \rho V}$$

where $C = 0.2 \times 10^{-6}$ farads

$U_0 = 2.0 \times 10^4$ volts

$C_p = 4.18 \text{ JK}^{-1}\text{g}^{-1}$

$\rho = 1.01 \text{ g cm}^{-3}$

$V = 1.0 \text{ cm}^3$

Using these values gives a theoretical temperature rise of 9.5°C .

Therefore, 94% of the energy stored in the capacitor is dissipated in the reaction solution.

3.2 UV/Visible Absorption Spectroscopy

3.2.1 Apparatus

The majority of absorption measurements were made on a Zeiss DMR-10 double beam recording spectrophotometer equipped with a thermostatted ($\pm 0.1^\circ\text{C}$) cell block. A few measurements were also made on a Zeiss PMQ II single beam spectrophotometer. The DMR-10 has been automated¹³ using an Intel SDK-8080 microprocessor, which receives data from the DMR-10 via the instrument's digital readout

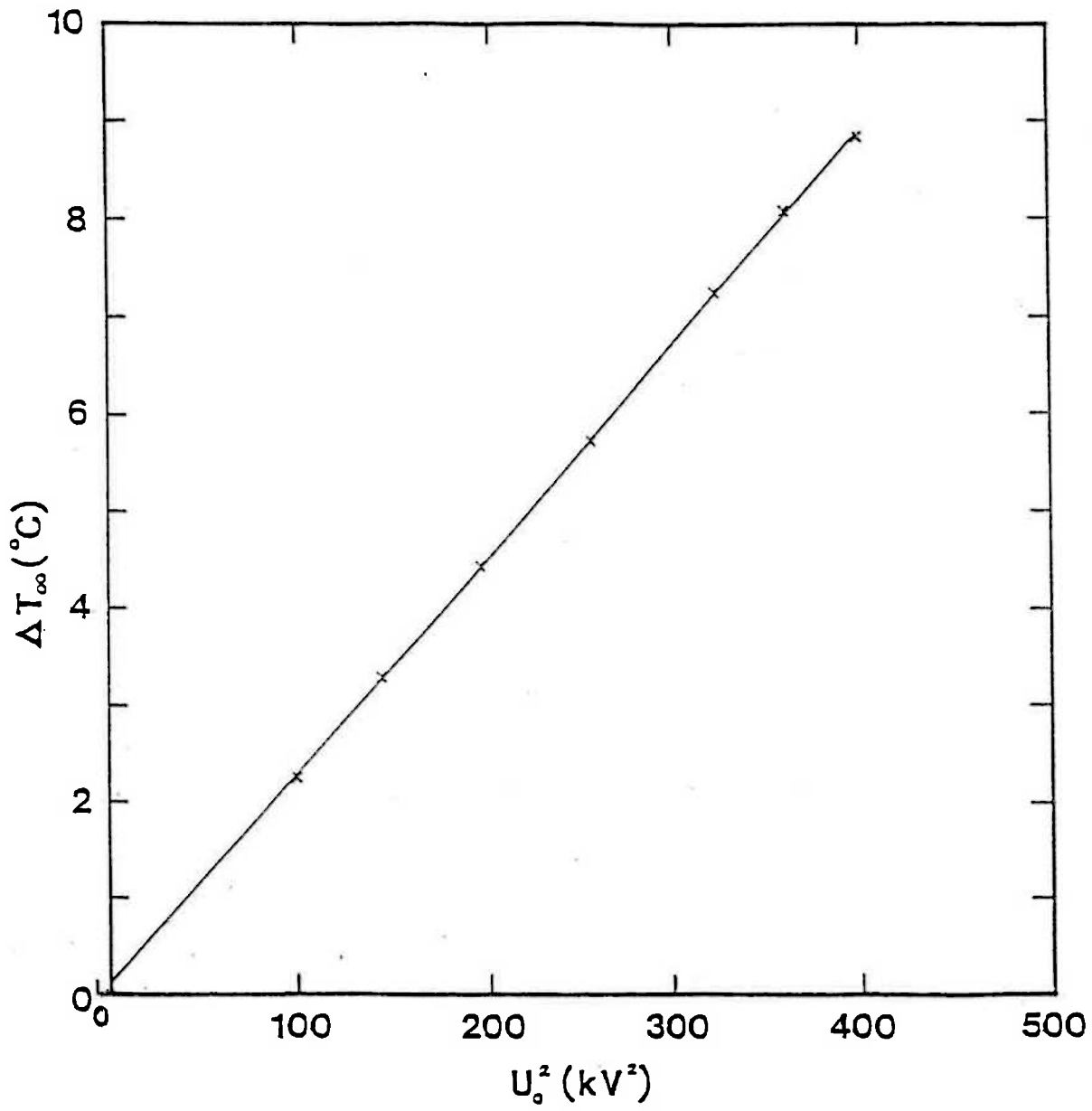


Fig. 3.3: Calibration curve for the temperature-jump apparatus

accessory. User communication is achieved through several switches and indicator lights on the front panel of the microprocessor, and via an ASR-33 Teletype equipped with a paper tape punch. During the recording of a spectrum the data are stored in the memory of the microprocessor. When all the information has been collected for a particular solution, the data are punched onto paper tape in ASCII format. At the end of the day's work the data are transferred from paper tape to a CDC Cyber 173 computer for analysis. A conversion program enables the data to be rewritten in alphanumeric format.

Quartz spectrophotometer cells of a variety of pathlengths were used. The temperature was maintained at a constant value with the aid of a MGW Lauda Thermo-boy temperature controller, which circulated water through the cell block. The solution temperature was monitored, as in the case of the temperature-jump calibration, by the use of a thermistor in the reference cell.

3.2.2 Experimental Procedure

A number of precautions were taken to obtain the maximum accuracy in the measurements. So that any cell mismatching could be allowed for, a baseline was recorded with solvent in both sample and reference cells prior to each set of measurements. The cells were then left in position throughout the measurements, and solutions were removed by suction. The sample cell was rinsed thoroughly with each solution to be studied prior to the recording of its spectrum.

Each spectrum was recorded in duplicate with wavelength increments of 2 nm between the pre-set wavelength limits.

An integration time of 1.6 seconds was allowed at each wavelength. Once the data had been transferred to the Cyber 173 computer, the program DMR01 allowed repetitive scans to be averaged, the baseline spectrum to be subtracted, and corrections due to solution thermal expansion to be made. A further program, ZETAPLT, enabled the corrected spectra to be plotted on a Zeta 1453 plotter.

3.3 Circular Dichroism

The circular dichroism measurements were made on a Jasco J-40CS recording spectropolarimeter, to which was added an Intel SDK-8085 microprocessor.¹⁴ The microprocessor can be used to control the operations of the spectropolarimeter, i.e. the wavelength step size, the wavelength range to be scanned, and the integration time at each wavelength. At the end of a scan the data collected can be printed out on a Teletype as voltages, which on multiplication by a conversion factor are re-expressed as ellipticities. It was found, however, that during the time taken for a scan the baseline of the instrument drifted. Thus, in order to eliminate the effect of this drift, measurements were made for the solution and baseline alternately at each wavelength, and the wavelength was changed manually. An integration time of 48 seconds and a time constant of 0.25 seconds were used for all the measurements. Each sensitivity setting of the spectropolarimeter was calibrated by using a standard solution of D-10-camphorsulphonic acid, which is known to have a molar ellipticity of $7,260 \text{ deg cm}^2 \text{ decimol}^{-1}$ at 290 nm.^{15,16}

The molar ellipticities, $[\theta]$, of all dye solutions were calculated using equation (3.30).

$$[\theta] = \frac{100 \cdot \psi}{l \cdot c} \quad (3.30)$$

where ψ = ellipticity (deg)

l = cell pathlength (cm)

c = dye concentration (mol dm^{-3})

The units of $[\theta]$ resulting from this equation are $\text{deg cm}^2 \text{decimol}^{-1}$. The molar circular dichroism, $\Delta\epsilon$, is simply related to the molar ellipticity by the following expression.

$$\Delta\epsilon = \frac{[\theta]}{3,300} \quad (3.31)$$

where $\Delta\epsilon$ is expressed in units of $\text{dm}^3 \text{mol}^{-1} \text{cm}^{-1}$. Since molar ellipticity appears to be more commonly used than molar circular dichroism in literature concerning the cyclodextrins, all of the circular dichroism results presented have been expressed in units of molar ellipticity.

3.4 Linear Dichroism

3.4.1 Preparation of Films

Poly (vinyl alcohol) films were cast from a 5% w/v solution of PVA (J.T. Baker Chemical Co.) in an ethanol water mixture (1:5 v/v). When dry, the films were cut into strips of dimensions 3 x 2.5 cm. The dye, whose dichroic spectrum was to be measured, was then introduced into the film by soaking it in an aqueous solution of the dye for approximately 3 hours. After leaving the

film overnight on a glass plate, the film was slowly stretched in a mechanical stretching device¹⁷ until a stretch ratio* greater than 4 was obtained. The film was then mounted in a brass cell for measurement.

3.4.2 Measurement of Spectra

Dichroic spectra were determined by the use of a Zeiss PMQ II single beam spectrophotometer with a wide window photomultiplier detector, which effectively eliminates light intensity losses due to the scattering of the films.^{17,18} A Glan-Taylor calcite polariser was mounted in the light path in such a way as to allow it to be rotated through 90°, thus enabling the plane of polarisation of the light to be changed while maintaining the same portion of the film in the light path. Absorbances were measured with light polarised parallel and perpendicular to the direction of stretch over the required wavelength range. The absorbances were then corrected by subtracting the absorbance due to the PVA, determined by the use of a film prepared under the same conditions as those described above, but without the introduction of dye. The dichroic ratio, R, can be calculated using the expression,

$$R = \frac{A_{//}}{A_{\perp}} \quad (3.32)$$

where $A_{//}$ and A_{\perp} are the absorbances with light polarised parallel and perpendicular to the direction of stretch respectively.

* Two marks were made on the film with ink before stretching. The stretch ratio is defined as the ratio of the distances between these marks after and before stretching.

Assuming that the dye molecules orientate themselves along the direction of stretch, the linear dichroism method enables the direction of polarisation of the dye's electronic absorption bands to be estimated. It is also a useful method for the detection of severely overlapping bands.

3.5 Fluorescence Spectroscopy

The fluorescence spectra* were recorded using a Perkin-Elmer 3000 fluorescence spectrometer with a thermostatted cell holder. A Philips PM 8100 chart recorder was used to plot the spectra. All measurements were made in a 1.0 cm pathlength quartz fluorescence cell at 25°C.

* Strictly the spectra should be referred to as luminescence spectra, since the exact origin of the emission is uncertain.

Bibliography

1. Eigen, M., *Disc. Faraday Soc.*, 17, 194 (1954).
2. Czerlinski, G. and M. Eigen, *Z. Elektrochem.*, 63, 652 (1959).
3. Bernasconi, C.J., "Relaxation Kinetics", Academic Press Inc., New York, 1976.
4. Schelly, Z.A. and E.M. Eyring, *J. Chem. Ed.*, 48, A639 (1971).
5. Eigen, M. and L. DeMayer, in "Techniques of Chemistry" (G.G. Hammes, ed.), Vol. VI, part II, chapter III, Wiley (Interscience), New York, 1973.
6. Amdur, I. and G.G. Hammes, "Chemical Kinetics", McGraw-Hill Inc., New York, 1966.
7. Gutfreund, H., "Enzymes: Physical Principles", Wiley (Interscience), Bristol, 1975.
8. Eigen, M. and L. DeMaeyer, in "Technique of Organic Chemistry" (S.L. Friess, E.S. Lewis and A. Weissberger, eds.), Vol. VIII, part II, chapter XVIII, Wiley (Interscience), New York, 1963.
9. Blagrove, R.J., Ph.D. Thesis, University of Adelaide (1968).
10. Hammes, G.G., in "Techniques of Chemistry" (G.G. Hammes, ed.), Vol. VI, part II, chapter IV, Wiley (Interscience), New York, 1973.
11. Collins, P.R., Ph.D. Thesis, University of Adelaide (1979).
12. Schiller, R.L., Honours Report, University of Adelaide (1981).
13. Boehm, G., Ph.D. Thesis, University of Adelaide (1981).
14. Fornasiero, D., Ph.D. Thesis, University of Adelaide (1981).
15. Connell, K.E., Honours Report, University of Adelaide (1984).
16. Cassim, J.Y. and J.T. Yang, *Biochemistry*, 8, 1947 (1969).
17. Kelly, G.R., Ph.D. Thesis, University of Adelaide (1974).
18. Bott, C.C. and T. Kurucsev, *J. Chem. Soc., Faraday Trans II*, 71, 749 (1975).

CHAPTER IV

CHAPTER IV: THE INTERACTION OF METHYL ORANGE
WITH THE CYCLODEXTRINS

4.1 Introduction

Although the interaction between methyl orange (MO) and the cyclodextrins (CD) was first studied as far back as 1953,¹ and has been investigated by various workers²⁻¹⁸ since then, a number of questions remain unanswered, particularly regarding the mechanism of complex formation. Before describing the experiments which have been performed, however, some of the contributions made by previous workers should be discussed.

Broser, Lautsch and co-workers¹⁻⁴ studied the interaction of both the acidic and basic forms of methyl orange with α - and β -CD spectrophotometrically. The spectral changes observed with increasing CD concentration were interpreted as being due to the formation of 1:1 inclusion complexes. In acidic solution a particularly large spectral change was observed, which was found to be due to a shift of the tautomeric equilibrium between the red "azonium" form and the colourless "ammonium" form of the methyl orange zwitterion. The dissociation and prototypic equilibria of methyl orange and its CD inclusion complexes are shown in Fig. 4.1. Broser and Lautsch also found that there is a decrease in the pKa of methyl orange by approximately one pH unit on inclusion by CD. This change, they showed, is a consequence of the greater stability of the inclusion complex of the basic form of the guest molecule compared to that of the acidic form.

About ten years later Cramer et al.⁶ found that methyl orange and α -CD can form complexes with higher stoichiometric ratios in

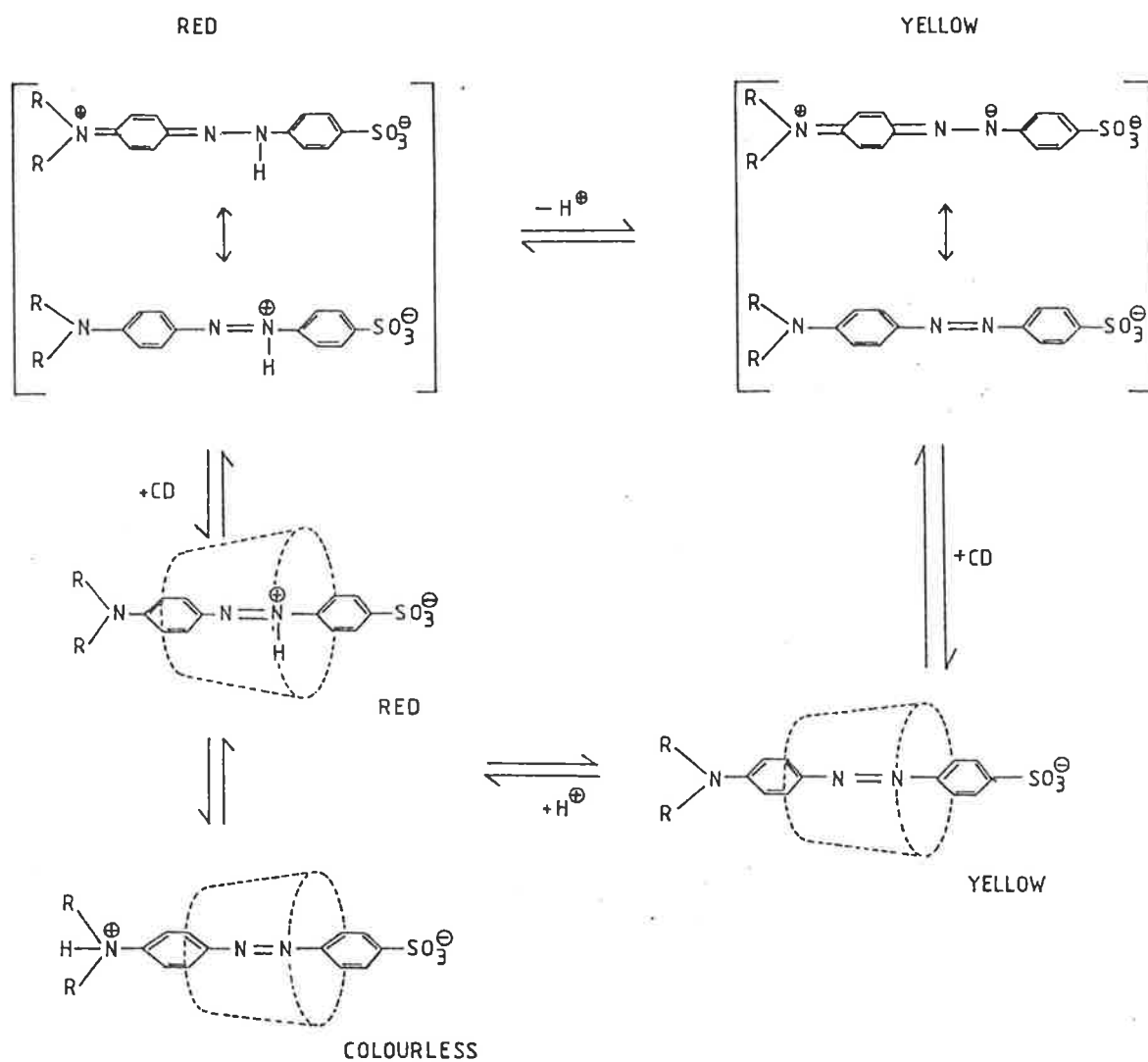


Fig. 4.1: Dissociation and prototropic equilibria of methyl orange and its cyclodextrin (α - or β -) inclusion complexes.¹⁹

addition to a 1:1 complex. This is indicated by the appearance of two non-related isosbestic points in the spectrum of methyl orange with varying α -CD concentrations (pH9, 13°C). Thus, at concentrations of CD between 0 and $5 \times 10^{-3} \text{ mol dm}^{-3}$ an isosbestic point was observed at 443 nm. On raising the CD concentration, a second isosbestic point appeared at 455 nm. Cramer's group then ceased their work on methyl orange to concentrate on dyes with which only a 1:1 complex is possible.

The structure of the α -CD-methyl orange complex in the solid state was determined by Harata¹¹ using the X-ray method. It was found that α -CD forms a 2:1 complex with methyl orange. The α -CD molecules form a channel structure, built up by the stacking of the CD rings. The methyl orange anions occur within the CD channel with a statistical disorder of four different arrangements.

The complexation of methyl orange by γ -CD has so far been the subject of only one communication. Hirai et al.¹⁶ studied the interaction of methyl orange and γ -CD spectrophotometrically, and concluded that the larger cavity of γ -CD was capable of including two molecules of the dye. Thus, it appears that methyl orange can combine with the cyclodextrins in a range of different stoichiometric ratios depending on the relative sizes of the dye and the cyclodextrin cavity.

Apparent association constants (i.e. obtained by assuming 1:1 complex formation only) for α - and β -CD with methyl orange have been collected from the literature and are listed in Table 4.1. A comparison of the values for α - and β -CD shows that the complexes of methyl orange with α -CD are significantly more stable than those

K_{app} ($\text{dm}^3 \text{ mol}^{-1}$)				
	α -CD	Ref.	β -CD	Ref.
MO (basic)	8.93×10^3	1	2.82×10^3	13
	4.5×10^3	7	3.8×10^3	16
	1.13×10^4	14	3.98×10^3	1
	6.2×10^3	17	2.63×10^3	14
	7.84×10^3	18	2.97×10^3	18
MO (acidic)	8.93×10^2	2	3.98×10^2	2
	7.7×10^2	4	2.82×10^2	13
	7.7×10^2	8	3.70×10^2	14
	8.00×10^2	14		
	1.03×10^3	19		
	4.7×10^2	17		

Table 4.1: Apparent association constants for the inclusion of methyl orange by cyclodextrin.

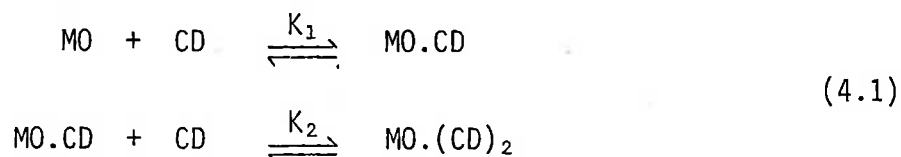
with β -CD. This is probably due to the smaller cavity of α -CD, which would result in a tighter fit between the dye and the cyclodextrin.

Numerous examples have been reported in the literature of complex formation between the cyclodextrins and substituted benzenes, as well as more complicated aromatic species.¹⁹ Thus, the dumb-bell-shaped methyl orange structure suggests that in this case both the dimethylaniline end and the benzenesulphonate end of the molecule might be capable of inclusion. Model building, using Corey-Pauling-Koltun (CPK) space-filling molecular models, also shows the possibility of inclusion from both ends, since both ends appear to fit the cavity of a given cyclodextrin equally well.

As mentioned above, it has been found that a complex of methyl orange and α -CD with a host-guest ratio of 2:1 can be isolated in the solid state.¹¹ The structure of this complex, however, is unlikely to be the same as that formed in solution. Lammers et al.²⁰ have pointed out that, in the case of crystallised cyclodextrin inclusion complexes, the guest molecule could be included either in intermolecular cavities, formed by the crystal lattice, or in the cavities of the cyclodextrins themselves. In the case of inclusion complexes in solution, however, the guest molecule can only be included in the cyclodextrin cavity, since the whole complex is surrounded by solvating water molecules.

Although the structure of the complex may be different in solution and the solid state, it appears, from the results, described above, of Cramer et al.,⁶ that a 2:1 complex can form in solution. The appearance of two unrelated isosbestic points in

the visible absorption spectrum seems to imply the existence of two consecutive cyclodextrin binding equilibria. Thus, for α -CD at least, the following scheme can be proposed.



It is possible that the complex MO.CD may not have a single unique structure, but rather two possible structures may exist, in which either the dimethylaniline or the benzenesulphonate end of the dye is included. This is still consistent with the observation of an isosbestic point at low cyclodextrin concentrations, since the two 1:1 complexes would both be in equilibrium with free dye and cyclodextrin, and hence the ratio of their concentrations would have a constant value, regardless of the concentration of cyclodextrin (see Appendix C). The second step in the above scheme would then involved the inclusion of whichever end of the dye was not included in the first step. It is most likely, however, because of the different shapes and physico-chemical properties of the dimethylamino and sulphonate groups, that one end of the methyl orange anion is included by the cyclodextrins preferentially. This has, in fact, been found experimentally by Susuki and Sasaki,¹⁵ who examined the complexes of methyl orange with α - and β -CD using nuclear magnetic resonance (NMR). Based on chemical shift data, they interpreted their results as indicating that methyl orange is included predominantly from the dimethylamino group end.

In order to investigate this phenomenon further, the means which has been adopted is to exclude the possibility of inclusion

from one end and subsequently to compare the degree of complexation to that found originally. One method of doing this is to use a methyl orange derivative with a bulky group at one end, so that only the other end could possibly fit within the cyclodextrin cavity. This method will be discussed further in the following chapter. In addition, it is also possible to modify slightly the cyclodextrin structure, which is likely to change the preferences of the cyclodextrin for each end of the methyl orange. The ionisable secondary hydroxyl groups of the cyclodextrins provide a possible means of doing this.

It has been found using ^{13}C -NMR that the C-2 and C-3 resonances of α - and β -CD are particularly sensitive to changes in the pH,²¹ thus suggesting that acid dissociation involves both the OH-2 and OH-3 groups around the secondary hydroxyl rim of the cyclodextrins. The pK_a of these groups has been determined by Gelb and co-workers²² by titration with sodium hydroxide to be 12.3 for α -CD at 25°C. For β - and γ -CD the corresponding values, which have been similarly determined, are 12.2²² and 12.1²³ respectively. Thus, if the pH of an aqueous cyclodextrin solution is increased to a value exceeding the pK_a , the cyclodextrin will gain a negative charge, which will be delocalised around the wide rim of the cavity. It is anticipated, then, that the negative charge on the cyclodextrin would greatly hinder the approach of the negatively charged benzenesulphonate end of methyl orange to the cyclodextrin cavity, whereas the effect on the approach of the uncharged dimethylaniline end would be much less. The basic experimental method, therefore, has been to investigate the interaction of methyl orange with the cyclodextrins

above and below the pK_a of the secondary hydroxyl groups, i.e. in 1 mol dm^{-3} sodium hydroxide solution (pH 13.4^{*}) and in 0.1 mol dm^{-3} di-sodium hydrogenphosphate buffer at pH 9.0.

As shown in the introduction to the thesis, the ability of the cavities of β - and γ -CD to include two aromatic moieties is well established. It is likely, then, that the scheme (4.1), proposed earlier for the complexation of methyl orange with α -CD, may not be sufficient to explain all the phenomena observed in the study of the dye's interaction with β - and γ -CD. In these cases the possibility of the inclusion of two methyl orange molecules simultaneously within the cyclodextrin cavity must also be considered.

* The pH measurements were made using a Radiometer PHM64 research pH meter, which had been standardised with the standard pH buffers: $0.010 \text{ mol dm}^{-3}$ Borax (pH 9.2) and $0.050 \text{ mol dm}^{-3}$ potassium hydrogen phthalate (pH 4.0). No allowance has been made for alkaline error. Nevertheless, it is expected that the pH of the 1 mol dm^{-3} sodium hydroxide solution would be well in excess of the pK_a of the secondary hydroxyl groups of the cyclodextrins.

4.2 Properties of the Methyl Orange Anion

The pK_a of methyl orange has been determined as 3.4.² All of the results presented, except where explicitly stated otherwise, have been derived from measurements made at pH values well in excess of the pK_a . Thus, contributions from the acidic form of the dye have generally been neglected, and the results refer to the basic form alone.

Methyl orange is known to aggregate in aqueous solution, as evidenced by deviations from Beer's law. At dye concentrations up to $1 \times 10^{-3} \text{ mol dm}^{-3}$, however, the deviations are quite small.²⁴ Thus, since all of the experiments described have been performed at dye concentrations of the order of $3 \times 10^{-5} \text{ mol dm}^{-3}$, any complications due to dye aggregation have been considered as negligible.

Temperature-jump studies of methyl orange were carried out at 465 and 430 nm (pH 9.0, 25°C). At 465 nm, a relaxation occurring within the heating time of the apparatus (10 μ seconds), and characterised by a decrease in absorbance was observed. No relaxation was observed at 430 nm. Under the same experimental conditions the equilibrium spectrum exhibited an analogous variation with temperature, the change at 465 nm being significantly greater than that expected due to solution expansion. An isosbestic point was observed in the region of 430 nm, which explains why no relaxation was observable at this wavelength. The small amplitude of the absorbance change observed, and the rapidity of the relaxation suggest that the effect may be due to slight changes in the solvation of the methyl orange anion, or to a small conformational change. Since no accurate measurements of

the relaxation time were possible, however, this process was not investigated further.

In order to explain the effects of the cyclodextrins on the absorption and circular dichroic spectra of methyl orange, it has been found that a knowledge of the origin of the electronic transitions occurring in the visible region is desirable. For compounds of the azobenzene series, both $\pi \rightarrow \pi^*$ and $n \rightarrow \pi^*$ transitions have been reported.²⁵⁻²⁸ As can be seen from the energy level diagram (Fig. 4.2), there are, in principle, one $\pi \rightarrow \pi^*$ transition and two $n \rightarrow \pi^*$ transitions associated with the azo group. For planar trans-azo compounds with C_{2h} symmetry, however, only the $\pi \rightarrow \pi^*$ (${}^1B_u \leftarrow {}^1A_g$) and $n_a \rightarrow \pi^*$ (${}^1A_u \leftarrow {}^1A_g$) transitions are allowed. The $n_s \rightarrow \pi^*$ (${}^1B_g \leftarrow {}^1A_g$) transition is forbidden due to symmetry selection rules.^{25,26} By reference to the character table for the C_{2h} point group it can be seen that the expected transition moment directions for the $\pi \rightarrow \pi^*$ and $n_a \rightarrow \pi^*$ transitions are parallel to and perpendicular to the molecular plane respectively.

In the case of azobenzene only the frequency of the $n_a \rightarrow \pi^*$ transition lies in the visible region, and thus it is this transition which is responsible for the colour. The $\pi \rightarrow \pi^*$ transition occurs at a much higher frequency, resulting in absorption in the ultraviolet region.²⁷ In the case of azobenzene derivatives, such as methyl orange, which have an auxochrome in the *para* position, the $\pi \rightarrow \pi^*$ band is red shifted, so that it overlaps with the $n_a \rightarrow \pi^*$ band,^{27,28} thus greatly increasing the visible absorption, and enabling their use as dyestuffs.

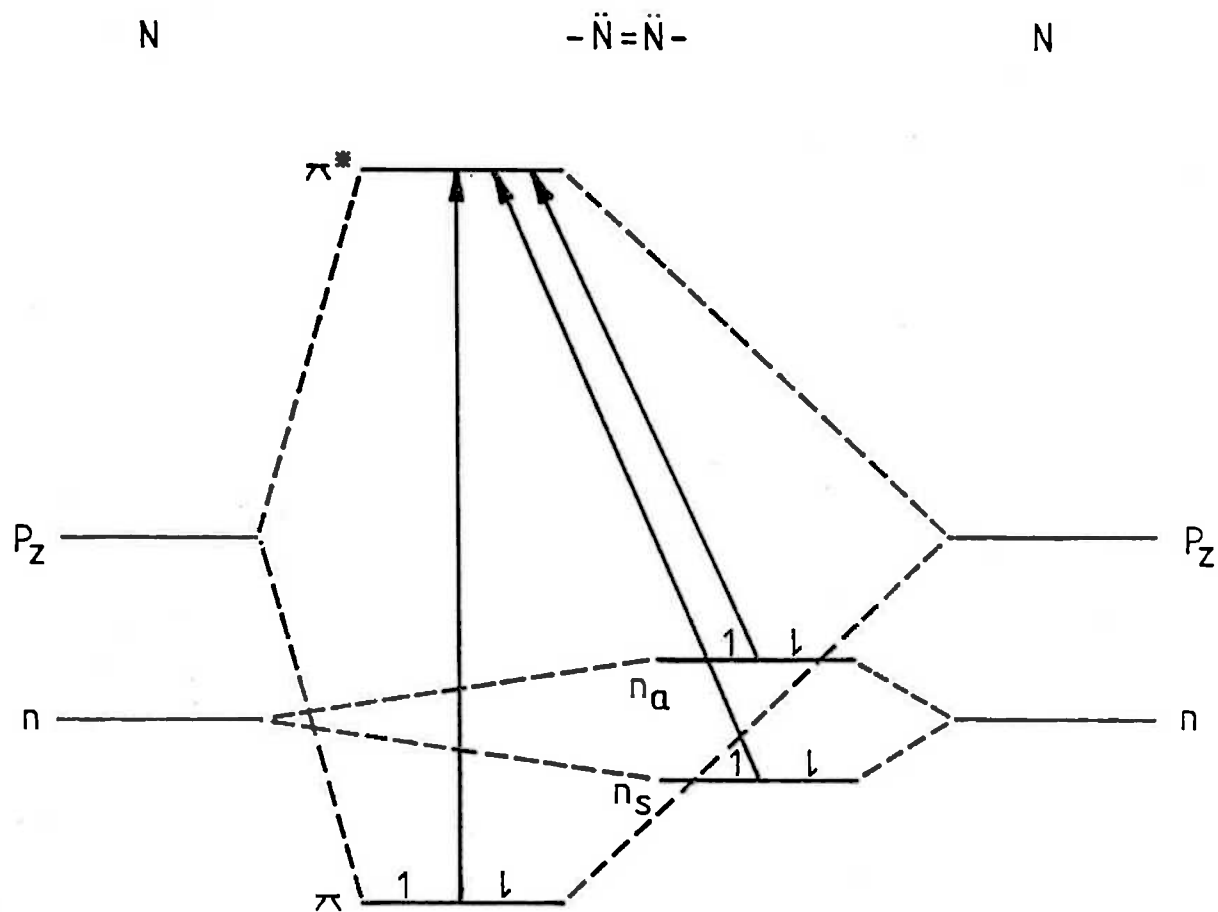


Fig. 4.2: Energy-level diagram for the azo group.²⁹

Note: For clarity the n and π energy levels have been offset.

A number of workers have found that p-substituted dimethylamino, amino and hydroxy azobenzene derivatives exhibit an additional long-wavelength absorption band, which is not apparent in the absorption spectra of other derivatives of azobenzene.^{30,31} In the case of methyl orange the presence of two high-intensity overlapping absorption bands has been confirmed by the following experimental observations.

- 1) An increase in temperature of an aqueous solution of methyl orange causes an increase in absorbance in the range 350-430 nm and a decrease in absorbance in the range 430-550 nm. If the experimental absorption band was due to a single band, increasing the temperature would merely increase the bandwidth and decrease the amplitude.
- 2) In aqueous solution the absorption curve of methyl orange is very broad, and is skewed towards low wavelengths. On transfer to ethanol the curve becomes skewed towards high wavelengths (see Fig. 4.3).

The origin of these transitions was investigated further by measuring the linear dichroism of methyl orange in stretched films (see Fig. 4.4). Assuming that the dye molecules orientate with the long molecular axis parallel to the direction of stretch, the large value of the dichroic ratio (R) indicates that the transition moment of the dominant transition is polarised approximately along the line interconnecting the two phenyl groups, which is consistent with the results of Popov and Smirnov.³² The relatively constant value of R across the absorption curve indicates that any contributions from transitions of different

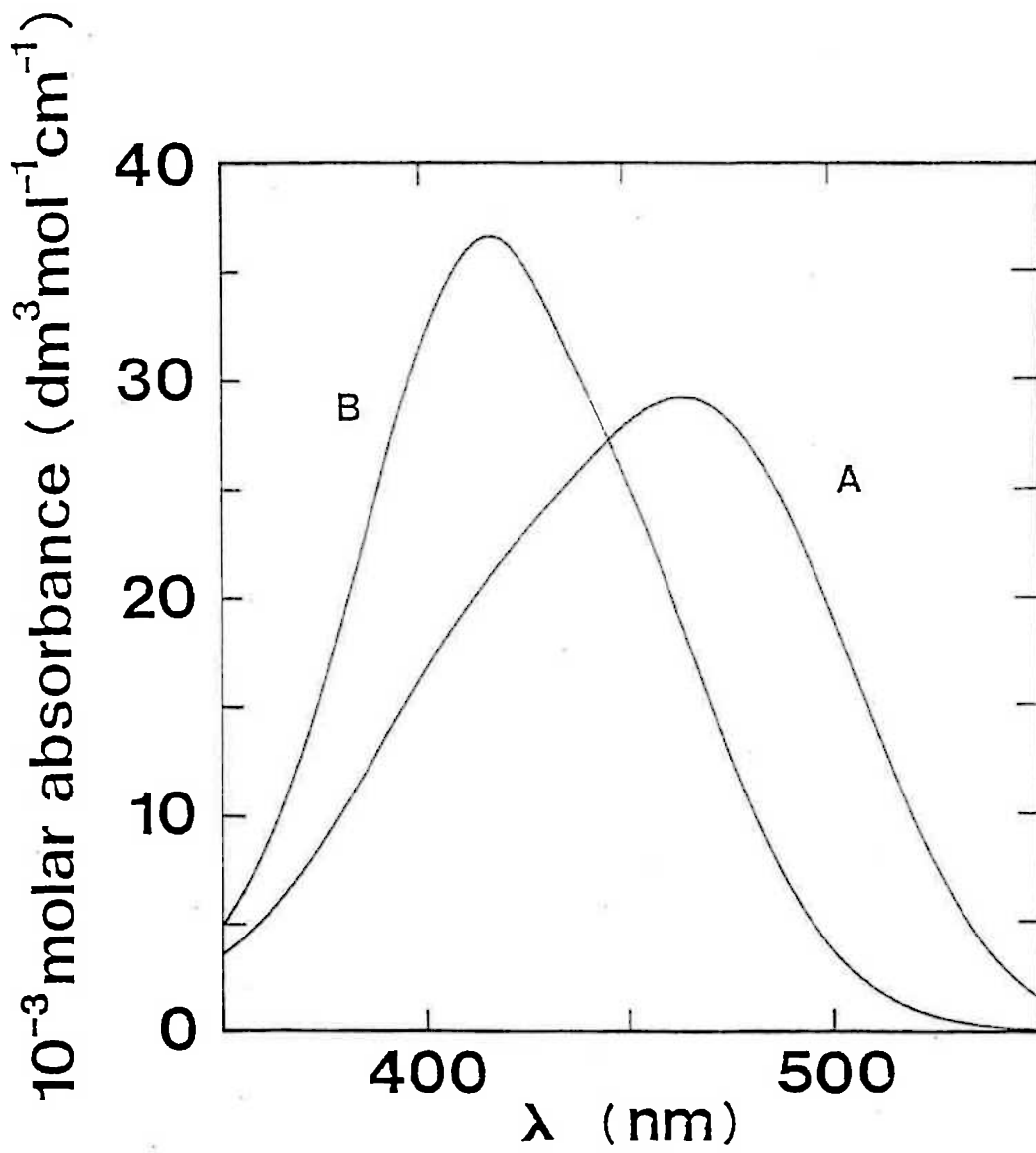


Fig. 4.3: Visible absorption spectrum of methyl orange ($4 \times 10^{-5} \text{ mol dm}^{-3}$) in aqueous solution (A) and in ethanol (B).

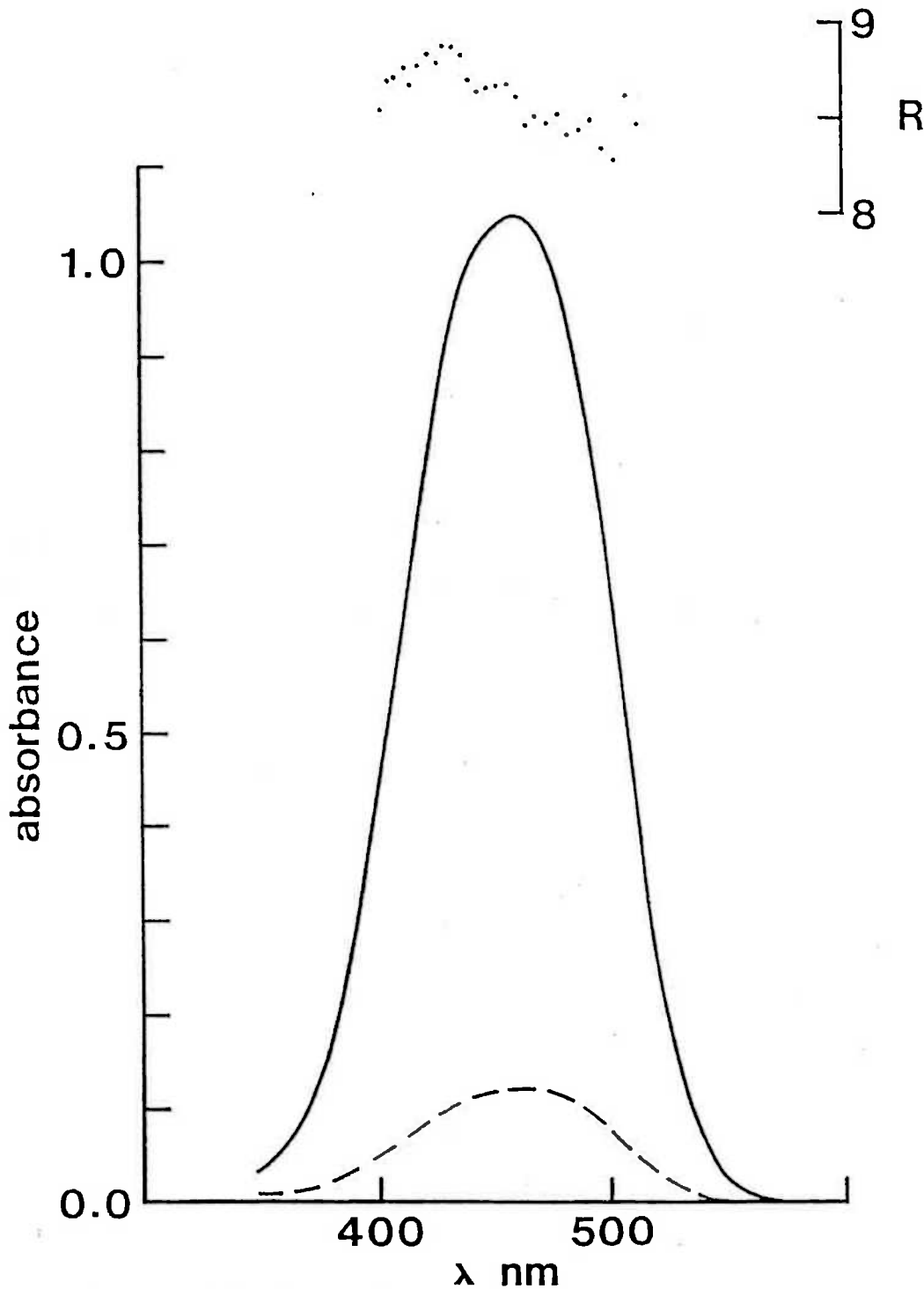


Fig. 4.4: Linear dichroic spectrum of methyl orange in stretched poly (vinyl alcohol) film (left hand ordinate). Solid curve = light polarised parallel to stretch Dashed curve = light polarised perpendicular to stretch Absorbance units are arbitrary. The ratio of the parallel and perpendicular absorbances, R , are shown as individual points and refer to the right hand ordinate.

polarisation are minimal.* Thus, it would appear that the two high-intensity overlapping absorption bands are both due to transitions polarised along the long axis of the molecule. As stated above, the expected transition moment direction for the $n_a \rightarrow \pi^*$ transition is perpendicular to the plane of the molecule. Hence, the constancy of R implies that this transition must have quite a small intensity, which is consistent with intensities quoted for this transition in similar compounds.^{27,28} It would seem most likely, then, that the two overlapping bands are due to $\pi \rightarrow \pi^*$ transitions. Molecular-orbital calculations on the π -system, however, have shown that only a single high-intensity transition, polarised approximately along the line connecting the phenyl moieties, occurs in the visible region.³³

According to Brode,³⁰ the presence of two overlapping bands suggests the presence of two distinct methyl orange species in solution. Brode noted that all the azobenzene derivatives which exhibit these two bands have a substituent in the *para* position capable of donating an electron-pair to the π -system. Using resonance theory, he then showed that a consequence of such a substituent would be an enhancement of the basicity of the nitrogen atom of the azo group which is furthest from the substituted benzene

* The slight drop in R on the long wavelength side of the absorption peak perhaps indicates a small contribution from a transition polarised more along the short axis of the molecule.

ring (see Fig. 4.5). To explain the overlapping bands, Brode suggested the formation of a hydrated species, in which water hydrogen bonds to one of the azo nitrogens. The hydrogen bonding interaction would presumably result in a further withdrawal of electrons from the *para* substituent, causing a distortion of the π -electron cloud relative to the non-hydrogen-bonded species, and a wavelength shift of the absorption maximum. Although the magnitude of the wavelength shift (approximately 60 nm) is unusually large for a solvent effect on a $\pi \rightarrow \pi^*$ transition, Brode's hypothesis is the only one proposed to this stage which adequately explains the absorption spectra of this group of dyes.

Reeves and co-workers³¹ have successfully applied Brode's hypothesis to explain the effect on the absorption spectrum of the binding of methyl orange to bovine serum albumin, human serum albumin and surfactant micelles. Considering first the effects of temperature and solvent changes on the spectrum of methyl orange alone, they attributed the high and low wavelength bands to the hydrogen-bonded and non-hydrogen-bonded species respectively. They then interpreted the spectral changes observed on binding of methyl orange to various hydrophobic sites as being the result of a diminution in hydrogen bonding with the aqueous solvent. As will be shown later, some of the effects of cyclodextrin on the visible absorption and circular dichroic spectra of methyl orange can also be easily explained by a decrease in dye-solvent hydrogen bonding.

Before proceeding to discuss the interaction of methyl orange with the cyclodextrins, the possibility must be considered that the

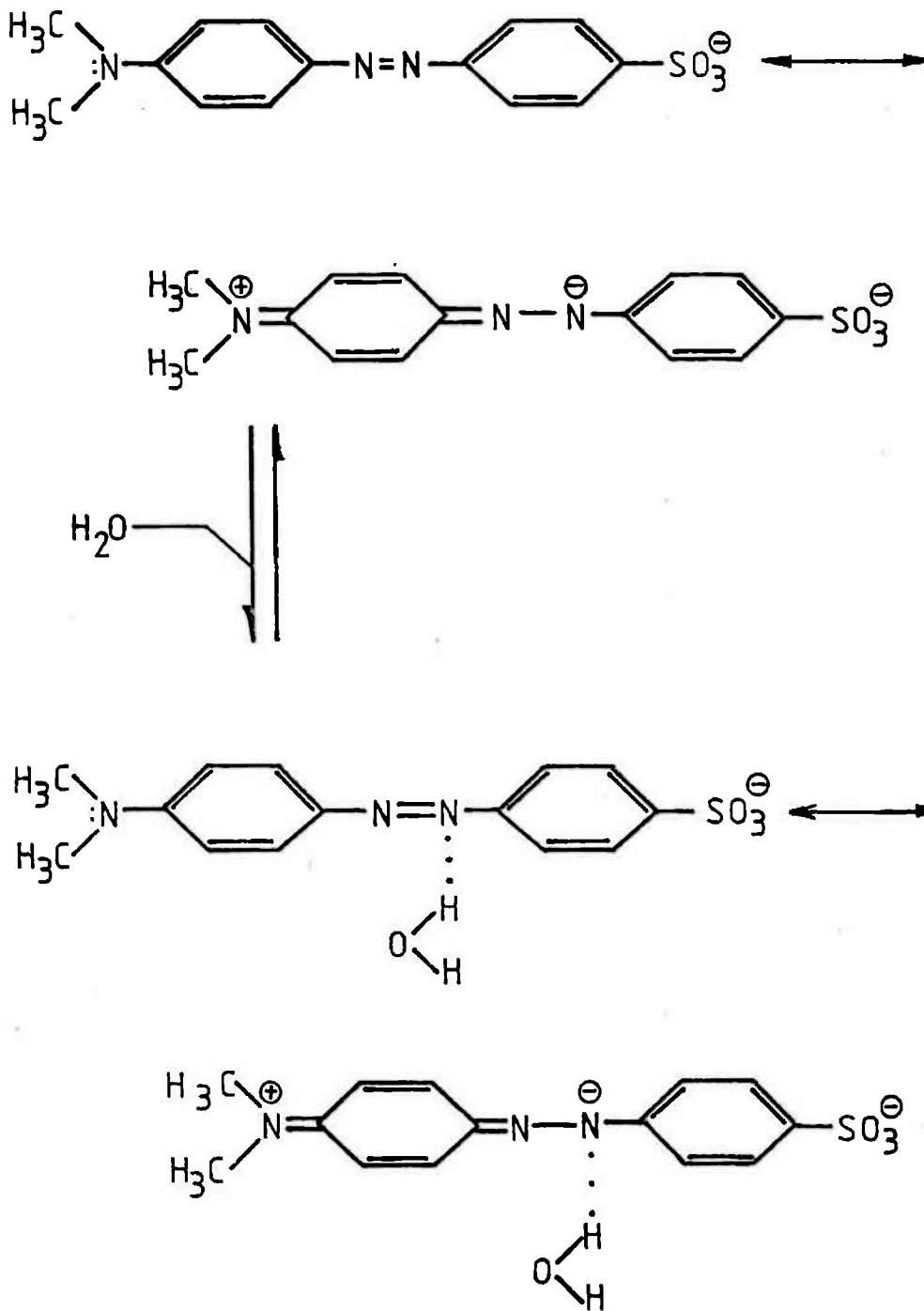


Fig. 4.5: Hydrogen bonding interaction of water with the azo nitrogens of methyl orange.

presence of cyclodextrin might cause a change in solvent structure. In this case the methyl orange spectrum might be altered even without any interaction between methyl orange and cyclodextrin occurring. In order to investigate this possibility, the spectrum of methyl orange was recorded in water, and in a 0.2 mol dm^{-3} aqueous solution of glucose (see Fig. 4.6), which would presumably cause a similar change in solvent structure to the cyclodextrins, but without the possibility of inclusion. It can be seen that only a very small increase in molar absorptivity is observed at this high glucose concentration. Thus, the relatively large spectral changes generally observed on the addition of cyclodextrin can be confidently attributed to a direct interaction between the methyl orange and cyclodextrin molecules.

4.3 The Interaction of Methyl Orange with α -Cyclodextrin

4.3.1 Results at pH 9.0

a) Temperature-Jump

At α -CD concentrations $\geq 1 \times 10^{-3} \text{ mol dm}^{-3}$, a fast relaxation was observed at 465 nm, characterised by a decrease in absorbance. The amplitude of the relaxation increased with increasing cyclodextrin concentration, thus indicating the participation of cyclodextrin in the reaction. The relaxation time (τ) appeared to decrease with increasing cyclodextrin concentration, however τ was too close to the heating time of the apparatus to allow an accurate determination of rate constants.

The variation of the equilibrium spectrum with temperature was found to be consistent with that observed in the temperature-jump

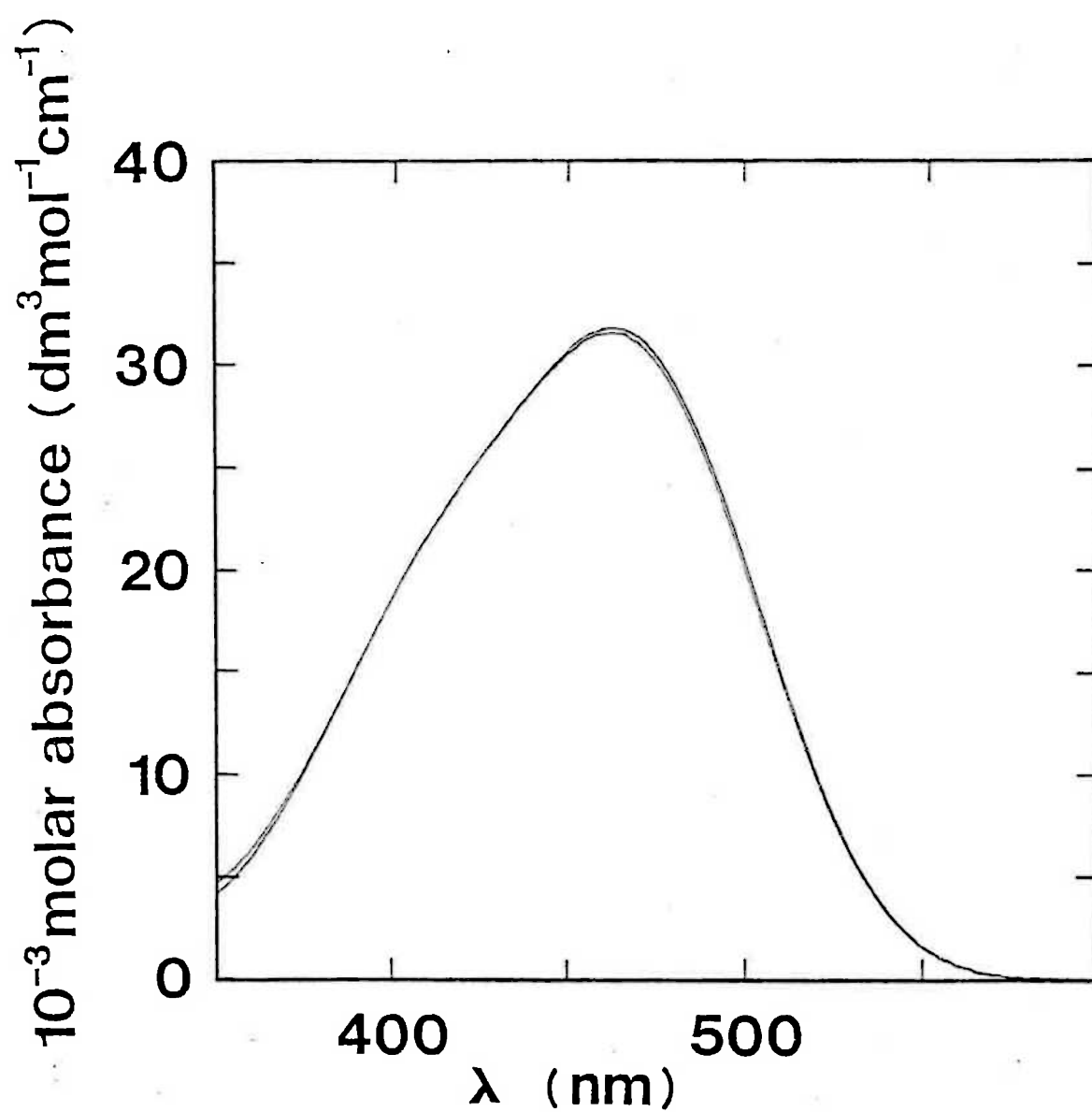


Fig. 4.6: Visible absorption spectrum of methyl orange ($4 \times 10^{-5} \text{ mol dm}^{-3}$) in water (lower curve) and in a 0.2 mol dm^{-3} aqueous solution of glucose (upper curve).

experiment. At α -CD concentrations $< 1 \times 10^{-3} \text{ mol dm}^{-3}$, the change in absorbance with a ten degree increase in temperature is no greater than that observed for methyl orange alone. At α -CD concentrations $\geq 1 \times 10^{-3} \text{ mol dm}^{-3}$, the decrease in absorbance at 465 nm due to the temperature rise increases with increasing α -CD concentration.

The fact that the relaxation is only observed at high cyclodextrin concentrations, in comparison with the methyl orange concentration, suggests that it may be due to the equilibrium between the 1:1 and 2:1 complexes.

b) Absorption Spectra

The effect of inclusion within α -CD on the absorption spectrum of methyl orange has previously been published by Cramer et al.⁶. A blue shift of the λ_{max} is observed, thus indicating a change in the environment of the methyl orange anion towards a more ethanol-like or less water-like environment (cf. Fig. 4.3). The appearance of two non-related isosbestic points, and their significance has been discussed earlier. A number of workers^{1,7,14,17,18} have determined apparent association constants for the interaction, assuming 1:1 complex formation, and these are listed in Table 4.1. There appears to be quite a deal of variation between the values quoted. Considering each determination to be equally valid, however, the average value of the apparent association constant is $7.8 (\pm 2.6) \times 10^3 \text{ dm}^3 \text{ mol}^{-1}$.

c) Induced Circular Dichroism

The induced circular dichroic spectrum of methyl orange in a thirty-fold excess of α -CD is shown in Fig. 4.7. Since it can

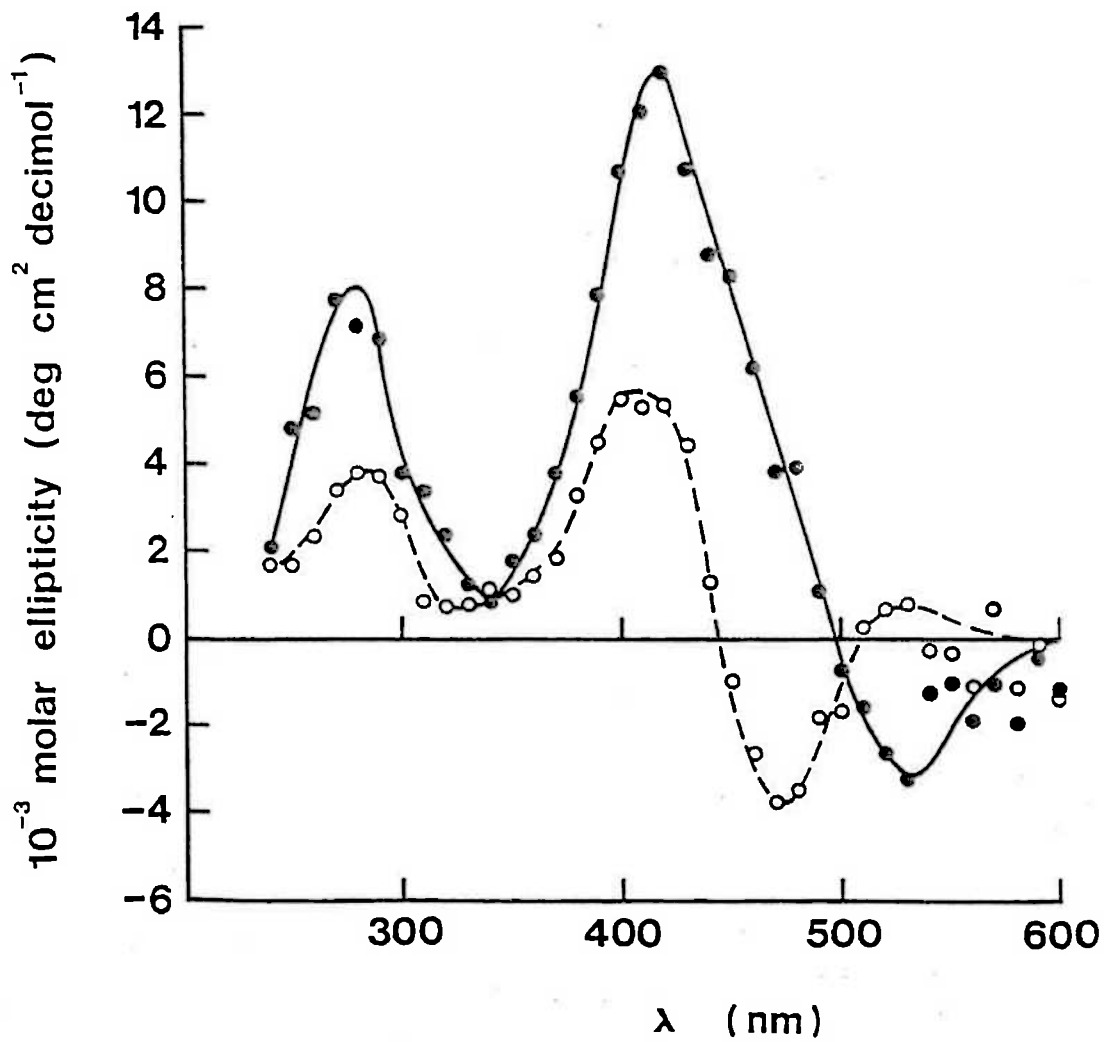


Fig. 4.7: Induced circular dichroic spectrum of methyl orange (4×10^{-5} mol dm⁻³) in the presence of α -CD (1×10^{-3} mol dm⁻³) at pH 9.0 (solid curve) and pH 13.4 (dashed curve).

be shown from CPK model building that only axial inclusion* of methyl orange within the α -CD cavity is possible, the large positive circular dichroic signal at approximately 415 nm must be due to a transition polarised predominantly along the long axis of the methyl orange molecule (see Appendix D). Conversely, the small negative circular dichroic signal at approximately 530 nm must be due to a transition polarised predominantly along the short axis of the molecule.

If the explanation of the absorption spectrum of methyl orange, which was proposed by Brode³⁰ (see Sec. 4.2), is applied, then the peak at 415 nm is most likely due to a $\pi \rightarrow \pi^*$ transition of a non-hydrogen-bonded methyl orange species. If an inclusion complex of a hydrogen-bonded methyl orange species was formed, a positive circular dichroic signal at higher wavelengths would be expected. Thus, the appearance of the circular dichroic spectrum would seem to suggest that water is excluded from the cyclodextrin cavity on complex formation.

The small negative circular dichroic signal at approximately 530 nm is probably due to the low-intensity $n_a \rightarrow \pi^*$ transition, which according to symmetry considerations is polarised perpendicular to the long axis of the molecule.

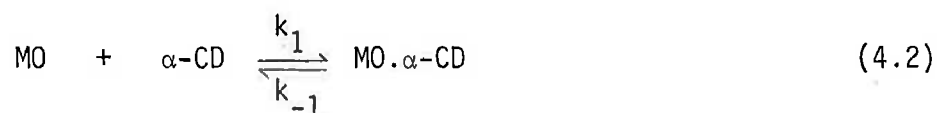
* The term axial inclusion implies that the long molecular axis of the guest is approximately parallel to the principal symmetry axis of the cyclodextrin.

4.3.2 Results at pH 13.4

a) Temperature-Jump

A rapid relaxation, with a very small amplitude, and characterised by an increase in absorbance, was observed at 465 nm. The reciprocal relaxation time was found to increase linearly with increasing α -CD concentration (see Fig. 4.8). A slower relaxation, with a slightly larger amplitude, but also characterised by an increase in absorbance, was also observed. In this case, however, the relaxation time was found to be independent of the α -CD concentration.

The concentration dependence of the faster relaxation suggests that it is probably due to the formation of a 1:1 complex, as described below.



By following the derivation given in Sec. 3.1.1, it can be shown that the reciprocal relaxation time is given by the following equation:

$$1/\tau_1 = k_1([\overline{\text{MO}}] + [\overline{\alpha\text{-CD}}]) + k_{-1} \quad (4.3)$$

Fitting the data to this equation using the DATAFIT routine (see Appendix B), yields the following values for the rate constants:

$$\begin{aligned} k_1 &= 5.3(\pm 0.7) \times 10^7 \text{ dm}^3 \text{ mol}^{-1} \text{ sec}^{-1} \\ k_{-1} &= 1.6(\pm 8.4) \times 10^3 \text{ sec}^{-1} \end{aligned}$$

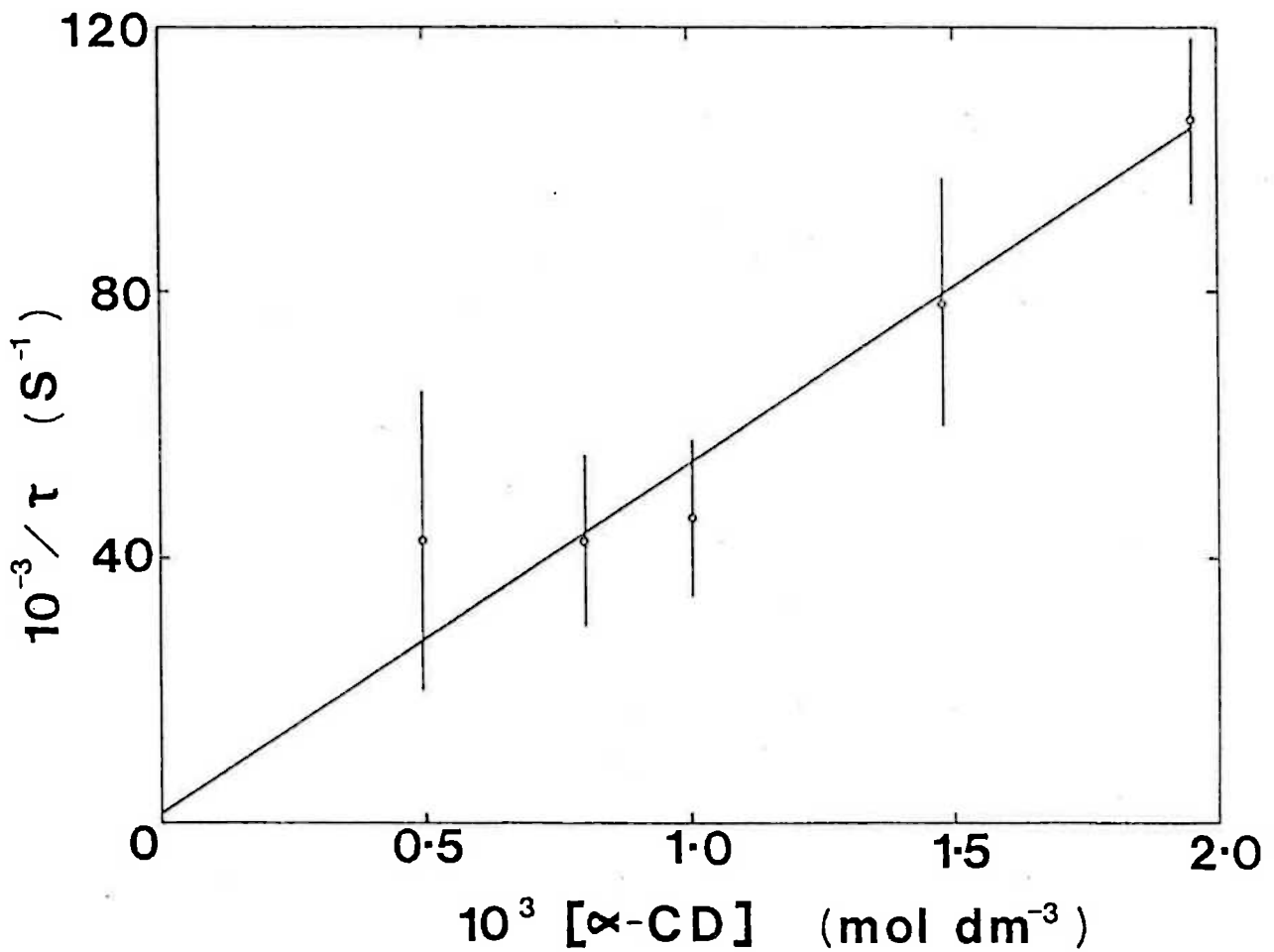


Fig. 4.8: Reciprocal relaxation times for MO/ α -CD mixtures as a function of total α -CD concentration at pH 13.4, 25°C. The solid curve represents the best fit of the data to equation (4.3).

The large errors in the values of the rate constants are a consequence of the very small amplitude of the relaxation.*

The fact that the slower relaxation shows no concentration dependence suggests that it may be due to a conformational change of the inclusion complex, or to changes in the solvation of the complex, as has been proposed by Hersey and Robinson.¹⁷ The average value of the reciprocal relaxation time for this process was $1.64 (\pm 0.22) \times 10^3 \text{ sec}^{-1}$.

b) Absorption Spectra

The effect of α -CD on the absorption spectrum of methyl orange in 1 mol dm^{-3} NaOH solution is very similar to that observed by Cramer et al.⁶ at pH 9.0. Again there is a blue shift of λ_{max} , and two non-related isosbestic points are apparent (see Fig. 4.9). At α -CD concentrations $\leq 5 \times 10^{-3} \text{ mol dm}^{-3}$, an isosbestic point is observed at 444 nm. On increasing the α -CD concentration, a new isosbestic point appears at approximately 459 nm.

If the data used are restricted to spectra recorded at α -CD concentrations $\leq 5 \times 10^{-3} \text{ mol dm}^{-3}$, values can be obtained for the equilibrium constant (K_1) for the binding of the first cyclodextrin, and for the molar absorptivity (ϵ_1) of the 1:1 complex (see Fig. 4.10). At any wavelength the observed absorbance (A) can be assumed to be given by,

$$A = \epsilon_{\text{MO}}[\text{MO}]_0 + (\epsilon_1 - \epsilon_{\text{MO}}) [\text{MO} \cdot \alpha\text{-CD}] \quad (4.4),$$

where $[\text{MO}]_0$ = total concentration of methyl orange added

$[\text{MO} \cdot \alpha\text{-CD}]$ = equilibrium concentration of the 1:1 complex.

By combining this equation with the following expression for the

* Consequently no value of K_1 was evaluated.

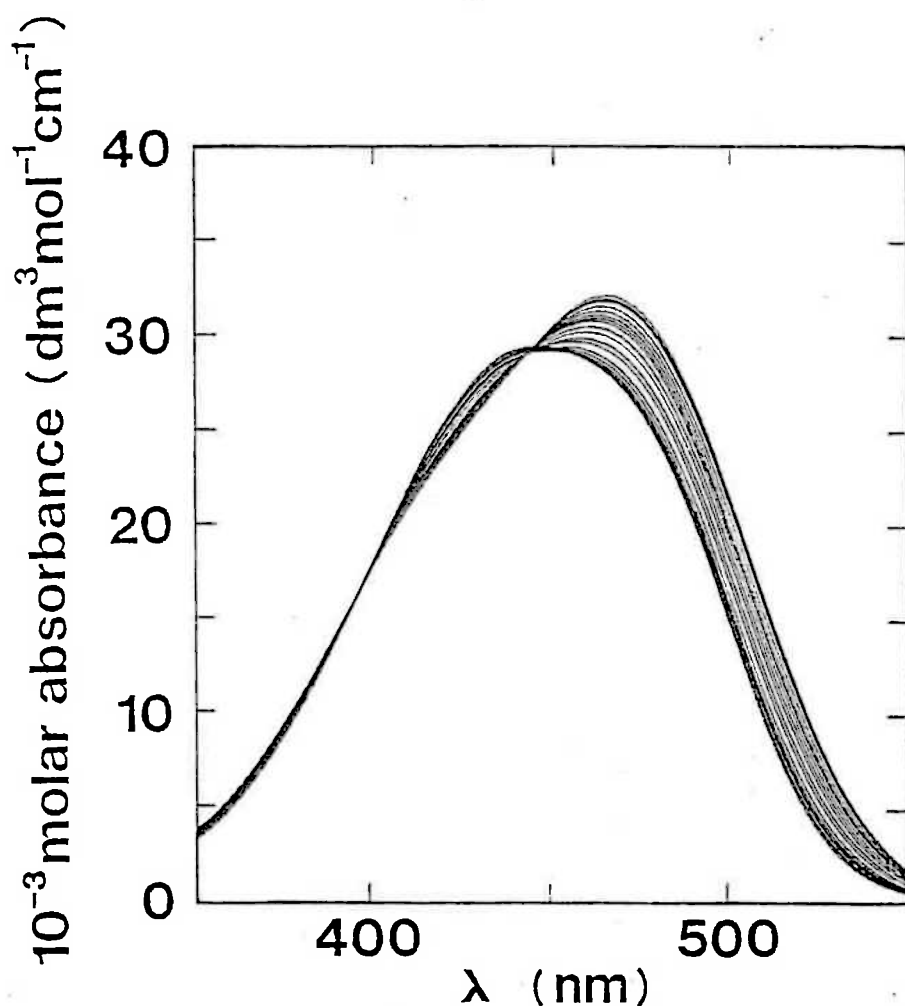


Fig. 4.9: Visible absorption spectrum of methyl orange ($4 \times 10^{-5} \text{ mol dm}^{-3}$) at pH 13.4 alone and in the presence of increasing concentrations of α -CD ranging from 5×10^{-5} to $2 \times 10^{-2} \text{ mol dm}^{-3}$.

The α -CD causes an increase in absorbance in the range 400-440 nm, and a decrease in absorbance at wavelengths $\geq 460 \text{ nm}$.

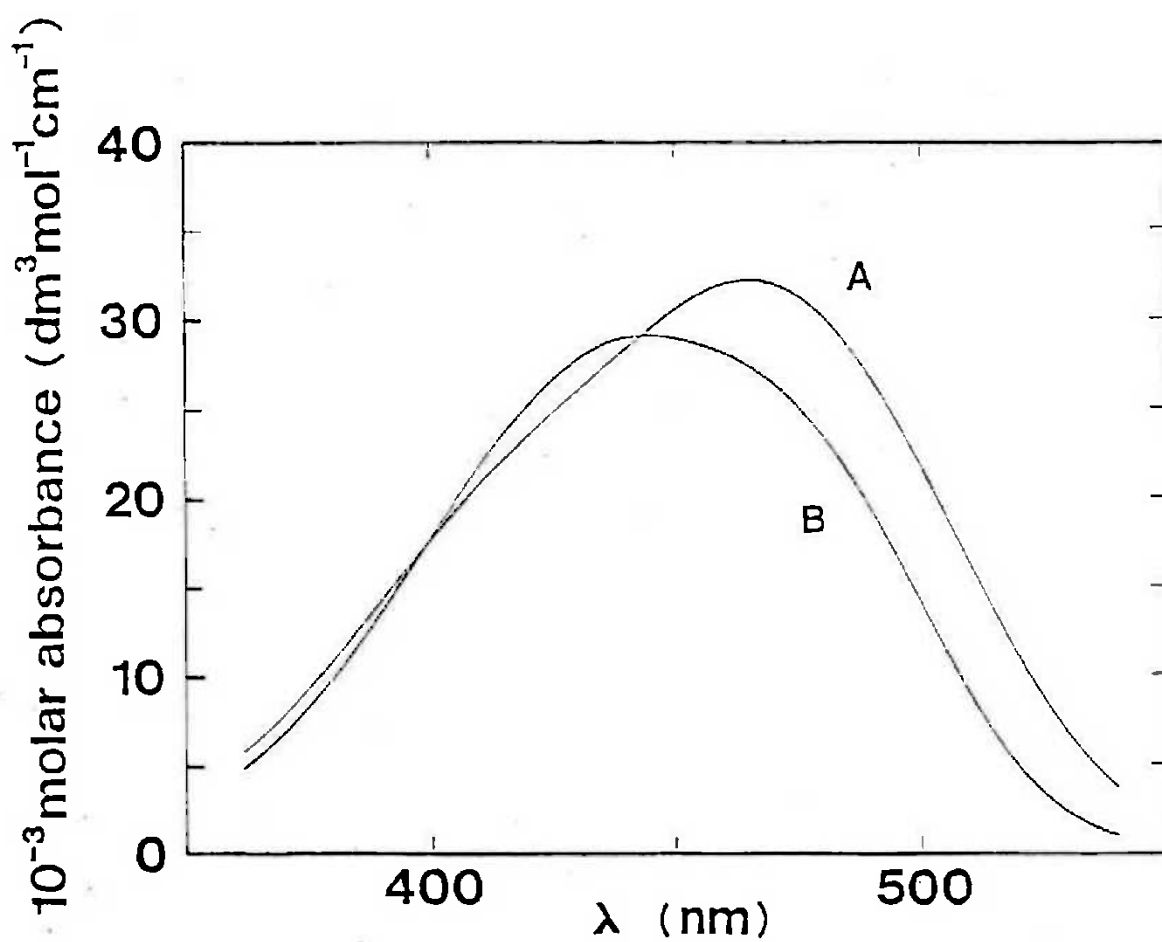


Fig. 4.10: Derived spectrum of the MO: α CD complex (B) compared to the spectrum of MO alone (A) at pH 13.4.

equilibrium constant, the data could be fitted using the non-linear least-squares fitting routine, DATAFIT (see Appendix B).

$$K_1 = \frac{[\text{MO} \cdot \alpha\text{-CD}]}{([\text{MO}]_0 - [\text{MO} \cdot \alpha\text{-CD}])([\text{CD}]_0 - [\text{MO} \cdot \alpha\text{-CD}])} \quad (4.5)$$

The fitting was carried out over all the monitored wavelengths, except those where small absorbance changes prevented DATAFIT from converging to a satisfactory minimum. The values of K_1 , obtained at 2 nm intervals, were found to be constant across the entire wavelength range (540-362 nm). The individual K_1 values were therefore weighted according to their estimated uncertainties, and averaged to give the following value:

$$K_1 = 7.48 (\pm 0.21) \times 10^2 \text{ dm}^3 \text{ mol}^{-1}$$

By comparing this value with those of the apparent association constant for the methyl orange/ α -CD interaction, quoted in Table 4.1, it can be seen that the deprotonation of α -CD causes a significant reduction in its binding affinity for methyl orange. Two possible reasons could account for this. The first is that electrostatic repulsion between the negatively charged sulphonate group of the methyl orange anion and the now negatively charged cyclodextrin hinders the association of the two components. The second possibility is that the deprotonation of the cyclodextrin causes a change in its structure or solvation, which results in an intrinsically lower binding affinity. The fact that both 1:1 and 2:1 complex formation can still occur, and that the value of K_1 is still quite large suggests, however, that inclusion occurs predominantly at the uncharged dimethylamino group end of the dye.

Thus, these results are in agreement with the earlier NMR results of Susuki and Sasaki,¹⁵ as well as the kinetic measurements of Hersey and Robinson.¹⁷

c) Induced Circular Dichroism

The induced circular dichroic spectrum of methyl orange in a thirty-fold excess of α -CD is shown in Fig. 4.7. The spectrum is similar to that observed in pH 9.0 buffer, except that there is a reduction in the intensities of the majority of the peaks. This reduction is probably due to a looser binding of the dye within the cyclodextrin cavity.

4.4 The Interaction of Methyl Orange with β -Cyclodextrin

4.4.1 Results at pH 9.0

a) Temperature-Jump

A relaxation was observed at 465 nm, which was characterised by a decrease in absorbance. The amplitude of the relaxation varied with the α -CD concentration, thus indicating the cyclodextrin's participation in the reaction. The relaxation time, however, appeared to be independent of the β -CD concentration within the concentration range studied (see Fig. 4.11). The average value of the reciprocal relaxation times determined is as follows:

$$\frac{1}{\tau}_{av} = 1.74 (\pm 0.11) \times 10^4 \text{ sec}^{-1}$$

The independence of the relaxation time of the cyclodextrin concentration suggests that the relaxation may be due to a conformational change of an inclusion complex. The absence of any concentration dependence, however, makes the confident assignment

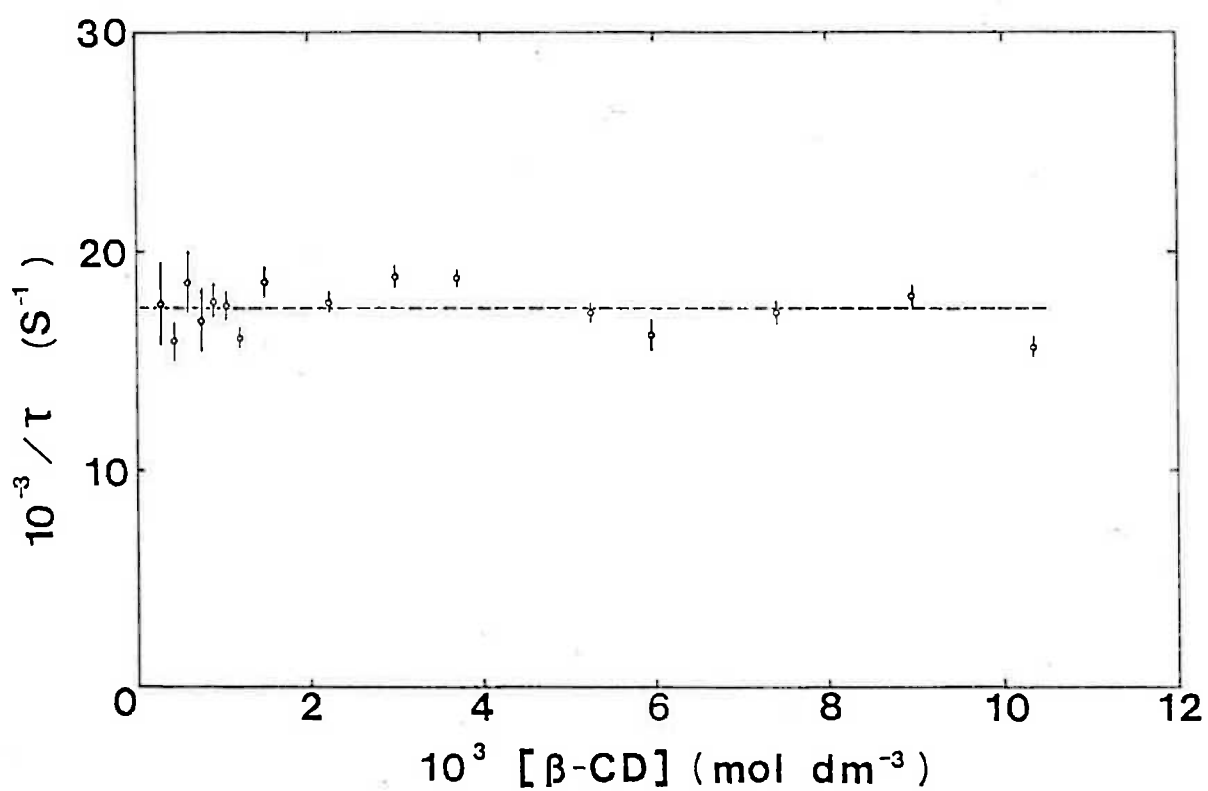


Fig. 4.11: Reciprocal relaxation times for MO/ β -CD mixtures as a function of total β -CD concentration at pH 9.0, 25°C. The dashed line represents the average of the observed reciprocal relaxation times.

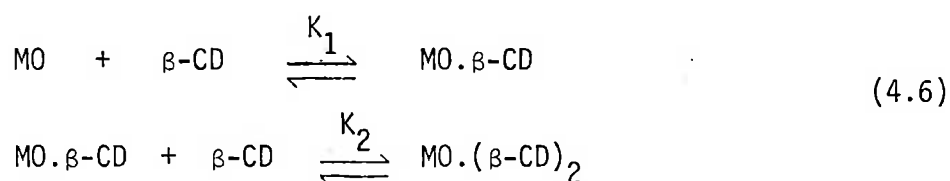


of a mechanism impossible, since any number of mechanisms could be operative, if the values of the rate constants and equilibrium constants are such that no apparent variation in τ is observed over the concentration range studied.

b) Absorption Spectra

The effect of β -CD on the absorption spectrum of methyl orange appears, at first sight, to be very similar to that of α -CD. A blue shift of λ_{\max} is observed, and an isosbestic point which shifts with increasing cyclodextrin concentration is again apparent (see Fig. 4.12). At β -CD concentrations $< 4 \times 10^{-4}$ mol dm $^{-3}$, an isosbestic is observed at approximately 454 nm. At β -CD concentrations $> 4 \times 10^{-4}$ mol dm $^{-3}$, the isosbestic point shifts to 466 nm.

The presence of a shifting isosbestic point implies that two or more inclusion complexes of different stoichiometric ratios occur simultaneously. Thus, the simplest explanation is that a reaction scheme analogous to that proposed for α -CD is followed:



It has been found, however, that the data cannot be fitted using this model.

If the data are fitted to a simple 1:1 complex formation, it is found that a satisfactory convergence occurs at the majority of wavelengths, although the value of K_1 derived is not constant across the entire wavelength range. In the range

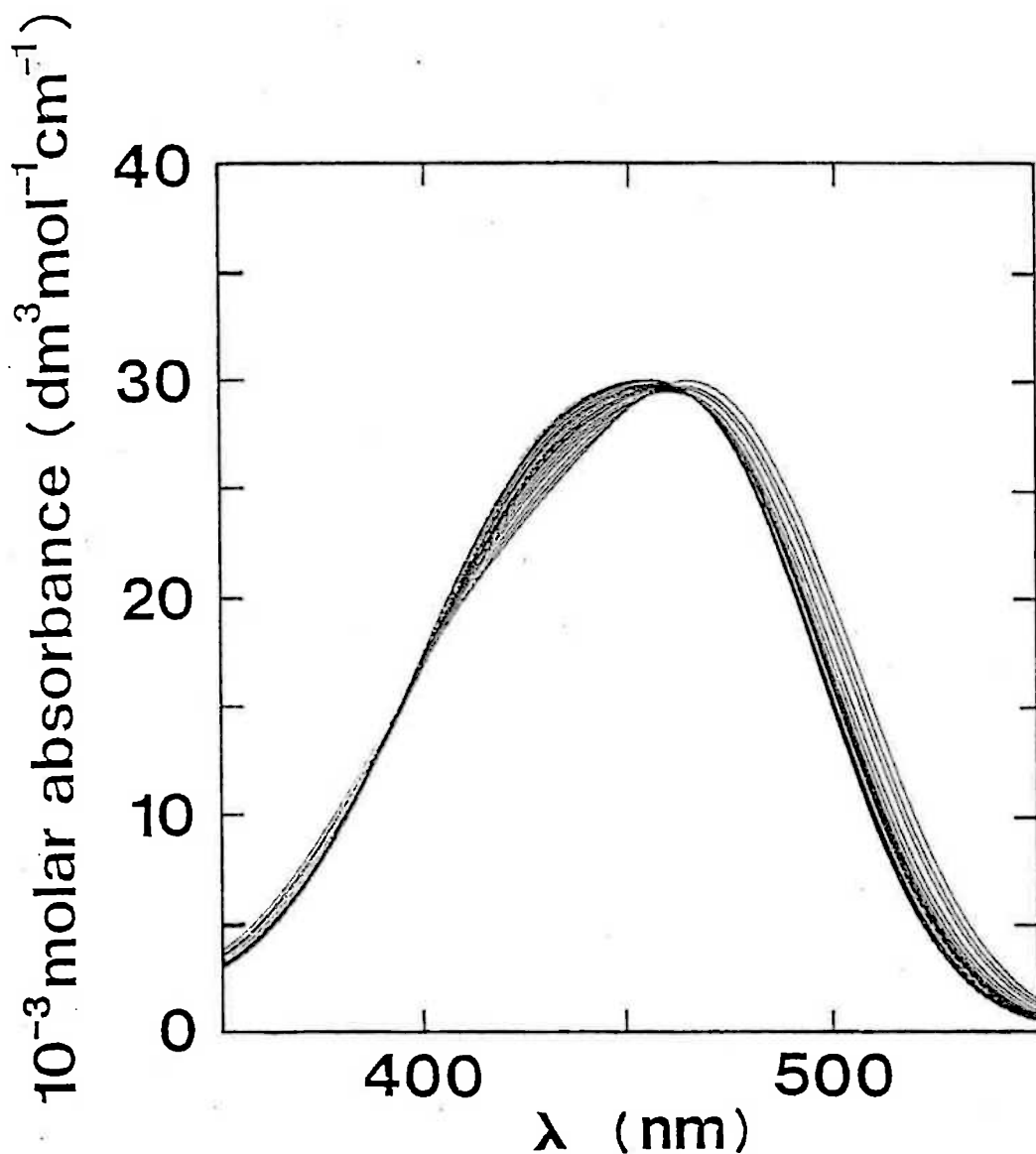


Fig. 4.12: Visible absorption spectrum of methyl orange ($4 \times 10^{-5} \text{ mol dm}^{-3}$) at pH 9.0 alone and in the presence of increasing concentrations of β -CD ranging from 7.5×10^{-5} to $1.2 \times 10^{-2} \text{ mol dm}^{-3}$.

The β -CD causes an increase in absorbance in the range 400-440 nm, and a decrease in absorbance at wavelengths ≥ 470 nm.

540-470 nm, the value of K_1 determined is of the order of $3 \times 10^3 \text{ dm}^3 \text{ mol}^{-1}$, whereas in the range 440-420 nm, it is approximately $1.5 \times 10^3 \text{ dm}^3 \text{ mol}^{-1}$. This inconsistency in K_1 is apparent even if the data are restricted to very low β -CD concentrations. Thus, although an adequate fit can be obtained at a given wavelength, the lack of a constant K_1 value implies that another complex, besides the 1:1, is formed at low β -CD concentrations.

The majority of association constants for the methyl orange/ β -CD system, quoted in the literature (see Table 4.1), have been determined at a single wavelength using the Hildebrand-Benesi method.³⁴ These determinations have assumed 1:1 complex formation, and neglected the presence of complexes of other stoichiometric ratios. The values quoted, therefore, are only apparent association constants. In order to determine a similar apparent association constant, the values of K_1 , determined across the entire wavelength range, 540-408 nm, by fitting to a 1:1 complex model only, have been averaged, and the following value derived, which is in agreement with the literature values.

$$K_{\text{app}} = 2.16(\pm 0.90) \times 10^3 \text{ dm}^3 \text{ mol}^{-1}$$

At this stage it is not possible to state conclusively the origin of the complications observed in the fitting of the methyl orange/ β -CD spectral data. The fact that similar complications are not observed in the case of the interaction of methyl orange with α -CD (pH 13.4) implies, however, that they are related to the larger cavity size of β -CD. Therefore, since the

ability of the cavity of β -CD to include two aromatic moieties has been reported by several workers (see Introduction p. 6), it is a distinct possibility that the complexities observed in the case of β -CD are due to the formation of species in which β -CD includes two methyl orange molecules, i.e. $(MO)_2 \cdot \beta\text{-CD}$ and/or $(MO)_2 \cdot (\beta\text{-CD})_2$. The construction of space-filling models appears to support this possibility, although it would seem that, due to steric crowding, the two methyl orange molecules could not penetrate each β -CD cavity to the same extent.

Similar complexities in the fitting of the spectra have also been observed in the case of the interaction between methyl orange and permethylated β -cyclodextrin.³⁵ In this case, however, kinetic evidence exists, which is consistent with one host-two guest complexation.

c) Induced Circular Dichroism

The induced circular dichroic spectrum of methyl orange in a thirty-fold excess of β -CD is shown in Fig. 4.13. If it is assumed that methyl orange is included axially by β -CD, then the induced circular dichroic spectrum of the dye should be very similar to that observed in the presence of α -CD (see Fig. 4.7). In fact, the spectra are distinctly different. Although a sharp positive peak still occurs at 415 nm, a new positive peak now appears at approximately 505 nm, and there is a suggestion of a negative signal in the region of 450 nm.

The differences in the circular dichroic spectra induced by α - and β -CD could be interpreted in two possible ways. The first is that they indicate different orientations of the methyl orange

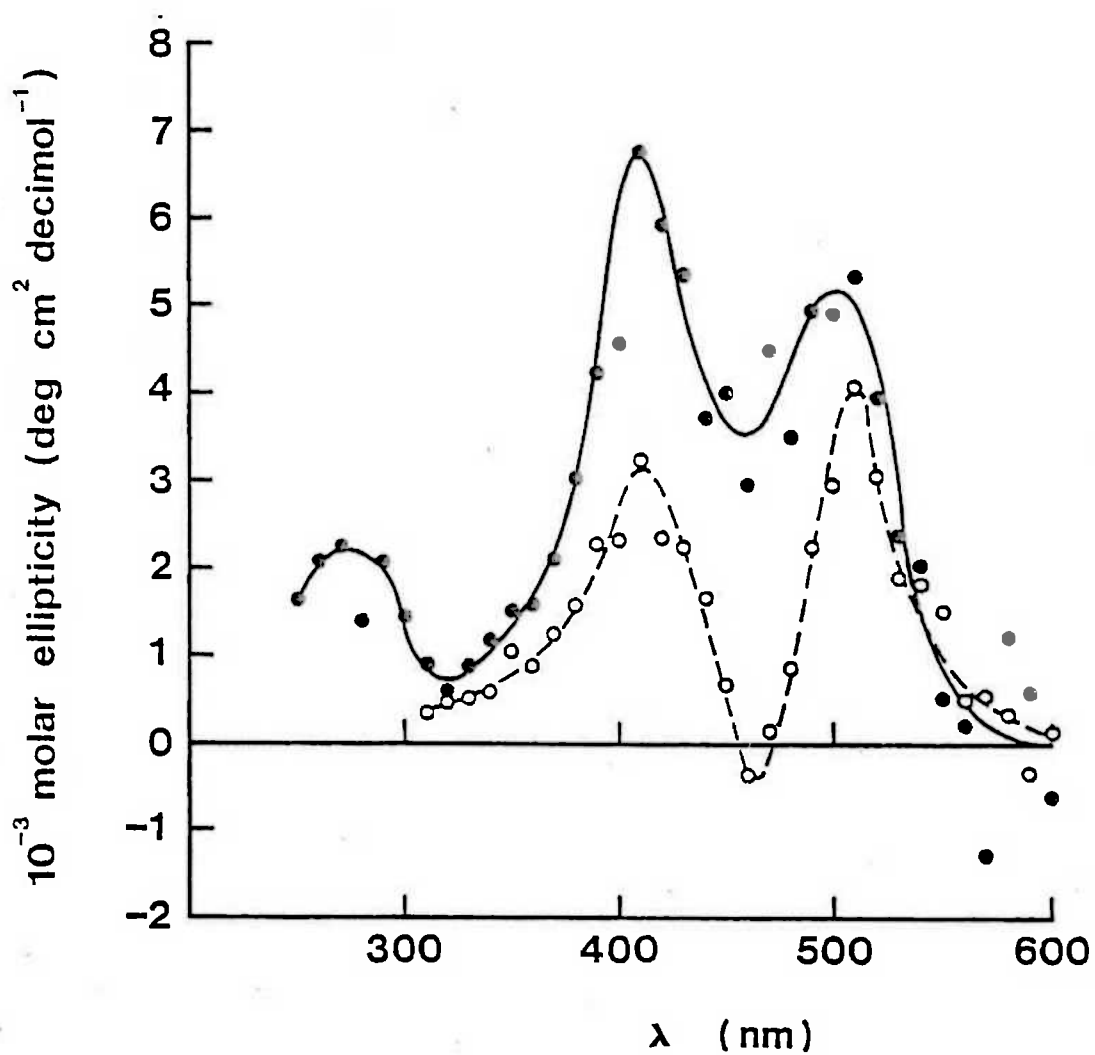


Fig. 4.13: Induced circular dichroic spectrum of methyl orange (4×10^{-5} mol dm⁻³) in the presence of β -CD (1×10^{-3} mol dm⁻³) at pH 9.0 (solid curve) and pH 13.4 (dashed curve).

anion within the cyclodextrin cavity. If this was the case, then, depending on the extent of the change in orientation, there would be a reversal in sign of some or all of the circular dichroic signals. Since model building appears to show that only axial inclusion could give sufficient penetration of the cavity for complex formation, however, a more likely explanation is that, in the case of β -CD, the spectrum is due to the combination of spectra of two or more species. The circular dichroic spectrum could then perhaps be attributed to the presence of both monomerically and dimerically included methyl orange, as has been earlier suggested to explain the absorption spectral data.

4.4.2 Results at pH 13.4

a) Temperature-Jump

A relaxation of very small amplitude was observed at 465 nm, which was characterised by a decrease in absorbance. The relaxation time appeared to be independent of the β -CD concentration, within the concentration range 1×10^{-3} - 1×10^{-2} mol dm⁻³. The average value of the reciprocal relaxation times determined is as follows:

$$1/\tau_{av} = 2.69(\pm 0.36) \times 10^4 \text{ sec}^{-1}$$

As was the case at pH 9.0, the independence of the relaxation time of the cyclodextrin concentration suggests that the relaxation may be due to a conformational change of an inclusion complex. Because of the small concentration range over which the relaxation is observable, however, no confident assignment of a mechanism can be made.

b) Absorption spectra

The effect of β -CD on the absorption spectrum of methyl orange in 1 mol dm^{-3} NaOH is shown in Fig. 4.14. As is the case at pH 9.0, a blue shift of λ_{max} , and a shifting isosbestic point are observed. At β -CD concentrations $\leq 4 \times 10^{-3} \text{ mol dm}^{-3}$, an isosbestic point is apparent at 450 nm. At higher β -CD concentrations, the isosbestic point shifts towards higher wavelengths.

The data were fitted to a simple 1:1 complex formation model. As was the case at pH 9.0, satisfactory convergence was obtained at the majority of wavelengths studied, but the value of the association constant determined varied across the wavelength range. In the range 540-470 nm a value of approximately $7.5 \times 10^2 \text{ dm}^3 \text{ mol}^{-1}$ was derived, whereas in the range 440-420 nm a value of approximately $4 \times 10^2 \text{ dm}^3 \text{ mol}^{-1}$ was obtained. At lower wavelengths still, 390-362 nm, the value again rose to approximately $9 \times 10^2 \text{ dm}^3 \text{ mol}^{-1}$. Thus, it appears that at pH 13.4 as well as pH 9.0 an additional inclusion complex is present, resulting in an inconsistent value of the association constant. Nevertheless, averaging the values across the entire wavelength range, one can derive the following apparent association constant.

$$K_{\text{app}} = 7.9(\pm 1.2) \times 10^2 \text{ dm}^3 \text{ mol}^{-1}$$

If this value is compared to that obtained for the methyl orange/ β -CD interaction at pH 9.0, i.e. $2.16 \times 10^3 \text{ dm}^3 \text{ mol}^{-1}$, it can be seen that the deprotonation of β -CD causes a significant reduction in its binding affinity for methyl orange, as was earlier found to be the case for α -CD. The fact that complex formation can

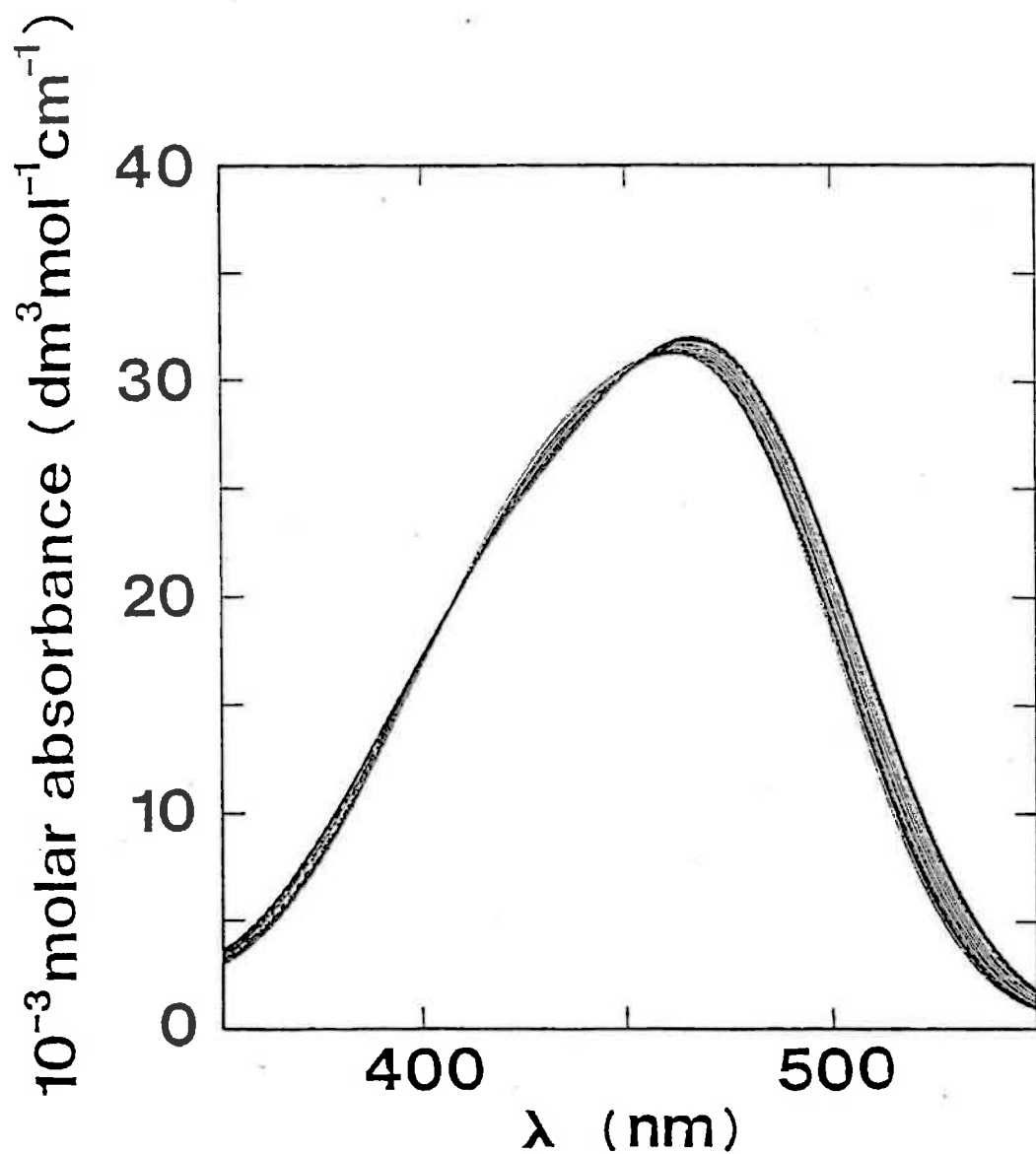


Fig. 4.14: Visible absorption spectrum of methyl orange ($4 \times 10^{-5} \text{ mol dm}^{-3}$) at pH 13.4 alone and in the presence of increasing concentrations of β -CD ranging from 3×10^{-5} to $1 \times 10^{-2} \text{ mol dm}^{-3}$.

The β -CD causes an increase in absorbance in the range 410-450 nm, and a decrease in absorbance at wavelengths ≥ 460 nm.

still occur, however, with such a large association constant suggests that inclusion may occur predominantly at the uncharged dimethylamino group end of the dye.

c) Induced Circular Dichroism

The induced circular dichroic spectrum of methyl orange in a thirty-fold excess of β -CD is shown in Fig. 4.13. The spectrum is similar to that observed at pH 9.0, in that the peaks occur at the same positions. The negative peak at approximately 450nm, however, has become much more obvious. Overall there is a reduction in the intensity of the circular dichroic signal, which suggests that the methyl orange anion is bound less tightly at pH 13.4 than at pH 9.0.

4.5 The Interaction of Methyl Orange with γ -Cyclodextrin

4.5.1 Results at pH 9.0

a) Temperature-Jump

Temperature-jump studies of solutions of methyl orange and γ -CD revealed a relaxation characterised by an increase in absorbance at 465 nm. The reciprocal relaxation times ($1/\tau$) of this process are given in Table 4.2, and appear in Fig. 4.15, plotted against the total γ -CD concentration. The dependence of $1/\tau$ on concentration indicates that the observed relaxation is coupled to other faster processes, occurring within the heating time of the apparatus, and which are characterised by small absorbance changes at the monitored wavelength. A variety of reaction schemes have been considered in explanation of the kinetic results. The scheme below gave the best fit to the $1/\tau$ data, and

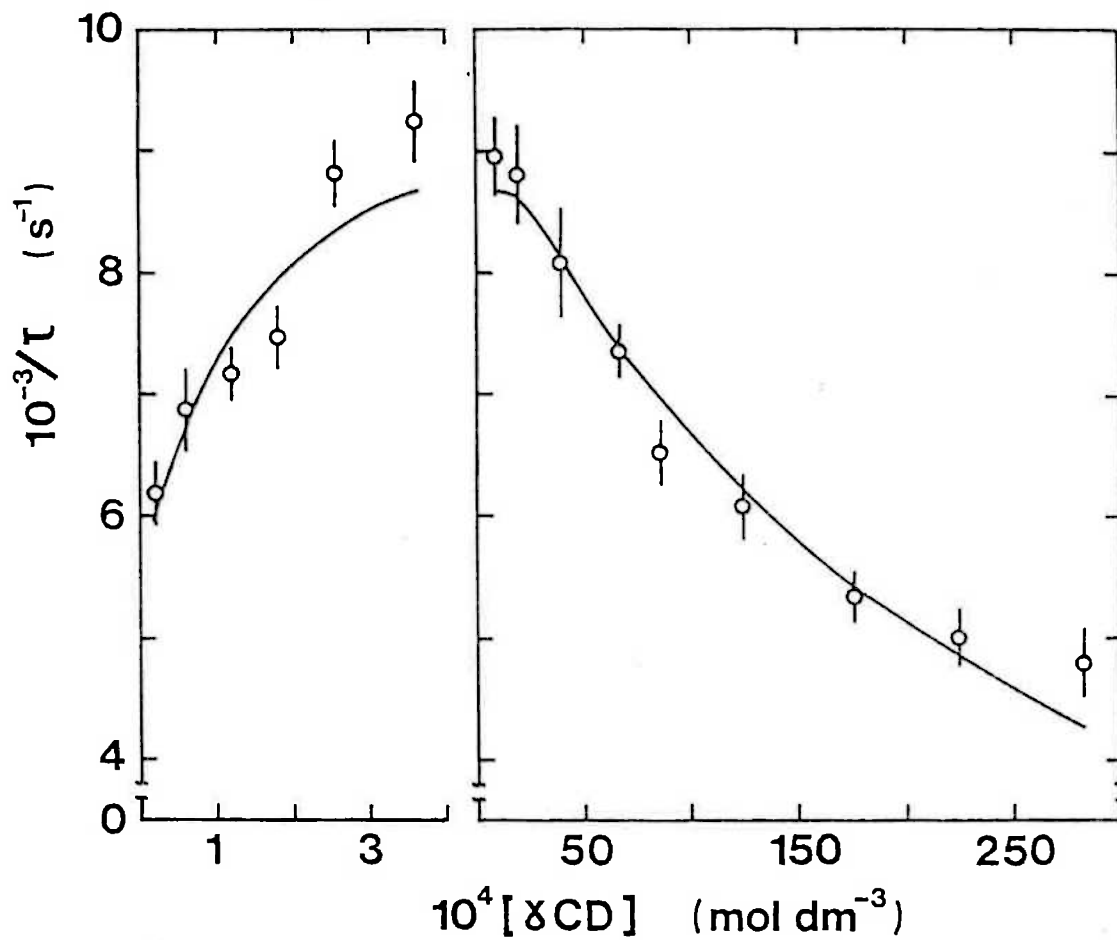
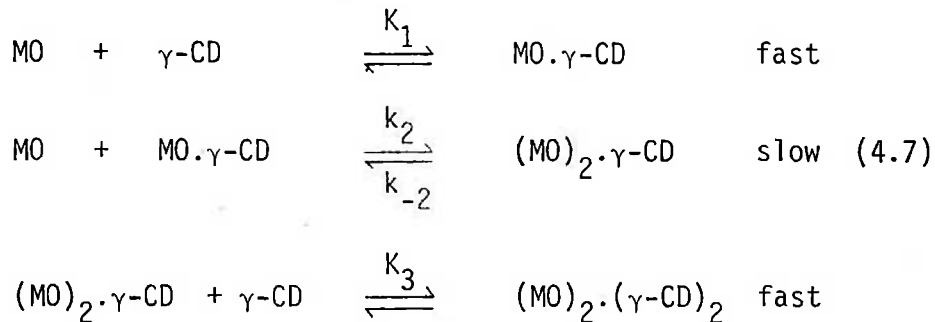


Fig. 4.15: Reciprocal relaxation times for MO/ γ -CD mixtures as a function of total γ -CD concentration at pH 9.0, 25°C. The solid curve represents the best fit of the data to equation (4.8).

yielded equilibrium constants which were consistent with values independently calculated from equilibrium spectrophotometric data.



In scheme (4.7), $\text{MO}\cdot\gamma\text{-CD}$ is an inclusion complex of methyl orange within $\gamma\text{-CD}$, $(\text{MO})_2\cdot\gamma\text{-CD}$ is an inclusion complex comprising a methyl orange dimer within $\gamma\text{-CD}$, and $(\text{MO})_2\cdot(\gamma\text{-CD})_2$ is an inclusion complex of the methyl orange dimer (which is considered to be in a parallel plane head-to-tail arrangement³⁶) axially included within two $\gamma\text{-CD}$ molecules. Provided that the first and last steps are sufficiently fast to be considered in equilibrium throughout the relaxation of the second step, the reaction scheme predicts a single exponential relaxation characterised by τ . Using the substitution method of Czerlinski³⁷ (see Appendix E), the following equation may be derived for the variation of τ with concentration:

$$\begin{aligned}
 1/\tau = & k_2 \frac{[\text{MO}][[\text{MO}] + [\text{MO}\cdot\gamma\text{-CD}] + 4[\gamma\text{-CD}]]}{[\text{MO}] + [\gamma\text{-CD}] + 1/K_1} \quad (4.8) \\
 & + k_{-2} \frac{[(\text{MO})_2\cdot\gamma\text{-CD}] + 1/K_3}{[\gamma\text{-CD}] + [(\text{MO})_2\cdot\gamma\text{-CD}] + 1/K_3}
 \end{aligned}$$

where all concentrations are equilibrium values.

The $1/\tau$ data were fitted to Eq.(4.8) by using the DATAFIT routine. The best-fit line is shown in Fig. 4.15, and the derived parameters are as follows:

$$k_2 = 9.4(\pm 5.1) \times 10^9 \text{ dm}^3 \text{ mol}^{-1} \text{ sec}^{-1}$$

$$k_{-2} = 4.8(\pm 0.8) \times 10^3 \text{ sec}^{-1}$$

$$K_1 = 45(\pm 7) \text{ dm}^3 \text{ mol}^{-1}$$

$$K_2 = 2.0(\pm 1.1) \times 10^6 \text{ dm}^3 \text{ mol}^{-1}$$

$$K_3 = 6.1(\pm 2.5) \times 10^3 \text{ dm}^3 \text{ mol}^{-1}$$

The errors in the rate and equilibrium constants were also derived from the DATAFIT routine, and represent one standard deviation.

b) Absorption Spectra

The visible absorption spectrum of methyl orange ($\sim 4 \times 10^{-5} \text{ mol dm}^{-3}$), alone and in the presence of γ -CD concentrations ranging from 2×10^{-5} to $3 \times 10^{-2} \text{ mol dm}^{-3}$, is shown in Figs. 4.16 and 4.17.

As can be seen from the figures, a shifting isosbestic point is again observed, thus implying the existence of more than two environments for the methyl orange anion. In accordance with the reaction scheme proposed above, the observed absorbance (A) can be assumed to be given by the following equation:

$$A = \epsilon_{\text{MO}}[\text{MO}] + \epsilon_{\text{MO}\cdot\gamma\text{-CD}}[\text{MO}\cdot\gamma\text{-CD}] \quad (4.9)$$

$$+ 2\epsilon_{(\text{MO})_2\cdot\gamma\text{-CD}}[(\text{MO})_2\cdot\gamma\text{-CD}] + 2\epsilon_{(\text{MO})_2\cdot(\gamma\text{-CD})_2}[(\text{MO})_2\cdot(\gamma\text{-CD})_2]$$

where all concentrations are equilibrium values.

The equilibrium spectra of Figs. 4.16 and 4.17 were fitted to this equation by using the routine DATAFIT at all monitored wavelengths, except those in the regions of the pseudo-isosbestic points, where the small changes in absorbance prevented DATAFIT from

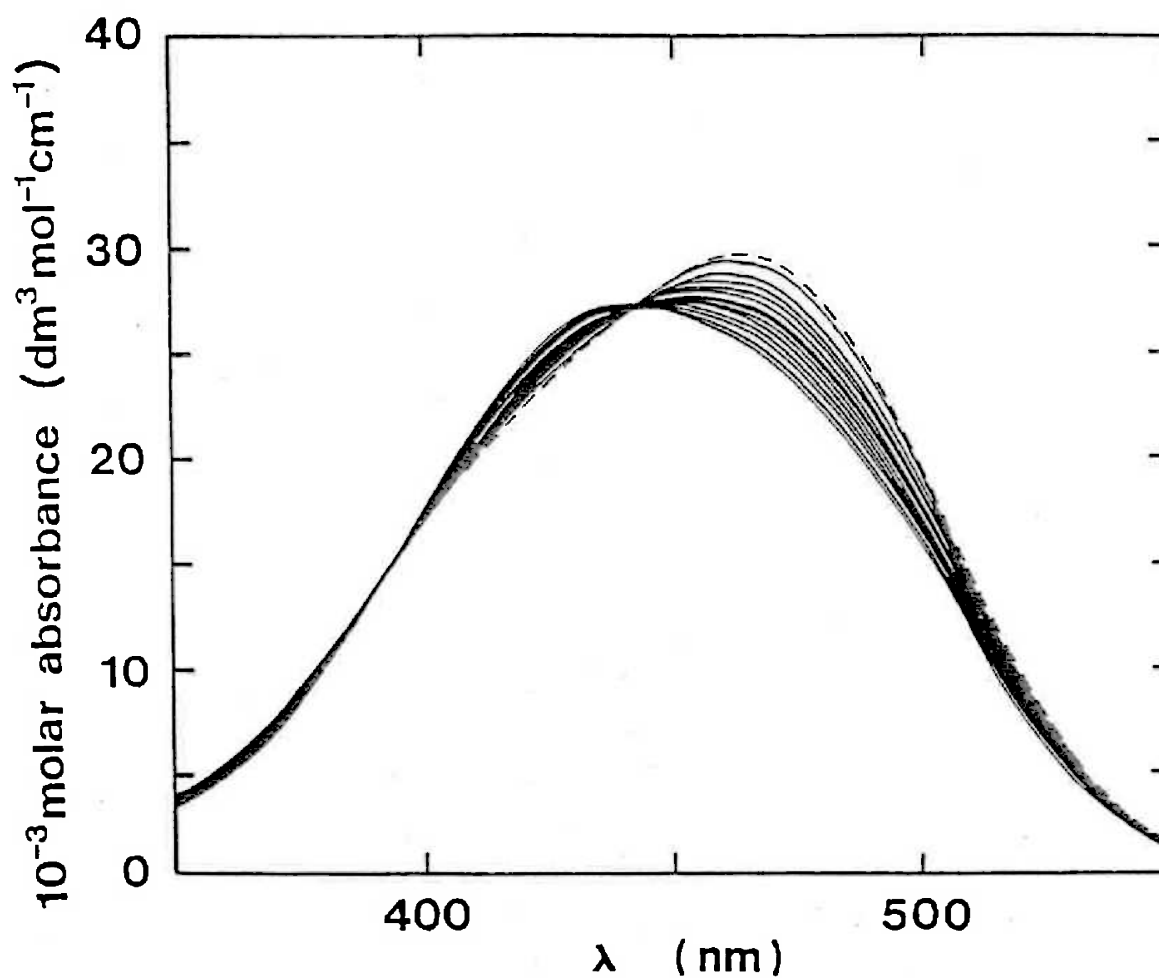


Fig. 4.16: Visible absorption spectrum of methyl orange ($4 \times 10^{-5} \text{ mol dm}^{-3}$) at pH 9.0 alone (dashed line) and in the presence of increasing concentrations of γ -CD ranging from 2.0×10^{-5} to $3.8 \times 10^{-4} \text{ mol dm}^{-3}$ (full lines).

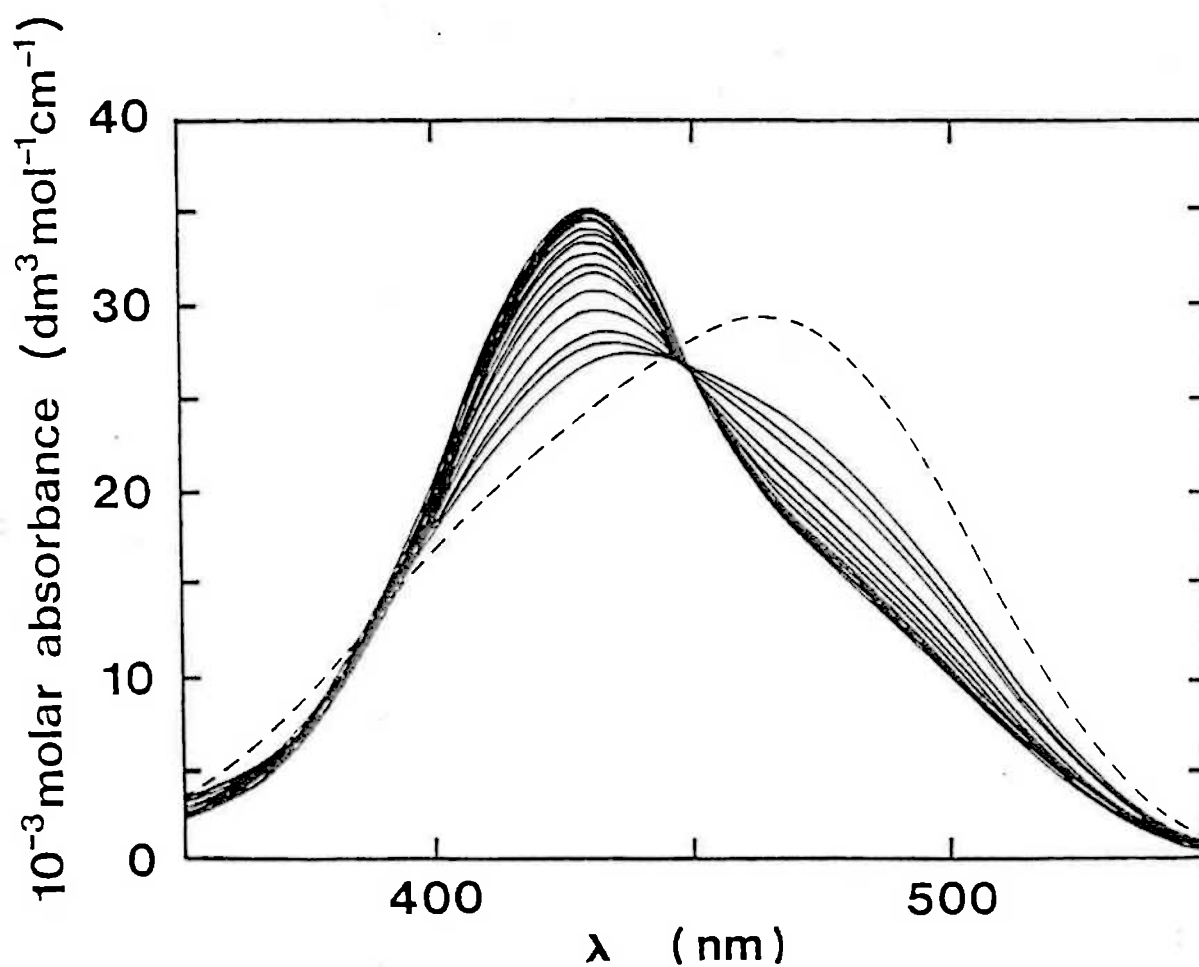
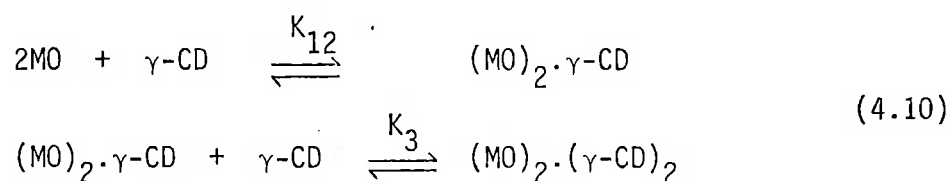


Fig. 4.17: Visible absorption spectrum of methyl orange ($4 \times 10^{-5} \text{ mol dm}^{-3}$) at pH 9.0 alone (dashed line) and in the presence of increasing concentrations of γ -CD ranging from 5.0×10^{-4} to $3.0 \times 10^{-2} \text{ mol dm}^{-3}$ (full lines).

converging to a best-fit value. It was found that the best fit to the equilibrium spectra was obtained if $[MO \cdot \gamma\text{-CD}]$ was taken to be negligible. Consequently, the reaction scheme, Eq.(4.7), simplifies to Eq.(4.10), in which $K_{12} = K_1 k_2 / k_{-2}$ of Eq.(4.7).



The K_{12} and K_3 values, calculated at 2 nm intervals in the ranges 412-440 nm and 460-540 nm, were weighted according to their estimated uncertainties, and averaged to give the values shown in Table 4.3. The temperature dependence of the equilibrium constants enabled the calculation of the corresponding ΔH° and ΔS° values (also shown in Table 4.3) by using Eq.(4.11).

$$\ln K = - \frac{\Delta H^\circ}{RT} + \frac{\Delta S^\circ}{R}
 \tag{4.11}$$

These K_{12} and K_3 values, together with the directly determined molar absorptivities of methyl orange, were used to derive the spectra of $(MO)_2 \cdot \gamma\text{-CD}$ and $(MO)_2 \cdot (\gamma\text{-CD})_2$ shown in Fig. 4.18, using DATAFIT.

The agreement between K_{12} (25.0°) = $3.8 (\pm 0.2) \times 10^7 \text{ dm}^6 \text{ mol}^{-2}$ (obtained from the equilibrium spectra) and $K_1 k_2 / k_{-2} = K_{12}$ (25.0°) = $9.0 (\pm 5.1) \times 10^7 \text{ dm}^6 \text{ mol}^{-2}$ (obtained from the τ data) is reasonable. The K_3 (25.0°) values, $4.7 (\pm 0.9) \times 10^2 \text{ dm}^3 \text{ mol}^{-1}$ and $6.1 (\pm 2.5) \times 10^3 \text{ dm}^3 \text{ mol}^{-1}$, derived from the equilibrium spectra and τ data respectively, agree less well, but, as the proportion of $(MO)_2 \cdot (\gamma\text{-CD})$ is very small, except at the higher concentrations of $\gamma\text{-CD}$, this is not unexpected.

Temperature (°C)	K_{12} (dm ⁶ mol ⁻²)	K_3 (dm ³ mol ⁻¹)
15.0	$5.5(\pm 0.8) \times 10^7$	$5.5(\pm 1.7) \times 10^2$
25.0	$3.8(\pm 0.2) \times 10^7$	$4.7(\pm 0.9) \times 10^2$
35.0	$1.2(\pm 0.4) \times 10^7$	$2.3(\pm 0.1) \times 10^2$
	$\Delta H_{12}^\circ = -56(\pm 6) \text{ kJ mol}^{-1}$	
	$\Delta S_{12}^\circ = -47(\pm 61) \text{ JK}^{-1} \text{ mol}^{-1}$	
	$\Delta H_3^\circ = -32(\pm 4) \text{ kJ mol}^{-1}$	
	$\Delta S_3^\circ = -58(\pm 42) \text{ JK}^{-1} \text{ mol}^{-1}$	

Table 4.3: Equilibrium constants, enthalpies, and entropies for the inclusion of methyl orange in γ -cyclodextrin (pH 9.0) from equilibrium spectra.

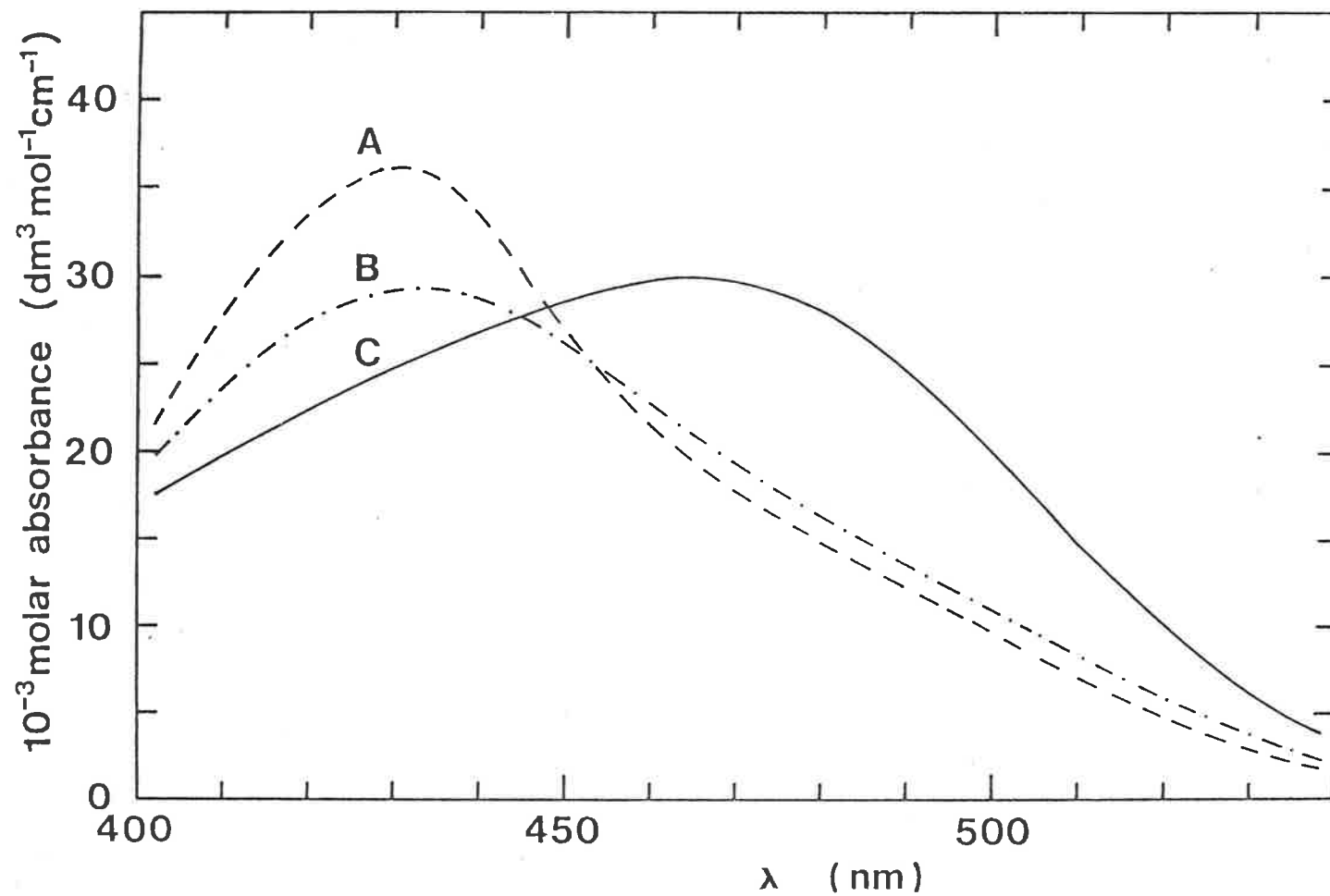


Fig. 4.18: Derived spectra of the $(\text{MO})_2 \cdot (\gamma\text{CD})_2$ (A) and $(\text{MO})_2 \cdot \gamma\text{CD}$ (B) complexes compared with the spectrum of MO alone (C) at pH 9.0.

c) Induced Circular Dichroism

The induced circular dichroic spectrum of methyl orange in a thirty-fold excess of γ -CD (see Fig. 4.19) differs markedly from that of methyl orange in a similar excess of α -CD or β -CD, which have been described earlier. This suggests that the environment of the methyl orange chromophore in γ -CD is very different from that experienced in either α - or β -CD. The spectrum arising from the methyl orange/ γ -CD interaction is characteristic of dimeric methyl orange, in which the $\pi \rightarrow \pi^*$ transition moments are almost parallel (see Appendix D). Dimeric methyl orange has previously been observed in association with poly-L-lysine, in which system both a blue shift in the absorption spectrum, and two peaks of opposite sign in the circular dichroic spectrum occurred.³⁸

4.5.2 Results at pH 13.4

a) Temperature-Jump

Temperature-jump studies of solutions of methyl orange and γ -CD in 1 mol dm^{-3} NaOH revealed a relaxation characterised by an increase in absorbance at 465 nm. The reciprocal relaxation times ($1/\tau$) of this process are given in Table 4.4, and appear in Fig.4.20, plotted against the total γ -CD concentration. The $1/\tau$ data were fitted to the three step mechanism described earlier (see Eq.(4.7)), omitting the first eight data points. The best-fit line is shown in Fig. 4.20, and the derived parameters are as follows:

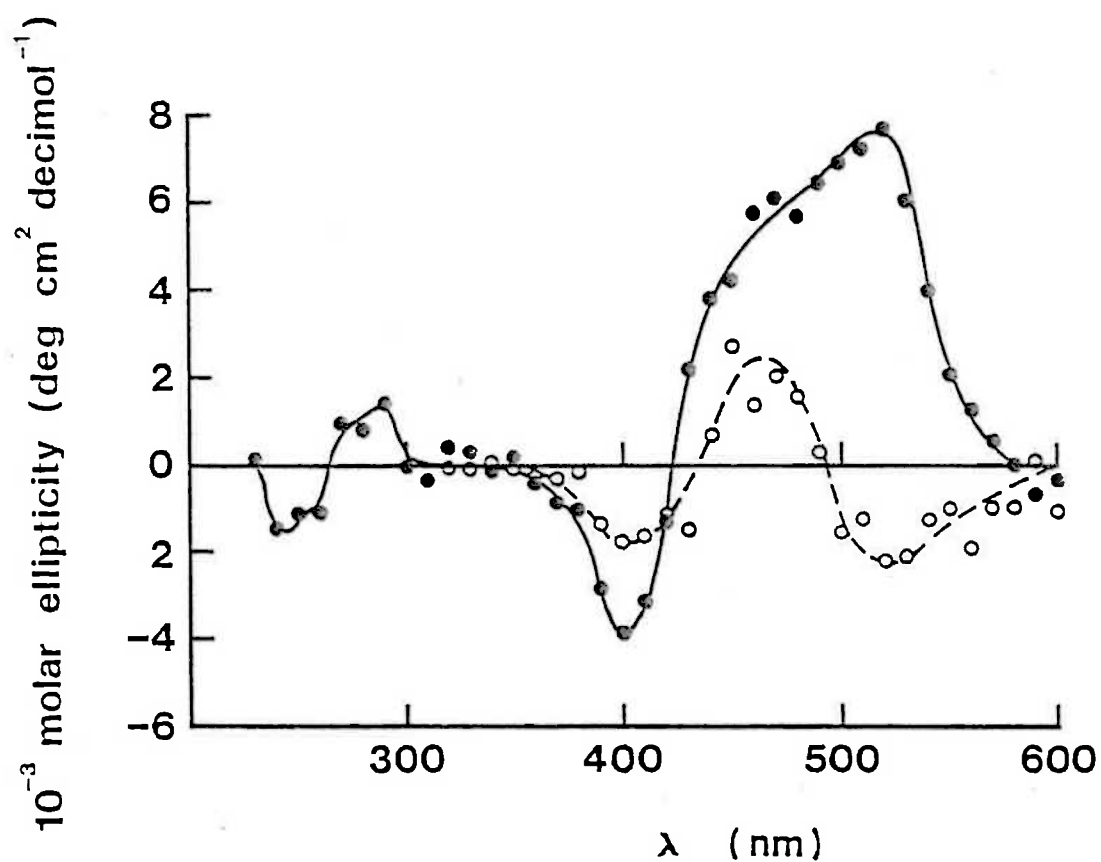


Fig. 4.19: Induced circular dichroic spectrum of methyl orange ($4 \times 10^{-5} \text{ mol dm}^{-3}$) in the presence of γ -CD ($1 \times 10^{-3} \text{ mol dm}^{-3}$) at pH 9.0 (solid curve) and pH 13.4 (dashed curve).

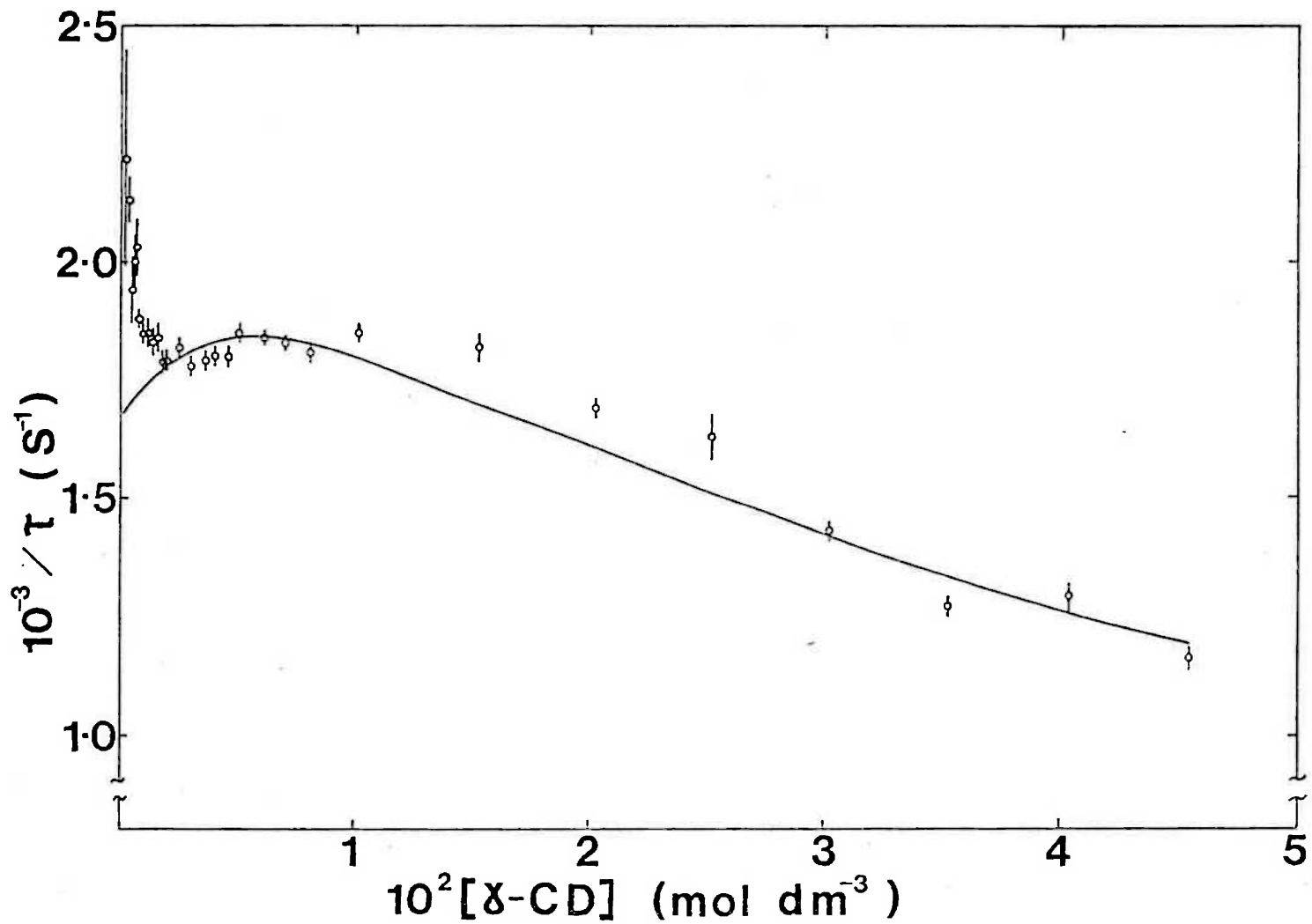


Fig. 4.20: Reciprocal relaxation times for MO/ γ -CD mixtures as a function of total γ -CD concentration at pH 13.4, 25°C. The solid curve represents the best fit of the data to equation (4.8).

$$\begin{aligned}
 k_2 &= 3(\pm 28) \times 10^7 \text{ dm}^3 \text{ mol}^{-1} \text{ sec}^{-1} \\
 k_{-2} &= 1.67(\pm 0.05) \times 10^3 \text{ sec}^{-1} \\
 K_1 &= 40(\pm 190) \text{ dm}^3 \text{ mol}^{-1} \\
 K_2 &= 2(\pm 17) \times 10^4 \text{ dm}^3 \text{ mol}^{-1} \\
 K_3 &= 40(\pm 330) \text{ dm}^3 \text{ mol}^{-1}
 \end{aligned}$$

The model was found to be unable to fit the data at low cyclodextrin concentrations, possibly because the first and third steps may not be completely decoupled from the slower second step at these concentrations. It should also be noted that the large values of the errors in the parameters are a consequence of the small percentage change of the reciprocal relaxation time across the entire cyclodextrin concentration range.

A comparison of the results obtained at pH 9.0 and pH 13.4 shows that the deprotonation of γ -cyclodextrin causes a deceleration of the relaxation process observed. The major cause for this deceleration appears to be a decrease in the value of k_2 , i.e. the rate of the dimerisation step of the mechanism (4.7) seems to be decreased.

b) Absorption Spectra

The visible absorption spectrum of methyl orange ($\sim 3 \times 10^{-5} \text{ mol dm}^{-3}$) alone and in the presence of γ -CD concentrations ranging from 5×10^{-5} to $3 \times 10^{-2} \text{ mol dm}^{-3}$ is shown in Fig. 4.21. The similarity of the spectral change to that observed at pH 9.0 indicates that the complex formed consists of an included methyl orange dimer. The presence of an isosbestic point at 450 nm suggests, however, that only two spectroscopically distinguishable species occur in significant concentration. Thus, the data were

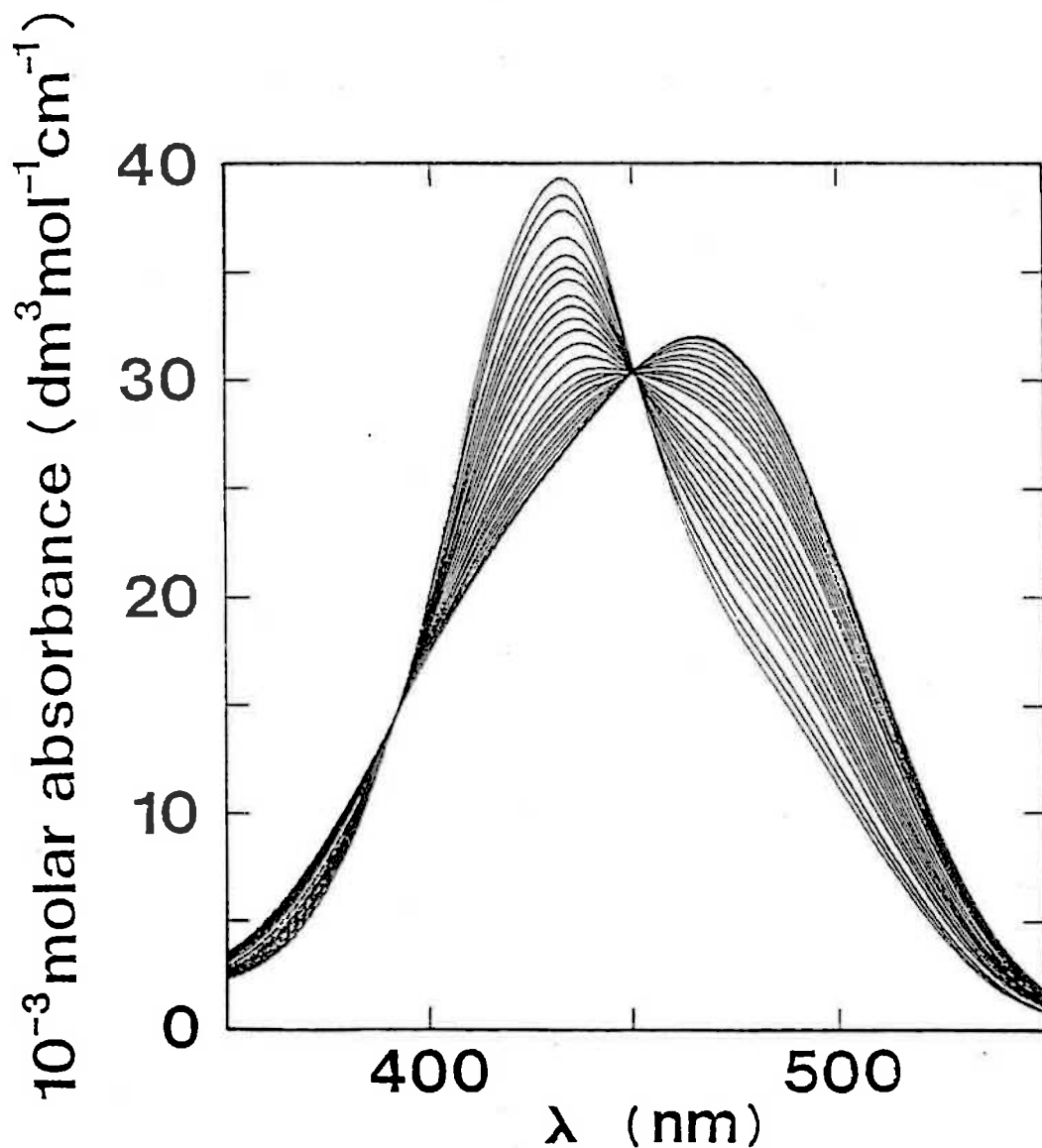
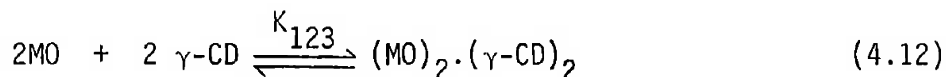


Fig. 4.21: Visible absorption spectrum of methyl orange ($3 \times 10^{-5} \text{ mol dm}^{-3}$) at pH 13.4 alone and in the presence of increasing concentrations of γ -CD ranging from 5×10^{-5} to $3 \times 10^{-2} \text{ mol dm}^{-3}$.

The γ -CD causes an increase in absorbance in the range 390-440 nm, and a decrease in absorbance at wavelengths $\geq 450 \text{ nm}$.

fitted to a single step equilibrium model:



It was found that the normal fitting procedure could not be used, because the large value of K_{123} resulted in a very shallow minimum, and thus prevented convergence. In this case, then, an alternative method for the determination of the association constant was used. This method is described in Appendix B. The value of the association constant obtained, averaging over the wavelength range 540-362 nm, is as follows

$$K_{123} = 1.99(\pm 0.62) \times 10^9 \text{ dm}^9 \text{ mol}^{-3}$$

The derived spectrum of the 2:2 complex is shown in Fig. 4.22.

If the above value of K_{123} is compared to the corresponding value derived at pH 9.0 (25.0°), i.e. $K_{12}K_3 = K_{123} = 1.8(\pm 0.4) \times 10^{10} \text{ dm}^9 \text{ mol}^{-3}$, it can be seen that the deprotonation of γ -CD causes a significant reduction in its binding affinity for methyl orange, as was earlier found to be the case for α - and β -CD.

c) Induced Circular Dichroism

The induced circular dichroic spectrum of methyl orange in a thirty-fold excess of γ -CD at pH 13.4 is shown in Fig. 4.19. A comparison of this spectrum to that observed at pH 9.0 shows that there is a large decrease in intensity, indicative of weaker binding of methyl orange at pH 13.4. It should also be noted that the peak at approximately 530 nm has changed signs, from positive at pH 9.0 to negative at pH 13.4. A number of possible reasons could account for this. One possibility is that the orientation

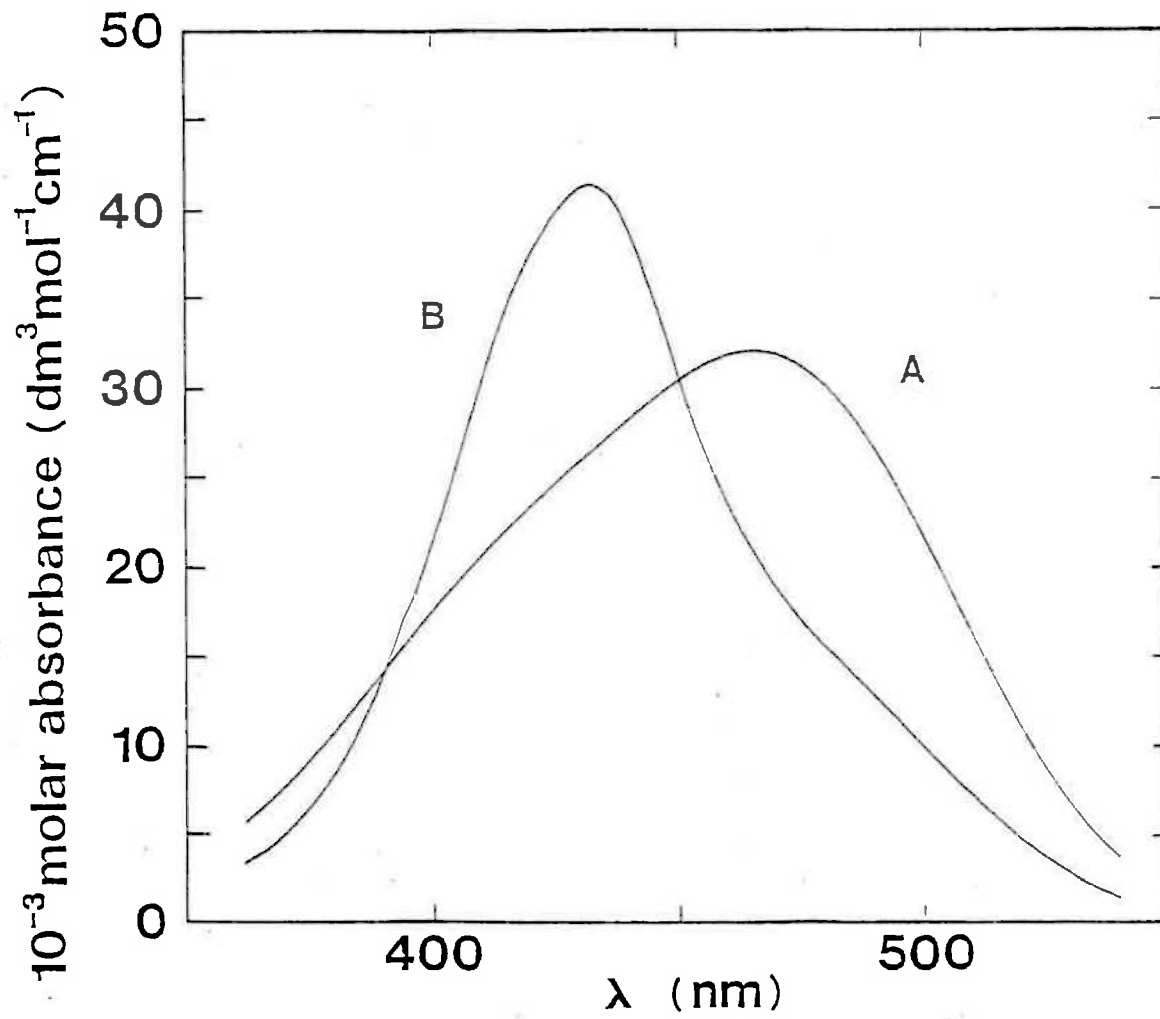


Fig. 4.22: Derived spectrum of the $(\text{MO})_2 \cdot (\gamma\text{CD})_2$ complex (B) compared with the spectrum of MO alone (A) at pH 13.4.

of the methyl orange dimer within the cyclodextrin cavity is different at the two pH values. Another possibility is that the structure of the dimer itself is significantly different at pH 9.0 and 13.4. A third possibility is that the coupling between the transition moments of the guest and the cyclodextrin is altered on deprotonation of the cyclodextrin. A combination of these three effects could also be occurring. Thus, it is not possible at this stage to assign a definite cause to the changes in the induced circular dichroic spectrum caused by deprotonation of the cyclodextrin.

[MO] (mol dm ⁻³ x 10 ⁵)	[γ -CD] (mol dm ⁻³)	$1/\tau$ (sec ⁻¹ x 10 ⁻³)
4.14(±0.03)	2.036(±0.028) x 10 ⁻⁵	6.18(±0.27)
4.10(±0.03)	6.077(±0.073) x 10 ⁻⁵	6.87(±0.34)
4.09(±0.03)	1.211(±0.018) x 10 ⁻⁴	7.16(±0.22)
4.07(±0.03)	1.811(±0.024) x 10 ⁻⁴	7.46(±0.26)
4.06(±0.03)	2.553(±0.028) x 10 ⁻⁴	8.81(±0.28)
4.04(±0.03)	3.597(±0.040) x 10 ⁻⁴	9.24(±0.34)
3.55(±0.02)	8.491(±0.062) x 10 ⁻⁴	8.95(±0.33)
3.54(±0.02)	1.952(±0.014) x 10 ⁻³	8.80(±0.41)
3.54(±0.02)	3.938(±0.027) x 10 ⁻³	8.07(±0.45)
3.51(±0.02)	6.663(±0.029) x 10 ⁻³	7.35(±0.22)
3.52(±0.02)	8.598(±0.037) x 10 ⁻³	6.51(±0.26)
3.52(±0.02)	1.240(±0.005) x 10 ⁻²	6.07(±0.27)
3.50(±0.02)	1.762(±0.007) x 10 ⁻²	5.34(±0.21)
3.51(±0.02)	2.243(±0.009) x 10 ⁻²	5.00(±0.24)
3.50(±0.02)	2.820(±0.010) x 10 ⁻²	4.79(±0.28)

Table 4.2: Concentrations and observed reciprocal relaxation times for the inclusion of methyl orange by γ -cyclodextrin at pH 9.0, 25.0°C.

Note: The errors in the concentrations were estimated from the known uncertainties in weighing. The errors in $1/\tau$ were estimated from the linear regressions of ln(volts) versus time data derived from oscilloscope photographs.

[MO] (mol dm ⁻³ x 10 ⁵)	[γ-CD] (mol dm ⁻³)	¹ / _τ (sec ⁻¹ x 10 ⁻³)
2.71(±0.01)	2.066(±0.026) x 10 ⁻⁴	2.22(±0.23)
2.71(±0.01)	4.051(±0.032) x 10 ⁻⁴	2.13(±0.05)
2.73(±0.01)	4.980(±0.036) x 10 ⁻⁴	1.94(±0.07)
2.72(±0.01)	6.052(±0.039) x 10 ⁻⁴	2.00(±0.06)
2.71(±0.01)	7.064(±0.043) x 10 ⁻⁴	2.03(±0.06)
2.71(±0.01)	8.064(±0.046) x 10 ⁻⁴	1.88(±0.02)
2.71(±0.01)	9.789(±0.052) x 10 ⁻⁴	1.85(±0.02)
2.72(±0.01)	1.206(±0.006) x 10 ⁻³	1.85(±0.03)
2.71(±0.01)	1.392(±0.007) x 10 ⁻³	1.83(±0.03)
2.72(±0.01)	1.607(±0.007) x 10 ⁻³	1.84(±0.03)
2.72(±0.01)	1.810(±0.008) x 10 ⁻³	1.79(±0.02)
2.71(±0.01)	2.014(±0.009) x 10 ⁻³	1.79(±0.02)
2.73(±0.01)	2.522(±0.010) x 10 ⁻³	1.82(±0.02)
2.70(±0.01)	3.005(±0.012) x 10 ⁻³	1.78(±0.02)
2.69(±0.01)	3.508(±0.014) x 10 ⁻³	1.79(±0.02)
2.72(±0.01)	4.035(±0.016) x 10 ⁻³	1.80(±0.02)
2.70(±0.01)	4.549(±0.017) x 10 ⁻³	1.80(±0.02)
2.71(±0.01)	5.045(±0.019) x 10 ⁻³	1.85(±0.02)
2.70(±0.01)	6.097(±0.023) x 10 ⁻³	1.84(±0.01)
2.72(±0.01)	7.029(±0.026) x 10 ⁻³	1.83(±0.01)
2.70(±0.01)	8.091(±0.029) x 10 ⁻³	1.81(±0.02)
2.71(±0.01)	1.013(±0.004) x 10 ⁻²	1.85(±0.02)
2.72(±0.01)	1.519(±0.006) x 10 ⁻²	1.82(±0.03)
2.71(±0.01)	2.023(±0.008) x 10 ⁻²	1.69(±0.02)
2.73(±0.01)	2.520(±0.009) x 10 ⁻²	1.63(±0.05)
2.68(±0.01)	3.015(±0.011) x 10 ⁻²	1.43(±0.02)
2.74(±0.01)	3.524(±0.013) x 10 ⁻²	1.27(±0.02)
2.73(±0.01)	4.032(±0.016) x 10 ⁻²	1.29(±0.03)
2.71(±0.01)	4.539(±0.018) x 10 ⁻²	1.16(±0.02)

Table 4.4: Concentrations and observed reciprocal relaxation times for the inclusion of methyl orange by γ-cyclodextrin at pH 13.4, 25.0°C.

Bibliography

1. Broser, W. and W. Lautsch, *Z.Naturforsch.*, 8b, 711 (1953).
2. Broser, W., *Z.Naturforsch.*, 8b, 722 (1953).
3. Lautsch, W., W. Broser, W. Biedermann and H. Gnichtel, *Angew.Chem.*, 66, 123 (1954).
4. Lautsch, W., W. Bandel and W. Broser, *Z.Naturforsch.*; 11b, 282 (1956).
5. Casu, B. and L. Rava, *Ric.Sci.*, 36, 733 (1966).
6. Cramer, F., W. Saenger and H.-Ch. Spatz, *J.Am.Chem.Soc.*, 89, 14 (1967).
7. van Etten, R.L., J.F. Sebastian, G.A. Clowes and M.L. Bender, *J.Am.Chem.Soc.*, 89, 3242 (1967).
8. van Hooidek, C. and C.C. Gross, *Rec.Trav.Chim.Pay-Bas.*, 89, 845 (1970).
9. Yamada, K., J. Morimoto and H. Iida, *J.Fac.Eng.Chiba Univ.*, 24, 71 (1973).
10. McMullan, R.K., W. Saenger, J. Fayos and D. Mootz, *Carbohydr. Res.*, 31, 37 (1973).
11. Harata, K., *Bull.Chem.Soc.Jpn.*, 49, 1493 (1976).
12. Fawcett, V., D.A. Long, T. Ridley and M.A. Stuckey, *Proc.5th Int.Conf.Raman Spectrosc.*, 1976, 228.
13. Szejtli, J., Z. Budai and M. Kajtar, *Magyar Kemiai Folyoirat*, 84, 68 (1978).
14. Matsui, Y. and K. Mochida, *Bull.Chem.Soc.Jpn.*, 51, 673 (1978).
15. Suzuki, M. and Y. Sasaki, *Chem.Pharm.Bull.*, 27, 609 (1979).
16. Hirai, H., N. Toshima and S. Uenoyama, *Polymer J.*, 13, 607 (1981).

17. Hersey, A. and B.H. Robinson, *J.Chem.Soc., Faraday Trans I*, 80, 2039 (1984).
18. Fujita, K., S. Ejima and T. Imoto, *J.Chem.Soc.Chem.Commun.*, 1984, 1277.
19. Szejtli, J., "Cyclodextrins and Their Inclusion Complexes", Akademiai Kiado, Budapest, 1982.
20. Lammers, J.N.J.J., J.L. Kooole and J. Hurkmans, *Die Stärke*, 23, 167 (1971).
21. Colson, P., H.J. Jennings and I.C.P. Smith, *J.Am.Chem.Soc.*, 96, 8081 (1974).
22. Gelb, R.I., L.M. Schwartz, J.J. Bradshaw and D.A. Laufer, *Bioorg.Chem.*, 9, 299 (1980).
23. Gelb, R.I., L.M. Schwartz and D.A. Laufer, *Bioorg.Chem.*, 11, 274 (1982).
24. Quadrifoglio, F. and V. Crescenzi, *J.Colloid Interfac.Sci.*, 35, 447 (1971).
25. Bock, H., *Angew.Chem.Int.Ed.Engl.*, 4, 457 (1965).
26. Kortüm, G. and H. Rau, *Ber.Bunsenges.physik.Chem.*, 68, 973 (1964).
27. Zollinger, H., "Azo and Diazo Chemistry. Aliphatic and Aromatic Compounds", Interscience, New York, 1961.
28. Kroner, J. and H. Bock, *Chem.Ber.*, 101, 1922 (1968).
29. Jaffé, H.H. and M. Orchin, "Theory and Applications of Ultraviolet Spectroscopy", Wiley, New York, 1962.
30. Brode, W.R., I.L. Seldin, P.E. Spoerri and G.M. Wyman, *J.Am.Chem.Soc.*, 77, 2762 (1955).
31. Reeves, R.L., R.S. Kaiser, M.S. Maggio, E.A. Sylvestre and W.H. Lawton, *Can.J.Chem.*, 51, 628 (1973).

32. Popov, K.R. and L.V. Smirnov, *Opt.Spectrosk.*, 30, 628 (1971).
33. Kurucsev, T., unpublished results, University of Adelaide (1981).
34. Benesi, H.A. and J.H. Hildebrand, *J.Am.Chem.Soc.*, 71, 2703 (1949).
35. Doddridge, B.G., unpublished results, University of Adelaide (1984).
36. Coates, E., *J.Soc.Dyers Colour.*, 85, 355 (1969).
37. Czerlinski, G.H., "Chemical Relaxation", Dekker, New York, 1966.
38. Hatano, M., M. Yoneyama, Y. Sato and Y. Kawamura, *Biopolymers*, 12, 2423 (1973).

CHAPTER V

CHAPTER V: THE INTERACTION OF TROPAEOLIN WITH
THE CYCLODEXTRINS

5.1 Introduction

As stated in the introduction to the previous chapter, one method of investigating the binding to cyclodextrin of a dye such as methyl orange, which has two groups capable of inclusion, is to exclude the possibility of inclusion at one end by the introduction of a bulky group. Thus, the investigation of the interaction between the cyclodextrins and the azo dye tropaeolin 000 no. 2 (TR), which is alternatively known as orange II, may shed further light on the methyl orange/cyclodextrin systems.

A comparison of the structures of methyl orange and tropaeolin (see Introduction, Fig. II) shows that in the case of tropaeolin the dimethylaniline moiety of methyl orange has been replaced by a β -naphthol moiety. The construction of CPK space-filling models seems to suggest that the naphthalene group is too large for inclusion within the cavity of α -CD, whereas complexes with β - and γ -CD would appear possible. Thus, in the case of α -CD only the benzenesulphonate end of tropaeolin should be able to penetrate the cavity sufficiently to enable complex formation. A comparison of the binding affinities of methyl orange and tropaeolin for α -CD, then, may assist in the determination of which portion of the methyl orange molecule is preferentially included.

Another, perhaps more important, reason for studying the interaction of tropaeolin with the cyclodextrins is to test the generality of the mechanism proposed for one host-two guest

complexation for the methyl orange/ γ -CD system. Although the formation of one host-two guest complexes has been well established using equilibrium methods, the mechanism of their formation is still in dispute. Thus, in order to be able to confidently state that the proposed mechanism is generally applicable, a number of consistent examples are required.

The only other research group so far to have investigated the tropaeolin/cyclodextrin interaction has been that of Suzuki and co-workers.¹⁻⁴ The major techniques which they have used for their investigation have been ^1H - and ^{13}C - nuclear magnetic resonance (NMR) and circular dichroism. Some of their results, however, seem somewhat ambiguous, particularly their NMR data, which yield different values of the association constant depending on which nucleus is observed.⁴ This highlights the advantage of visible absorption methods that the data collected depend upon the environment of the entire molecule, rather than that of individual atoms.

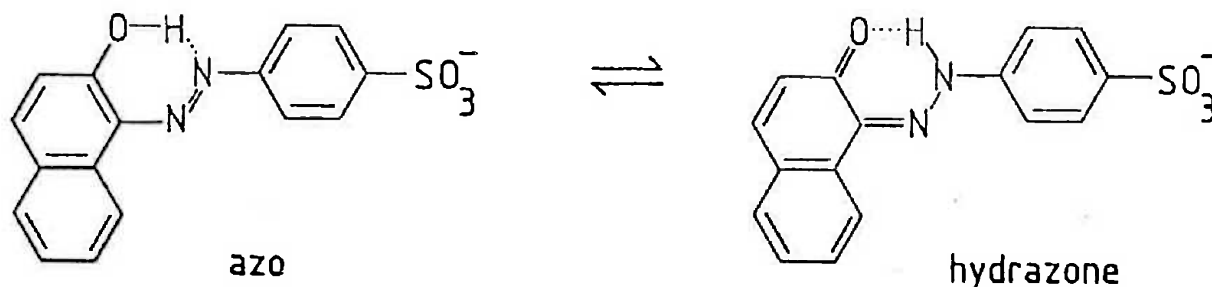
5.2 Properties of the Tropaeolin Anion

The pK_a of the hydroxyl group of tropaeolin has been determined as 11.4.⁵ The reason that the pK_a is so high is that an intramolecular hydrogen bond exists between the hydrogen of the hydroxyl group and one of the azo nitrogens. In the case of the isomer of tropaeolin, in which the hydroxyl group is *para* to the azo group and is thus unable to participate in hydrogen bonding, the pK_a decreases to a value of 8.2.

The UV/visible absorption spectrum of tropaeolin was found to be invariant within the pH range 2.0-6.0 in the presence of

aqueous solutions of 0.05 mol dm^{-3} glycine/HCl or 0.10 mol dm^{-3} acetate buffer, which indicates that no significant shifts in protonic equilibria occur under these conditions. Thus, since all of the results presented, except where explicitly stated otherwise, have been derived from measurements made at pH 5.5, contributions from any forms of the dye other than the tropaeolin mono-anion have generally been neglected.

From investigations of visible absorption spectra it has been found that in solution phenylazonaphthols, such as tropaeolin, exist in a tautomeric equilibrium between azo and hydrazone forms,^{5,6} as shown below.



The position of the equilibrium seems to depend on the polarity of the solvent.⁶ In aqueous solution, however, it is the hydrazone form which predominates.

Temperature-jump studies of tropaeolin were carried out at 480 nm (pH 5.5, 25°C). A relaxation occurring within the heating time of the apparatus (5 μ seconds) and characterised by a decrease in absorbance was observed. The magnitude of this relaxation is proportional to the total tropaeolin concentration.

This is followed by a slower relaxation, which produces an increase in absorbance, and whose amplitude never exceeds 15% of that of the fast relaxation. The total absorbance change arising from the two relaxations is consistent with the temperature variation of the equilibrium spectrum. However, since the fast relaxation is outside the experimental time scale it is not considered further.

Tropaeolin is known to aggregate in aqueous solution, as evidenced by deviations from Beer's law.^{7,8} Thus, it seems possible that the slow relaxation may be due to the dimerisation of the dye:



The increase in absorbance characterising this relaxation is consistent with a shift towards the monomer side of the equilibrium with an increase in temperature. The total tropaeolin concentration range, over which this single exponential relaxation may be quantitatively studied, is limited to $2 \times 10^{-5} - 6 \times 10^{-5}$ mol dm⁻³, as a consequence of the small absorbance changes and the high molar absorbance of tropaeolin. The reciprocal relaxation time, $1/\tau = 2.24 (\pm 0.40) \times 10^3 \text{ sec}^{-1}$, exhibits no significant variation within this experimental concentration range. The expected variation of $1/\tau$ with total tropaeolin concentration, $[\text{TR}]_0$, for the dimerisation equilibrium is described by the following equation⁹:

$$1/\tau^2 = k_{-d}^2 (8K_D[\text{TR}]_0 + 1) \quad (5.2)$$

where $K_D = k_d/k_{-d}$

Spectrophotometric studies of tropaeolin solutions have enabled the following value of the dimerisation constant, K_D , to be derived from the variation of the apparent molar absorbance of the dye with concentration:

$$K_D = 9.10 (\pm 4.28) \times 10^2 \text{ dm}^3 \text{ mol}^{-1}$$

This compares with the literature values of 1.32×10^{37} and $7.1 \times 10^2 \text{ dm}^3 \text{ mol}^{-1}$ ⁸, which were obtained at a lower ionic strength.

Using the derived value of K_D , it is found that over the concentration range studied $8K_D[\text{TR}]_0 \ll 1$, so that Eq. (5.2) reduces to

$$1/\tau^2 \approx k_{-d}^2 \quad (5.3)$$

Therefore, if it is assumed that the relaxation observed is actually due to dimerisation, the following values of the rate constants can be calculated:

$$k_{-d} \approx 2.24 (\pm 0.40) \times 10^3 \text{ sec}^{-1}$$

$$k_d \approx 2.0 (\pm 1.0) \times 10^6 \text{ dm}^3 \text{ mol}^{-1} \text{ sec}^{-1}$$

The linear dichroism of tropaeolin in stretched poly (vinyl alcohol) film is shown in Fig. 5.1. It can be seen that over the range 400-550 nm the absorbance parallel to the direction of stretch is substantially greater than that perpendicular to the direction of stretch, and that the dichroic ratio is relatively constant. Assuming that the dye molecules orientate with the long molecular axis parallel to the direction of stretch

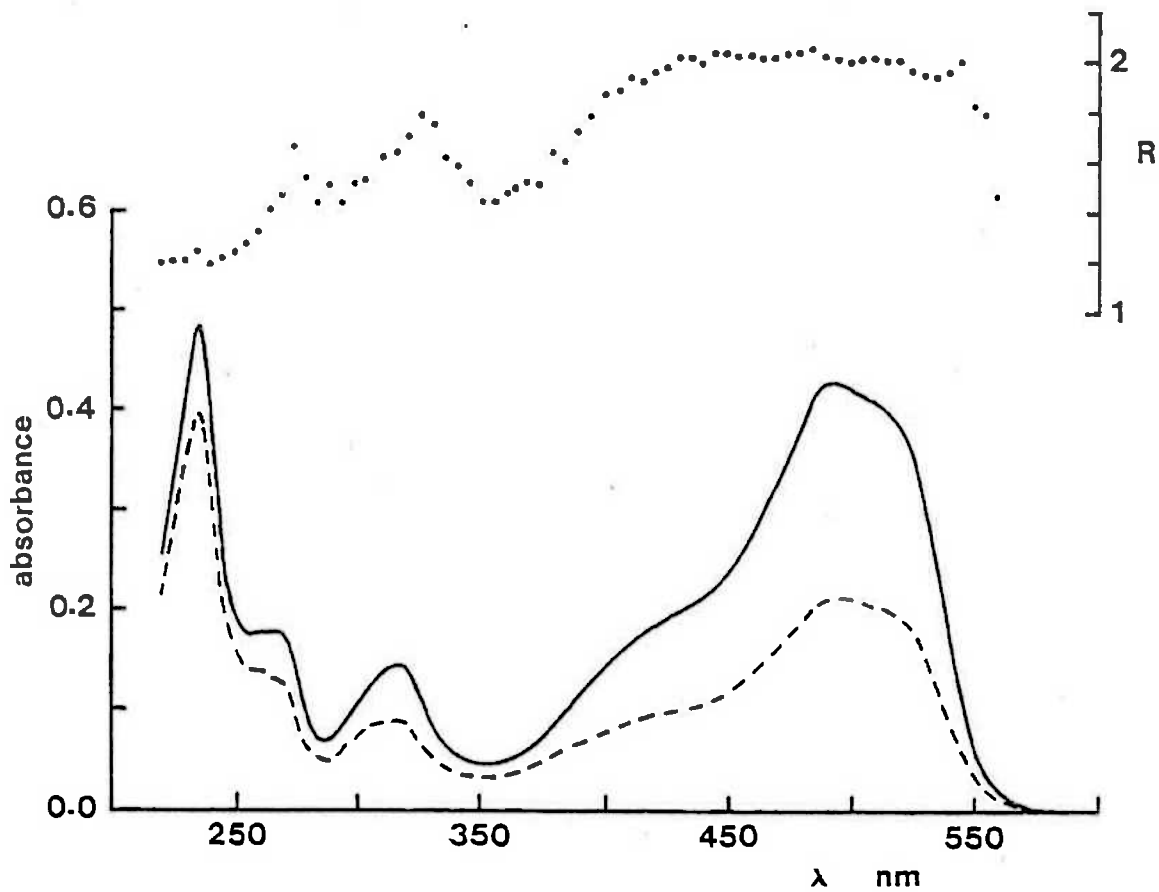


Fig. 5.1: Linear dichroic spectrum of tropaeolin in stretched poly (vinyl alcohol) film (left hand ordinate).

Solid curve = light polarised parallel to stretch

Dashed curve = light polarised perpendicular to stretch

Absorbance units are arbitrary.

The ratio of the parallel and perpendicular absorbances,

R , are shown as individual points and refer to the

right hand ordinate.

these results indicate that the absorption bands in this range are polarised approximately along a line interconnecting the naphthalenyl and phenyl groups, which is consistent with the results of Popov.¹⁰

Solutions of tropaeolin ($3.8 \times 10^{-5} \text{ mol dm}^{-3}$) show a very weak luminescence band, centred at approximately 550 nm (see Fig. 5.2). Luminescence spectra for o-hydroxy azo compounds have previously been reported.^{11,12} However, these spectra have been recorded in hydrocarbon solvents, and at very low temperatures (77 and 93K), in contrast to the results presented here, which have been obtained from aqueous solutions at 298K. According to Nurmukhametov et al.¹¹ the luminescence of o-hydroxy azo compounds is due to the presence of the intramolecular hydrogen bond, which reduces the probability of deactivation through vibrational processes. Gabor et al,¹² however, suggested that the luminescence is due to the hydrazone tautomer of these compounds.

As stated in the preceding chapter, the possibility must be considered that the presence of cyclodextrin in a dye solution may cause a spectral change, even without any direct interaction between dye and cyclodextrin occurring. In order to eliminate this possibility, the spectrum of tropaeolin was recorded in water and in a 0.03 mol dm^{-3} aqueous solution of glucose (see Fig. 5.3). It can be seen that the spectra are almost indistinguishable. Thus, any spectral changes observed on the addition of cyclodextrin can be attributed to complexation with the dye.

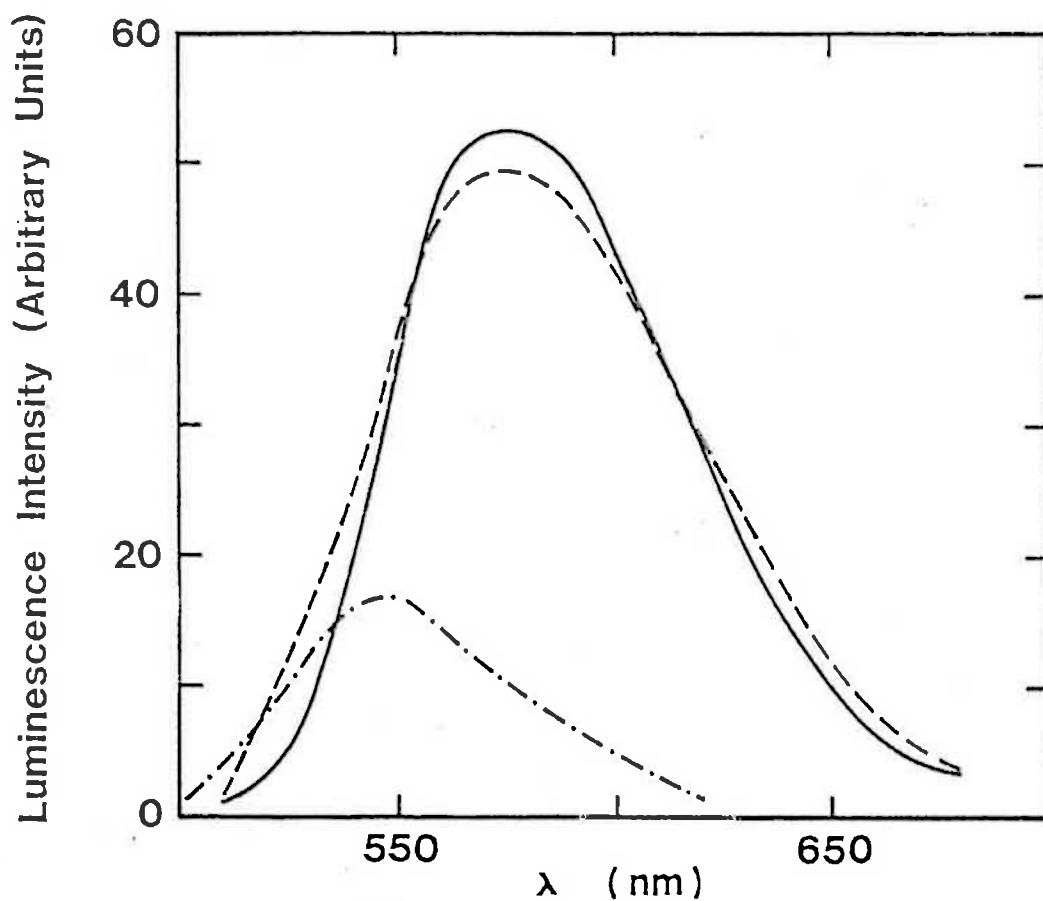


Fig. 5.2: Luminescence spectrum ($\lambda_{\text{ex}} = 380$ nm) of tropaeolin ($3.8 \times 10^{-5} \text{ mol dm}^{-3}$) alone (dotted curve) and in the presence of β -CD (dashed curve) and γ -CD (solid curve) at pH 5.5, 25°C. The β - and γ -CD concentrations were 9.9×10^{-3} and $1.0 \times 10^{-2} \text{ mol dm}^{-3}$ respectively.

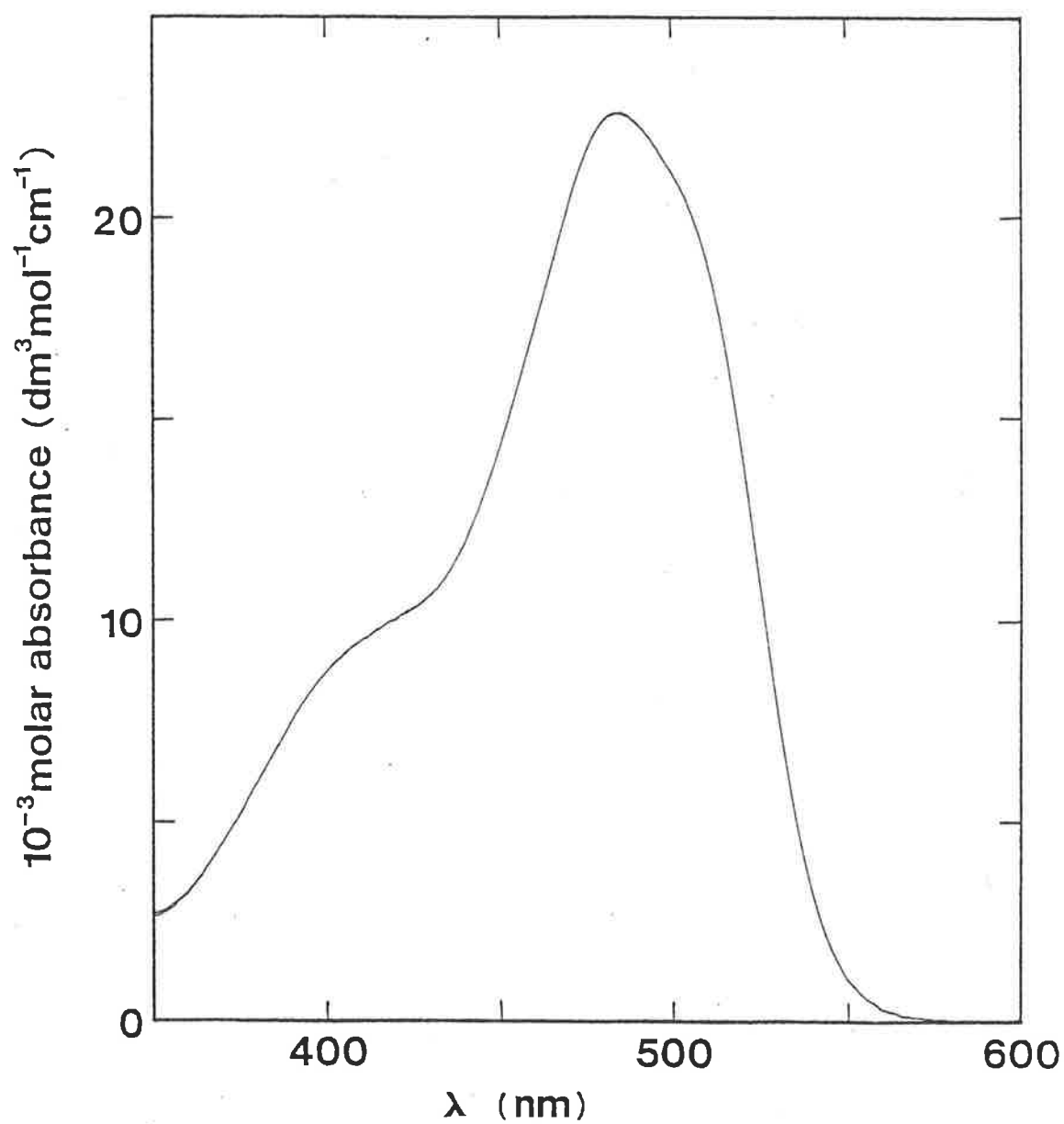


Fig. 5.3: Visible absorption spectrum of tropaeolin ($3.9 \times 10^{-5} \text{ mol dm}^{-3}$) in water and in a 0.03 mol dm^{-3} aqueous solution of glucose.

5.3 The Interaction of Tropaeolin with α -Cyclodextrin

The addition of α -CD ($1.01 \times 10^{-2} \text{ mol dm}^{-3}$) to an aqueous solution of tropaeolin ($3.86 \times 10^{-5} \text{ mol dm}^{-3}$) resulted in no significant changes in the dye's absorption or luminescence spectra, neither was any induced circular dichroism apparent. Temperature-jump studies revealed no relaxations other than those observed for the dye alone. Thus, it appears that α -CD is either not able to include the tropaeolin anion, or the association constant is too low for the detection of an inclusion complex.

If these results are compared to those of the methyl orange/ α -CD system, which gave significant spectral changes and a large association constant, the data support the previous assertion that it is the uncharged dimethylaniline end of methyl orange rather than the negatively charged benzenesulphonate end which is preferentially included by the cyclodextrin cavity.

5.4 The Interaction of Tropaeolin with β -Cyclodextrin

a) Temperature-Jump

Temperature-jump studies of tropaeolin and β -CD revealed a relaxation characterised by an increase in absorbance at 480 nm, whose amplitude was substantially greater than that of the slow relaxation observed for the dye alone, at all except the lowest β -CD concentrations. The reciprocal relaxation times ($1/\tau$) of this process are given in Table 5.1, and appear in Fig. 5.4, plotted against the total β -CD concentration. The variation of $1/\tau$ with β -CD concentration is similar to that presented earlier for methyl orange in the presence of γ -CD, and also for the interaction of crystal violet with γ -CD,¹³ which were both found to be consistent

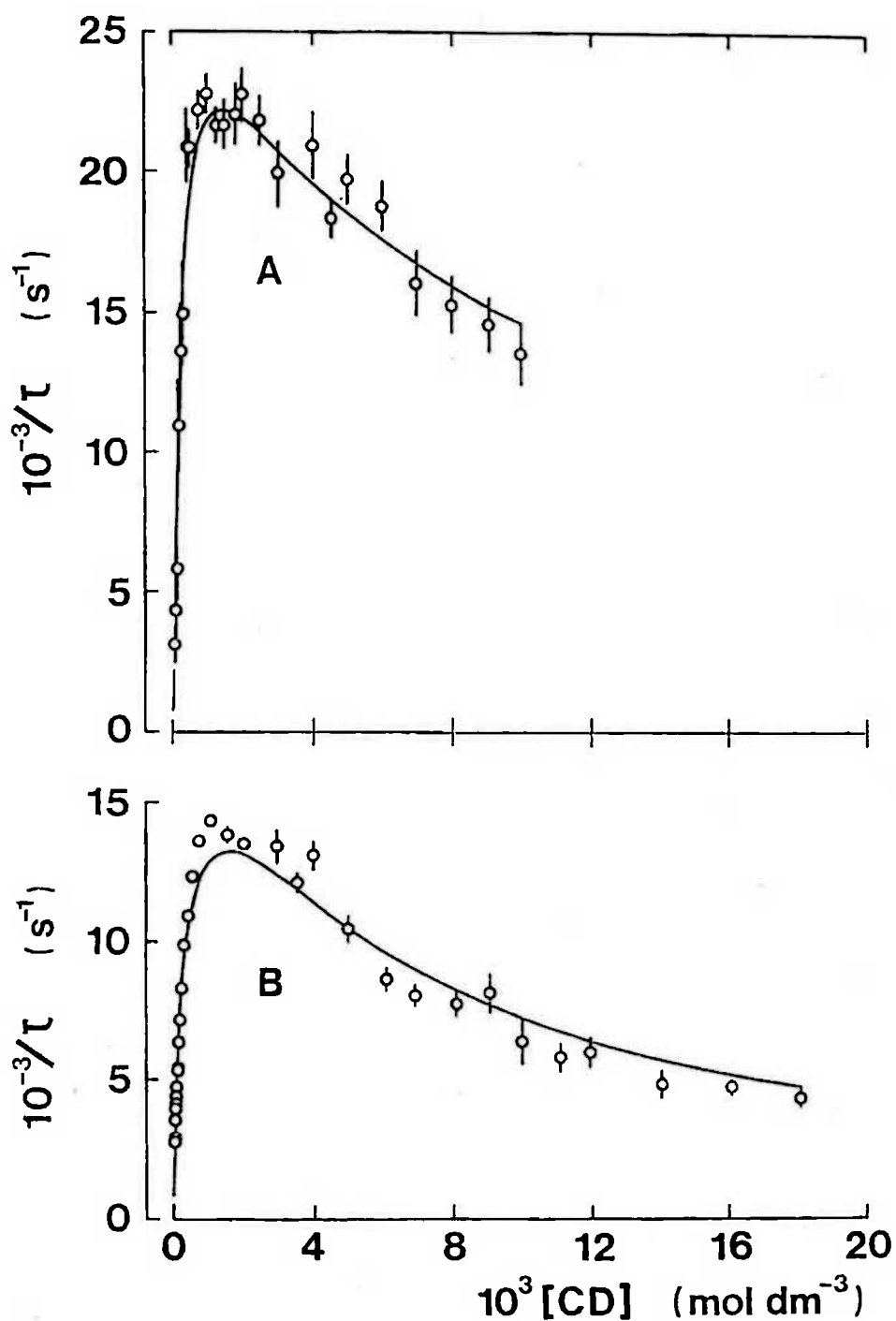
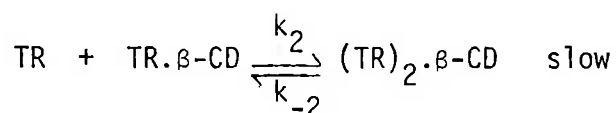
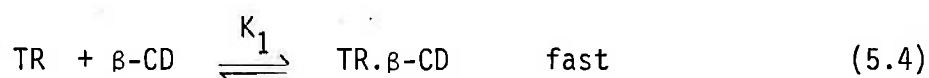


Fig. 5.4: Reciprocal relaxation times for TR/ β -CD (A) and TR/ γ -CD mixtures (B) as a function of total cyclodextrin concentration at pH 5.5, 25°C.

The solid curve represents the best fit of the data to equations (5.5) and (5.9) for β - and γ -CD respectively.

with a mechanism involving dimerisation of the dye within the cyclodextrin cavity. In the case of the tropaeolin/ β -CD interaction the results are best described by the following scheme:



Using the method of Bernasconi¹⁴ or Czerlinski,⁹ equation (5.5) may be derived for the variation of $1/\tau$ with concentration.

$$1/\tau = k_2 \cdot \frac{[\text{TR}]([\text{TR}] + [\text{TR}\cdot\beta\text{-CD}] + 4[\beta\text{-CD}])}{[\text{TR}] + [\beta\text{-CD}] + 1/K_1} + k_{-2} \quad (5.5)$$

where all concentrations are equilibrium values.

The $1/\tau$ data were fitted to equation (5.5) by using the DATAFIT routine. The best-fit line is shown in Fig. 5.4, and the derived parameters are given below.

$$k_2 = 5 (\pm 6) \times 10^9 \text{ dm}^3 \text{ mol}^{-1} \text{ sec}^{-1}$$

$$k_{-2} = 1.3 (\pm 1.5) \times 10^3 \text{ sec}^{-1}$$

$$K_1 = 7.1 (\pm 0.7) \times 10^2 \text{ dm}^3 \text{ mol}^{-1}$$

$$K_2 = 4 (\pm 7) \times 10^6 \text{ dm}^3 \text{ mol}^{-1}$$

The large uncertainties in the parameters are a consequence of the small relaxation amplitudes observed at low β -CD concentrations.

b) Absorption Spectra

The visible absorption spectrum of tropaeolin ($3.8 \times 10^{-5} \text{ mol dm}^{-3}$), alone and in the presence of β -CD concentrations ranging from 4×10^{-5} to $5 \times 10^{-3} \text{ mol dm}^{-3}$, is shown in Fig. 5.5.

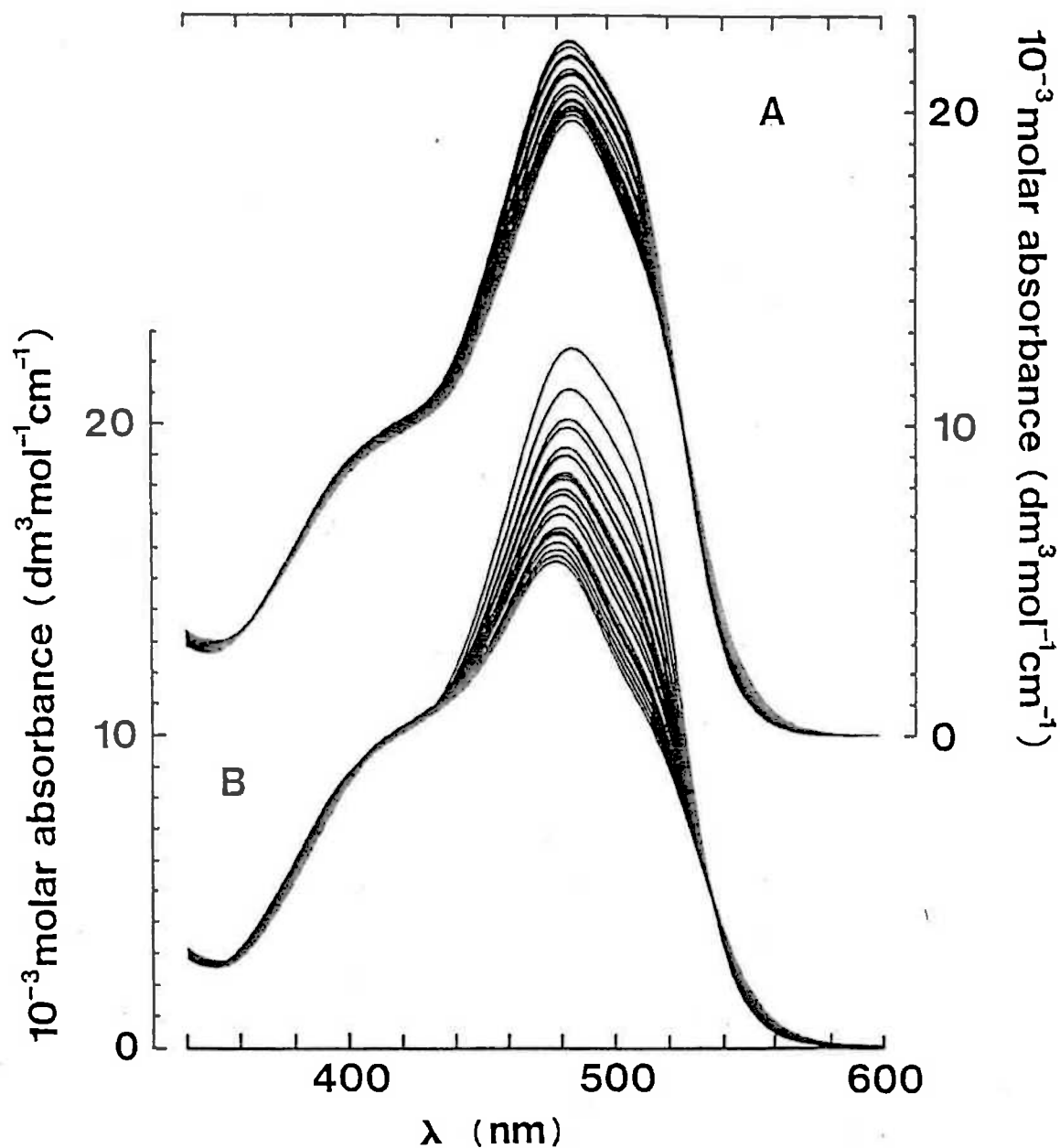
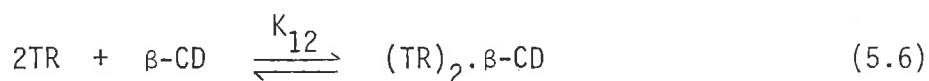


Fig. 5.5: Visible absorption spectrum of tropaeolin ($3.8 \times 10^{-5} \text{ mol dm}^{-3}$) in the presence of β -CD (data set A - right hand scale) and γ -CD (data set B - left hand scale) at 25°C . In both cases the molar absorbance observed at 480 nm decreases systematically as the cyclodextrin concentration increases. The β - and γ -CD concentration ranges were 0 - 4.99×10^{-3} and 0 - $2.56 \times 10^{-3} \text{ mol dm}^{-3}$ respectively.

A hypochromic effect and a slight red shift of approximately 3 nm were observed on complexation. Although the temperature-jump results indicate the existence of two coupled equilibria and three different environments for the tropaeolin anion, attempts to fit the absorbance data to this mechanism failed to give a unique fit. A possible reason for this is that one of the species has a negligible concentration across the entire cyclodextrin concentration range and therefore does not significantly contribute to the absorbance. Another possibility is that the absorption spectrum of two of the species are indistinguishable. Therefore, in order to find a value for the association constant, the two steps of scheme (5.4) were combined to give equation (5.6):



In accordance with this scheme the observed absorbance (A) can be assumed to be given by equation (5.7):

$$A = \epsilon_{\text{TR}}[\text{TR}] + 2\epsilon_{(\text{TR})_2 \cdot \beta\text{-CD}}[(\text{TR})_2 \cdot \beta\text{-CD}] \quad (5.7)$$

The equilibrium spectra of Fig. 5.5 were fitted to equation (5.7) by using the routine DATAFIT at all monitored wavelengths, except those in the regions where small changes in absorbance prevented DATAFIT from converging to a best-fit value. The K_{12} values, calculated at 2 nm intervals in the range 440-500 nm were weighted according to their estimated uncertainties, and averaged to give the following value:

$$K_{12} = 2.03 (\pm 0.21) \times 10^7 \text{ dm}^6 \text{ mol}^{-2}$$

Using this value of K_{12} , together with the directly determined molar absorptivities of tropaeolin, the spectrum of the $(\text{TR})_2 \cdot \beta\text{-CD}$

complex was derived, and this is shown in Fig. 5.6.

c) Induced Circular Dichroism

The induced circular dichroic spectrum of tropaeolin in a hundred-fold excess of β -CD is shown in Fig. 5.7. Although the linear dichroism results (in the absence of cyclodextrin) seem to show that the absorption bands of tropaeolin in the range 500-550 nm are polarised approximately along the long axis of the molecule, the circular dichroic spectrum induced by β -cyclodextrin exhibits both positive and negative signals in this range. This is consistent with dimer formation within the cyclodextrin cavity, which would result in the splitting of each monomer absorption band into two bands with mutually perpendicular transition moments due to the exciton interaction (see Appendix D).

d) Luminescence Spectrum

The luminescence spectrum of tropaeolin in a two hundred and fifty-fold excess of β -CD is shown in Fig. 5.2. It can be seen a large enhancement of the dye's luminescence is observed. Whether the luminescence is actually fluorescence or phosphorescence, it is not possible to say without measurements of the luminescence lifetime. Fluorescence enhancements have often been observed on complexation with cyclodextrin (see Sec. 2.1). Since it seems that tropaeolin forms a dimer within the β -CD cavity, however, it is perhaps more likely that it is in fact an enhancement in phosphorescence which is observed (see Appendix D).

5.5 The Interaction of Tropaeolin with γ -Cyclodextrin

a) Temperature-Jump

Temperature-jump studies of solutions of tropaeolin and γ -CD

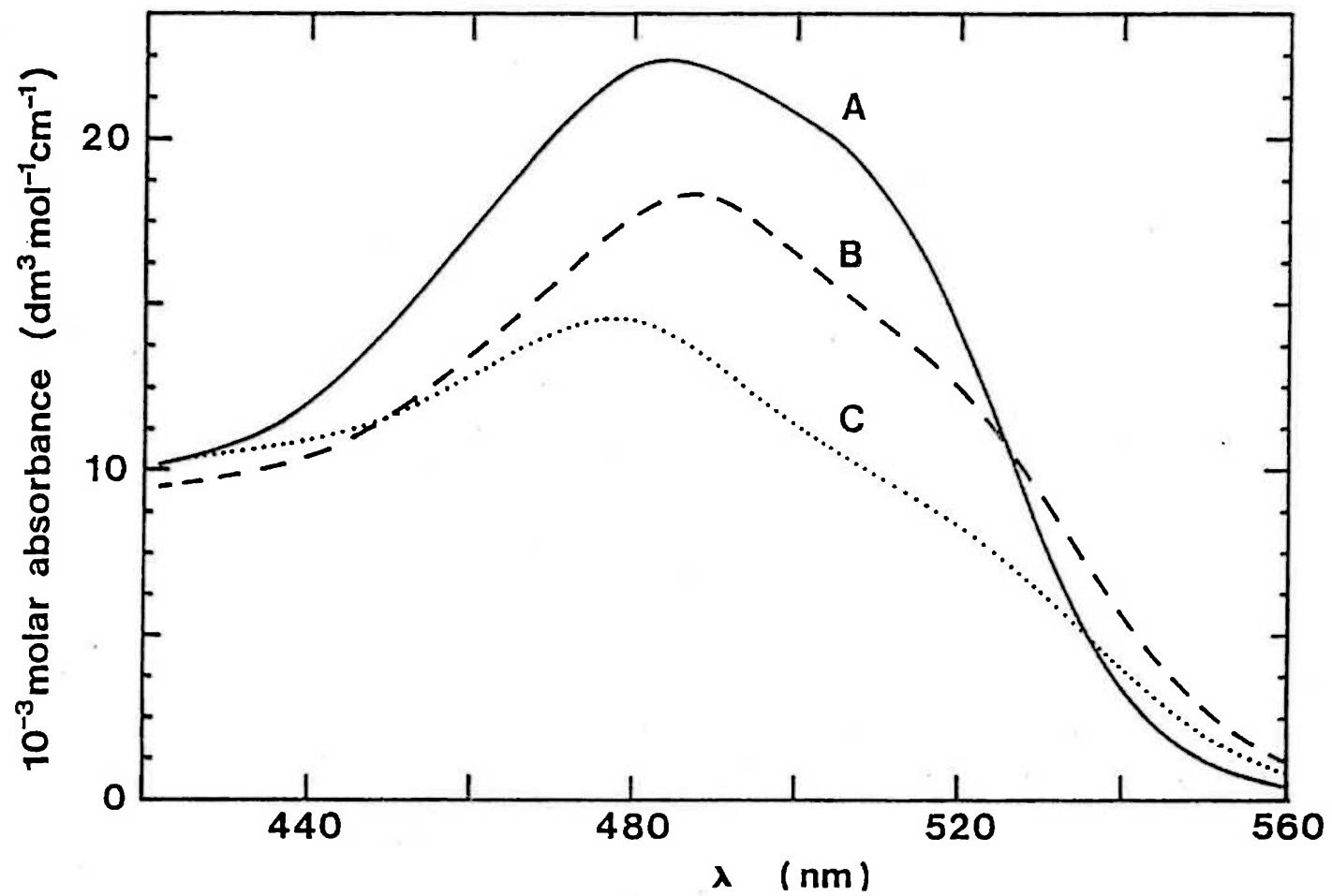


Fig. 5.6: Derived spectra of the $(\text{TR})_2 \cdot \beta\text{-CD}$ (B) and $(\text{TR})_2 \cdot \gamma\text{-CD}$ (C) complexes compared to the spectrum of TR alone (A).

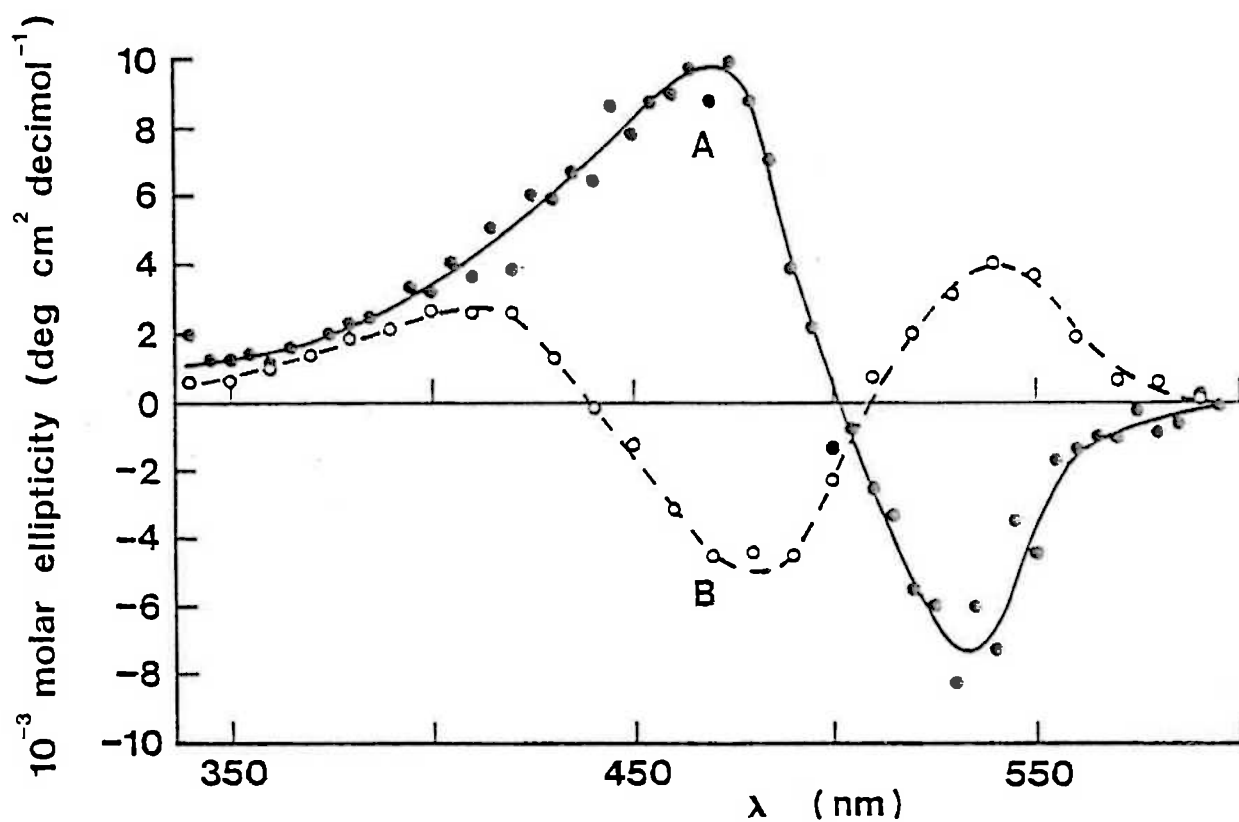
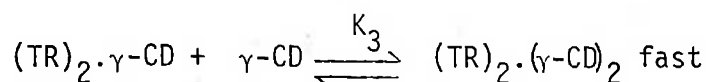
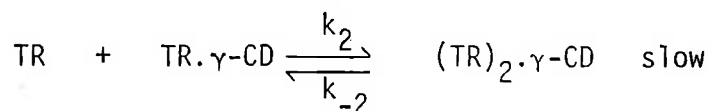
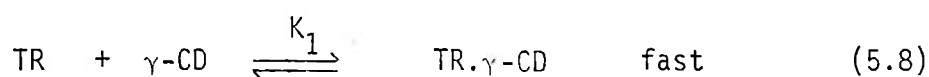


Fig. 5.7: Induced circular dichroic spectrum of tropaeolin ($3.8 \times 10^{-5} \text{ mol dm}^{-3}$) in the presence of β -CD (B) and γ -CD (A). The β - and γ -CD concentrations were 4.0×10^{-3} and $3.4 \times 10^{-3} \text{ mol dm}^{-3}$ respectively.

revealed a relaxation characterised by an increase in absorbance at 480 nm, whose amplitude was substantially greater than that of the slow relaxation observed for the dye alone, over the entire γ -CD concentration range studied. The reciprocal relaxation times ($1/\tau$) of this process are given in Table 5.2, and appear in Fig. 5.4, plotted against total γ -CD concentration. As in the case of the interaction with β -CD, the variation of $1/\tau$ with cyclodextrin concentration suggests a mechanism involving dimerisation of the dye within the cyclodextrin cavity. In the case of the tropaeolin/ γ -CD interaction, however, the results are best described by a three step mechanism:



This mechanism is the same as that earlier proposed for the methyl orange/ γ -CD interaction (equation (4.7)). Thus the equation characterising the variation of $1/\tau$ with γ -CD concentration (equation (5.9)) is identical to equation (4.8) except that TR has replaced MO:

$$1/\tau = k_2 \cdot \frac{[\text{TR}] ([\text{TR}] + [\text{TR}\cdot\gamma\text{-CD}] + 4[\gamma\text{-CD}])}{[\text{TR}] + [\gamma\text{-CD}] + 1/K_1} \quad (5.9)$$

$$+ k_{-2} \cdot \frac{[(\text{TR})_2\cdot\gamma\text{-CD}] + 1/K_3}{[\gamma\text{-CD}] + [(\text{TR})_2\cdot\gamma\text{-CD}] + 1/K_3}$$

where all concentrations are equilibrium values.

The $1/\tau$ data were fitted to equation (5.9) by using the DATAFIT routine. The best-fit line is shown in Fig. 5.4, and the derived parameters are given below:

$$k_2 = 2.27 (\pm 0.61) \times 10^9 \text{ dm}^3 \text{ mol}^{-1} \text{ sec}^{-1}$$

$$k_{-2} = 1.35 (\pm 0.23) \times 10^3 \text{ sec}^{-1}$$

$$K_1 = 4.18 (\pm 1.47) \times 10^2 \text{ dm}^3 \text{ mol}^{-1}$$

$$K_2 = 1.68 (\pm 0.54) \times 10^6 \text{ dm}^3 \text{ mol}^{-1}$$

$$K_3 = 1.77 (\pm 1.54) \times 10^2 \text{ dm}^3 \text{ mol}^{-1}$$

b) Absorption Spectra

The visible absorption spectrum of tropaeolin ($3.8 \times 10^{-5} \text{ mol dm}^{-3}$), alone and in the presence of γ -CD concentrations ranging from 1×10^{-5} to $2.5 \times 10^{-3} \text{ mol dm}^{-3}$, is shown in Fig. 5.5. A large hypochromic effect and a blue shift of approximately 7 nm were observed on complexation. The spectral variations were analysed through the analogous equilibrium to that shown in equation 5.6 by using the DATAFIT routine. In order to prevent contributions from the species $(\text{TR})_2 \cdot (\gamma\text{-CD})_2$, only spectra recorded at cyclodextrin concentrations $\leq 5 \times 10^{-4} \text{ mol dm}^{-3}$ were used.*

The K_{12} values, calculated at 2 nm intervals in the range 470-520 nm, were weighted according to their estimated uncertainties and averaged to give the following value:

$$K_{12} = 4.10 (\pm 0.11) \times 10^8 \text{ dm}^6 \text{ mol}^{-2}$$

* The spectral changes caused by the formation of the 2:2 complex were too small to enable the determination of its formation constant.

This value compares with $K_1K_2 = 7.0 (\pm 3.3) \times 10^8 \text{ dm}^6 \text{ mol}^{-2}$ derived from the temperature-jump data, and indicates a satisfactory degree of internal consistency. Using the value of K_{12} above, together with the directly determined molar absorptivities of tropaeolin, the spectrum of the $(\text{TR})_2 \cdot \gamma\text{-CD}$ complex was derived, and this is shown in Fig. 5.6.

It may be noted that the spectra of $(\text{TR})_2 \cdot \beta\text{-CD}$ and $(\text{TR})_2 \cdot \gamma\text{-CD}$ in the visible region both show a hypochromic effect relative to the spectrum of free dye. This has also been observed on dimerisation in the absence of cyclodextrin.⁸ The differences in the spectra of $(\text{TR})_2 \cdot \beta\text{-CD}$ and $(\text{TR})_2 \cdot \gamma\text{-CD}$, however, suggest that the two complexes have a slightly different structure, presumably caused by the differences in cavity sizes.

A comparison of the K_{12} values derived from the spectra shows that the $(\text{TR})_2 \cdot \gamma\text{-CD}$ complex is approximately twenty times more stable than the $(\text{TR})_2 \cdot \beta\text{-CD}$ complex. Thus, it appears that $\gamma\text{-CD}$, because of its larger cavity size, is better able to accommodate the tropaeolin dimer.

c) Induced Circular Dichroism

The induced circular dichroic spectrum of tropaeolin in a hundred-fold excess of $\gamma\text{-CD}$ is shown in Fig. 5.7. As was the case with $\beta\text{-CD}$, both positive and negative peaks are seen in the range 400-550 nm, which is thus consistent with dimer formation. However, the reversal in sign for the bands, centred at approximately 475 and 535 nm, on comparing $\beta\text{-CD}$ to $\gamma\text{-CD}$, implies different geometries for the inclusion complexes in each case. For example, the reversal could be accounted for by a difference

in the orientation of the dimer with respect to the cyclodextrin cavity, or by a difference in the structure of the dimer itself.

d) Luminescence Spectrum

The luminescence spectrum of tropaeolin in a two hundred and fifty-fold excess of γ -CD is shown in Fig. 5.2. A large enhancement of the dye's luminescence was observed, which is very similar to that exhibited in the presence of β -CD.

5.6 The Interaction of the Tropaeolin Di-anion with the Cyclodextrins

The addition of α -, β -, or γ -CD ($2 \times 10^{-3} \text{ mol dm}^{-3}$) to a solution of tropaeolin ($3.8 \times 10^{-5} \text{ mol dm}^{-3}$) in 1 mol dm^{-3} NaOH (pH 13.4) resulted in no significant changes in the dye's absorption spectrum, suggesting that inclusion does not occur.

At this high pH the hydroxyl group of the dye becomes deprotonated and hence the dye possesses a double negative charge. The cyclodextrins also become negatively charged due to the loss of a proton from one of the secondary hydroxyl groups. Thus, the fact that inclusion does occur for β - and γ -CD at pH 5.5, but not at pH 13.4 could be due to electrostatic repulsion. The negative charges on the tropaeolin would presumably hinder dimerisation of the dye, and the negative charge on the cyclodextrin would hinder the association of the dye and cyclodextrin. An alternative explanation could be that the tropaeolin di-anion, because of its double negative charge, is more strongly solvated than the tropaeolin mono-anion. Hence, the removal of the solvating water molecules from the di-anion, and its transfer into the cyclodextrin cavity may be energetically unfavourable.

Table 5.1: Concentrations and observed reciprocal relaxation times for the inclusion of TR by β -CD (pH 5.5, 25°C).

[TR] (mol dm ⁻³ x 10 ⁵)	[β -CD] (mol dm ⁻³)	¹ / _{τ} (sec ⁻¹ x 10 ⁻³)
3.81(±0.03)	3.97(±0.06) x 10 ⁻⁵	3.11(±0.68)
3.80(±0.03)	8.0 (±0.1) x 10 ⁻⁵	4.35(±1.90)
3.78(±0.03)	1.20(±0.02) x 10 ⁻⁴	5.83(±1.86)
3.79(±0.03)	1.80(±0.02) x 10 ⁻⁴	10.96(±1.68)
3.75(±0.03)	2.40(±0.03) x 10 ⁻⁴	13.63(±2.09)
3.75(±0.03)	2.99(±0.04) x 10 ⁻⁴	14.95(±2.27)
3.81(±0.03)	3.96(±0.03) x 10 ⁻⁴	20.90(±1.31)
3.73(±0.03)	4.88(±0.04) x 10 ⁻⁴	20.87(±0.71)
3.79(±0.03)	7.39(±0.05) x 10 ⁻⁴	22.17(±0.73)
3.77(±0.03)	9.84(±0.06) x 10 ⁻⁴	22.76(±0.73)
3.76(±0.03)	1.235(±0.008) x 10 ⁻³	21.64(±0.65)
3.72(±0.03)	1.480(±0.009) x 10 ⁻³	21.65(±0.87)
3.81(±0.03)	1.79(±0.01) x 10 ⁻³	22.04(±1.13)
3.71(±0.03)	1.98(±0.01) x 10 ⁻³	22.76(±0.96)
3.78(±0.03)	2.49(±0.02) x 10 ⁻³	21.83(±0.93)
3.75(±0.03)	3.01(±0.02) x 10 ⁻³	19.96(±1.18)
3.69(±0.03)	4.00(±0.02) x 10 ⁻³	20.94(±1.23)
3.78(±0.02)	4.53(±0.02) x 10 ⁻³	18.38(±0.70)
3.80(±0.03)	4.99(±0.03) x 10 ⁻³	19.75(±0.89)
3.80(±0.02)	5.99(±0.02) x 10 ⁻³	18.76(±0.89)
3.78(±0.02)	6.98(±0.03) x 10 ⁻³	16.07(±1.15)
3.75(±0.02)	7.98(±0.03) x 10 ⁻³	15.30(±1.01)
3.75(±0.02)	9.06(±0.04) x 10 ⁻³	14.60(±0.97)
3.75(±0.02)	9.98(±0.04) x 10 ⁻³	13.53(±1.07)

Table 5.2: Concentrations and observed reciprocal relaxation times for the inclusion of TR by γ -CD (pH 5.5, 25°C).

[TR] (mol dm ⁻³ x 10 ⁵)	[γ -CD] (mol dm ⁻³)	$1/\tau$ (sec ⁻¹ x 10 ⁻³)
3.82(±0.04)	1.00(±0.02) x 10 ⁻⁵	2.81(±0.04)
3.81(±0.04)	2.03(±0.03) x 10 ⁻⁵	2.99(±0.04)
3.77(±0.04)	2.87(±0.04) x 10 ⁻⁵	3.61(±0.04)
3.82(±0.04)	3.95(±0.06) x 10 ⁻⁵	3.97(±0.04)
3.84(±0.04)	4.88(±0.07) x 10 ⁻⁵	4.22(±0.04)
3.87(±0.05)	5.85(±0.08) x 10 ⁻⁵	4.46(±0.05)
3.81(±0.04)	7.0 (±0.1) x 10 ⁻⁵	4.81(±0.05)
3.88(±0.04)	7.6 (±0.1) x 10 ⁻⁵	5.10(±0.05)
3.85(±0.04)	9.0 (±0.1) x 10 ⁻⁵	5.41(±0.06)
3.83(±0.05)	1.00(±0.01) x 10 ⁻⁴	5.39(±0.05)
3.85(±0.05)	1.20(±0.02) x 10 ⁻⁴	6.34(±0.08)
3.82(±0.04)	1.58(±0.02) x 10 ⁻⁴	7.19(±0.10)
3.85(±0.05)	2.01(±0.03) x 10 ⁻⁴	8.29(±0.09)
3.82(±0.05)	2.95(±0.04) x 10 ⁻⁴	9.85(±0.12)
3.85(±0.05)	3.91(±0.04) x 10 ⁻⁴	10.92(±0.18)
3.85(±0.05)	5.21(±0.05) x 10 ⁻⁴	12.34(±0.20)
3.82(±0.04)	7.23(±0.07) x 10 ⁻⁴	13.59(±0.15)
3.84(±0.04)	1.04(±0.01) x 10 ⁻³	14.33(±0.17)
3.81(±0.04)	1.55(±0.02) x 10 ⁻³	13.84(±0.17)
3.81(±0.03)	1.99(±0.01) x 10 ⁻³	13.48(±0.25)
3.80(±0.03)	2.94(±0.02) x 10 ⁻³	13.40(±0.60)
3.71(±0.03)	3.52(±0.02) x 10 ⁻³	12.10(±0.38)
3.76(±0.03)	3.98(±0.02) x 10 ⁻³	13.06(±0.50)
3.80(±0.03)	4.98(±0.02) x 10 ⁻³	10.43(±0.50)
3.80(±0.03)	6.09(±0.03) x 10 ⁻³	8.62(±0.44)
3.79(±0.03)	6.91(±0.03) x 10 ⁻³	8.04(±0.38)
3.79(±0.03)	8.10(±0.04) x 10 ⁻³	7.75(±0.47)

cont'd.

Table 5.2 cont'd.

[TR] (mol dm ⁻³ x 10 ⁵)	[γ-CD] (mol dm ⁻³)	¹ / _τ (sec ⁻¹ x 10 ⁻³)
3.80(±0.03)	9.04(±0.04) x 10 ⁻³	8.13(±0.75)
3.77(±0.03)	9.99(±0.04) x 10 ⁻³	6.39(±0.82)
3.80(±0.03)	1.108(±0.005) x 10 ⁻²	5.82(±0.53)
3.79(±0.03)	1.194(±0.005) x 10 ⁻²	4.83(±0.50)
3.80(±0.03)	1.403(±0.006) x 10 ⁻²	4.75(±0.26)
3.78(±0.03)	1.805(±0.007) x 10 ⁻²	4.34(±0.30)

Bibliography

1. Suzuki, M. and Y. Sasaki, *Chem.Pharm.Bull.*, 27, 1343 (1979).
2. Suzuki, M., Y. Sasaki and M. Suguira, *Chem.Pharm.Bull.*, 27, 1797 (1979).
3. Suzuki, M. and Y. Sasaki, *Chem.Pharm.Bull.*, 29, 585 (1981).
4. Suzuki, M. and Y. Sasaki, *Chem.Pharm.Bull.*, 32, 832 (1984).
5. Zollinger, H., "Azo and Diazo Chemistry. Aliphatic and Aromatic Compounds", Interscience, New York, 1961.
6. Reeves, R.L. and R.S. Kaiser, *J.Org.Chem.*, 35, 3670 (1970).
7. Milicevic, B. and G. Eigenmann, *Helv.Chim.Acta*, 47, 1039 (1964).
8. Reeves, R.L., M.S. Maggio and S.A. Harkaway, *J.Phys.Chem.*, 83, 2359 (1979).
9. Czerlinski, G.H., "Chemical Relaxation", Marcel Dekker, New York, 1966.
10. Popov, K.R., *Opt.Spectrosk.*, 33, 51 (1972).
11. Nurmukhametov, R.N., D.N. Shigorin, Yu.I. Kozlov and V.A. Puchkov, *Opt.Spectrosk.*, 11, 606 (1961).
12. Gabor, G., Y. Frei, D. Gegiou, M. Kaganowitch and E. Fischer, *Israel J.Chem.*, 5, 193 (1967).
13. Schiller, R.L., J.H. Coates and S.F. Lincoln, *J.Chem.Soc., Faraday Trans. I*, 80, 1257 (1984).
14. Bernasconi, C.F., "Relaxation Kinetics", Academic Press, New York, 1976.

CHAPTER VI

CHAPTER VI: THE INTERACTION OF ROCCELLIN WITH THE
CYCLODEXTRINS.

6.1 Introduction

The interaction between the azo dye roccellin (RO), alternatively known as acid red 88 or naphthalene red J, and the cyclodextrins has not previously been investigated. Matsui and Mochida,¹ however, have studied the interaction of the *para*-hydroxy isomer of roccellin with α - and β -cyclodextrin. They found no evidence of complex formation with α -CD, which they interpreted as indicating that the cavity of α -CD is too small for the inclusion of a naphthyl group of the dye. On the addition of β -CD they observed significant changes in the absorption spectrum of the dye, which they suggested was due to the formation of a 1:1 inclusion complex. They did not extend their investigation to the interaction of the dye with γ -CD.

The similarity of the structure of roccellin to that of its *para*-hydroxy isomer and also to that of tropaeolin suggests that roccellin may be a suitable guest molecule for β - and/or γ -CD. The major aim of the investigation is to determine whether or not roccellin, with its larger aromatic residues in comparison with methyl orange and tropaeolin, can form a dimer within the cavities of β - or γ -CD, and if possible determine the mechanism of complex formation.

6.2 Properties of the Roccellin Anion

Aqueous solutions of roccellin exhibit a red colour, which deepens on the addition of a small amount of 1 mol dm^{-3} sodium

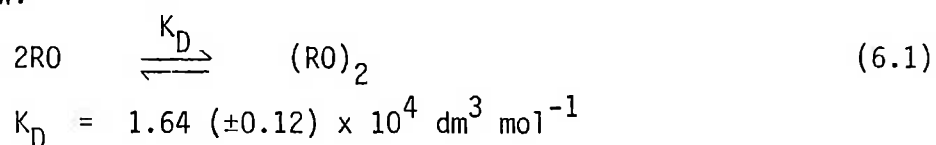
hydroxide solution. This colour change occurs in the pH range 11-12. Thus, by analogy with tropaeolin, it seems most likely that the pK_a of the hydroxyl group of roccellin is close to 11.4. Since all of the results presented, except where explicitly stated otherwise, have been derived from measurements made on solutions in water ($pH \approx 7$), contributions from any forms of the dye other than the roccellin mono-anion have generally been neglected.

The similarity of the structures of roccellin and tropaeolin suggests that, as well as possessing an intramolecular hydrogen bond, roccellin could also undergo azo-hydrazone tautomerisation. Since the solvent used (water) is polar, however, the hydrazone form should be the predominant species.²

The most important difference between roccellin and the dyes previously studied is that it has a large tendency to aggregate, which is enhanced by the addition of salts. For the utilisation of the Joule-heating temperature-jump apparatus, solutions of high ionic strength are required, to allow the rapid passage of charge between the electrodes of the temperature-jump cell. At high ionic strengths, however, it was found that roccellin is insoluble. Therefore, no temperature-jump experiments could be made. An alternative kinetic method, which does not require high salt concentrations, is the pressure-jump technique. This is another chemical relaxation method, in which a rapid decrease in pressure is used to perturb the equilibrium, rather than a sudden rise in temperature. A pressure-jump apparatus, similar in design to that described in the literature,³ is currently undergoing development in this laboratory. Preliminary experiments

on solutions of the dye alone showed no evidence of any relaxations. The absorbance of solutions of roccellin in the presence of β - or γ -CD were found to be slightly pressure dependent, however the relaxations observed were within the response time of the instrument (approximately 1 millisecond), thus preventing the determination of the relaxation times. Therefore, no kinetic information is available on the dimerisation of the dye, or on its interaction with the cyclodextrins.

In order to determine the dimerisation constant of the dye, a series of dye solutions ($0.2\text{--}16 \times 10^{-5} \text{ mol dm}^{-3}$) were prepared in water, and the absorbance measured at a fixed wavelength (510 nm) on a Zeiss PMQ II spectrophotometer. From the variation of the apparent molar absorbance of the dye with concentration, the dimerisation constant, K_D , describing the equilibrium, equation (6.1), was determined, and this is given below.

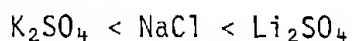


In order to avoid contributions to the absorption spectrum from roccellin dimers when investigating the interaction of the dye with the cyclodextrins, all absorption spectra were recorded at a very low dye concentration ($2 \times 10^{-6} \text{ mol dm}^{-3}$), so that the vast majority of the dye was in the monomer form.

An approximation to the visible absorption spectrum of the dimer was obtained by recording the spectra of dye solutions, to

which varying amounts of lithium sulphate ($0-0.5 \text{ mol dm}^{-3}$) had been added. It was found that there was a large decrease in intensity of the band at approximately 505 nm, followed by an increase in intensity of a band at approximately 440 nm as the lithium sulphate concentration increased (see Fig. 6.1). No isosbestic points were observed, indicating the formation of higher aggregates than the dimer. Thus, the major effect of dimerisation on the visible absorption spectrum is to cause a decrease in intensity of the main absorption band.

Lithium sulphate was chosen as the salt used in the above experiment, because it was found that the dye was more soluble in solutions of lithium sulphate than in those of any other salt tried. Its solubility in various salt solutions was found to increase in the order,



The differences in solubility are probably due to the size of the cation and the extent of its hydration. According to a number of workers^{4,5} the cations aid aggregation by binding between the negatively charged sulphonate groups, and thus decreasing repulsion (see Fig. 6.2).

In contrast to tropaeolin, roccellin does not exhibit a luminescence spectrum in aqueous solution at 25°C. However, if lithium sulphate is added, a band appears at approximately 600 nm, which increases in intensity and shifts towards 620 nm as the lithium sulphate concentration is increased (see Fig. 6.3). Accordingly, this band is attributable to roccellin aggregates (dimers, trimers, etc.).

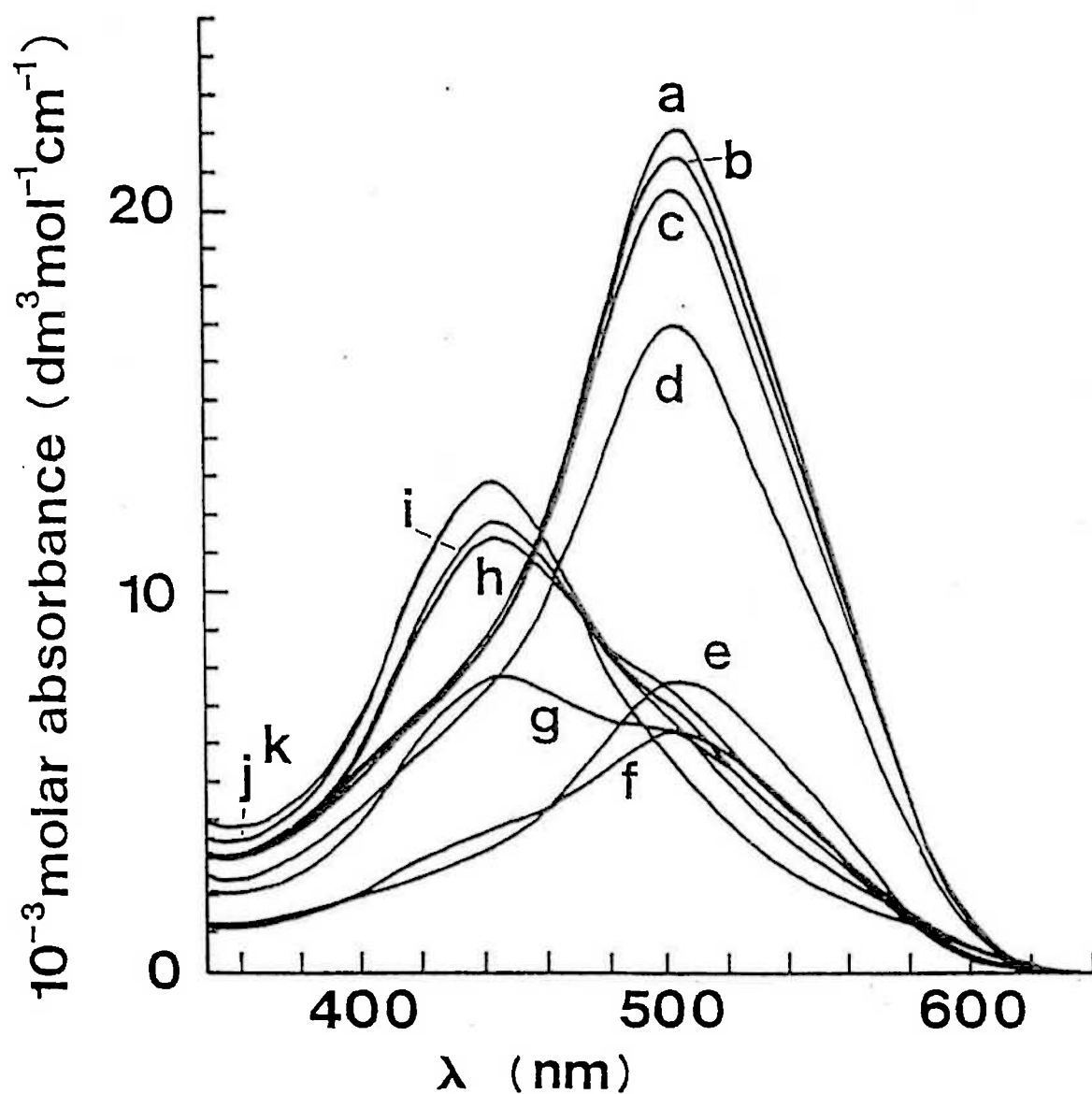


Fig. 6.1: Visible absorption spectrum of roccellin ($5 \times 10^{-5} \text{ mol dm}^{-3}$) in the presence of increasing concentrations of lithium sulphate at 25°C .

$[\text{Li}_2\text{SO}_4] = 0, 0.01, 0.05, 0.075, 0.10, 0.15, 0.20, 0.225, 0.25, 0.30$ and 0.50 mol dm^{-3} from a to k.

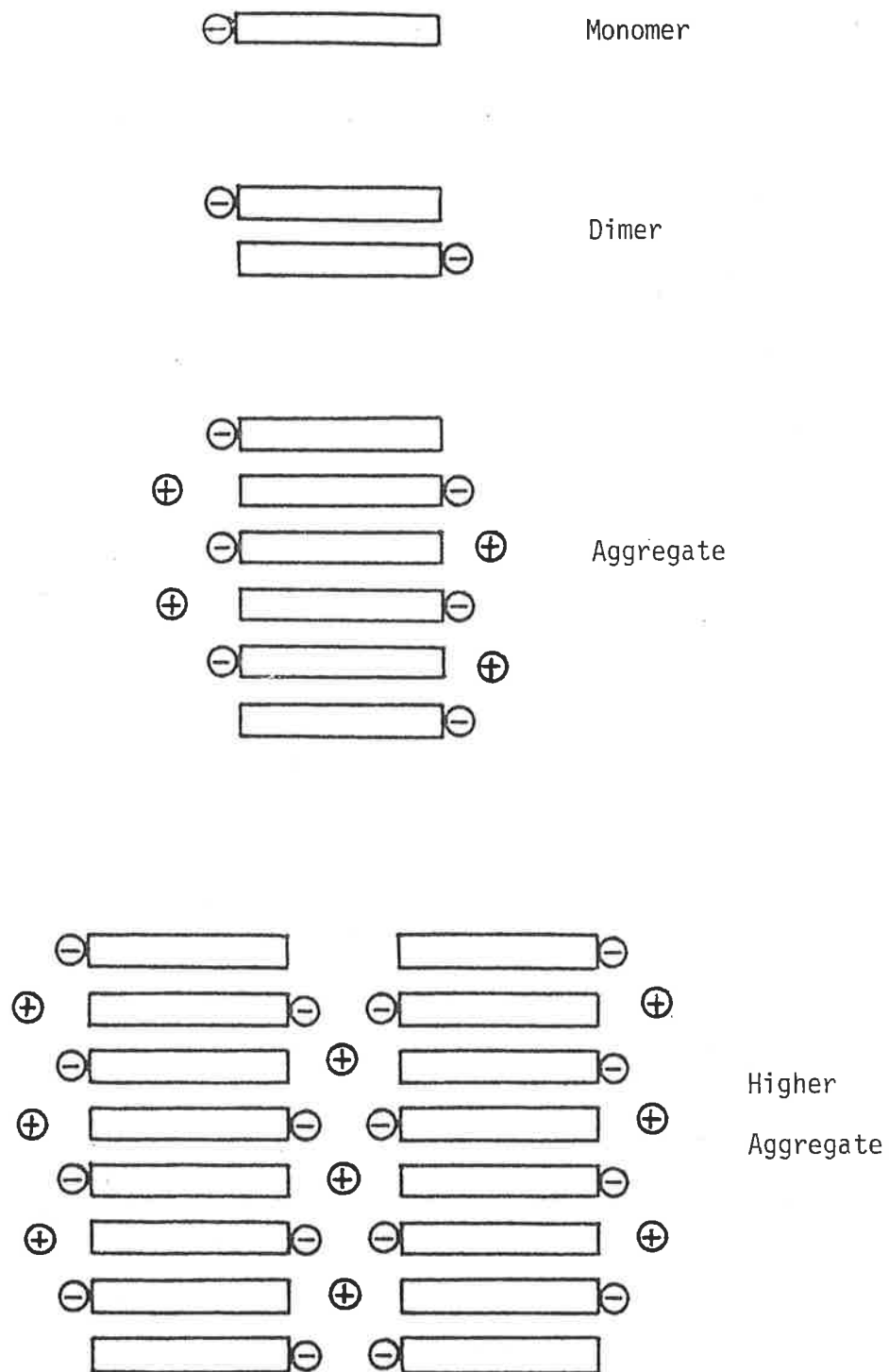


Fig. 6.2: Schematic diagram of the aggregation of a mono-sulphonated planar azo dye, facilitated by positively charged counter-ions.

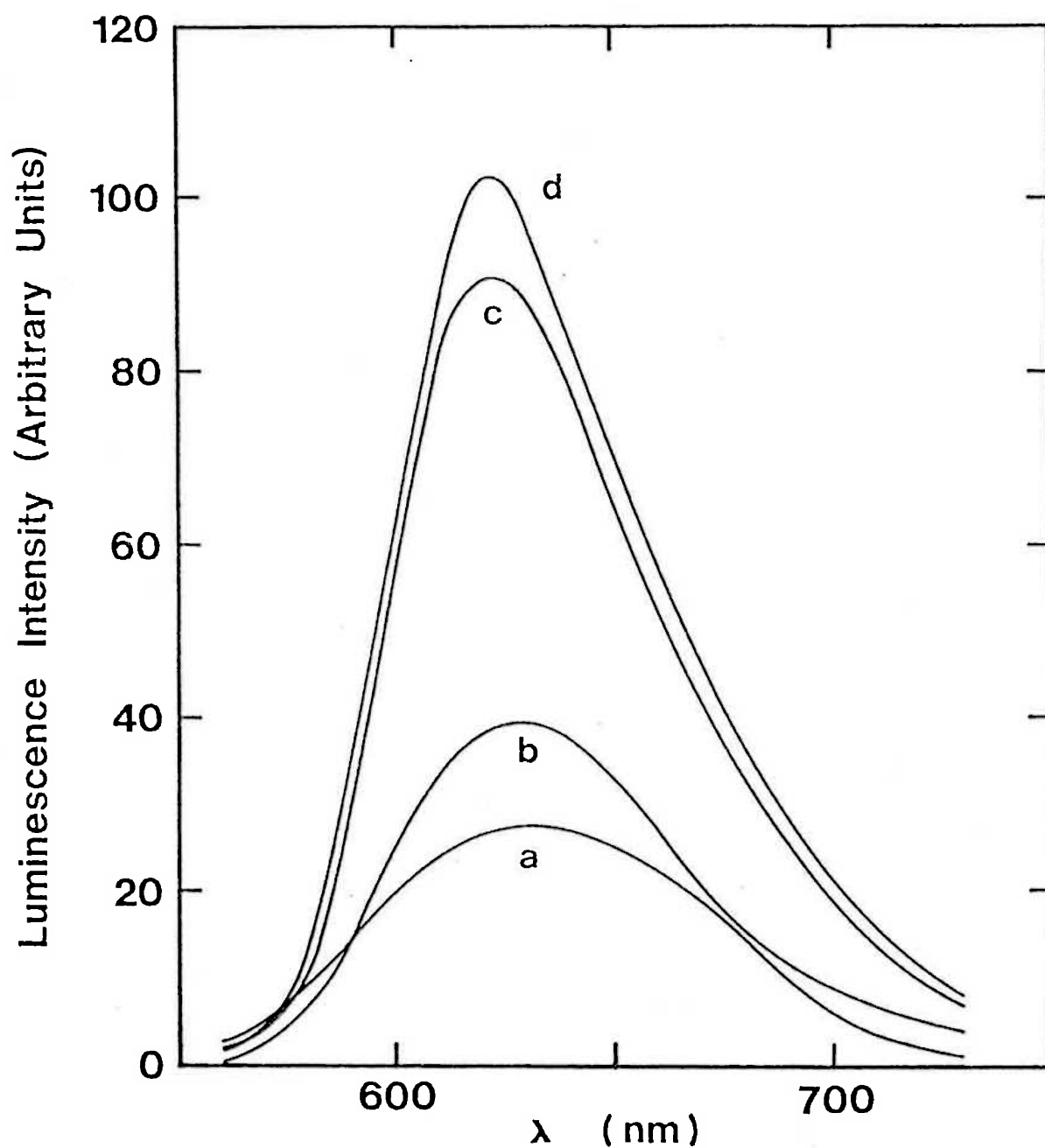


Fig. 6.3: Luminescence spectrum ($\lambda_{\text{ex}} = 420 \text{ nm}$) of roccellin ($4.9 \times 10^{-5} \text{ mol dm}^{-3}$) in the presence of increasing concentrations of lithium sulphate at 25°C .

$[\text{Li}_2\text{SO}_4] = 0.15, 0.20, 0.30$ and 0.50 mol dm^{-3} from a to d.

The linear dichroism of roccellin in stretched poly(vinyl alcohol) film is shown in Fig. 6.4. It can be seen that over the range 450-580 nm the absorbance parallel to the direction of stretch is substantially greater than that perpendicular to the direction of stretch, and that the dichroic ratio is relatively constant. Assuming that the dye molecules orientate with the long molecular axis parallel to the direction of stretch, these results indicate that the absorption bands in this range are polarised approximately along a line interconnecting the centres of the two naphthyl groups.

Before proceeding to discuss the interaction of roccellin with the cyclodextrins, the possibility must be considered that the presence of cyclodextrin may cause a spectral change, even without any direct interaction between dye and cyclodextrin occurring. In order to eliminate this possibility, the spectrum of roccellin was recorded in water and in a 0.01 mol dm^{-3} aqueous solution of glucose (see Fig. 6.5). It can be seen that only a very small increase in molar absorbance is observed in comparison with the much larger effects caused by the addition of the cyclodextrins. Thus, the effects caused by the cyclodextrins can be confidently attributed to complexation with the dye.

6.3 The Interaction of Roccellin with α -Cyclodextrin

The addition of α -CD ($4.04 \times 10^{-3} \text{ mol dm}^{-3}$) to an aqueous solution of roccellin ($4.01 \times 10^{-5} \text{ mol dm}^{-3}$) resulted in no significant changes in the dye's absorption and no measurable luminescence, neither was any induced circular dichroism apparent. Thus, it appears that α -CD is either not able to include the roccellin anion, or else the association constant is too low for

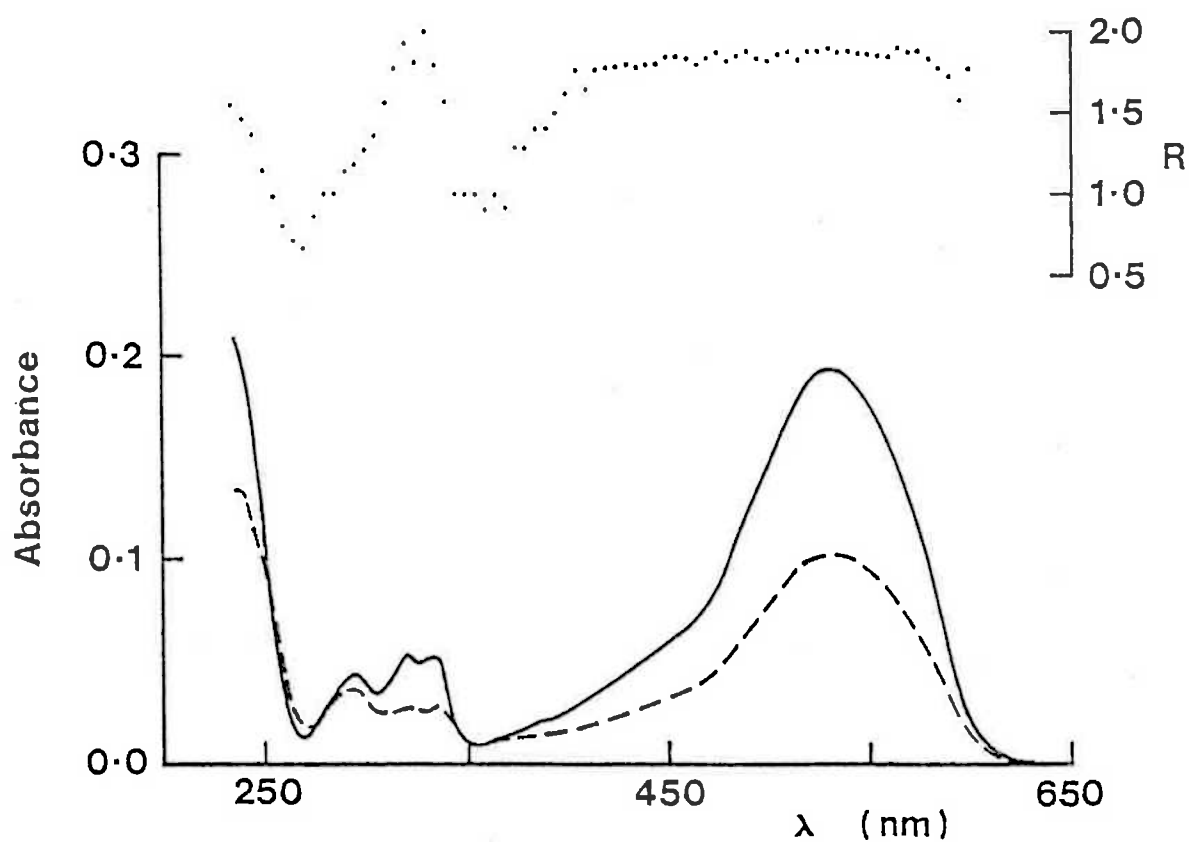


Fig. 6.4: Linear dichroic spectrum of roccellin in stretched poly (vinyl alcohol) film (left hand ordinate).
 Solid curve = light polarised parallel to stretch.
 Dashed curve = light polarised perpendicular to stretch.
 Absorbance units are arbitrary.
 The ratio of the parallel and perpendicular absorbances, R , are shown as individual points and refer to the right hand ordinate.

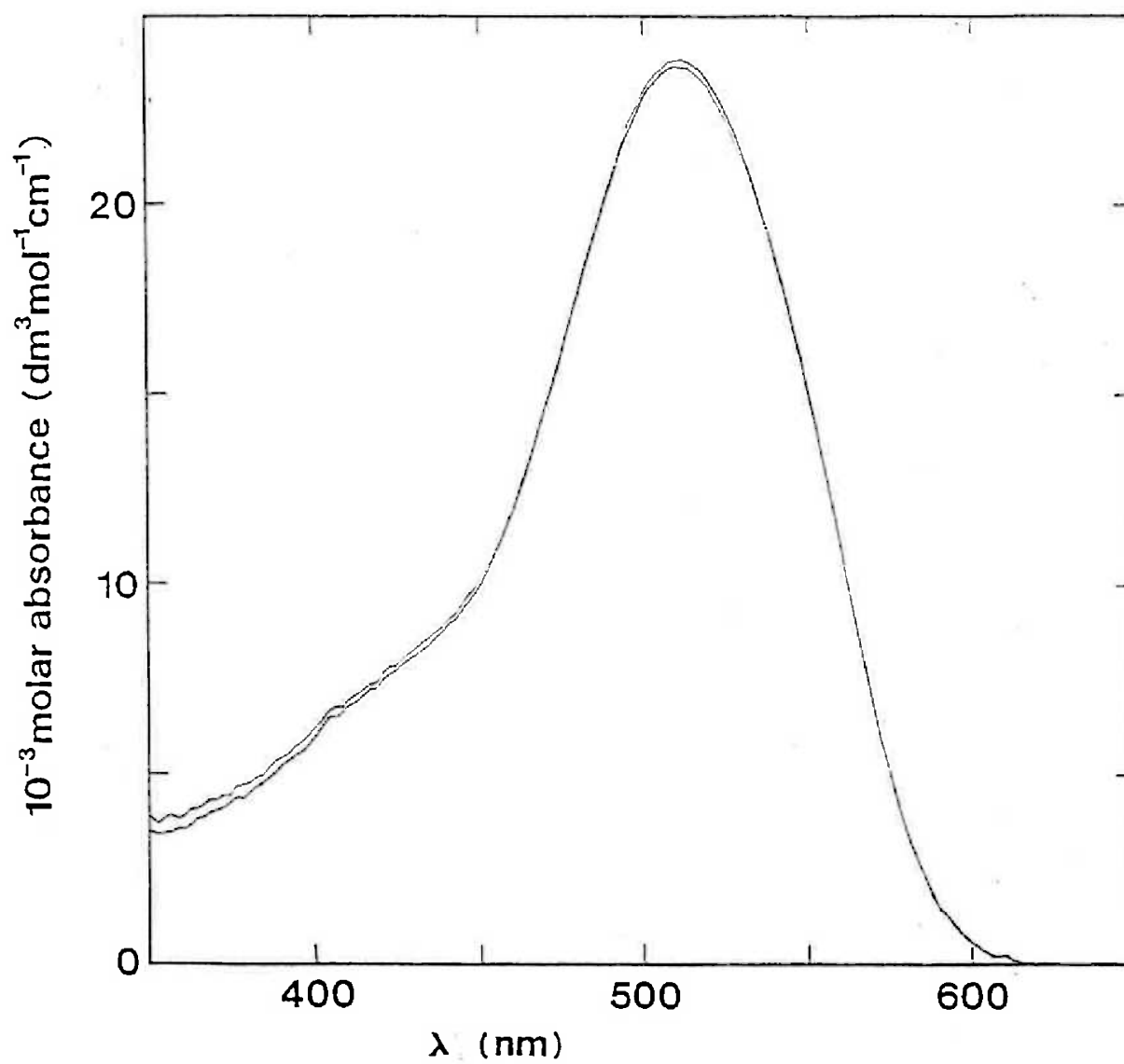


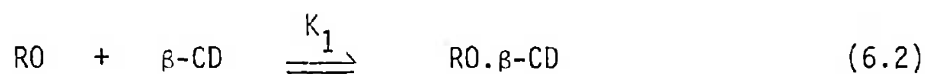
Fig. 6.5: Visible absorption spectrum of roccellin (2.0×10^{-6} mol dm^{-3}) in water (lower curve) and in a 0.01 mol dm^{-3} aqueous solution of glucose (upper curve).

the detection of inclusion. Based on CPK molecular model building, it seems most likely that the naphthyl groups of roccellin are too large to fit inside the cavity of α -CD.

6.4 The Interaction of Roccellin with β -Cyclodextrin

a) Absorption Spectra

The visible absorption spectrum of roccellin (2.0×10^{-6} mol dm^{-3}) alone and in the presence of β -CD concentrations ranging from 5×10^{-5} to 2×10^{-3} mol dm^{-3} is shown in Fig. 6.6. A small hypochromic effect was observed on complexation, but no wavelength shift was detectable. It was found that the data are adequately described by a 1:1 complex formation equilibrium:



In accordance with this scheme the observed absorbance (A) can be assumed to be given by equation (6.3).

$$A = \epsilon_{\text{RO}}[\text{RO}] + \epsilon_{\text{RO} \cdot \beta\text{-CD}}[\text{RO} \cdot \beta\text{-CD}] \quad (6.3)$$

The equilibrium spectra of Fig. 6.6 were fitted to equation (6.3) by using the routine DATAFIT at all monitored wavelengths, except those where small changes in absorbance prevented DATAFIT from converging to a best-fit value. The K_1 values, calculated at 2 nm intervals in the range 570-462 nm were weighted according to their estimated uncertainties, and averaged to give the following value.

$$K_1 = 7.20 (\pm 0.88) \times 10^2 \text{ dm}^3 \text{ mol}^{-1}$$

Using this value of K_1 , together with the directly determined molar absorptivities of roccellin, the spectrum of the RO. β -CD

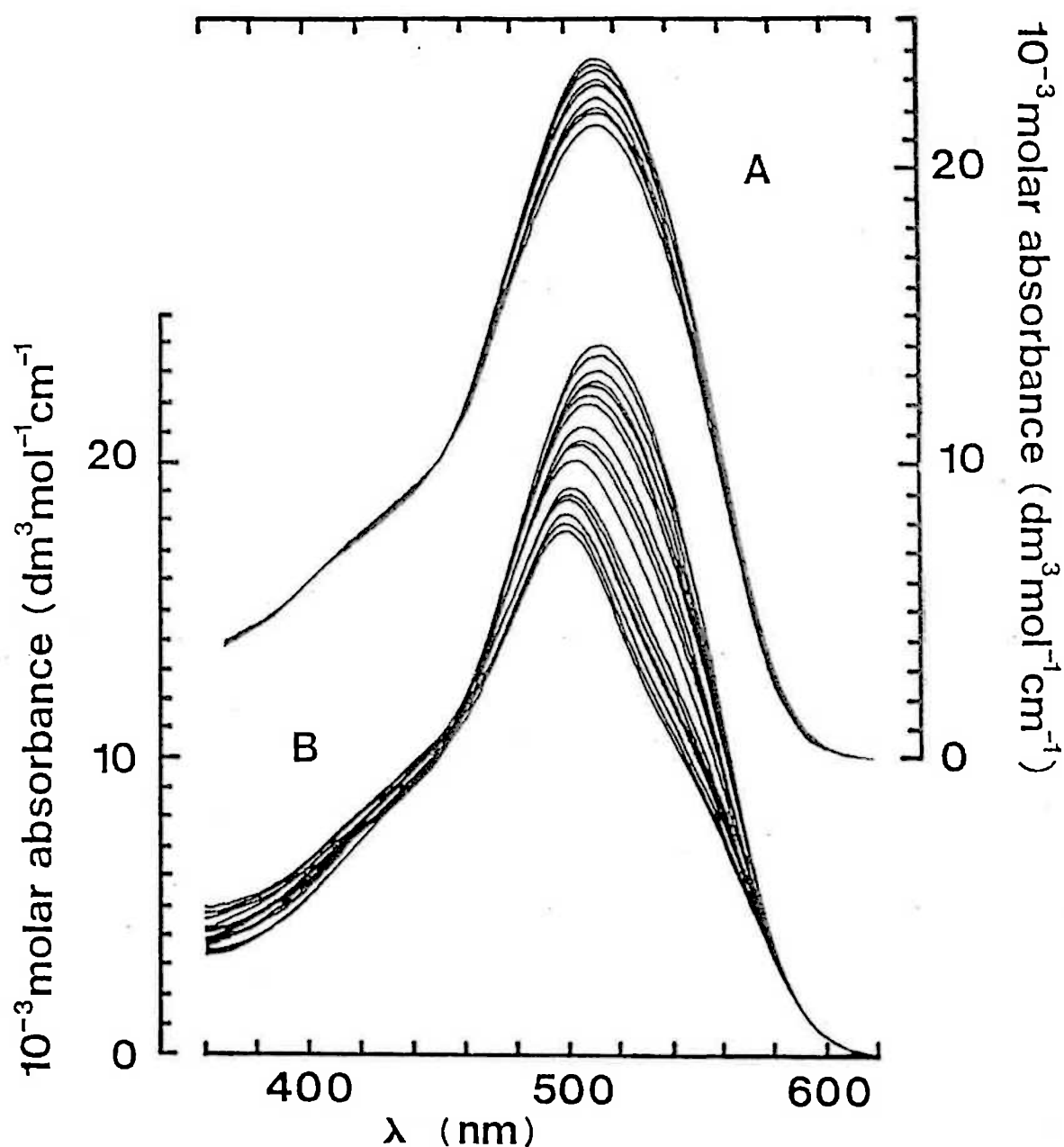


Fig. 6.6: Visible absorption spectrum of roccellin ($2.0 \times 10^{-6} \text{ mol dm}^{-3}$) in the presence of β -CD (data set A - right hand scale) and γ -CD (data set B - left hand scale) at 25°C . In both cases the molar absorbance observed at 500 nm decreases systematically as the cyclodextrin concentration increases. The β - and γ -CD concentration ranges were $0 - 2 \times 10^{-3}$ and $0 - 5 \times 10^{-4} \text{ mol dm}^{-3}$ respectively.

complex was derived, and this is shown in Fig. 6.7.

It is interesting to note the similarity of the K_1 values determined for the RO/ β -CD system ($7.20 \times 10^2 \text{ dm}^3 \text{ mol}^{-1}$), and that derived from temperature-jump measurements for the TR/ β -CD system ($7.1 \times 10^2 \text{ dm}^3 \text{ mol}^{-1}$). This similarity suggests that it may be the β -naphthol moiety of the dyes which is preferentially included by β -CD in both cases.

b) Induced Circular Dichroism

The induced circular dichroic spectrum of roccellin in a hundred-fold excess of β -CD is shown in Fig. 6.8. The spectrum exhibits only positive signals, and no splitting due to exciton interactions is apparent. Thus, the spectrum appears to be consistent with the formation of a 1:1 complex.

c) Luminescence Spectrum

The luminescence spectrum of roccellin in a hundred-fold excess of β -CD is shown in Fig. 6.9. As was previously found with tropaeolin, the inclusion of the dye results in the enhancement of its luminescence. (In the absence of β -CD the dye exhibits no measurable luminescence under these conditions.) This enhancement is presumably due to the protection that the cyclodextrin cavity confers on the dye from collisional interactions with various quenching agents, such as water and dissolved oxygen.

6.5 The Interaction of Roccellin with γ -Cyclodextrin

a) Absorption Spectra

The visible absorption spectrum of roccellin ($2.0 \times 10^{-6} \text{ mol dm}^{-3}$) alone and in the presence of γ -CD concentrations ranging from 2.5×10^{-7} to $5 \times 10^{-4} \text{ mol dm}^{-3}$ is shown in Fig. 6.6. A

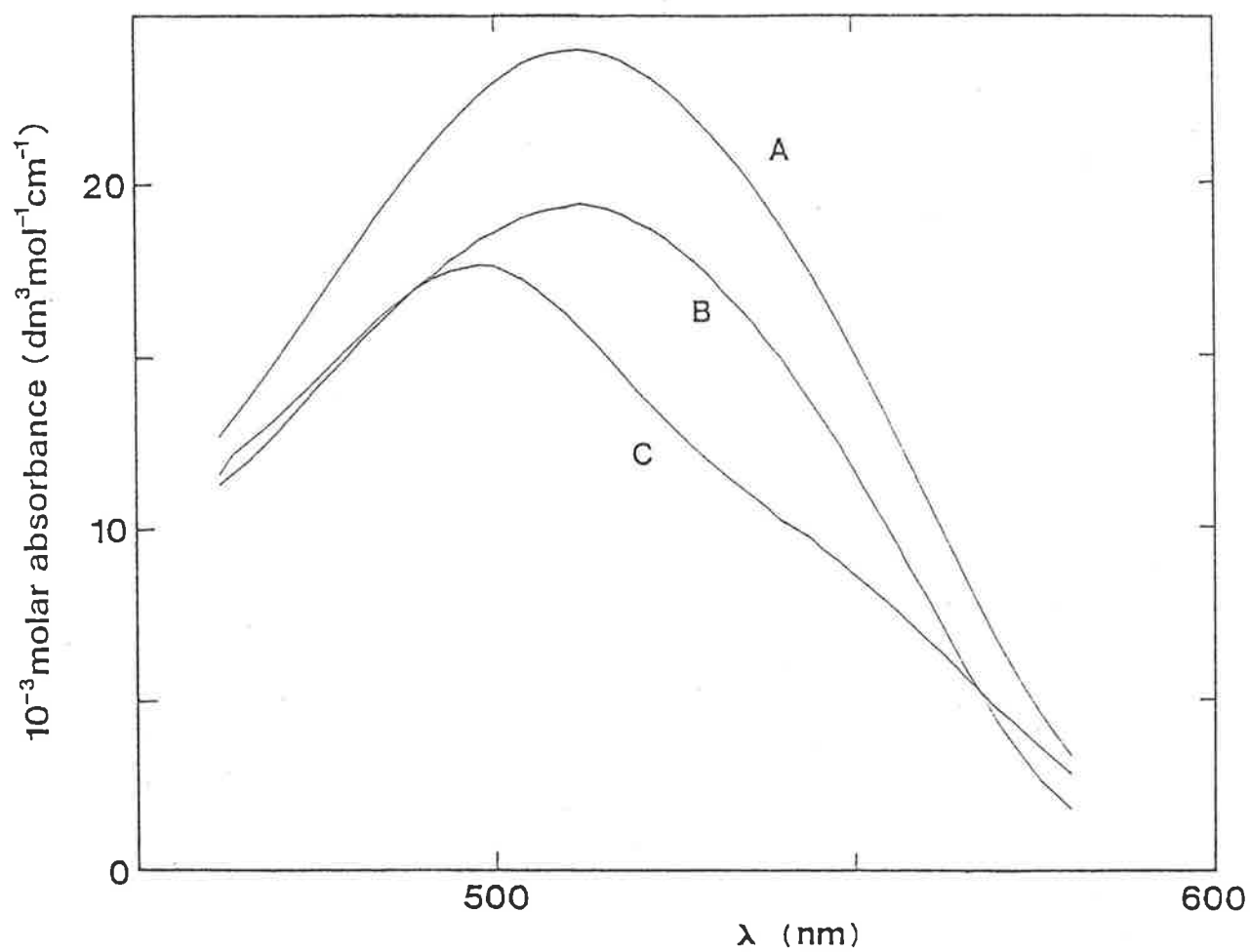


Fig. 6.7: Derived spectra of the $\text{R0} \cdot \beta\text{-CD}$ (B) and $(\text{R0})_2 \cdot \gamma\text{-CD}$ (C) complexes compared to the spectrum of R0 alone (A).

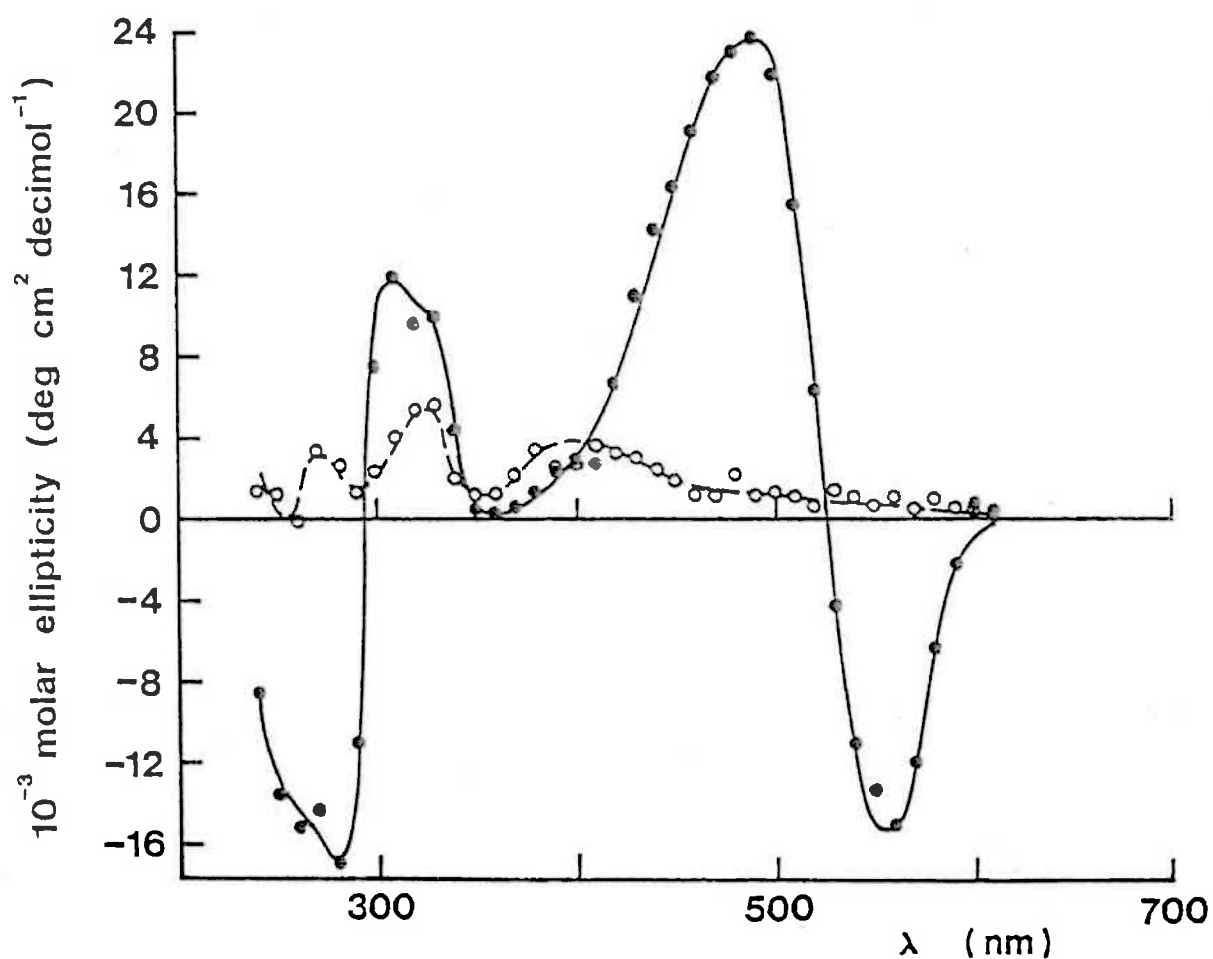


Fig. 6.8: Induced circular dichroic spectrum of roccellin in the presence of β -CD (dashed curve) and γ -CD (solid curve) at 25°C.

Dashed curve: $[\text{RO}] = 4.0 \times 10^{-5} \text{ mol dm}^{-3}$, $[\beta\text{-CD}] = 4.0 \times 10^{-3} \text{ mol dm}^{-3}$.

Solid curve: $[\text{RO}] = 8.0 \times 10^{-6} \text{ mol dm}^{-3}$, $[\gamma\text{-CD}] = 8.0 \times 10^{-4} \text{ mol dm}^{-3}$.

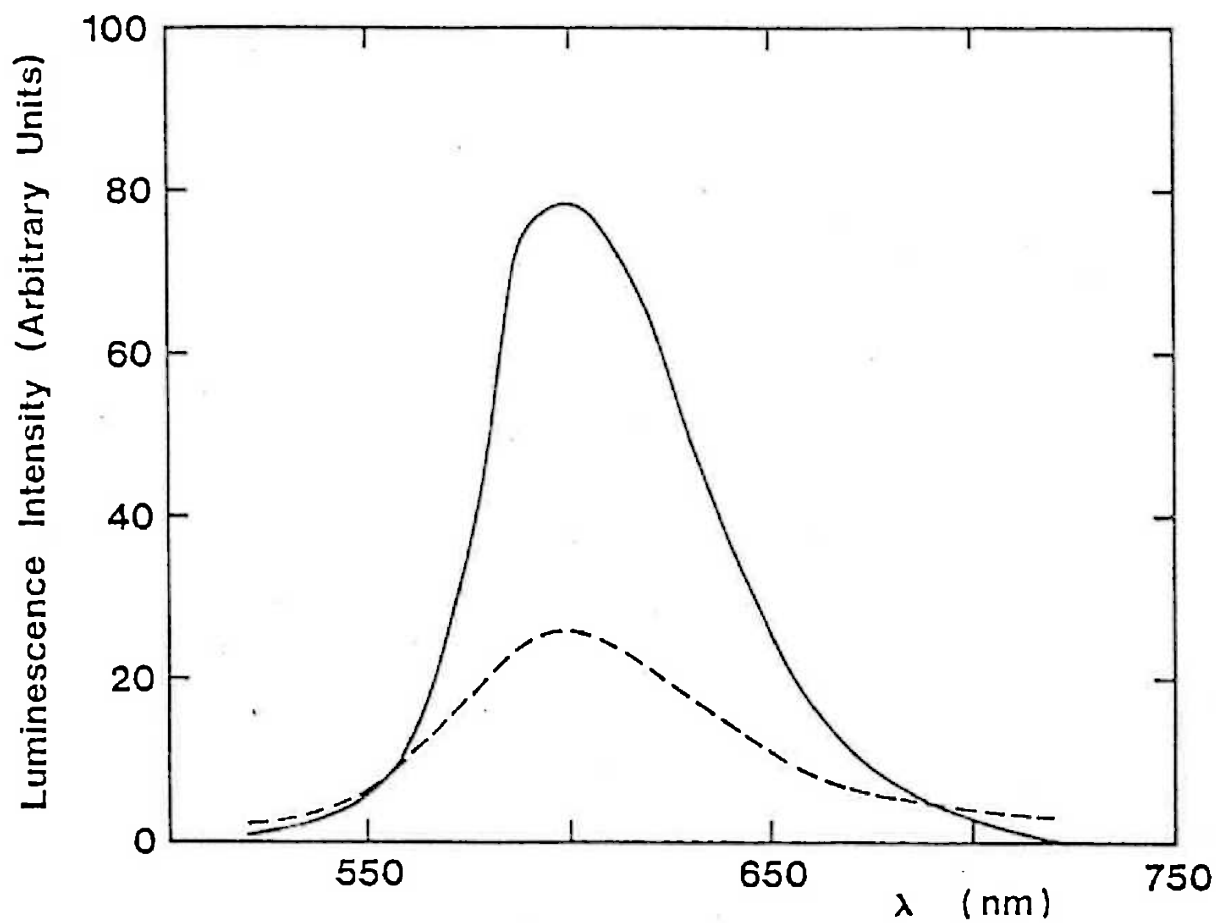
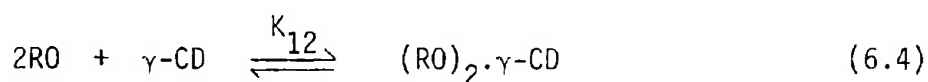


Fig. 6.9: Luminescence spectrum ($\lambda_{\text{ex}} = 420$ nm) of roccellin (4.0×10^{-5} mol dm $^{-3}$) in the presence of 4.0×10^{-3} mol dm $^{-3}$ β -CD (dashed curve) and γ -CD (solid curve) at 25°C.

large hypochromic effect and a blue shift of approximately 15 nm were observed on complexation. In contrast to the roccellin/ β -CD system, significant changes in the spectrum of the dye are observed even at cyclodextrin concentrations at which the dye is in excess. This indicates either that roccellin forms a 1:1 complex with γ -CD but with a much higher association constant than for the β -CD system, or more likely that dimerisation of the dye occurs within the γ -CD cavity. Thus, the data can be described by the following equilibrium:



It was found that the normal fitting procedure could not be used, because the large value of K_{12} resulted in a very shallow minimum and thus prevented convergence (see Appendix B). In this case, then, the determination of the association constant was carried out by using an alternative method, which combines the programs MOLABS and ROCEQU. The value of the association constant obtained, averaging over the wavelength range 580-464 nm, is as follows:

$$K_{12} = 9.0 (\pm 1.8) \times 10^{10} \text{ dm}^6 \text{ mol}^{-2}$$

Using this value of K_{12} , together with the directly determined molar absorptivities of roccellin, the spectrum of the $(\text{RO})_2 \cdot \gamma\text{-CD}$ complex was derived, and this is shown in Fig. 6.7.

b) Induced Circular Dichroism

The induced circular dichroic spectrum of roccellin in a hundred-fold excess of γ -CD is shown in Fig. 6.8. The positive and negative signals observed are characteristic of exciton splitting caused by dimerisation of the dye within the γ -CD cavity.

The relatively large values of the molar ellipticity indicate strong coupling between the transition moments of the dye and those of the glucose residues of the cyclodextrin.

c) Luminescence Spectrum

The luminescence spectrum of roccellin in a hundred-fold excess of γ -CD is shown in Fig. 6.9. Again an enhancement of the dye's luminescence is observed. However, the intensity of the luminescence spectrum in the presence of γ -CD is over twice that observed in the presence of β -CD. Since it has been observed earlier that luminescence enhancement occurs on aggregation of the dye, the more intense luminescence spectrum exhibited in the presence of γ -CD is consistent with dimerisation within the γ -CD cavity.

6.6 The Interaction of the Roccellin Di-anion with the Cyclodextrins

The addition of α - or γ -CD ($4 \times 10^{-3} \text{ mol dm}^{-3}$) to a solution of roccellin ($4 \times 10^{-5} \text{ mol dm}^{-3}$) in 1 mol dm^{-3} NaOH (pH 13.4) resulted in no significant changes in the dye's absorption spectrum, and no induced circular dichroism could be detected. On the addition of β -CD, however, a hypochromic effect was observed in the visible region (see Fig. 6.10), and an induced circular dichroic spectrum was apparent (see Fig. 6.11). Thus, only β -CD appears to be able to include the dye in its di-anion form. It should be noted, however, that at this high pH not only does the dye have a double negative charge due to deprotonation of its hydroxyl group, but the secondary hydroxyl groups of the cyclodextrin will also be partially negatively charged, since their pK_a is approximately 12.2.⁶ A possible reason for the lack of a complex with γ -CD is therefore that repulsion between the

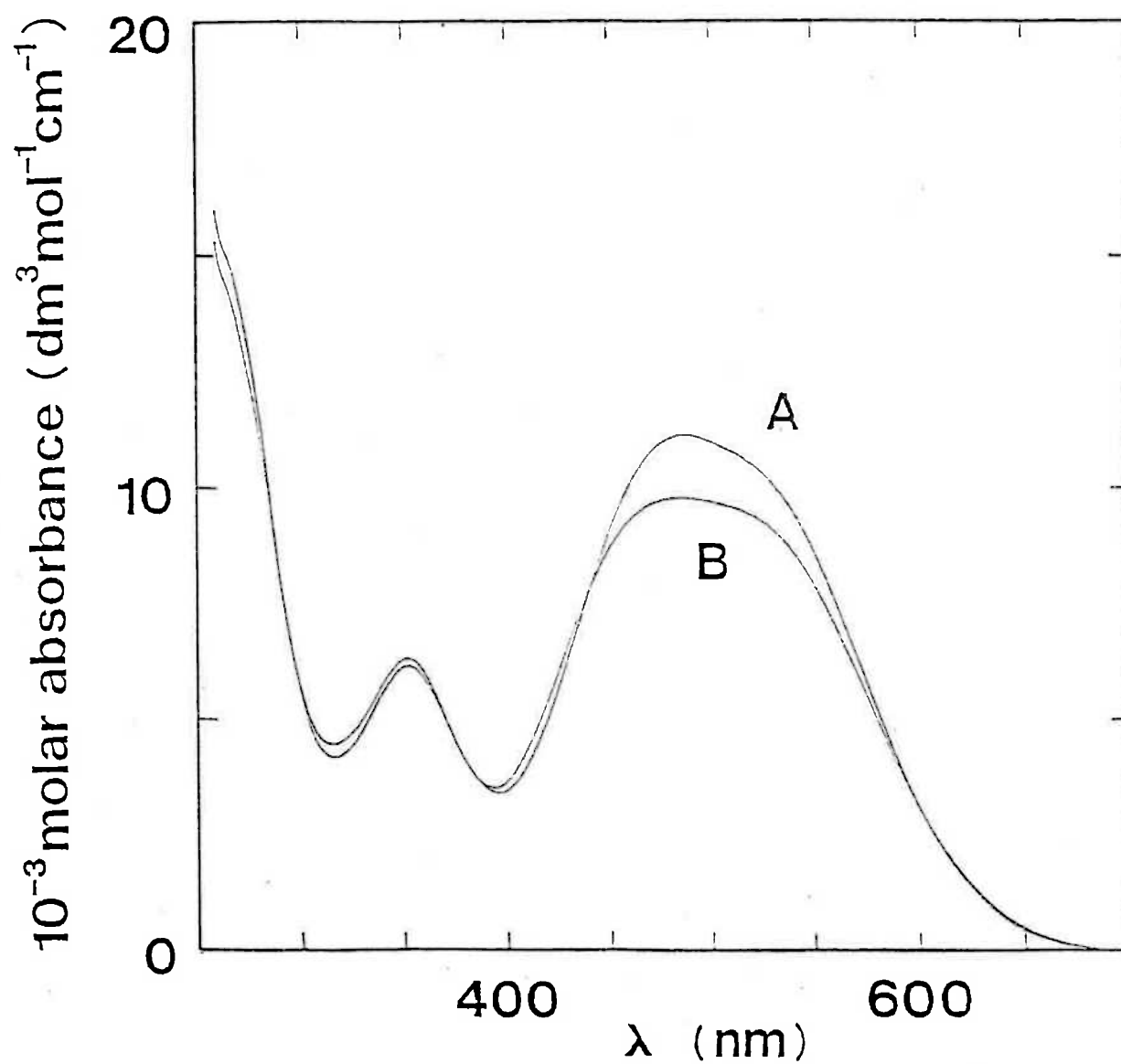


Fig. 6.10: Visible absorption spectrum of roccellin ($4.1 \times 10^{-5} \text{ mol dm}^{-3}$) alone (curve A) and in the presence of $4.0 \times 10^{-3} \text{ mol dm}^{-3}$ β -CD (curve B) at pH 13.4, 25°C.

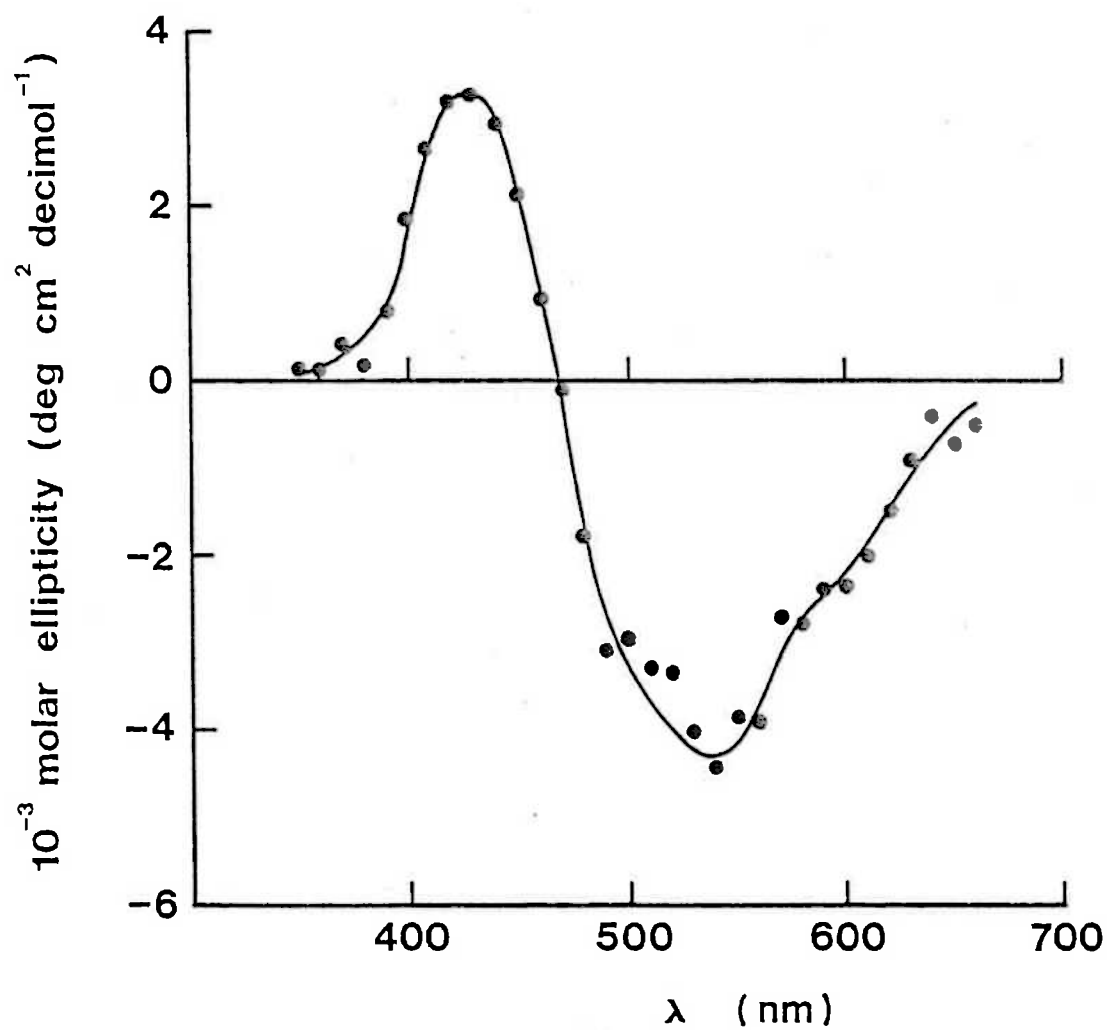


Fig. 6.11: Induced circular dichroic spectrum of roccellin (4.0×10^{-5} mol dm⁻³) in the presence of 4.0×10^{-3} mol dm⁻³ β -CD at pH 13.4, 25°C.

negative charges of the dye and the cyclodextrin prevents complex formation. However, this would also be the case for β -CD, with which a complex does occur. Therefore, a more likely explanation is that γ -CD can only form a stable complex with a roccellin dimer (a roccellin monomer being held only very weakly), and that the dimer is prevented from forming due to charge repulsion or possibly stronger hydration of the dye at the higher pH, as a consequence of its higher negative charge.

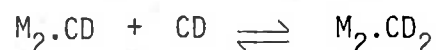
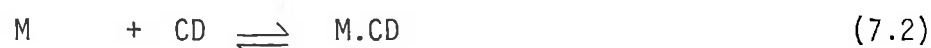
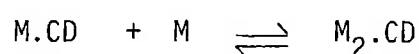
Bibliography

1. Matsui, Y. and K. Mochida, *Bull.Chem.Soc.Jpn.*, 51, 673 (1978).
2. Reeves, R.L. and R.S. Kaiser, *J.Org.Chem.*, 35, 3670 (1970).
3. Davis, J.S. and H. Gutfreund, *F.E.B.S. Letters*, 72, 199 (1976).
4. Giles, C.H., V.G. Agnihotri and N. McIver, *J.Colloid and Interfac.Sci.*, 50, 24 (1975).
5. Craven, B.R., J.C. Griffith and J.G. Kennedy, *Aust.J.Chem.*, 28, 1971 (1975).
6. Gelb, R.I., L.M. Schwartz, J.J. Bradshaw and D.A. Laufer, *Bioorg.Chem.*, 9, 299 (1980).

CHAPTER VII

CHAPTER VII: GENERAL DISCUSSION AND CONCLUSIONS

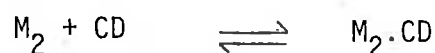
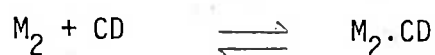
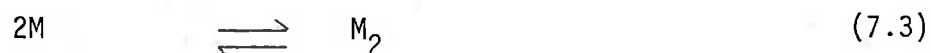
The major finding of this thesis is that certain azo dyes are able to form one host-two guest and occasionally two host-two guest complexes with β - and γ -cyclodextrin by dimerisation of the dye within the cyclodextrin cavity (equations (7.1) and (7.2)). The mechanisms proposed have been derived on the basis of results obtained by temperature-jump relaxation spectrophotometry, a direct kinetic method, in contrast to mechanisms suggested by previous workers based upon equilibrium measurements of fluorescence intensities alone.¹⁻⁴



where M = dye monomer

CD = cyclodextrin

Alternative mechanisms, involving dimerisation outside the cyclodextrin cavity (equations (7.3) and (7.4)), have also been considered, but they cannot explain the observed kinetics.



Another mechanism for two host-two guest complexation, which involves the aggregation of two 1:1 inclusion complexes (equation (7.5)), has been proposed by Hamai¹ to explain the interaction of naphthalene with β -cyclodextrin. The same mechanism has also been suggested by Herkstroeter et al.⁴ for the pyrenylbutyrate/ γ -cyclodextrin system. Both of these studies, however, relied on equilibrium fluorescence measurements. Therefore, although this mechanism is quite feasible, no direct kinetic evidence for the aggregation of 1:1 complexes has yet been presented.



In the case of one host-two guest complexation only a single mechanism (equation (7.1)) has up to now been found to apply. Not only do the azo dyes form one host-two guest complexes via this scheme, but the kinetic results of Schiller et al.⁷ suggest that crystal violet, a triphenylmethane dye, also complexes with γ -cyclodextrin according to this mechanism. Thus, although the number of examples is too few to state definitely that this is the sole mechanism of one host-two guest complexation, it does nevertheless seem that this mechanism is quite widely applicable.

The kinetics of 1:1 complex formation of azo dyes with α -cyclodextrin have been investigated by several workers.^{5,6} In the majority of cases the reaction was very rapid, however the rate constants were measurable by using the techniques of stopped-flow or temperature-jump spectrophotometry. A similar situation has been found in this study for the interaction of

methyl orange with α -cyclodextrin. An inspection of the literature values of the rate constants derived suggests that the major determinant of the rate of complex formation is the relative sizes of the guest and the cyclodextrin cavity, and hence the degree of steric hindrance. In the case of one host-two guest and two host-two guest complexation it has been assumed that the first step of the mechanism, involving the formation of a 1:1 complex, is much more rapid than the inclusion of the second guest molecule. Since it is a necessary requirement of one host-two guest and two host-two guest complexation that the volume of the cyclodextrin cavity is much larger than that occupied by a single guest molecule, the amount of steric hindrance in the 1:1 complex would be negligible. Therefore, the assumption of a rapid formation of a 1:1 complex is probably valid.

Dimer formation within the cyclodextrin cavity occurs at dye concentrations at which, in the absence of cyclodextrin, the amount of dimer in free solution is negligible. Hence, γ -cyclodextrin effectively increases the dimerisation constant, K_d , of all three dyes studied, and in the case of tropaeolin an increase in K_d is also observed on the addition of β -cyclodextrin. This implies that the dye dimer is more stable when included within the cyclodextrin cavity than when free in solution. Two possible reasons could account for this increase in stability:

- 1) the presence of cyclodextrin facilitates the association of the dye monomers.
- 2) the presence of cyclodextrin hinders the dissociation of the dye dimer.

Intuitively it would seem that the second possibility is the most likely, since the dye dimer is held within the cyclodextrin cavity by various secondary forces. Some evidence has been found, however, which suggests that the first hypothesis is correct. Tropaeolin was found to exhibit a slow temperature-jump relaxation in the absence of cyclodextrin. It was suggested that this relaxation may be due to the dimerisation of the dye. If this assignment is correct, then it is found that the forward rate constant for dimerisation, k_d , is approximately a thousand times less than the forward rate constant for dimerisation within the γ -cyclodextrin cavity, k_2 . A similar relationship has been found in the case of crystal violet.⁷ An explanation has been proposed^{7,8} for this apparent facilitation of dimerisation within the cyclodextrin cavity. It has been suggested that a dye monomer, when included within the hydrophobic cyclodextrin cavity, is partially desolvated and that, on formation of a one host-two guest complex, the interaction between the included dye monomer and the approaching dye monomer facilitates the expulsion of solvating water molecules and the consequent completion of dimer formation within the cyclodextrin cavity. In contrast, the formation of the dye dimer in water in the absence of cyclodextrin occurs less readily, since the dye monomers are fully solvated and consequently the interaction between them is less easily established.

Since the dyes chosen for investigation have aromatic residues of varying sizes, the results obtained enable something to be said about the specificity of the cyclodextrin cavities.

Consider the results presented in Table 7.1. The cavity of α -cyclodextrin appears to be able to include only a single phenyl residue. The cavity of β -cyclodextrin seems to be able to include two phenyl residues or a naphthyl and a phenyl residue, but it is unable to include two naphthyl residues. The cavity of γ -cyclodextrin, however, appears to be large enough to admit two naphthyl residues, a naphthyl and a phenyl residue, or two phenyl residues. This dependence of the stoichiometric ratio on the cavity size implies that a good fit between the guest and host component molecules is necessary for stable complex formation, which is consistent with the participation of van der Waals forces in stabilising the resultant complex.

It has also been found that the uncharged end of the dyes rather than the negatively charged sulphonate end is preferentially included. A possible reason for this is that the sulphonate group is strongly solvated, so that removal of the solvating water molecules in order to form a complex with cyclodextrin is not favoured. High stability constants have been observed for complexes of negatively charged aromatic species⁹ (e.g. the *para*-nitrophenolate anion) with the cyclodextrins, however in these cases the negative charge is generally delocalised around the whole π -system, in contrast to the localised charge of the sulphonate group.

The results which have been presented on the interaction of the dyes with the cyclodextrins in sodium hydroxide solution show that, when negatively charged, the cyclodextrins are not as readily able to form inclusion complexes with the dyes as when they are

		Cyclodextrin		
		α	β	γ
Anionic Dye	MO	1:2	1:1 or 2:1	2:2
	TR	-	2:1	2:2
	RO	-	1:1	2:1

Table 7:1: The stoichiometric ratios (guest:host) of the most stable complex species.

Note: a dash indicates no complex formation.

in their uncharged form. Two possible explanations could be proposed to explain this observation. Firstly, since the dyes are all negatively charged, charge repulsion between the dyes and the cyclodextrin could hinder association. However, since it appears that, if possible, an uncharged residue is included in preference to the negatively charged sulphonate end of the dye, a more likely explanation is that the deprotonation of the cyclodextrin results in an intrinsic reduction in its binding affinity, perhaps due to the expected enhancement of its solvation.

The complete elucidation of the mechanisms of cyclodextrin inclusion complex formation is difficult, and it seems that various experimental approaches are required in order to obtain a clear picture of the inclusion process. The participation of solvating water appears to be very likely, and the formation of a complex may rely on competing factors, e.g. the relative stabilities of the guest when solvated by water and when complexed by van der Waals forces to the cyclodextrin. In the case of the azo dyes investigated, although the exact role of water has not been determined, mechanisms for one host-two guest and two host-two guest complexation have been proposed which adequately explain the experimental observations.

Bibliography

1. Hamai, S., *Bull.Chem.Soc.Jpn.*, 55, 2721 (1982).
2. Kano, K., I. Takenoshita and T. Ogawa, *Chem.Lett.*, 1982, 321.
3. Kobayashi, N., R. Saito, H. Hino, Y. Hino, A. Ueno and T. Osa, *J.Chem.Soc. Perkin Trans. II*, 1983, 1031.
4. Herkstroeter, W.G., P.A. Martic and S. Farid, *J.Chem.Soc. Perkin Trans. II*, 1984, 1453.
5. Cramer, F., W. Saenger and H. -Ch. Spatz, *J.Am.Chem.Soc.*, 89, 14 (1967).
6. Hersey, A. and B.H. Robinson, *J.Chem.Soc. Faraday Trans I*, 80, 2039 (1984).
7. Schiller, R.L., J.H. Coates and S.F. Lincoln, *J.Chem.Soc. Faraday Trans. I*, 80, 1257 (1984).
8. Clarke, R.J., J.H. Coates and S.F. Lincoln, *J.Chem.Soc. Faraday Trans I*, 80, 3119 (1984).
9. Connors, K.A. and J.M. Lipari, *J.Pharm.Sci.*, 65, 379 (1976).

APPENDICES

APPENDIX A: MATERIALS

The α -, β - and γ -cyclodextrin were obtained from Sigma Chemical Company, and were used without further purification. They were stored as the anhydrous material over phosphorous pentoxide in a vacuum desiccator. Methyl orange (B.D.H., LR grade) was used without further purification. Elemental analysis was consistent with the dye being the tetrahydrate. Tropaeolin 000 no. 2 (B.D.H.) was purified by salting out from hot distilled water using sodium acetate, after which it was recrystallised three times from distilled water and then twice from ethanol. Roccellin (Sigma) was purified by salting out from hot distilled water with sodium acetate, recrystallised twice from distilled water, and the crystals were then washed with cold ethanol. Elemental analyses of both tropaeolin and roccellin were consistent with the dyes being the monohydrate. The analytical reagent grade compounds KH_2PO_4 (B.D.H.), Na_2HPO_4 (B.D.H.), K_2SO_4 (B.D.H.), Li_2SO_4 (B.D.H.), NaCl (Univar), sodium acetate (B.D.H.) and glycine (B.D.H.) were used without further purification. Aqueous sodium hydroxide solutions were prepared by the dilution of the contents of a B.D.H. concentrated volumetric solution ampoule.

All measurements were made on freshly prepared dye solutions, and exposure to light was kept to a minimum. No adsorption of the dyes to glass or quartz was detected. All volumetric glassware was cleaned by prolonged soaking in Decon 90 solution, followed by extensive rinsing in distilled water. All solutions were diluted by weight from stock solutions prepared using A-grade volumetric apparatus.

The azo dyes used have numerous alternative names. The systematic names, the colour index numbers and some of the commercial names are listed below.^{1,2}

Methyl Orange

p-[(p-Dimethylamino)phenylazo]benzenesulphonic acid

sodium salt

C.I. Acid Orange 52

C.I. 13025

Helianthin

Orange III

Tropaeolin D

Tropaeolin 000 no. 2

p-(2-Hydroxy-1-naphthylazo)benzenesulphonic acid sodium salt

C.I. Acid Orange 7

C.I. 15510

Orange II

Betanaphthol orange

Roccellin

p-(2-Hydroxy-1-naphthylazo)naphthalenesulphonic acid sodium

salt

C.I. Acid Red 88

C.I. 15620

Naphthalene Red J

APPENDIX B: COMPUTATIONAL METHODS

Apart from the determination of relaxation times from temperature-jump data, which were carried out on a Computer Products LSI-11 minicomputer, all the computations were performed on a CDC Cyber 173 computer. The programs used were written in either FORTRAN IV or FORTRAN V. Since the programs are too lengthy to allow full listings to be given, the essential features of each program will merely be described.

PROGRAM CDXKIN

From the values of the relaxation times determined and the initial concentrations of dye and cyclodextrin, this program calculates equilibrium constants and rate coefficients describing the dye-cyclodextrin interaction. A variety of different reaction schemes can be considered, so as to find the mechanism which best fits the data. The program incorporates the following four basic subroutines.

1) VALIN

This subroutine merely reads the data, including estimated uncertainties, from the input file.

2) MODEL

This subroutine defines the expected dependence of the reciprocal relaxation time on the equilibrium dye, cyclodextrin and inclusion complex concentrations for each reaction mechanism considered.

3) NEWRAP

For each successive estimate of the equilibrium constants,

this subroutine uses the Newton-Raphson method³ to calculate equilibrium concentrations of the dye, cyclodextrin and inclusion complexes from the input values of the initial concentrations of dye and cyclodextrin.

4) DATAFIT

This is a non-linear weighted least squares fitting procedure, which was written by Dr. T. Kurucsev of this department. The subroutine enables the data to be fitted to the equation defined by subroutine MODEL.

PROGRAM CDXEQU

From the measured absorbances at a particular wavelength of dye solutions over a range of cyclodextrin concentrations, this program calculates equilibrium constants for the dye-cyclodextrin equilibria occurring, as well as molar absorptivities of the complexes formed. As was the case with CDXKIN, a variety of equilibrium reaction schemes can be considered. Again the program contains the subroutines VALIN, MODEL, NEWRAP and DATAFIT, however in this case subroutine MODEL defines the expected dependence of the absorbance on the equilibrium concentrations of the dye, cyclodextrin and inclusion complexes. The wavelength at which the calculation is carried out can be varied, so that the absorption spectra of the complexes formed can be determined.

In certain cases, e.g. the roccellin/ γ -cyclodextrin interaction, where the association constant is very large, this program cannot give an accurate value of the association constant, because of the shallowness of the minimum being sought by the least squares method,

i.e. the calculated absorbance is very insensitive to perturbations in the value of the association constant. In these cases an alternative method has been used, which involves the successive application of programs MOLABS and ROCEQU.

PROGRAM MOLABS

For the interaction of a dye and a cyclodextrin which can be described by a single equilibrium, this program calculates the molar absorptivity at a particular wavelength of the complex formed, by extrapolation of a double reciprocal plot of the change in the apparent molar absorptivity of the dye versus the cyclodextrin concentration to infinite cyclodextrin concentration. The absorption spectrum of the complex can be obtained by varying the wavelength at which the calculation is performed.

PROGRAM ROCEQU

For each wavelength and each concentration of cyclodextrin this program calculates the equilibrium concentrations of dye, cyclodextrin and complex from the absorbance and the values of the molar absorptivities of the complex (derived from MOLABS) and the free dye (derived from the spectrum of the dye alone). The ratio of the equilibrium complex concentration to that of the dye and the cyclodextrin then enables a value of the association constant to be determined. The values of the association constant, calculated at each wavelength and cyclodextrin concentration, are then averaged to give the final value quoted.

PROGRAM CALCMET

This program uses the Newton-Raphson method to calculate

equilibrium concentrations of dye, cyclodextrin and inclusion complexes from input values of the initial concentrations of dye and cyclodextrin, and assumed values of the association constants. It also calculates the expected variation of the reciprocal relaxation time with these equilibrium concentrations based on assumed values of the rate constant. Thus, this is merely a utility program, which has been used to check the validity of the equations comprising the NEWRAP subroutines, and also to simulate the temperature-jump data.

PROGRAM DMRO01

This program is used for the averaging of repetitive UV/vis. absorption spectra. The program subtracts the baseline, averages the absorbances, allows for expansion due to temperature variation and creates three output files for further analysis. The program was written in FORTRAN IV by Mr. G. Boehm of this department, but it has recently been updated to FORTRAN V.

PROGRAM ZETAPLT

This program reads one of the output files from DMRO01, calculates origin and scaling factors, and creates a plot file, which enables the spectral data to be plotted on a Zeta 1453 plotter. The resultant plot displays the molar absorptivities versus wavelength for a series of concentrations on the same axes.

APPENDIX C: ISOSBESTIC POINTS

If the total concentration of an absorbing species is fixed, an isosbestic point is defined as a point in the UV/visible absorption spectrum at which the absorbance is independent of the concentration of an additional non-absorbing species, with which the absorbing species reacts. Thus, in the case of dye-cyclodextrin interactions an isosbestic point would be observable, if at some wavelength the dye absorbance is independent of the cyclodextrin concentration.

It is sometimes stated in the literature that the observation of such an isosbestic point indicates the formation of a 1:1 complex,⁴⁻⁶ however this is quite incorrect. The presence of an isosbestic point merely indicates that only two spectroscopically distinguishable species are present in significant concentrations. For example, a 2:1 complex may form in addition to a 1:1 complex, however if the absorption spectrum of the 1:1 complex is indistinguishable from that of the free dye or of the 2:1 complex, or if the concentration of the 1:1 complex is negligible, an isosbestic point could still be observed.

It is also possible that an isosbestic point may be observed for a system in which two complexes with different absorption spectra but with the same stoichiometric ratio are present, if the ratio of the concentrations of the two species is constant. In this case an averaged spectrum of the two species is seen, and they are thus spectroscopically indistinguishable. Consider the scheme below, describing the formation of two 1:1 cyclodextrin inclusion compounds with different absorption spectra.



If the total dye concentration is fixed, conservation of mass requires that,

$$\Delta C_A + \Delta C_{ACD'} + \Delta C_{ACD''} = 0 \tag{C2}$$

From the expressions for the equilibrium constants it can be shown that,

$$C_{ACD''} = C_{ACD'} \times K_2/K_1$$

$$\therefore \Delta C_{ACD''} = \Delta C_{ACD'} \times K_2/K_1 \tag{C3}$$

Substituting (C3) into (C2) it is found that,

$$\Delta C_{ACD'} = -\Delta C_A / (1 + K_2/K_1) \tag{C4}$$

$$\Delta C_{ACD''} = -\Delta C_A / (1 + K_1/K_2) \tag{C5}$$

Now the absorbance, assuming that the cyclodextrin is non-absorbing, is given by

$$A = \epsilon_1 C_A + \epsilon_2 C_{ACD'} + \epsilon_3 C_{ACD''}$$

By differentiation generally it can be shown that,

$$\Delta A = \epsilon_1 \Delta C_A + \epsilon_2 \Delta C_{ACD'} + \epsilon_3 \Delta C_{ACD''} \tag{C6}$$

Substituting for $\Delta C_{ACD'}$ and $\Delta C_{ACD''}$ from (C4) and (C5) gives,

$$\Delta A = \left[\epsilon_1 - \frac{\epsilon_2}{(1 + K_2/K_1)} - \frac{\epsilon_3}{(1 + K_1/K_2)} \right] \Delta C_A \tag{C7}$$

For an isosbestic point to occur, any change in the equilibrium concentration of dye caused by the addition of cyclodextrin must not cause a change in absorbance. Thus, at a particular wavelength the following equation must hold.

$$\epsilon_1 - \epsilon_2 \cdot \left(\frac{K_1}{K_1 + K_2} \right) - \epsilon_3 \cdot \left(\frac{K_2}{K_1 + K_2} \right) = 0 \quad (C8)$$

Since this expression contains no concentration terms, it satisfies the necessary condition for an invariant isosbestic point.

From the above discussion it can be seen that the presence of an isosbestic point does not allow anything to be said about the number of complexes formed or about their stoichiometries. The absence of an isosbestic point, however, is direct evidence for the presence of two or more complexes of different stoichiometries.

APPENDIX D: MOLECULAR EXCITON THEORY

The molecular exciton model is a state interaction theory, which has been proposed to explain differences in the properties (particularly spectroscopic) of molecular aggregates in comparison to those of the single molecule. If, on aggregation, the intermolecular electron overlap is small, so that the molecular units preserve their individuality in an aggregate, the molecular exciton model will satisfy the requirements of a perturbation theory. We may then seek solutions for the aggregate in terms of the wave functions and energies of the states of the component molecules. The theoretical consideration of the exciton model which follows is based on a review by Kasha et al.⁷.

The ground state wave function, ψ_0 , for a molecular dimer has the unique description,

$$\psi_0 = \psi_a \psi_b \quad (D1)$$

where ψ_A and ψ_B represent the ground state wave functions of molecule A and B respectively.

The Hamiltonian operator for the dimer is,

$$\hat{H} = \hat{H}_A + \hat{H}_B + \hat{V}_{AB} \quad (D2)$$

where \hat{H}_A and \hat{H}_B are the Hamiltonian operators of the isolated molecules, and \hat{V}_{AB} is the intermolecular perturbation potential.

The energy of the ground state of the dimer is given, from the basic postulates of quantum theory, as

$$E_0 = \iint \psi_A \psi_B \hat{H} \psi_A \psi_B d\tau_A d\tau_B \quad (D3)$$

which factorises into

$$E_0 = E_A + E_B + \iint \psi_A \psi_B \hat{V}_{AB} \psi_A \psi_B d\tau_A d\tau_B \quad (D4)$$

The last term represents the van der Waals interaction energy (an energy lowering) between the ground states of molecules A and B, and E_A and E_B are the ground state energies of the isolated molecules.

The excited state dimer wave functions (exciton wave functions) may be written as

$$\psi_E = r\psi_A^\dagger \psi_B + s\psi_A \psi_B^\dagger \quad (D5)$$

where ψ_A^\dagger and ψ_B^\dagger represent excited state wave functions for a particular excited state under study of molecules A and B respectively, and r and s are coefficients to be determined. The time-independent Schrödinger equation for the excited state in question is

$$\hat{H} (r\psi_A^\dagger \psi_B + s\psi_A \psi_B^\dagger) = E_E (r\psi_A^\dagger \psi_B + s\psi_A \psi_B^\dagger) \quad (D6)$$

Multiplying both sides of this equation by $\psi_A^\dagger \psi_B$ and integrating over coordinates for molecules A and B yields (assuming orthogonality),

$$r \iint \psi_A^\dagger \psi_B \hat{H} \psi_A^\dagger \psi_B d\tau_A d\tau_B + s \iint \psi_A^\dagger \psi_B \hat{H} \psi_A \psi_B^\dagger d\tau_A d\tau_B = rE_E \quad (D7)$$

Multiplying both sides of equation (D6) by $\psi_A \psi_B^\dagger$ and proceeding as before leads to

$$r \iint \psi_A \psi_B^\dagger \hat{H} \psi_A^\dagger \psi_B d\tau_A d\tau_B + s \iint \psi_A \psi_B^\dagger \hat{H} \psi_A \psi_B^\dagger d\tau_A d\tau_B = sE_E \quad (D8)$$

Now we define the following terms,

$$\hat{H}_{AA}(=\hat{H}_{BB}) = \iint \psi_A^\dagger \psi_B \hat{H} \psi_A^\dagger \psi_B d\tau_A d\tau_B \quad (D9)$$

$$\hat{H}_{AB}(=\hat{H}_{BA}) = \iint \psi_A^\dagger \psi_B \hat{H} \psi_A \psi_B^\dagger d\tau_A d\tau_B \quad (D10)$$

Substituting these terms into equations (D7) and (D8) yields the following two simultaneous equations,

$$r(\hat{H}_{AA}-E_E) + s\hat{H}_{AB} = 0 \quad (D11)$$

$$r\hat{H}_{BA} + s(\hat{H}_{BB}-E_E) = 0 \quad (D12)$$

These equations, if they are to have solutions other than the trivial one that $r=s=0$, must have solutions given by the following determinantal equation,

$$\begin{vmatrix} \hat{H}_{AA}-E_E & \hat{H}_{AB} \\ \hat{H}_{BA} & \hat{H}_{BB}-E_E \end{vmatrix} = 0 \quad (D13)$$

Due to the equivalence of \hat{H}_{AA} to \hat{H}_{BB} , and \hat{H}_{AB} to \hat{H}_{BA} , it can be shown that the roots, E_E , of this equation are

$$E_E' = \hat{H}_{AA} + \hat{H}_{AB} \quad (D14)$$

$$E_E'' = \hat{H}_{AA} - \hat{H}_{AB} \quad (D15)$$

Substituting (D14) into equation (D11) yields

$$\hat{H}_{AB} (s-r) = 0 \quad \therefore r = s \text{ for } E_E'$$

Similarly, substituting (D15) into equation (D11) yields

$$\hat{H}_{AB} (r+s) = 0 \quad \therefore r = -s \text{ for } E_E''$$

Now substituting for s in equation (D5) yields,

$$\psi_{E'} = r(\psi_A^\dagger \psi_B + \psi_A \psi_B^\dagger)$$

$$\psi_{E''} = r(\psi_A^\dagger \psi_B - \psi_A \psi_B^\dagger)$$

After normalisation these two equations become,

$$\psi_{E'} = \frac{1}{\sqrt{2}} (\psi_A^\dagger \psi_B + \psi_A \psi_B^\dagger) \quad (D16)$$

$$\psi_{E''} = \frac{1}{\sqrt{2}} (\psi_A^\dagger \psi_B - \psi_A \psi_B^\dagger) \quad (D17)$$

Evaluating $E_{E'}$ and $E_{E''}$ by substituting for \hat{H}_{AA} and \hat{H}_{AB} into equations (D14) and (D15) from equations (D9) and (D10) yields,

$$E_{E'} = E_A^\dagger + E_B + \iint \psi_A^\dagger \psi_B \hat{V}_{AB} \psi_A^\dagger \psi_B d\tau_A d\tau_B + \iint \psi_A^\dagger \psi_B \hat{V}_{AB} \psi_A \psi_B^\dagger d\tau_A d\tau_B \quad (D18)$$

$$E_{E''} = E_A^\dagger + E_B + \iint \psi_A^\dagger \psi_B \hat{V}_{AB} \psi_A^\dagger \psi_B d\tau_A d\tau_B - \iint \psi_A^\dagger \psi_B \hat{V}_{AB} \psi_A \psi_B^\dagger d\tau_A d\tau_B \quad (D19)$$

The last term in equations (D18) and (D19) is the exciton splitting term, ϵ .

$$\epsilon = \iint \psi_A^\dagger \psi_B \hat{V}_{AB} \psi_A \psi_B^\dagger d\tau_A d\tau_B \quad (D20)$$

This term represents an interaction energy due to the exchange of excitation energy between molecule A and molecule B. The third term in equations (D18) and (D19) is analogous to the corresponding term in equation (D4), and represents the van der Waals interaction (energy lowering) between an excited molecule A and the ground state molecule B. The transition energy for the dimer will be given by the difference between equation (D18) or (D19) and equation (D4). Thus,

$$\Delta E_{\text{dimer}} = E_A^{\dagger} - E_A + \iint \psi_A^{\dagger} \psi_B \hat{V}_{AB} \psi_A^{\dagger} \psi_B d\tau_A d\tau_B \\ - \iint \psi_A \psi_B \hat{V}_{AB} \psi_A \psi_B d\tau_A d\tau_B \pm \iint \psi_A^{\dagger} \psi_B \hat{V}_{AB} \psi_A \psi_B^{\dagger} d\tau_A d\tau_B$$

If we represent the difference of the van der Waals terms as ΔD then,

$$\Delta E_{\text{dimer}} = \Delta E_{\text{unit}} + \Delta D \pm \epsilon \quad (\text{D21})$$

As is evident from equation (D21), the exciton model describes a resonance splitting of the excited state energy levels on dimerisation. The ground state of the dimer is merely displaced relative to the monomer ground state due to the van der Waals interaction.

Although the exciton interaction could be described by a purely quantum mechanical treatment, a simpler method, which has found wide application, employs a quasi-classical vector model. Consider an electric dipole transition* of a molecule from the ground state, m , to an electronically excited state, n . This transition has associated with it an electric transition dipole moment, $\vec{\mu}_{nm}$, which is related to the change in polarisation of the molecule during the transition. It is given by the integral,

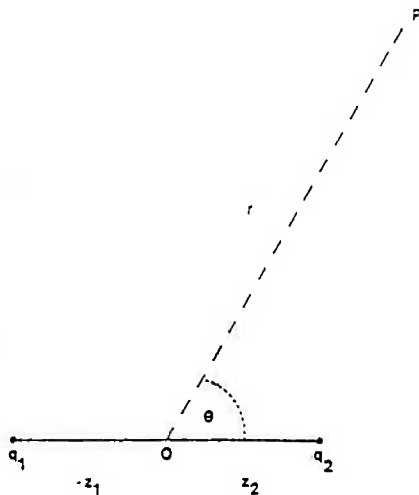
$$\vec{\mu}_{nm} = \int \psi_n \vec{\mu} \psi_m d\tau \quad (\text{D22})$$

where $\vec{\mu}$ is the instantaneous electric dipole moment of the molecule in the ground state.

* An electronic transition caused by the interaction of the instantaneous electric dipole moment of the molecule with the electric component of electromagnetic radiation.

It is important to note that the transition moment is a vector quantity. Its direction determines the direction of polarisation of the electric vector of the electromagnetic radiation required for the transition to occur. The square of the magnitude of the transition moment is directly proportional to the intensity of the transition.

In the case of a dimer the exciton interaction can now be approximated by the electrostatic interaction between the electric transition moment dipoles of the component molecules. Consider the distribution of two charges, q_1 and q_2 , arranged about an origin O , which we take to lie at the centre, as shown below.



If a point P is taken such that its distance, r , from the origin is greater than the distances of the charges from the origin, z_1 and z_2 , it can be shown⁸ that the potential, V , due to the dipole at this point is given by

$$V = \frac{1}{4\pi\epsilon_0} \left\{ \frac{q}{r} + \frac{\mu}{r^2} + \frac{Q(3\cos^2\theta-1)}{2r^3} + \dots \right\} \quad (D23)$$

where $q = q_1 + q_2$ is the total charge

$\mu = q_2 z_2 - q_1 z_1$ is the dipole moment

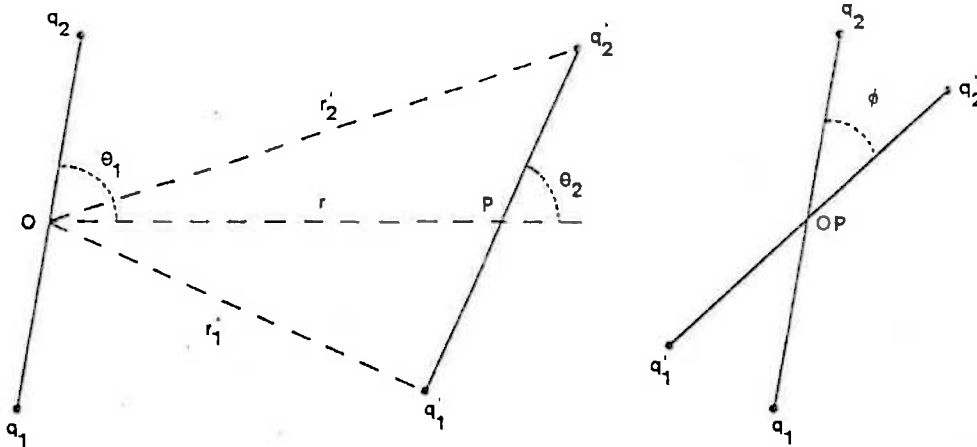
$Q = q_1 z_1^2 + q_2 z_2^2$ is the quadrupole moment

Now if we place a similar charge distribution, $q_1' q_2'$, so that its centre of mass lies at the point P (see below), then the electrostatic potential energy of interaction of the two distributions can be written as,

$$U_{e1} = q_1' V(r_1') + q_2' V(r_2') \quad (D24)$$

where $V(r_1')$ and $V(r_2')$ are the electrostatic potentials

due to the first distribution, $q_1 q_2$, at the charges q_1' and q_2' respectively.



By the substitution of equation (D23) into equation (D24), and by the application of various trigonometric formulae, it can be shown that the electrostatic energy arising from the dipole-dipole interaction is given by

$$(4\pi\epsilon_0)U_{e1} = -\frac{\mu\mu'}{r^3}\{2\cos\theta_1\cos\theta_2 - \sin\theta_1\sin\theta_2\cos\phi\} \quad (D25)$$

Thus, the exciton splitting term may be approximated by,

$$\epsilon = -\frac{\mu_{nm}^2}{r^3}\{2\cos\theta_1\cos\theta_2 - \sin\theta_1\sin\theta_2\cos\phi\} \quad (D26)$$

This representation of the exciton splitting energy is known as the point-dipole approximation. An important point to note regarding equation (D26) is that the angular dependent coefficient of the dipole-dipole interaction energy varies from positive to negative as one dipole is rotated with respect to the other. The interaction can therefore be attractive or repulsive depending on the relative orientations.

Consider a dimer in which the transition dipoles of the component molecules are arranged as shown in Fig. D1. The exciton splitting of the excited state in the dimer can be seen to be due to the two possible phase relationships of the transition moments, i.e. in-phase and out-of-phase. If the transition moments are in-phase, the dipole-dipole interaction is repulsive, and hence an increase in energy results. If the transition moments are out of phase, the dipole-dipole interaction is attractive and an energy lowering occurs. The resultant transition moments for each of the dimer transitions can be obtained from a vector sum of the monomer transition moments. It is interesting to note that for this particular arrangement of the monomer transition dipoles, which is the most likely arrangement for the intense long wavelength transition of the azo dyes investigated, the resultant dimer transition moment for the in-phase arrangement, μ'' , is significantly greater than that for the out-of-phase arrangement, μ' . Thus, the

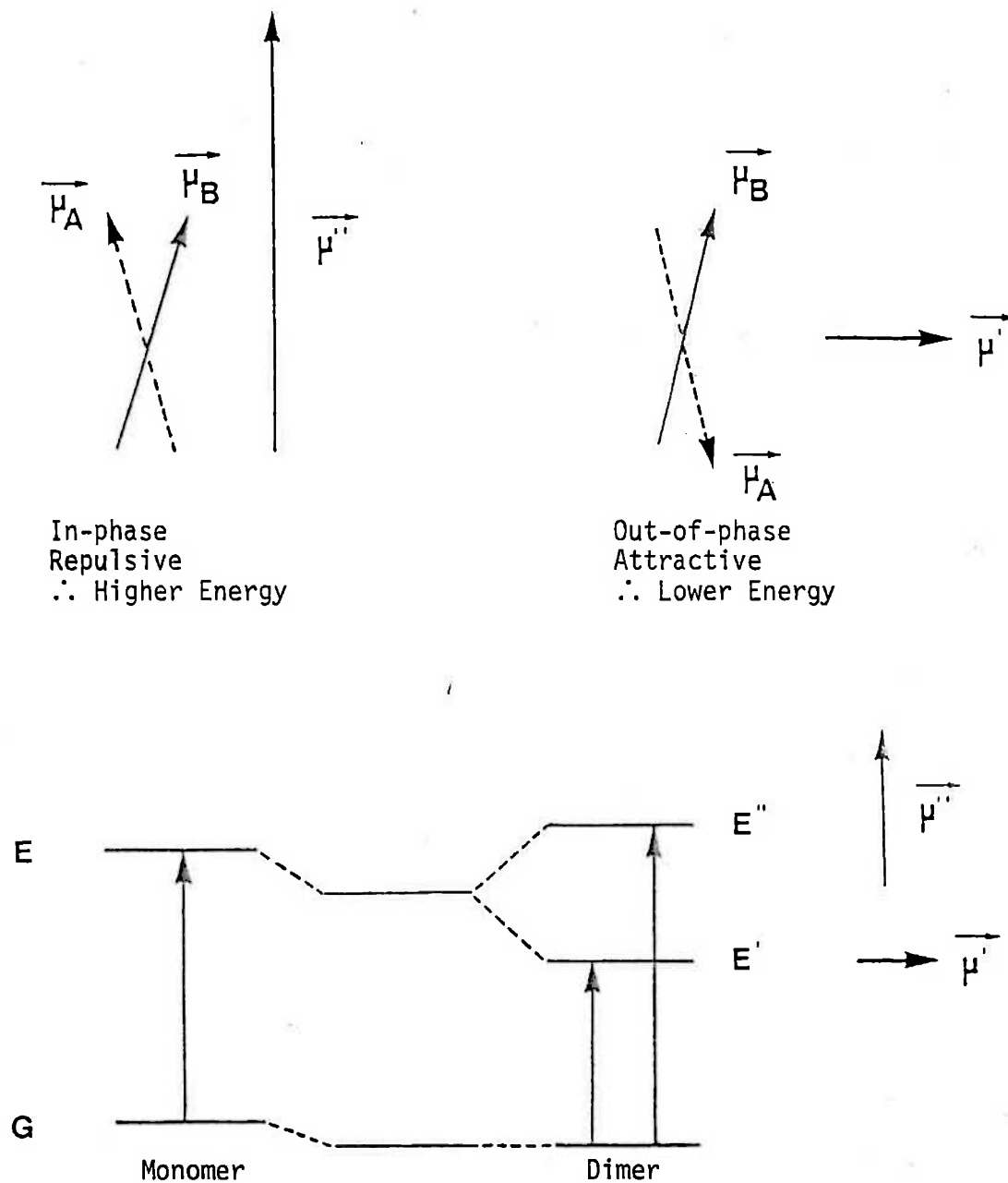


Fig. D1: Schematic representation of the exciton interaction.

Top, the two possible arrangements of the transition moments.

Bottom, energy levels of the monomer and dimer.

transition to the higher energy state in the dimer, E'' , would be much more intense than that to the lower energy state, E' , and accordingly a blue shift in the absorption spectrum of the compound would be expected upon dimerisation. Another important point to note is that the two resultant dimer transition moments are mutually perpendicular. This will be shown to have significance in the explanation of the effect of dimerisation on the induced circular dichroic spectrum. Another effect which is often observed on dimerisation is that of hyper/hypo-chromism, i.e. a change in intensity of absorption. This is caused by the interaction of the transition moments of different electronic transitions.

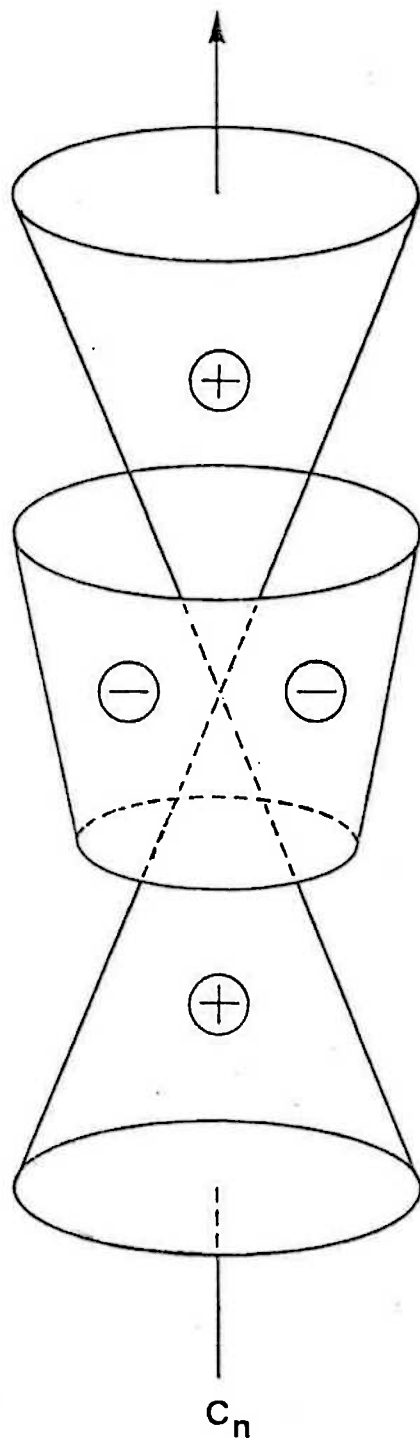
Circular dichroism is defined as the difference in absorption between left and right circularly polarised light by a dissymmetric medium or molecule, i.e.

$$\Delta\varepsilon = \varepsilon_L - \varepsilon_R$$

where ε_L and ε_R are the molar absorptivities of left and right circularly polarised light respectively.

In order for an electronic transition of a molecule to exhibit circular dichroism it must possess not only an electric transition moment but also a magnetic transition moment. It has been found, however, that even an achiral chromophore, which lacks a magnetic moment, is able to show an induced circular dichroic spectrum if it interacts with the transitions of other chromophores arranged chirally with respect to it. This is known as the dipole-coupling mechanism of circular dichroism production.⁹ Consider the inclusion of an achiral dye molecule within the cavity of a cyclodextrin. The electric transition moments of the glucose units

of the cyclodextrin are arranged chirally with respect to the electric transition moment of the included dye molecule. Thus, coupling between the electric transition moments of the glucose units and the guest molecule results in the appearance of a magnetic moment, hence allowing the observation of an induced circular dichroic spectrum in the same wavelength region as the guest's absorption spectrum. As can be seen from equation (D27), circular dichroism can have either a positive or a negative value depending on the relative magnitudes of the molar absorptivities of the compound with respect to left and right circularly polarised light. In the case of cyclodextrin inclusion compounds it has been found experimentally that the sign of the induced circular dichroism is determined by the orientation of the guest's electric transition moment with respect to the principal symmetry axis of the cyclodextrin molecule. A simple sector rule for predicting the sign of the circular dichroism induced in aromatic guests by the cyclodextrins has been proposed by Kajtar et al.¹⁰ (see Fig. D2). If the electric transition moment of the guest molecule lies within an imaginary double cone, whose centre coincides with that of the cyclodextrin and whose constructor forms an angle of approximately 30° with the principal symmetry axis of the cyclodextrin, then the induced circular dichroism will have a positive value. If the electric transition moment is outside this double cone, a negative circular dichroism signal will result. Now if we consider the case of a guest dimer included within the cyclodextrin cavity, it was found earlier that the directions of the transition moments of the two dimer transitions were mutually



$n = 6$ for α -cyclodextrin

7 for β -cyclodextrin

8 for γ -cyclodextrin

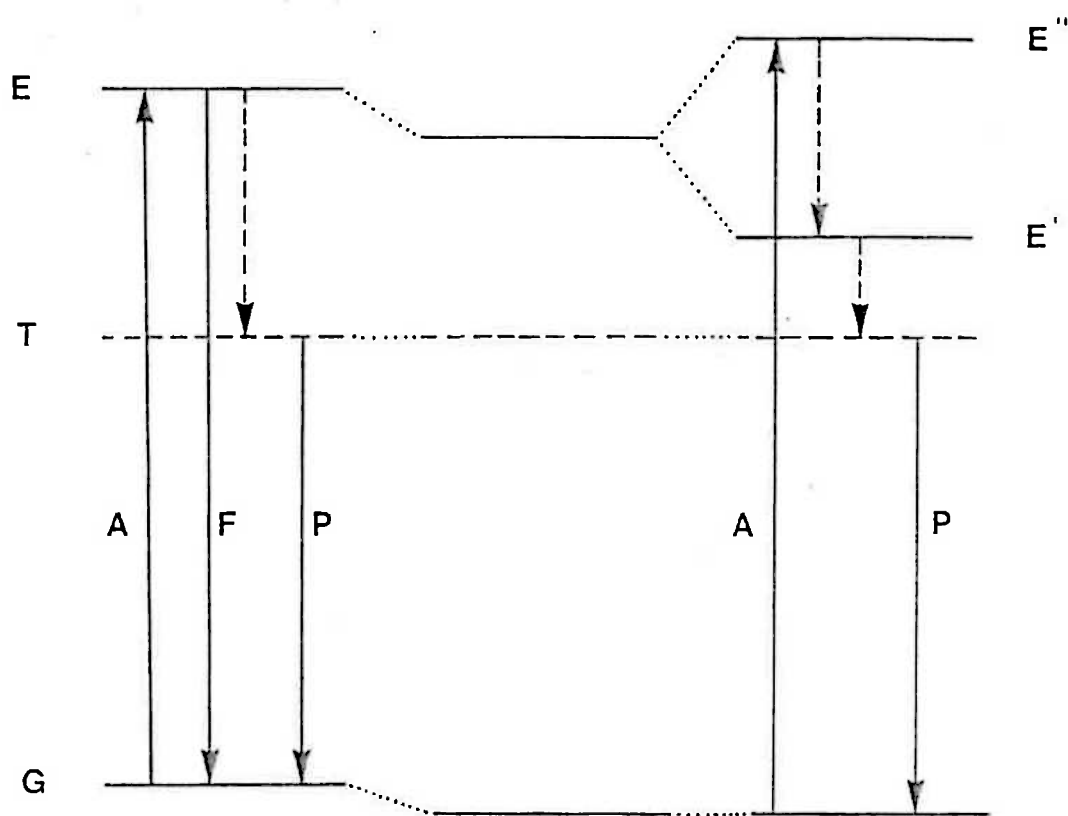
Fig. D2: Sector diagram for predicting the sign of circular dichroism bands induced in inclusion complexes of aromatic molecules with cyclodextrins.

perpendicular. Thus, if a guest dimer is included by cyclodextrin, it would be expected that both a positive and a negative circular dichroic signal would be apparent for each monomer transition.

In addition to the induced circular dichroism caused by the coupling of the dimer transition moments with the transition moments of the cyclodextrin glucose units, it is possible that the dimer may exhibit an induced circular dichroic spectrum of positive and negative signals of equal magnitude due to the dipole coupling of two identical monomeric transition moments. However, this will only occur if one particular fixed dissymmetric orientation of the dimer is favoured inside the cyclodextrin cavity over its mirror image.

A further spectral effect which is often observed on aggregation^{7,11} is a quenching of fluorescence and a corresponding increase in phosphorescence intensity*. Consider the energy level diagram shown in Fig. D3. Since the exciton splitting is dependent on the magnitude of the transition moment, only the singlet state of the molecule shows any significant splitting. The triplet state of the monomer remains nearly degenerate. In the case of near-parallel transition moments in the dimer, excitation will occur predominantly to the upper exciton singlet state, followed by rapid internal conversion between the two singlet states. Radiative transitions from the lower exciton state to the ground state

* Radiative de-excitation transitions between states of the same multiplicity are defined as fluorescence, whereas those between states of different multiplicity are termed phosphorescence.



A = absorption	G = ground state
F = fluorescence	E = excited state
P = phosphorescence	T = triplet state

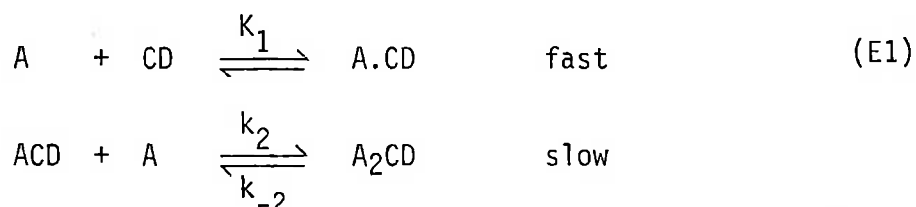
Fig. D3: Excitation and de-excitation pathways with and without exciton splitting.

will have a low probability due to the small value of the transition moment, and thus a decrease in fluorescence is expected on aggregation. Radiationless intersystem crossing, however, from the lower exciton singlet state to the triplet state results in an increase in phosphorescence intensity.

APPENDIX E: DERIVATION OF RECIPROCAL RELAXATION TIME

EXPRESSIONS

Consider the following mechanism, describing dimerisation of a dye, A, within the cavity of a cyclodextrin, CD.



If it is assumed that, after a temperature jump, the first reaction step relaxes much more rapidly than the second, then the first reaction step can be considered to be decoupled from the second and its reciprocal relaxation time is given by (see Sec. 3.1(a)),

$$1/\tau_1 = k_1 (\bar{C}_A + \bar{C}_{CD}) + k_{-1} \quad (E2)$$

In order to derive an expression describing the relaxation of the second step, we make use of the following differential rate equation

$$\frac{dC_{A_2 \cdot CD}}{dt} = k_2 C_{A \cdot CD} C_A - k_{-2} C_{A_2 \cdot CD} \quad (E3)$$

After the temperature jump it can easily be shown that, for a small perturbation,

$$\frac{d\Delta C_{A_2 \cdot CD}}{dt} = k_2 \bar{C}_{A \cdot CD} \Delta C_A + k_2 \bar{C}_A \Delta C_{A \cdot CD} - k_{-2} \Delta C_{A_2 \cdot CD} \quad (E4)$$

In order to find an expression for the relaxation time, the right hand side of this equation must be expressed in terms of $\Delta C_{A_2 \cdot CD}$ alone.

To do this we make use of the principle of mass conservation.

$$\Delta C_{CD} + \Delta C_{ACD} + \Delta C_{A_2CD} = 0 \quad (E5a)$$

$$\Delta C_A + \Delta C_{ACD} + 2\Delta C_{A_2CD} = 0 \quad (E5b)$$

Combining these two expressions, it can be shown that

$$\Delta C_{ACD} = -\Delta C_{CD} - \Delta C_{A_2CD} \quad (E6)$$

$$\Delta C_A = \Delta C_{CD} - \Delta C_{A_2CD} \quad (E7)$$

Now we can utilise the fact that the first step can be considered to be at equilibrium throughout the relaxation of the second.

$$\therefore K_1 = \frac{\bar{C}_{AD}}{\bar{C}_A \cdot \bar{C}_{CD}} \quad (E8)$$

$$\Rightarrow \bar{C}_{ACD} = K_1 \bar{C}_A \bar{C}_{CD} \quad (E9)$$

Differentiation of (E9) with respect to \bar{C}_{CD} , and a change of differentials to differences leads, on rearrangement, to

$$\Delta C_{ACD} = K_1 \bar{C}_A \Delta C_{CD} + K_1 \bar{C}_{CD} \Delta C_A \quad (E10)$$

Substituting for ΔC_{ACD} and ΔC_A from (E6) and (E7) respectively, it can be shown that

$$\Delta C_{CD} = \frac{K_1 \bar{C}_{CD} - 1}{K_1(\bar{C}_A + \bar{C}_{CD}) + 1} \cdot \Delta C_{A_2CD} \quad (E11)$$

Substituting for ΔC_{CD} back into (E6) and (E7), ΔC_{ACD} and ΔC_A can thus be expressed totally in terms of ΔC_{A_2CD}

$$\Delta C_{ACD} = - \frac{K_1(\bar{C}_A + 2\bar{C}_{CD})}{K_1(\bar{C}_A + \bar{C}_{CD}) + 1} \cdot \Delta C_{A_2CD} \quad (E12)$$

$$\Delta C_A = - \frac{K_1 \bar{C}_A + 2}{K_1(\bar{C}_A + \bar{C}_{CD}) + 1} \cdot \Delta C_{A_2CD} \quad (E13)$$

Now substituting for ΔC_{ACD} and ΔC_A back into (E4), it can be shown that

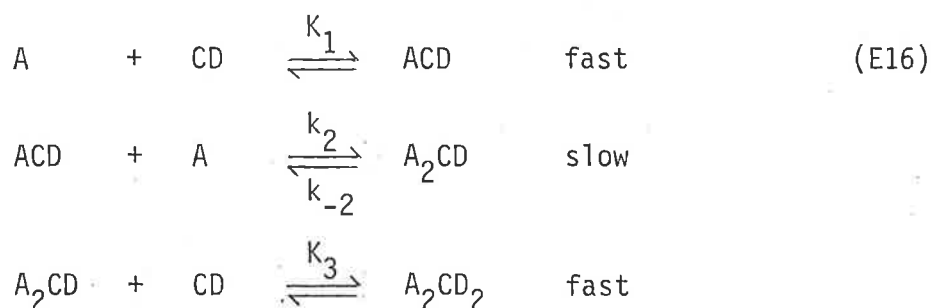
$$-\frac{d\Delta C_{A_2CD}}{dt} = \left[k_2 \frac{\bar{C}_A(\bar{C}_A + \bar{C}_{ACD} + 4\bar{C}_{CD})}{\bar{C}_A + \bar{C}_{CD} + 1/K_1} + k_{-2} \right] \Delta C_{A_2CD} \quad (E14)$$

Thus, by definition, the relaxation time of the second step is given by the expression

$$1/\tau_2 = k_2 \cdot \frac{\bar{C}_A(\bar{C}_A + \bar{C}_{ACD} + 4\bar{C}_{CD})}{\bar{C}_A + \bar{C}_{CD} + 1/K_1} + k_{-2} \quad (E15)$$

The method of derivation presented here is that described by Czerlinski,¹² however an alternative method,¹³ utilising matrix algebra, gives the same result.

Now consider the following mechanism, describing the formation of a 2:2 dye-cyclodextrin complex.



In this case an expression describing the relaxation of the second step can be derived by using the "substitution method" of Czerlinski. This involves considering the mechanism in two parts. An equation for $1/\tau_2$ is first derived by considering the first two reaction steps alone, and then another equation for $1/\tau_2$ is derived by

considering the second two reaction steps. The overall equation for $1/\tau_2$ is then obtained by a combination of these two equations. The equilibrium factor associated with k_2 is taken to be that derived from the consideration of the first two reaction steps, whereas that associated with k_{-2} is taken to be that derived from the consideration of the second two reaction steps.

The first two reaction steps have already been considered above, and this resulted in the following equation

$$1/\tau_2 = k_2 \cdot \frac{\bar{C}_A(\bar{C}_A + \bar{C}_{ACD} + 4\bar{C}_{CD})}{\bar{C}_A + \bar{C}_{CD} + 1/K_1} + k_{-2} \quad (E17)$$

If we now consider the second two steps, another expression for the reciprocal relaxation time can be derived from the following differential rate equation,

$$-\frac{dC_{ACD}}{dt} = k_2 C_{ACD} C_A - k_{-2} C_{A_2CD} \quad (E18)$$

After the temperature jump it can be shown that,

$$-\frac{d\Delta C_{ACD}}{dt} = k_2 \bar{C}_{ACD} \Delta C_A + k_2 \bar{C}_A \Delta C_{ACD} - k_{-2} \Delta C_{A_2CD} \quad (E19)$$

In order to find an expression for the relaxation time, the right hand side of this equation must be expressed in terms of ΔC_{ACD} alone. To do this we make use of the following equations, obtained by inspection,

$$\Delta C_A = \Delta C_{ACD} \quad (E20)$$

$$\Delta C_{CD} = -\Delta C_{A_2CD} \quad (E21)$$

and the mass conservation equation,

$$\Delta C_A + \Delta C_{ACD} + 2\Delta C_{A_2CD} + 2\Delta C_{A_2CD_2} = 0 \quad (E22)$$

Substituting for ΔC_A from (E20) into (E22) yields,

$$\Delta C_{A_2CD} = -\Delta C_{ACD} - \Delta C_{A_2CD_2} \quad (E23)$$

Now we can utilise the fact that the last step can be considered to be at equilibrium.

$$\therefore K_3 = \frac{\bar{C}_{A_2CD_2}}{\bar{C}_{A_2CD} \cdot \bar{C}_{CD}} \quad (E24)$$

$$\Rightarrow \bar{C}_{A_2CD_2} = K_3 \bar{C}_{A_2CD} \bar{C}_{CD} \quad (E25)$$

Differentiation of (E25) with respect to \bar{C}_{A_2CD} and a change of differentials to differences leads, on rearrangement, to

$$\Delta C_{A_2CD_2} = K_3 \bar{C}_{CD} \Delta C_{A_2CD} + K_3 \bar{C}_{A_2CD} \Delta C_{CD} \quad (E26)$$

Substituting for ΔC_{A_2CD} and ΔC_{CD} from (E23) and (E21) yields

$$\Delta C_{A_2CD_2} = - \frac{K_3 \bar{C}_{CD}}{K_3 (\bar{C}_{CD} + \bar{C}_{A_2CD}) + 1} \cdot \Delta C_{ACD} \quad (E27)$$

Substituting for $\Delta C_{A_2CD_2}$ back into (E23), ΔC_{A_2CD} can thus be expressed totally in terms of ΔC_{ACD} .

$$\Delta C_{A_2CD} = - \frac{K_3 \bar{C}_{A_2CD} + 1}{K_3 (\bar{C}_{CD} + \bar{C}_{A_2CD}) + 1} \cdot \Delta C_{ACD} \quad (E28)$$

Now substituting for ΔC_{A_2CD} and ΔC_A from (E28) and (E20) respectively back into (E19) it can be shown that

$$-\frac{d\Delta C_{ACD}}{dt} = \left[k_2(\bar{C}_A + \bar{C}_{ACD}) + k_{-2} \cdot \frac{K_3 \bar{C}_{A_2CD} + 1}{K_3(\bar{C}_{CD} + \bar{C}_{A_2CD}) + 1} \right] \Delta C_{ACD} \quad (E29)$$

Thus, by definition, the relaxation time of the second step, by consideration of the second two steps alone, is given by the expression,

$$1/\tau_2 = k_2(\bar{C}_A + \bar{C}_{ACD}) + k_{-2} \cdot \frac{\bar{C}_{A_2CD} + 1/K_3}{\bar{C}_{CD} + \bar{C}_{A_2CD} + 1/K_3} \quad (E30)$$

Now, combining equations (E17) and (E30) according to the substitution method the overall reciprocal relaxation time of the second step of the three step mechanism (E16) is given by the expression

$$1/\tau_2 = k_2 \cdot \frac{\bar{C}_A(\bar{C}_A + \bar{C}_{ACD} + 4\bar{C}_{CD})}{\bar{C}_A + \bar{C}_{CD} + 1/K_1} + k_{-2} \cdot \frac{\bar{C}_{A_2CD} + 1/K_3}{\bar{C}_{CD} + \bar{C}_{A_2CD} + 1/K_3} \quad (E31)$$

Bibliography

1. Colour Index, 3rd ed., The Society of Dyers and Colourists, Bradford (U.K.), 1971.
2. The Merck Index, 8th ed., Merck and Co., Inc., Rahway (U.S.A.), 1968.
3. Scarborough, J.B., "Numerical Mathematical Analysis", Johns Hopkins Press, Baltimore (U.S.A.), 1955.
4. Mochida, K., A. Kagita, Y. Matsui and Y. Date, *Bull.Chem.Soc.Jpn.*, 46, 3703 (1973).
5. Uekama, K., M. Otagiri, Y. Kanie, S. Tanaka and K. Ikeda, *Chem.Pharm.Bull.*, 23, 1421 (1975).
6. Matsui, Y. and K. Mochida, *Bull.Chem.Soc.Jpn.*, 51, 673 (1978).
7. Kasha, M., H.R. Rawls and M. Ashraf El-Bayoumi, *Pure Appl.Chem.*, 11, 371 (1965).
8. Maitland, G.C., M. Rigby, E.B. Smith and W.A. Wakeham, "Intermolecular Forces. Their Origin and Determination", Oxford University Press, Oxford, 1981.
9. Schellman, J.A., *Acc.Chem.Res.*, 1, 144 (1968).
10. Kajtar, M., Cs. Horvath-Toro, E. Kuthi and J. Szejtli, *Acta Chim.Acad.Sci.Hung.*, 110, 327 (1982).
11. McRae, E.G. and M. Kasha, *J.Chem.Phys.*, 28, 721 (1958).
12. Czerlinski, G.H., "Chemical Relaxation", Dekker, New York, 1966.
13. Bernasconi, C.F., "Relaxation Kinetics", Academic Press Inc., New York, 1976.

Clarke, R.J., Coates, J.H. & Lincoln, S.F. (1984) Kinetic and equilibrium studies of cyclomalto-octaose (γ -cyclodextrin)-methyl orange inclusion complexes. *Carbohydrate Research*, v. 127(2), pp. 181-191

NOTE:

This publication is included on pages 217-227 in the print copy of the thesis held in the University of Adelaide Library.

It is also available online to authorised users at:

[https://doi.org/10.1016/0008-6215\(84\)85352-5](https://doi.org/10.1016/0008-6215(84)85352-5)

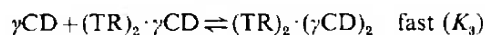
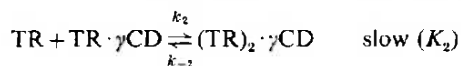
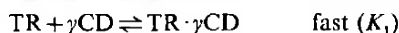
Complexation of Tropaeolin 000 No. 2 by β - and γ -Cyclodextrin

BY RONALD J. CLARKE, JOHN H. COATES* AND STEPHEN F. LINCOLN*

Department of Physical and Inorganic Chemistry, University of Adelaide,
South Australia 5001, Australia

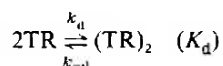
Received 23rd February, 1984

Measurements of the temperature-jump and equilibrium u.v.-visible and induced circular dichroic spectra of tropaeolin 000 No. 2 (TR) in the presence of α -, β - and γ -cyclodextrin (α CD, β CD and γ CD) have been carried out. Three complexation steps are detected in the presence of γ CD through the temperature-jump data (298.2 K):



where K_1 , K_2 and K_3 are $(4.18 \pm 1.47) \times 10^2$, $(1.68 \pm 0.54) \times 10^8$ and $(1.77 \pm 1.54) \times 10^2 \text{ dm}^3 \text{ mol}^{-1}$, respectively; $k_2 = (2.27 \pm 0.61) \times 10^9 \text{ dm}^3 \text{ mol}^{-1} \text{ s}^{-1}$ and $k_{-2} = (1.35 \pm 0.23) \times 10^3 \text{ s}^{-1}$. In the presence of β CD the third complexation was not detected and $K_1 = (7.1 \pm 0.7) \times 10^2$ and $K_2 = (4 \pm 7) \times 10^6 \text{ dm}^3 \text{ mol}^{-1}$; $k_2 = (5 \pm 6) \times 10^9 \text{ dm}^3 \text{ mol}^{-1} \text{ s}^{-1}$ and $k_{-2} = (1.3 \pm 1.5) \times 10^3 \text{ s}^{-1}$. No complexation reactions were detected in the presence of α CD. The equilibrium u.v.-visible spectra and the circular and linear dichroic spectra are consistent with these reaction schemes, but suggest different orientation and penetration for the $(\text{TR})_2$ dimer included in $(\text{TR})_2 \cdot \beta\text{CD}$ compared with $(\text{TR})_2 \cdot \gamma\text{CD}$.

For the equilibrium



the equilibrium constant $K_d = (9.10 \pm 4.28) \times 10^2 \text{ dm}^3 \text{ mol}^{-1}$ has been determined by u.v.-visible spectroscopy, and $k_{-d} = (2.24 \pm 0.40) \times 10^3 \text{ s}^{-1}$ has been estimated from temperature-jump experiments. Hence $k_d = (2.0 \pm 1.0) \times 10^6 \text{ dm}^3 \text{ mol}^{-1} \text{ s}^{-1}$. Thus the increase in stability of $(\text{TR})_2$ included in $(\text{TR})_2 \cdot \gamma\text{CD}$ and $(\text{TR})_2 \cdot \beta\text{CD}$ over that observed in the absence of cyclodextrin is a consequence of $k_2 \approx 10^3 k_d$.

The inclusion complexes formed by the cyclodextrins are currently subject to substantial investigation as they exhibit some of the characteristics of enzyme-substrate and drug-receptor interactions and are potentially important in the design of controlled chemical synthetic pathways.¹⁻⁵ The α -, β - and γ -cyclodextrins (CD), which are respectively six-, seven- and eight-membered α -1,4-linked cyclic oligomers of D-glucopyranose with internal annular radii of 5–6, 7–8 and 9–10 Å, respectively, present an opportunity to examine systematically the selectivity of cyclodextrins for substrates in the formation of inclusion complexes.^{6,7} The majority of reported studies of cyclodextrin inclusion-complex formation have been predominantly concerned with the determination of stability constants,^{8,9} but it was shown at an early stage that the inclusion-complex formation rates fall conveniently into the temperature-

jump spectrophotometric timescale.¹⁰ More recent studies of the inclusion of methyl orange¹¹ and crystal violet¹² by γ CD using this technique show the mechanism of the inclusion process to involve multiple equilibria, and in the case of the latter dye it was found that the dimerisation of crystal violet was accelerated *ca.* 10^3 -fold in the presence of γ CD. The latter observation is particularly interesting as the acceleration of the preassembly of reactant molecules is of considerable synthetic interest. Accordingly it is important to investigate the generality of this acceleration of dimerisation by cyclodextrins together with the mechanisms of inclusion complexation and the selectivity of the cyclodextrins in such complexations. In this study the aromatic azo dye tropaeolin 000 No. 2 (also known as orange II),¹³⁻¹⁵ which is known to dimerise in solution, has been selected as a probe to study the inclusion complexation reactions of α -, β - and γ -CD.

EXPERIMENTAL

Tropaeolin 000 No. 2 (B.D.H.) was purified by salting out from hot distilled water using sodium acetate after which it was recrystallised three times from distilled water and then twice from ethanol.¹⁶ Elemental analysis was consistent with the purified dye being the monohydrate. The α -, β - and γ -cyclodextrins (Sigma) were stored as the anhydrous material over P_2O_5 in a vacuum desiccator. The analytical-reagent-grade salts KH_2PO_4 (B.D.H.), Na_2HPO_4 (B.D.H.), K_2SO_4 (B.D.H.), NaCl (Univar), sodium acetate (B.D.H.) and glycine (B.D.H.) were used without further purification.

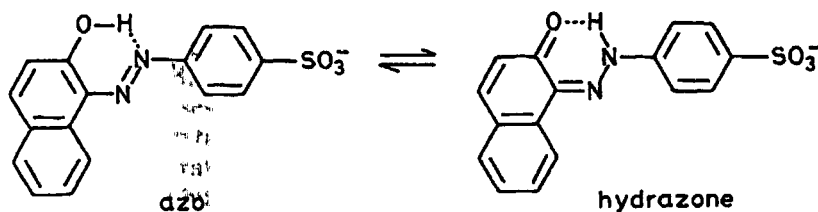
Tropaeolin solutions are known to 'age' slowly, probably as a result of nucleation,¹⁵ and in consequence all solutions studied were freshly prepared. Exposure to light was kept to a minimum prior to measurement. No adsorption of tropaeolin to glass or quartz was detected, nevertheless all volumetric glassware was cleaned at the same time by prolonged soaking in Decon 90 solution followed by extensive rinsing in triply distilled water to ensure a consistent surface history. The quartz spectrophotometer cells were carefully washed with each solution to be studied prior to the recording of its spectrum. All solutions were diluted by weight from stock solutions prepared using A-grade volumetric apparatus.

Visible spectra were measured in quartz cells using a Zeiss DMR10 double-beam spectrophotometer equipped with a thermostatted (± 0.1 K) cell block. Spectra were run in duplicate at 298.2 K, recorded digitally at 2 nm intervals in the range 340–600 nm, punched onto paper tape and analysed using a Cyber 173 computer. Temperature-jump spectrophotometric studies were carried out at 480 nm using equipment constructed to a design similar to that described in the literature.¹⁷ The temperature jump was 8.9 K with a heating time of *ca.* 5 μ s, and the observation temperature was 298.2 ± 0.1 K. Photomultiplier voltages for each transient were collected either as 1024 8-bit data points using a Data Lab DL905 transient recorder or as 4096 8-bit data points using a Data Lab DL910 and stored on magnetic tape. At least five transients were collected for each solution, then averaged and subjected to kinetic analysis using a Computer Products Spectrum II minicomputer. Circular dichroic spectra were measured on a JASCO J40-CS spectropolarimeter equipped with a microprocessor for averaging repeated measurements at each wavelength. Linear dichroic spectra were determined on stretched poly(vinyl alcohol) films¹⁸ using a Zeiss PMQ2 spectrophotometer.

RESULTS AND DISCUSSION

EQUILIBRIUM AND KINETIC ASPECTS

In water tropaeolin exists in a tautomeric equilibrium between its azo and hydrazone forms as shown below, with the latter form predominating.¹⁴ We find the u.v.–visible spectrum of tropaeolin to be invariant in water within the pH range 2.0–6.0 in the presence of either 0.05 mol dm⁻³ glycine + HCl or 0.10 mol dm⁻³ acetate buffer, which indicates that no significant shifts in protonic equilibria occur



under these conditions. (The pK_a of the hydroxy group is reported¹³ to be 11.4.) Thus the data discussed below, which were obtained from aqueous solutions buffered at pH 5.50 by 0.100 mol dm⁻³ phosphate buffer and 0.200 mol dm⁻³ in K₂SO₄ (selected to provide appropriate resistance for temperature-jump spectrophotometric experiments on the basis that SO₄²⁻ has a low tendency to be complexed by cyclodextrins¹⁶), pertain to the tropaeolin monoanion.

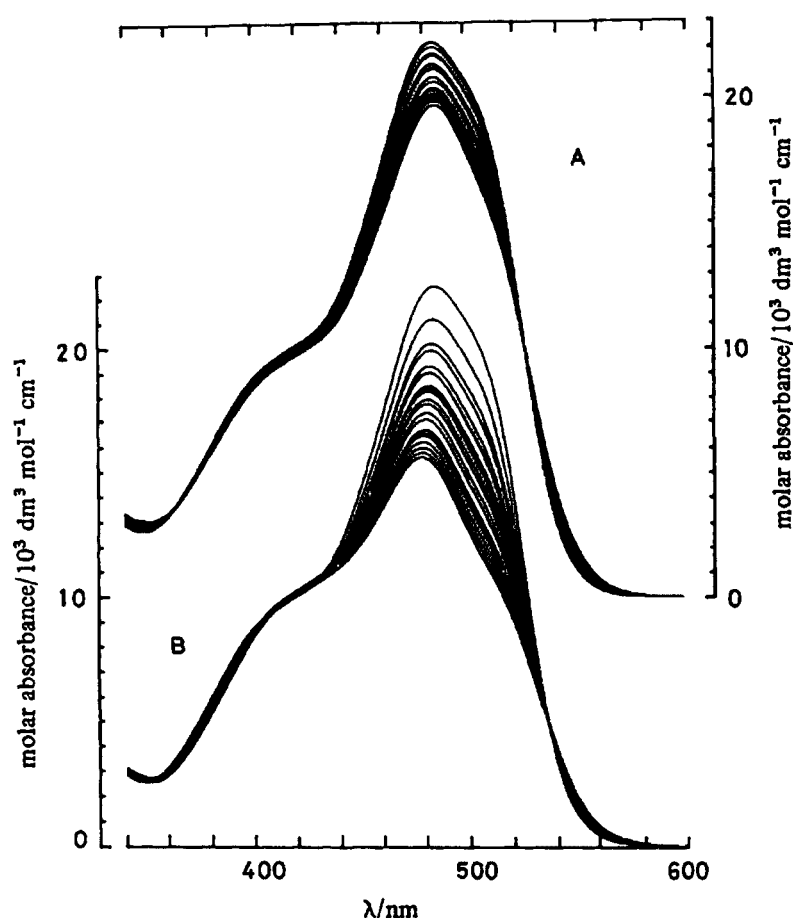


Fig. 1. Variation of the tropaeolin spectrum in the presence of β CD (data set A, right-hand scale) and γ CD (data set B, left-hand scale) at 298.2 K. In both cases the molar absorbance observed at 480 nm decreases systematically as the cyclodextrin concentration increases. The β CD and γ CD concentration ranges were $0-4.99 \times 10^{-3}$ and $0-2.56 \times 10^{-3}$ mol dm⁻³, respectively, and the tropaeolin concentration was 3.8×10^{-5} mol dm⁻³. The maximum β CD concentration is close to the solubility limit but the spectral variation with increase in $[\beta\text{CD}]$ is slight at $[\beta\text{CD}] > 4.99 \times 10^{-3}$ mol dm⁻³. The spectral variation observed in the $[\gamma\text{CD}]$ range 2.56×10^{-3} to 2.50×10^{-2} mol dm⁻³ is minimal and is not shown here.

Table 1. Initial concentrations and observed reciprocal relaxation times for the inclusion of TR by β CD at 298.2 K

[TR] ^a /10 ⁻⁵ mol dm ⁻³	[β CD] ^a /mol dm ⁻³	(1/ τ) ^b /10 ³ s ⁻¹
3.81 ± 0.03	(3.97 ± 0.06) × 10 ⁻⁵	3.11 ± 0.68
3.80 ± 0.03	(8.0 ± 0.1) × 10 ⁻⁵	4.35 ± 1.90
3.78 ± 0.03	(1.20 ± 0.02) × 10 ⁻⁴	5.83 ± 1.86
3.79 ± 0.03	(1.80 ± 0.02) × 10 ⁻⁴	10.96 ± 1.68
3.75 ± 0.03	(2.40 ± 0.03) × 10 ⁻⁴	13.63 ± 2.09
3.75 ± 0.03	(2.99 ± 0.04) × 10 ⁻⁴	14.95 ± 2.27
3.81 ± 0.03	(3.97 ± 0.03) × 10 ⁻⁴	20.90 ± 1.31
3.73 ± 0.03	(4.88 ± 0.04) × 10 ⁻⁴	20.87 ± 0.71
3.79 ± 0.03	(7.39 ± 0.05) × 10 ⁻⁴	22.17 ± 0.73
3.77 ± 0.03	(9.84 ± 0.06) × 10 ⁻⁴	22.76 ± 0.73
3.76 ± 0.03	(1.235 ± 0.008) × 10 ⁻³	21.64 ± 0.65
3.72 ± 0.03	(1.480 ± 0.009) × 10 ⁻³	21.65 ± 0.87
3.81 ± 0.03	(1.79 ± 0.01) × 10 ⁻³	22.04 ± 1.13
3.71 ± 0.03	(1.98 ± 0.01) × 10 ⁻³	22.76 ± 0.96
3.78 ± 0.03	(2.49 ± 0.02) × 10 ⁻³	21.83 ± 0.93
3.75 ± 0.03	(3.01 ± 0.02) × 10 ⁻³	19.96 ± 1.18
3.69 ± 0.03	(4.00 ± 0.02) × 10 ⁻³	20.94 ± 1.23
3.78 ± 0.02	(4.53 ± 0.02) × 10 ⁻³	18.38 ± 0.70
3.80 ± 0.03	(4.99 ± 0.03) × 10 ⁻³	19.75 ± 0.89
3.80 ± 0.02	(5.99 ± 0.02) × 10 ⁻³	18.79 ± 0.89
3.78 ± 0.02	(6.98 ± 0.03) × 10 ⁻³	16.07 ± 1.15
3.75 ± 0.02	(7.98 ± 0.03) × 10 ⁻³	15.30 ± 1.01
3.75 ± 0.02	(9.06 ± 0.04) × 10 ⁻³	14.60 ± 0.97
3.75 ± 0.02	(9.98 ± 0.04) × 10 ⁻³	13.53 ± 1.07

^a The errors in initial concentrations are estimated from known uncertainties in weighing.

^b The errors in 1/ τ are standard errors from the linear regressions of ln (voltage) against time.

The spectrum of tropaeolin exhibits a progressive decrease in molar absorbance in the range 420–520 nm as the concentration of either β CD or γ CD increases (fig. 1) with the latter cyclodextrin having the greatest effect. In contrast α CD induces negligible spectral change under the same conditions, and in consequence it is deduced that the interactions of the cyclodextrins with TR strengthen in the sequence α CD < β CD < γ CD. Qualitatively the spectral variations observed with increasing [β CD] and [γ CD] are similar to those observed on formation of the tropaeolin dimer¹⁵ (TR)₂ in the absence of cyclodextrin but the bathochromic (*ca.* 3 nm) and hypsochromic (*ca.* 7 nm) shifts from the TR absorbance maximum (480 nm) which occur with increase in [β CD] and [γ CD], respectively, indicate that the interaction of TR with these two cyclodextrins differs significantly. The isosbestic points observed in the presence of β CD and γ CD suggest the predominance of two absorbing species, but identification of the species in solution cannot be made from these data alone and is dependent on kinetic and other spectroscopic data which are discussed below.

Temperature-jump spectrophotometric studies at 480 nm of TR solutions alone and α -, β - and γ -CD solutions of TR show a fast relaxation occurring within the instrumental heating time (*ca.* 5 μ s) which produces a decrease in absorbance, the

Table 2. Initial concentrations and observed reciprocal relaxation times for the inclusion of TR by γ CD at 298.2 K

[TR] ^a /10 ⁻⁵ mol dm ⁻³	[γ CD] ^a /mol dm ⁻³	(1/ τ) ^b /10 ³ s ⁻¹
3.82 ± 0.04	(1.00 ± 0.02) × 10 ⁻⁵	2.81 ± 0.04
3.81 ± 0.04	(2.03 ± 0.03) × 10 ⁻⁵	2.99 ± 0.04
3.77 ± 0.04	(2.87 ± 0.04) × 10 ⁻⁵	3.61 ± 0.04
3.82 ± 0.04	(3.95 ± 0.06) × 10 ⁻⁵	3.97 ± 0.04
3.84 ± 0.04	(4.88 ± 0.07) × 10 ⁻⁵	4.22 ± 0.04
3.87 ± 0.05	(5.85 ± 0.08) × 10 ⁻⁵	4.46 ± 0.05
3.81 ± 0.04	(7.0 ± 0.1) × 10 ⁻⁵	4.81 ± 0.05
3.88 ± 0.04	(7.6 ± 0.1) × 10 ⁻⁵	5.10 ± 0.05
3.85 ± 0.04	(9.0 ± 0.1) × 10 ⁻⁵	5.41 ± 0.06
3.83 ± 0.05	(1.00 ± 0.01) × 10 ⁻⁴	5.39 ± 0.05
3.85 ± 0.05	(1.20 ± 0.02) × 10 ⁻⁴	6.34 ± 0.08
3.82 ± 0.04	(1.58 ± 0.02) × 10 ⁻⁴	7.19 ± 0.10
3.85 ± 0.05	(2.01 ± 0.03) × 10 ⁻⁴	8.29 ± 0.09
3.82 ± 0.05	(2.95 ± 0.04) × 10 ⁻⁴	9.85 ± 0.12
3.85 ± 0.05	(3.91 ± 0.04) × 10 ⁻⁴	10.92 ± 0.18
3.85 ± 0.05	(5.21 ± 0.05) × 10 ⁻⁴	12.34 ± 0.20
3.82 ± 0.04	(7.23 ± 0.07) × 10 ⁻⁴	13.59 ± 0.15
3.84 ± 0.04	(1.04 ± 0.01) × 10 ⁻³	14.33 ± 0.17
3.81 ± 0.04	(1.55 ± 0.02) × 10 ⁻³	13.84 ± 0.17
3.81 ± 0.03	(1.99 ± 0.01) × 10 ⁻³	13.48 ± 0.25
3.80 ± 0.03	(2.94 ± 0.02) × 10 ⁻³	13.40 ± 0.60
3.71 ± 0.03	(3.52 ± 0.02) × 10 ⁻³	12.10 ± 0.38
3.76 ± 0.03	(3.98 ± 0.02) × 10 ⁻³	13.06 ± 0.50
3.80 ± 0.03	(4.98 ± 0.02) × 10 ⁻³	10.43 ± 0.50
3.80 ± 0.03	(6.09 ± 0.03) × 10 ⁻³	8.62 ± 0.44
3.79 ± 0.03	(6.91 ± 0.03) × 10 ⁻³	8.04 ± 0.38
3.79 ± 0.03	(8.10 ± 0.04) × 10 ⁻³	7.75 ± 0.47
3.80 ± 0.03	(9.04 ± 0.04) × 10 ⁻³	8.13 ± 0.75
3.77 ± 0.03	(9.99 ± 0.04) × 10 ⁻³	6.39 ± 0.82
3.80 ± 0.03	(1.108 ± 0.005) × 10 ⁻²	5.82 ± 0.53
3.79 ± 0.03	(1.194 ± 0.005) × 10 ⁻²	5.99 ± 0.57
3.78 ± 0.03	(1.403 ± 0.006) × 10 ⁻²	4.83 ± 0.50
3.80 ± 0.03	(1.607 ± 0.007) × 10 ⁻²	4.75 ± 0.26
3.78 ± 0.03	(1.805 ± 0.007) × 10 ⁻²	4.34 ± 0.30

^{a, b} See table 1.

magnitude of which is proportional to the total [TR] and is little affected by the presence of the cyclodextrins. This is followed by a slow relaxation (tables 1 and 2) which produces an increase in absorbance, the magnitude of which, in the presence of TR alone, never exceeds 15% of the amplitude of the fast relaxation. The presence of α CD produces no detectable change in the relaxations observed in the presence of TR alone, which indicates that interaction between TR and α CD is not detectable, as was earlier deduced from the equilibrium spectral data. In contrast, in the presence of β CD the amplitude of the slow relaxation becomes greater than that of the fast relaxation approximately one-third of the way from the low end of the [β CD] range. In the presence of γ CD the slow relaxation is substantially greater in amplitude than

the fast relaxation over the entire $[\gamma\text{CD}]$ range studied (table 2). It is also found that the slow relaxations observed in the presence of βCD and γCD are substantially faster than the slow relaxation observed in the presence of TR alone. The constant and variable natures, respectively, of the fast and slow relaxations indicate that the fast process is little affected by the presence of cyclodextrin and may therefore pertain to a monomeric intramolecular TR process, whereas the slow relaxation, being substantially affected by the presence of β and γCD , probably arises from an intermolecular process involving a cyclodextrin. In all cases the total absorbance change arising from the two relaxations is consistent with the temperature variation of the equilibrium spectrum; however, as the fast relaxation is outside the experimental timescale it is not further considered and subsequent discussion refers to the slow relaxations only.

Tropeolin is known to dimerise¹⁵ in aqueous solutions:

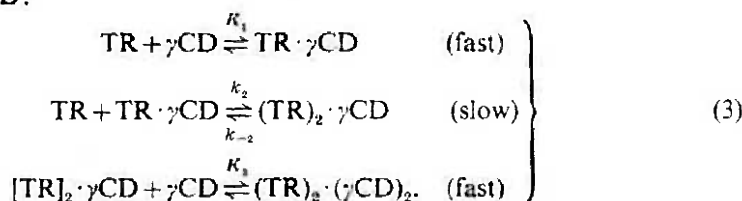


and the increase in absorbance characterising the slow relaxation is consistent with a shift towards the monomer side of the equilibrium with increasing temperature. The total $[\text{TR}]$ range over which this single-exponential relaxation may be quantitatively studied is limited to $(2-6) \times 10^{-5} \text{ mol dm}^{-3}$ as a consequence of the small absorbance changes and the high molar absorbances of the TR solutions. The reciprocal relaxation time, $1/\tau = (2.24 \pm 0.40) \times 10^3 \text{ s}^{-1}$, exhibits no significant variation within this experimental $[\text{TR}]$ range at 298.2 K. Eqn (2)¹² describes the expected variation of $1/\tau$ with total tropeolin concentration $[\text{TR}]_0$ for the dimerisation equilibrium (1):

$$1/\tau^2 = k_{-d}^2(8K_d[\text{TR}]_0 + 1). \quad (2)$$

Under our conditions $8K_d[\text{TR}]_0 \ll 1$, yielding $k_{-d} \approx 1/\tau = (2.24 \pm 0.40) \times 10^3 \text{ s}^{-1}$. U.v.-visible spectrophotometric studies of tropeolin solutions gave a value of $K_d = (9.10 \pm 4.28) \times 10^2$ at pH 5.5 in $0.100 \text{ mol dm}^{-3}$ phosphate and $0.200 \text{ mol dm}^{-3} \text{ K}_2\text{SO}_4$, which is comparable with the literature value of 7.1×10^2 obtained at lower ionic strength. Using our data it is thus found that $k_d = (2.0 \pm 1.0) \times 10^6 \text{ dm}^3 \text{ mol}^{-1} \text{ s}^{-1}$.

The variation of $1/\tau^*$ characterising TR/ γCD solutions in the $[\gamma\text{CD}]$ range 1.0×10^{-3} to $1.8 \times 10^{-2} \text{ mol dm}^{-3}$ at $[\text{TR}] \approx 3.8 \times 10^{-5} \text{ mol dm}^{-3}$ is shown in fig. 2, and the individual $1/\tau$ values appear in table 2. This variation of $1/\tau$ is similar to that observed for methyl orange¹¹ and crystal violet¹² in the presence of γCD and is consistent with the coupled relaxation of the three equilibria shown in reaction (3), where $\text{TR} \cdot \gamma\text{CD}$ is an inclusion complex of TR in γCD , $(\text{TR})_2 \cdot \gamma\text{CD}$ is an inclusion complex of $(\text{TR})_2$ in γCD , and $(\text{TR})_2 \cdot (\gamma\text{CD})_2$ is a complex in which both ends of $(\text{TR})_2$ are included by γCD :



* When $[\gamma\text{CD}] \geq 2.9 \times 10^{-3} \text{ mol dm}^{-3}$ a third and slower relaxation appeared which was $\leq 2\%$ amplitude of the main relaxation. In consequence the relaxation data were fitted to two exponential curves and it is the $1/\tau$ characterising the greatly predominant relaxation amplitude which is plotted in fig. 2 and quoted in table 2. The origin of the minor relaxation is not known.

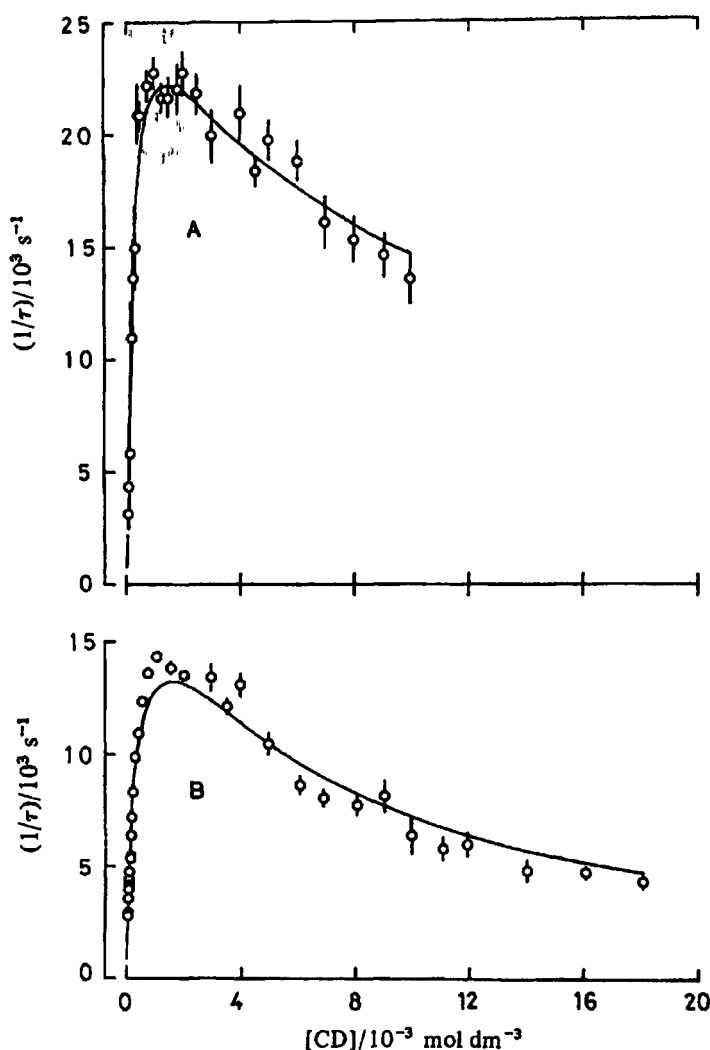


Fig. 2. (A) Variation of $1/\tau$ (298.2 K) characterising the TR/ β CD system with variation of the total [β CD]. The solid curve represents the best fit of the data to eqn (5). (B) The variation of $1/\tau$ (298.2 K) characterising the TR/ γ CD system with variation of the total [γ CD]. The solid curve represents the best fit of the data to eqn (4).

Using the method of Bernasconi¹⁹ or Czerlinski²⁰ eqn (4) may be derived for $1/\tau$ characterising the coupled equilibria of reaction (3):

$$1/\tau = k_2 \left(\frac{[\text{TR}]([\text{TR} \cdot \gamma\text{CD}] + [\text{TR}] + 4[\gamma\text{CD}])}{[\text{TR}] + [\gamma\text{CD}] + 1/K_1} \right) + k_{-2} \left(\frac{[(\text{TR})_2 \cdot \gamma\text{CD}] + 1/K_3}{[\gamma\text{CD}] + [(\text{TR})_2 \cdot \gamma\text{CD}] + 1/K_3} \right) \quad (4)$$

(all concentrations are equilibrium values).

The non-linear regression curve for the fit of the $1/\tau$ data to eqn (4), in which each datum point was weighted according to its experimental error, is shown in fig. 2 and the derived parameters appear in table 3. These $1/\tau$ data can also be fitted to the equation

$$1/\tau = k_2 \left(\frac{[\text{TR}]([\text{TR} \cdot \gamma\text{CD}] + [\text{TR}] + 4[\gamma\text{CD}])}{[\text{TR}] + [\gamma\text{CD}] + 1/K_1} \right) + k_{-2} \quad (5)$$

Table 3. Equilibrium and kinetic parameters (298.2 K)

system	$K_1/10^2 \text{ dm}^3 \text{ mol}^{-1}$	$K_2/10^5 \text{ dm}^3 \text{ mol}^{-1}$	$K_3/10^8 \text{ dm}^3 \text{ mol}^{-1}$	$k_2/10^9 \text{ dm}^3 \text{ mol}^{-1} \text{ s}^{-1}$	$k_{-2}/10^3 \text{ s}^{-1}$
tropaeolin/ β -cyclodextrin ^a	7.1 ± 0.7	40 ± 70	—	5 ± 6	1.3 ± 1.5
tropaeolin/ γ -cyclodextrin ^a	4.18 ± 1.47	16.8 ± 0.54	0.177 ± 0.154	2.27 ± 0.61	1.35 ± 0.23
tropaeolin ^a	—	$0.0091 \pm 0.0043 (= K_d)$	—	$0.0020 \pm 0.0010 (= k_d)$	$2.2 \pm 0.4 (= k_{-d})$
methyl orange/ γ -cyclodextrin ^b	0.45 ± 0.07	20 ± 11	6.1 ± 2.5	9.4 ± 5.1	4.8 ± 0.8
crystal violet/ γ -cyclodextrin ^c	4.63 ± 0.06	10.3 ± 0.9	—	1.73 ± 0.08	1.68 ± 0.07
crystal violet ^c	—	$ca. 0.006 (= K_d)$	—	$ca. 0.0009 (= k_d)$	$ca. 1.5 (= k_{-d})$

^a This study. ^b Ref. (11). ^c Ref. (12).

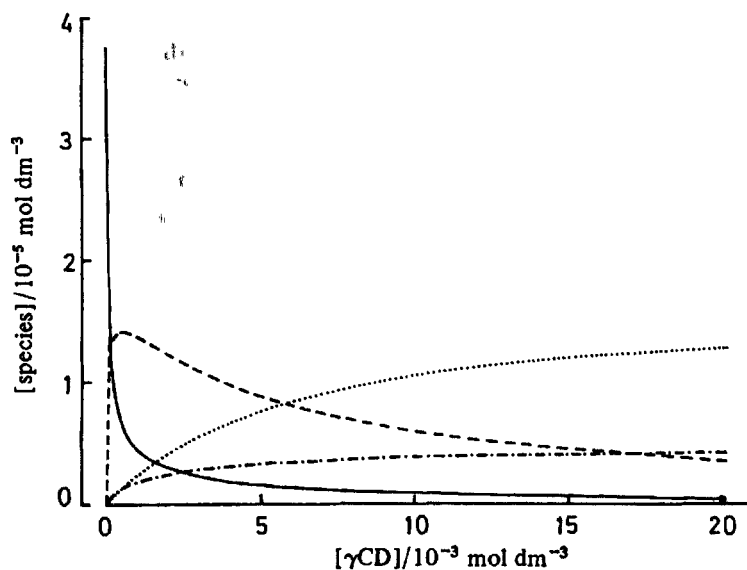


Fig. 3. Variation of (—) [TR], (---) [TR· γ CD], (-·-·-) [(TR) $_2$ · γ CD] and (·····) [(TR) $_2$ ·(γ CD) $_2$] with variation of total [γ CD] at constant total [TR] = 3.80×10^{-5} mol dm $^{-3}$. The species concentrations were calculated using $K_1 = 4.18 \times 10^2$ mol dm $^{-3}$, $K_2 = 1.68 \times 10^6$ mol dm $^{-3}$ and $K_3 = 1.77 \times 10^8$ mol dm $^{-3}$.

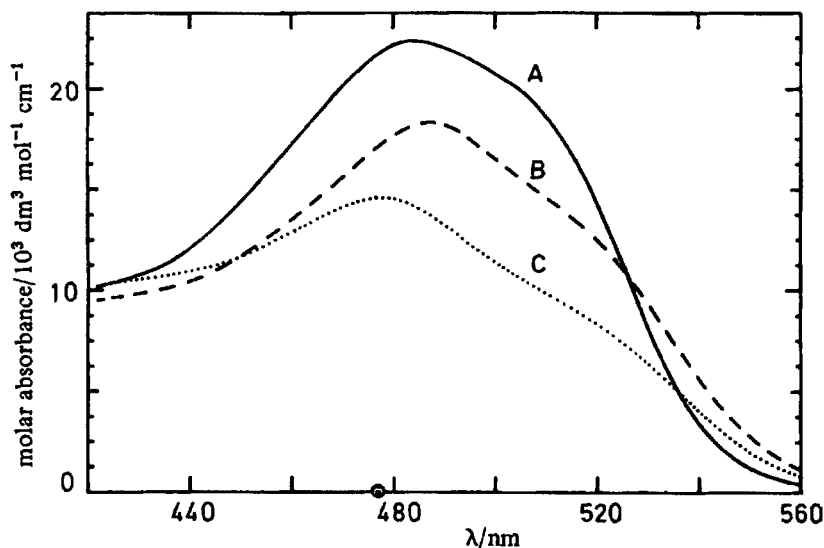


Fig. 4. Spectra of (A) TR, (B) (TR) $_2$ · β CD and (C) (TR) $_2$ · γ CD.

which characterises the variation of $1/\tau$ for the first two coupled equilibria shown in reaction (3) only. The errors in the parameters derived through eqn (5) are considerably greater than those derived through eqn (4), and thus it appears that the three coupled equilibria in reaction (3) best describe the TR/ γ CD system. In contrast, the variation of $1/\tau$ for the TR/ β CD system appears to be best described by eqn (5), which produces the regression curve shown in fig. 2 and the parameters given in table 3. The $1/\tau$ data for the TR/ β CD system may also be fitted to eqn (4), but the errors are substantially

greater than those obtained through eqn (5). As a consequence of the lesser relaxation amplitudes observed for the TR/ β CD system, particularly at low concentrations, the errors in $1/\tau$ are substantially greater than those observed for the TR/ γ CD system (table 2), and as a consequence the errors in k_2 and k_{-2} are also substantially greater. The $[\beta\text{CD}]$ range is restricted by the solubility of βCD , which is substantially less than that of γCD .¹

SPECTROSCOPIC ASPECTS

The variation of the concentration of species in solution with $[\gamma\text{CD}]$ is shown in fig. 3, which was generated using K_1 , K_2 and K_3 (table 3) derived from the temperature-jump spectrophotometric study. It was observed that although the equilibrium spectra of the TR/ γ CD system exhibit little variation at $[\gamma\text{CD}] > 2.56 \times 10^{-3} \text{ mol dm}^{-3}$, substantial variations in species concentrations do occur. Clearly a fortuitous combination of spectral characteristics and species concentrations render the observed solution spectra insensitive to changes in the positions of the equilibria shown in reaction (3) when $[\gamma\text{CD}] > 2.56 \times 10^{-3} \text{ mol dm}^{-3}$. Attempts to fit the spectral variation in the range 470–520 nm shown in fig. 1 to the three equilibria shown in reaction (3) using non-linear least-squares fitting procedures failed to produce a unique data fit. Accordingly data for fifteen solutions in the $[\gamma\text{CD}]$ range $0\text{--}5.00 \times 10^{-4} \text{ mol dm}^{-3}$ were fitted to the following equilibrium



and the derived $K_{12} = (4.10 \pm 0.11) \times 10^8 \text{ dm}^6 \text{ mol}^{-2}$. This value compares with $K_1 K_2 = (7.0 \pm 3.3) \times 10^8 \text{ dm}^6 \text{ mol}^{-2}$ derived from the temperature-jump spectrophotometric data and indicates a satisfactory degree of internal consistency for the TR/ γ CD system. Analysis of the spectral variation observed over the $[\gamma\text{CD}]$ range $0\text{--}5.00 \times 10^{-4} \text{ mol dm}^{-3}$ (fig. 1) according to the equilibrium shown in reaction (6) using the equilibrium constant $K_{12} = (4.10 \pm 0.11) \times 10^8 \text{ dm}^6 \text{ mol}^{-2}$ yields the spectrum of $(\text{TR})_2 \cdot \gamma\text{CD}$ shown in fig. 4. The concentrations of TR \cdot γCD and $(\text{TR})_2 \cdot (\gamma\text{CD})_2$ are shown to be small from temperature-jump measurements (fig. 3); thus their contribution has been neglected in the calculation above. Over the $[\gamma\text{CD}]$ range 5×10^{-4} to $2.5 \times 10^{-2} \text{ mol dm}^{-3}$ the small spectral variations (fig. 1) caused by the substantial variations in the concentrations of the species present (fig. 3) rendered reliable derivations of the spectra of TR \cdot γCD and $(\text{TR})_2 \cdot (\gamma\text{CD})_2$ impossible.

Analysis of the spectral variations of the TR/ β CD system through the analogous equilibrium to that shown in reaction (6) yields $K_{12} = (2.03 \pm 0.21) \times 10^7 \text{ dm}^6 \text{ mol}^{-2}$, which compares with $K_1 K_2 = (2.84 \pm 4.59) \times 10^6 \text{ dm}^6 \text{ mol}^{-2}$ derived from the temperature-jump spectrophotometric data. The large error in $K_1 K_2$, the source of which was discussed earlier, renders comparison with K_{12} semi-quantitative at best, and hence this aspect is not further pursued. Nevertheless the spectrum of $(\text{TR})_2 \cdot \beta\text{CD}$ derived (fig. 4) from the spectral variation in fig. 1 using the equilibrium constant $K_{12} = (2.03 \pm 0.21) \times 10^7 \text{ dm}^6 \text{ mol}^{-2}$ allows qualitative comparison with the spectra of TR and $(\text{TR})_2 \cdot \gamma\text{CD}$. (The concentration of TR \cdot βCD and its contribution to the spectral variation shown in fig. 1 is too small to permit a meaningful determination of the spectrum of this species.)

The circular dichroic spectra of solutions of TR in the presence of βCD or γCD (fig. 5) are obtained under conditions in which $(\text{TR})_2 \cdot \beta\text{CD}$ and $(\text{TR})_2 \cdot \gamma\text{CD}$ are the greatly predominant species. Fig. 5 shows that inclusion of the TR dimer in both β - and γ -cyclodextrin leads to induced circular dichroism. However, the differences in sign for the bands approximately centred at 475 and 535 nm imply different geometries

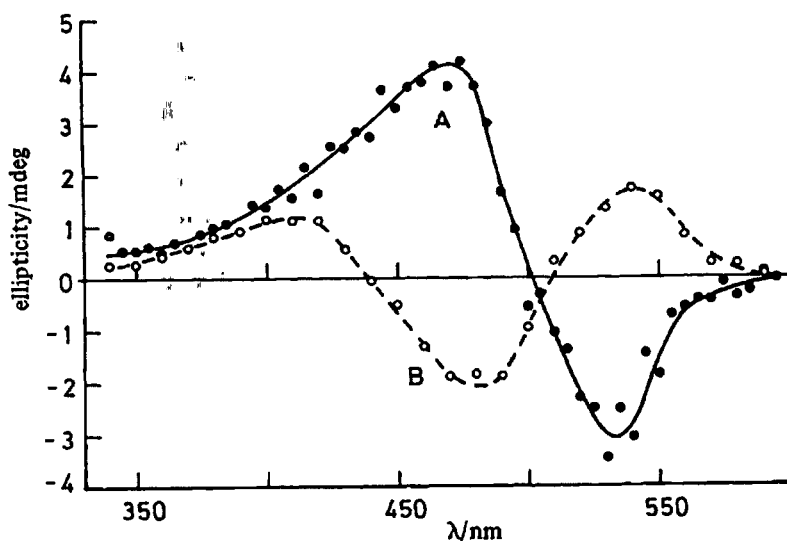


Fig. 5. (A) Circular dichroic spectrum of $(\text{TR})_2 \cdot \gamma\text{CD}$ (total $[\gamma\text{CD}]$ and $[\text{TR}] = 3.41 \times 10^{-5}$ and $3.75 \times 10^{-5} \text{ mol dm}^{-3}$, respectively). (B) Circular dichroic spectrum of $(\text{TR})_2 \cdot \beta\text{CD}$ (total $[\beta\text{CD}]$ and $[\text{TR}] = 4.00 \times 10^{-5}$ and $3.81 \times 10^{-5} \text{ mol dm}^{-3}$, respectively).

for the inclusion complexes in each case. Detailed interpretation is complex, since the formation of a dimer *per se* leads to exciton splitting of the monomer absorption bands, and inclusion leads to further interactions with the seven (βCD) or eight (γCD) chiral glucopyranose rings of the respective cyclodextrins.^{21, 22}

The linear dichroic spectra of TR adsorbed to poly(vinyl alcohol) film which was subsequently stretched are shown in fig. 6. When the film is stretched there is a tendency for the dye molecules to align with the direction of stretch. The absorbance parallel to the direction of stretch is seen to be substantially greater than that perpendicular to the direction of stretch, and over the range 400–500 nm the ratio, R , of these two absorbances is constant (fig. 6). This is consistent with the transition moment(s) of TR in this range being aligned approximately with the axis along which the trapped dye molecules are oriented in the stretched film. In this case the axis passes approximately through the sulphonato group and the more distant ring of the naphthalene residue.²³

The spectrum of TR in the range 400–550 nm could arise either from different electronic transitions or from a vibronic progression of a single electronic transition. The linear dichroism results do not allow one to distinguish between these possibilities. On dimerisation, however, exciton splitting as a consequence of dipole coupling of these transitions is expected to produce positive and negative rotational strengths; such behaviour is seen in fig. 5.^{21, 22} It has already been pointed out that the circular dichroic spectra of the dimers in $(\text{TR})_2 \cdot \beta\text{CD}$ and $(\text{TR})_2 \cdot \gamma\text{CD}$ are quite different, which probably means that the dimer geometries are different and/or that similar dimers are differently disposed within each cyclodextrin.

According to exciton theory,²² slight bathochromic and hypsochromic shifts such as those observed for $(\text{TR})_2 \cdot \beta\text{CD}$ and $(\text{TR})_2 \cdot \gamma\text{CD}$, respectively, (fig. 5) arise for dimers with idealised end-to-end in-line transition dipoles and parallel transition dipoles, respectively. In the case of TR molecules (which are unlikely to be planar) interacting together with an encapsulating cyclodextrin, the constituent monomer transition dipoles are likely to be in oblique, co-planar inclined or non-planar orientations. Nevertheless, a *prima facie* interpretation of the spectral shifts, taking into account

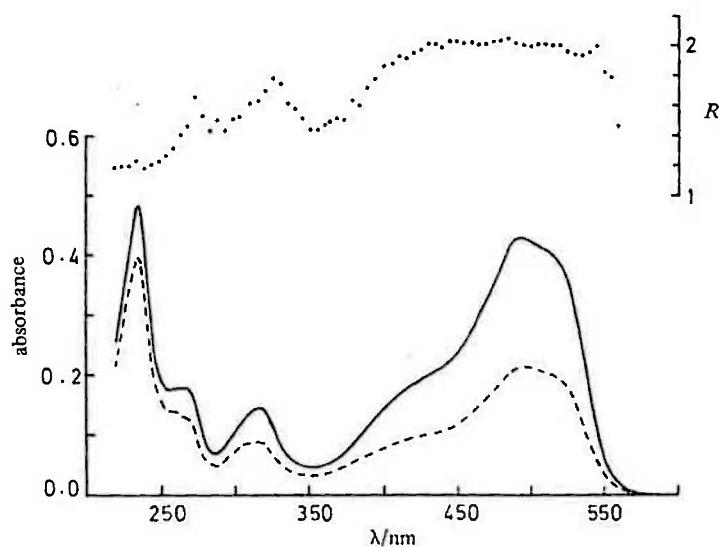
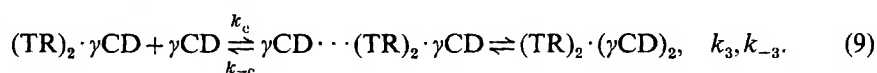
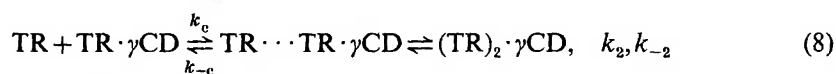
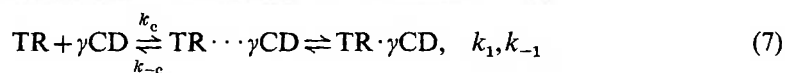


Fig. 6. Linear dichroic spectrum of TR on stretched poly(vinyl alcohol) film: (—) parallel to stretch and (---) perpendicular to stretch (left-hand ordinate). Absorbance units are arbitrary. The ratio of the parallel and perpendicular absorbances, R , are shown as individual points and refer to the right-hand ordinate.

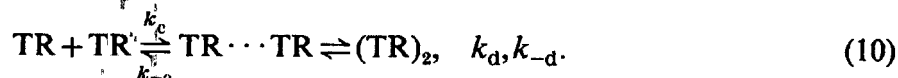
evidence from space-filling molecular models, suggests that in the $(\text{TR})_2 \cdot \gamma\text{CD}$ complex the TR molecules are antiparallel, largely superimposed and both inside the γCD . In the $(\text{TR})_2 \cdot \beta\text{CD}$ complex it is likely that one TR molecule is included, with the other antiparallel but displaced longitudinally and not inside the cyclodextrin. The antiparallel arrangements are likely since they would result in minimum mutual repulsion between the sulphonato groups.

MECHANISTIC ASPECTS

The inclusion of TR by γCD involves a sequence of sterically orienting interactions and solvation changes which are not separately identifiable from experiment. It is nevertheless informative to consider the formation of the various inclusion complexes in a reaction scheme truncated into two stages.¹² The first stage is the diffusion-controlled formation of a collisional complex typified by a formation rate constant $k_c \approx 10^{10} \text{ dm}^3 \text{ mol}^{-1} \text{ s}^{-1}$ in which the solvation of the two interacting species is little altered. The second stage, which involves substantial changes in the steric orientation and solvation,^{4,10} is the formation of the inclusion complex. These two stages are shown in reactions (7)–(9), which are expansions of reaction (3):



Reaction (10) shows the equivalent two states for the formation of $(\text{TR})_2$:



The rate constants to the right of these equilibria are the overall rate constants and correspond to those given in table 3 for reactions (8) and (10). As experimental kinetic data are available for reactions (8) and (10) the interactions shown therein are considered first.

As a consequence of $k_2 \approx 10^3 k_d$ the tropaeolin dimer, $(\text{TR})_2$, is *ca.* 10^3 more stable in $(\text{TR})_2 \cdot \gamma\text{CD}$ than in water alone. It is reasonable to assume that the $(\text{TR})_2$ structure is the same in both environments, as was discussed earlier, and also that k_c is similar for reactions (8) and (9). The steric constraints placed on the formation of $(\text{TR})_2$ in $(\text{TR})_2 \cdot \gamma\text{CD}$ are substantially greater than those placed on the formation of $(\text{TR})_2$ in water alone, and yet $k_2 \approx 10^3 k_d$. This suggests that the rates of steric orientation are not major determinants of k_2 and k_d and that the desolvation processes are the dominant rate-determining factors. In the solid state the γCD annulus is occupied by seventeen disordered water molecules,²⁴ and a similar situation is likely to prevail in solution. Thus the formation of $\text{TR} \cdot \gamma\text{CD}$ will result in expulsion of many of these water molecules from the annulus, and the included end of TR will be largely desolvated whilst the protruding end will be enveloped in the solvation shell of $\text{TR} \cdot \gamma\text{CD}$. An examination of molecular models suggests that TR fits loosely into the γCD annulus, and in consequence the second TR in the collisional species $\text{TR} \cdots \text{TR} \cdot \gamma\text{CD}$ encounters a partly desolvated TR in a partially hydrophobic environment. The entry of this second TR molecule into the annulus involves a complicated sequence of events. It is envisaged that the establishment of a strong dispersion-force interaction between the desolvated portion of the included TR and the entering TR facilitates the sequential expulsion of solvating water and the consequent completion of the dimer formation in $(\text{TR})_2 \cdot \gamma\text{CD}$. In comparison the formation of $(\text{TR})_2$ in water, where both TR entities in the collisional species $\text{TR} \cdots \text{TR}$ [reaction (10)] are fully solvated, the strong dispersion-force interaction is less readily established and consequently the dimerisation occurs less readily. The dissociation of $(\text{TR})_2 \cdot \gamma\text{CD}$ and $(\text{TR})_2$ requires the progressive insertion of water molecules between the planes of the $(\text{TR})_2$ dimer, and it is clear that the disruption of the considerable dispersion forces between the TR entities is likely to be a major determinant of k_{-2} and k_{-d} [reactions (8) and (10)]. The close similarity of these rate constants suggests that this is the dominant factor determining their magnitude. This model for the dimerisation of TR in the absence and presence of γCD is supported by the semiquantitative data characterising the $\text{TR}/\beta\text{CD}$ system (table 3) and also by that for the crystal violet/ γCD system (table 3). Thus whilst the model is simplistic, as it does not specifically consider the possible influences of hydrogen bonding of γCD hydroxy groups with TR or solvating water, or the influence of the strong dispersion force interactions thought to exist between included species and cyclodextrins,²⁵ its applicability to three different systems enhances its plausibility.

It was shown earlier that the formation of $\text{TR} \cdot \gamma\text{CD}$ is required to be a rapid pre-equilibrium in the treatment of the kinetics of formation of $(\text{TR})_2 \cdot \gamma\text{CD}$. (An analogous rapid pre-equilibrium exists in the methyl orange/ γCD and crystal violet/ γCD systems.^{11,12}) In the absence of direct determinations of k_1 and k_{-1} [reaction (7)] only estimates can be made of their magnitude. Nevertheless, as the largest directly determined rate constant for a 1:1 inclusion complex [k_1 (298.2) = $1.4 \times 10^8 \text{ dm}^3 \text{ mol}^{-1} \text{ s}^{-1}$] was observed for the *p*-nitrophenolate/ αCD system,¹⁰ a reasonable basis for estimating k_1 and k_{-1} for the $\text{TR}/\gamma\text{CD}$ system exists.

The annular radius of γ CD (9–10 Å) is considerably greater than that of α CD (5–6 Å), and hence the constraints on inclusion of a simply substituted phenyl group such as that of TR should be comparatively small for γ CD. As the formation of $(\text{TR})_2 \cdot \gamma\text{CD}$ is characterised by $k_2 = 2.27 \times 10^9 \text{ dm}^3 \text{ mol}^{-1} \text{ s}^{-1}$ it is probable that the relatively unhindered inclusion of TR to form $\text{TR} \cdot \gamma\text{CD}$ will be characterised by $k_1 \geq 2 \times 10^9 \text{ dm}^3 \text{ mol}^{-1} \text{ s}^{-1}$, on which basis $k_{-1} \geq 5 \times 10^7 \text{ s}^{-1}$ which is *ca.* 10^2 greater than k_{-1} reported for α CD systems.¹⁰ On this basis the formation equilibria of $\text{TR} \cdot \beta\text{CD}$ and the methyl orange/ γ CD and crystal violet/ γ CD systems are also found to be more labile than the α CD species. These observations are consistent with the rapid pre-equilibrium required to explain the variations of $1/\tau$ in fig. 2. Whilst it is anticipated that the larger cyclodextrins might produce the more facile equilibria as a consequence of the looser fit of γ CD to a given substrate, experimental confirmation is not yet available.

The formation of a species analogous to $(\text{TR})_2 \cdot (\gamma\text{CD})_2$ has been observed in the methyl orange/ γ CD system (table 2) but such a species is not observed in the crystal violet/ γ CD system, probably as a consequence of the steric hindrance engendered by the trigonal geometry of crystal violet. [The apparent absence of a $(\text{TR})_2 \cdot (\beta\text{CD})_2$ species may be a consequence of the small β CD annulus, but in view of the semiquantitative nature of the data for the TR/ β CD system it is not further considered.] The simultaneous inclusion of both ends of a dimer by γ CD has been the subject of only one report,¹¹ however, it is not surprising that such inclusion complexes should exist as the simultaneous inclusion of both ends of monomeric cinnamates²⁶ and fluorocinnamates²⁷ by the smaller α CD has been observed.

The apparent inability of α CD to form $\text{TR} \cdot \alpha\text{CD}$ is surprising as β CD readily forms $(\text{TR})_2 \cdot \beta\text{CD}$. It is possible that the spectra of TR and $\text{TR} \cdot \alpha\text{CD}$ do not differ greatly and that in consequence the latter species is not detected. Nevertheless as the spectral change accompanying the inclusion of $(\text{TR})_2$ is substantially a consequence of increased dimer formation, the absence of $(\text{TR})_2 \cdot \alpha\text{CD}$ may be unambiguously attributed to the small size of the α CD annulus, which in contrast to the annuli of β CD and γ CD is unable to accommodate $(\text{TR})_2$. The preferential inclusion of $(\text{TR})_2$ to form $(\text{TR})_2 \cdot \gamma\text{CD}$ (K_2) by comparison with the inclusion of TR to form $\text{TR} \cdot \gamma\text{CD}$ (K_1) is also observed for the TR/ β CD, methyl orange/ γ CD, and crystal violet/ γ CD systems (table 3), and appears to illustrate the increased stability which results from a close matching of the substrate and cyclodextrin annular sizes.

Our attention has been drawn to a paper²⁸ in which the interactions of a variety of azo dyes with α CD have been studied using the temperature-jump and stopped-flow methods. The temperature-jump relaxation times are of the same order of magnitude as those reported here but their concentration dependences are quite different. The mechanism suggested by Hersey and Robinson for α CD-azo dye interactions involves the formation of a binary complex followed by an isomerization step. Our results for β CD and γ CD are, on the other hand, compatible with formation of an included dye dimer. This result is not unexpected in view of the greater cavity sizes in β CD and γ CD compared with α CD and the known tendency of TR to dimerise.¹⁵

We thank Dr Tom Kurucsev for the use of his non-linear least-squares fitting program DATAFIT and for his advice on circular and linear dichroic spectroscopy.

¹ M. L. Bender and M. Komiyama, *Cyclodextrin Chemistry* (Springer, Berlin, 1978).

² W. Saenger, *Angew. Chem., Int. Ed. Engl.*, 1980, **19**, 344.

³ I. Tabushi, *Acc. Chem. Res.*, 1982, **15**, 66.

⁴ J. Szejtli, *Cyclodextrins and Their Inclusion Complexes* (Akadémiai Kiado, Budapest, 1982).

- ⁵ R. Breslow, *Chem. Br.*, 1983, 126.
- ⁶ K. Kano, I. Takenoshita and T. Ogawa, *Chem. Lett.*, 1982, 321.
- ⁷ A. Ueno, K. Takahashi, Y. Hino and T. Osa, *J. Chem. Soc., Chem. Commun.*, 1981, 194.
- ⁸ H. Kondo, H. Nokitani and K. Hiromi, *J. Biochem. (Tokyo)*, 1976, **79**, 393.
- ⁹ H. Hirai, N. Toshima and S. Uenoyama, *Polym. J.*, 1981, **13**, 607.
- ¹⁰ F. Cramer, W. Saenger and H-Ch. Spatz, *J. Am. Chem. Soc.*, 1967, **89**, 14.
- ¹¹ R. J. Clarke, J. H. Coates and S. F. Lincoln, *Carbohydr. Res.*, 1984, **127**, 181.
- ¹² R. L. Schiller, J. H. Coates and S. F. Lincoln, *J. Chem. Soc., Faraday Trans. 1*, 1984, **80**, 1257.
- ¹³ H. Zollinger, *Azo and Diazo Chemistry: Aliphatic and Aromatic Compounds* (Interscience, New York, 1961), p. 328.
- ¹⁴ R. L. Reeves and R. S. Kaiser, *J. Org. Chem.*, 1970, **35**, 3670.
- ¹⁵ R. L. Reeves, M. S. Maggio and S. A. Harkaway, *J. Phys. Chem.*, 1979, **83**, 2359.
- ¹⁶ K. Mochida, A. Kogita, Y. Matsui and Y. Date, *Bull. Chem. Soc. Jpn*, 1973, **46**, 3703.
- ¹⁷ G. G. Hammes, in *Techniques of Chemistry*, ed. G. G. Hammes (Wiley, New York, 1974), vol. iv, pt. 2.
- ¹⁸ C. C. Bott and T. Kurucsev, *J. Chem. Soc., Faraday Trans. 2*, 1975, **71**, 749.
- ¹⁹ C. F. Bernasconi, *Relaxation Kinetics* (Academic Press, New York, 1976).
- ²⁰ G. H. Czerlinski, *Chemical Relaxation* (Marcel Dekker, New York, 1966).
- ²¹ J. A. Schellman, *Acc. Chem. Res.*, 1968, **1**, 144.
- ²² M. Kasha, H. R. Rawls and M. Ashraf El-Bayoumi, *Pure Appl. Chem.*, 1965, **11**, 371.
- ²³ K. R. Popov, *Opt. Spectrosc.*, 1972, **33**, 51.
- ²⁴ J. M. MacLennan and J. J. Stezowski, *Biochem. Biophys. Res. Commun.*, 1980, **92**, 926.
- ²⁵ R. J. Bergeron, D. M. Pillor, G. Gibeily and W. P. Roberts, *Bio-org. Chem.*, 1978, **7**, 263.
- ²⁶ K. A. Connors and T. W. Rosanske, *J. Pharm. Sci.*, 1980, **69**, 173.
- ²⁷ I. R. Brereton, personal communication.
- ²⁸ A. Hersey and B. H. Robinson, *J. Chem. Soc., Faraday Trans. 1*, 1984, **80**, 2039.